N77-15438

NASA CR-144899

BOLTED JOINTS
IN GRAPHITE-EPOXY COMPOSITES

By L. J. Hart-Smith

Prepared under Contract NAS1-13172 by
DOUGLAS AIRCRAFT COMPANY,
McDONNELL DOUGLAS CORPORATION,
Long Beach, California

for

NATIONAL AERONAUTICS AND SPACE ADMINISTRATION

1. Report No.	2. Government Accession No.	3. Recipient's Catalog No.
NASA CR-144899		N77-15438

4. Title and Subtitle	5. Report Date
BOLTED JOINTS IN GRAPHITE-EPOXY COMPOSITES	JUNE 1976
	6. Performing Organization Code

7. Author(s)	8. Performing Organization Report No.
L. J. Hart-Smith	

9. Performing Organization Name and Address	10. Work Unit No.
Douglas Aircraft Company, McDonnell Douglas Corporation, 3855 Lakewood Blvd, Long Beach, California 90846.	11. Contract or Grant No. NAS1-13172

12. Sponsoring Agency Name and Address	13. Type of Report and Period Covered
National Aeronautics and Space Administration, Washington, D.C. 20546.	Contractor Report
	14. Sponsoring Agency Code

15. Supplementary Notes

16. Abstract

Experimental data generated during a comprehensive investigation of bolted joints in graphite-epoxy composites are presented. By interpreting these and other data, methods are provided for the analysis and design of such joints. The specimens tested incorporated quasi-isotropic and two near-quasi-isotropic patterns of the 0, $\pm\pi/4$, $\pi/2$ (0°, ±45°, 90°) family. Both all-graphite/epoxy laminates and hybrid graphite-glass/epoxy laminates were tested. The tests encompassed a range of geometries for each laminate pattern to cover the three basic failure modes — net section tension failure through the bolt hole, bearing and shearout. Static tensile and compressive loads were applied. A constant bolt diameter of 6.35 mm (0.25 in.) was used in the tests. The interaction of stress concentrations associated with multi-row bolted joints was investigated experimentally by testing single- and double-row bolted joints and open-hole specimens in tension. For tension loading, linear interaction was found to exist between the bearing stress reacted at a given bolt hole and the remaining tension stress running by that hole to be reacted elsewhere. The interaction under compressive loading was found to be non-linear. Most of the joints tested were of double-lap configuration using regular hexagon-head bolts. Comparitive tests were run using single-lap bolted joints and double-lap joints with pin connections (neither bolt head nor nut) and both of these joint types exhibited lower strengths than were demonstrated by the corresponding double-lap joints. The new empirical analysis methods developed here for single-bolt joints are shown to be capable of predicting the behavior of multi-row joints. The formulation permits further effects (such as different bolt sizes and environments) to be accounted for as data become available.

17. Key Words (Suggested by Author(s))	18. Distribution Statement
Bolted Joints Graphite-Epoxy Composites Stress Concentrations Experimental Results Empirical Analyses	Unclassified - unlimited.

19. Security Classif. (of this report)	20. Security Classif. (of this page)	21.
Unclassified	Unclassified	

* For sale by the National Technical Information Service, Springfield, Virginia 22151

FOREWARD

This report was prepared by the Douglas Aircraft Company, McDonnell Douglas Corporation, Long Beach, California under the terms of Contract NAS1-13172. The test specimens were fabricated at Douglas and tested at Langley Research Center. The program was sponsored by the National Aeronautics and Space Administration's Langley Research Center, Hampton, Virginia. Mr. M. B. Dow was the Contracting Agency's Technical Monitor.

CONTENTS

TABLES

* Note: Tables with A suffix are in S.I. Units; Tables with B suffix are in U.S. Customary Units; Tables with neither suffix cover both unit systems.

ILLUSTRATIONS

BOLTED JOINTS IN GRAPHITE-EPOXY COMPOSITES

By L. J. Hart-Smith

Douglas Aircraft Company, McDonnell Douglas Corporation

SUMMARY

The objectives of this report are to present the data generated during a comprehensive experimental investigation of bolted joints in graphite-epoxy composites and, by interpreting these and other data, to provide methods for the analysis and design of such joints. The specimens tested incorporated quasi-isotropic and two near quasi-isotropic patterns of the 0, $\pm\pi/4$, $\pi/2$ ($0°$, $\pm 45°$, $90°$) family. Both all-graphite/epoxy laminates and hybrid graphite-glass/epoxy laminates were tested.

The tests encompassed a range of geometries for each laminate pattern to cover the three basic failure modes — net section tension failure through the bolt hole, bearing, and shearout. A constant bolt diameter of 6.35 mm (0.25 inch) was used in the tests. The interaction of stress concentrations associated with multi-row bolted joints was investigated experimentally by testing single- and double-row bolted joints and open-hole specimens in tension. For tensile loading a linear interaction was found to exist between the bearing stress reacted at a given hole and the remaining tension stress running by that hole to be reacted elsewhere. The interaction under compressive loading was found to be non-linear. Most of the joints tested were of double-lap configuration using regular hexagon head bolts. Comparative tests were run using single-lap bolted joints and double-lap joints with pin connections (neither bolt head nor nut) and both of these joint types exhibited lower strengths than were demonstrated by the corresponding double-lap joints.

The new empirical analysis methods developed here for single-bolt joints are shown to be capable of predicting the behavior of multi-row joints. These methods are formulated to account for further effects (such as different bolt diameters and different environments) as data become available.

INTRODUCTION

Experience with bolted joints in composite structures for aerospace applications has indicated a need for greater analysis capability in joint design than has been needed for conventional ductile metals. Major problems contributing to this situation are the fact that bolted joints in composites fail at loads which are not close to either perfectly elastic or perfectly plastic predictions and that there is an almost unlimited number of possible combinations of composite material(s) and fiber patterns which may require bolted joints. Prior work in this area has been fragmented and too specific to provide a simple rational analysis method applicable to arbitrary composite joints. However, prior work has characterized the various failure modes and identified both the dominant factors and the joint parameters associated with such joints. This prior knowledge makes it possible to confine attention to ranges of joint parameters near the optimums and to plan an in-depth experimental study in association with the development of analysis methods, both to explain the tests and to predict the capability of joint geometries other than those for which test data exist.

The purpose of this investigation was to conduct a series of tests on bolted joints in graphite-epoxy composites and develop empirical analysis methods. The fiber patterns tested include the quasi-isotropic pattern and two near-isotropic patterns. The graphite-epoxy used (Thornel 300 / Narmco 5208) is a current high-strength material of moderate modulus and is used widely throughout the composites industry. About one half of the specimens tested were from laminates that had the fibers aligned with the load direction replaced by S-glass. These hybrid laminates exhibited greater stress concentration relief at bolt holes than did the all-graphite materials. The findings of this investigation are supplemented with those from prior work.

Conventional fabrication and testing techniques were used throughout. The laminates for each pattern and material combination were cured in large single sheets to minimize any effect of processing variables. Most of the test specimens were so designed as to permit the generation of multiple results from each. The test specimens covered the entire range of joint geometries of practical interest. The tests were conducted at room temperature. The experimental

investigation employed a single bolt diameter, 6.35 mm (0.25 in.), throughout. Therefore the specific strength values derived do not account for the known sensitivity to scale effect for bolts of other sizes. The analysis techniques developed permit straightforward extension to account for such effects as operating temperature and bolt diameter, as well as to other composite material systems, once the appropriate test data have been generated.

While a considerable body of information about experiments on bolted joints in composite structures can be found in the literature, there appears to be no other comparable analytical investigation. The analyses which have been reported are mostly of finite elements and, as such, apply to specific situations which are covered in greater depth than is possible with the empirical methods developed here, but which do not lend themselves to such comprehensive parametric studies as the empirical methods permit.

The significance of the material presented in this report is that empirical analysis methods have been developed for bolted joints in graphite-epoxy composites and that these methods cover a range of geometries, fiber patterns and material combinations of practical interest so that efficient joints can be designed. The methods are applicable to both single- and multiple-bolt joints and are capable of extension to account for other factors and new material systems as data become available. The test program employed here can serve as a model to account for such variables as new composite materials, larger bolt diameters, and different operating environments.

The units used for physical quantities in this report are given both in U.S. Customary Units and in the International System of Units (SI) (ref. 1).

SYMBOLS

C	constant
d	bolt diameter
e	edge distance from middle of bolt
F_{br}	material allowable bearing strength
F_{tu}	material allowable tensile ultimate strength
k_b, k_t	interaction coefficients (defined in equation 26)

k_{bc}	composite stress concentration factor at failure, with respect to bearing stress
k_{be}	elastic isotropic stress concentration factor, with respect to bearing stress
k_{tc}	composite stress concentration factor at failure, with respect to net section tension stress
k_{te}	elastic isotropic stress concentration factor, with respect to net section tension stress
P	load
t	laminate thickness
w	specimen width
θ	coefficient (defined in equation 2)
σ, σ_t	laminate tensile stress
σ_b	laminate bearing stress
τ_s	laminate in-plane shear stress

EXPERIMENTAL INVESTIGATION

This section of the report explains the choice of materials and fiber patterns employed in this program, describes the test specimens, the test procedures, and the characteristic failure modes, and presents a compilation of the test results. These results are interpreted in the succeeding section. The test results are classified here according to failure mode.

TEST SPECIMENS

Materials

The laminates from which the bolted joint specimens were fabricated were made of the Thornel 300 / Narmco 5208 graphite-epoxy composite. This material was selected because of its widespread use throughout the U.S. composites industry at the start of this program. It is a high-strength material of intermediate modulus and has been found to have such a mix of properties as to make it attractive for aerospace applications. About half of the specimens had the longitudinal plies replaced by S-1014 glass fibers impregnated with the same Narmco 5208 resin. All cross plies ($\pm\pi/4$ and $\pi/2$) were graphite. The compos-

ite material from which the laminates were fabricated was in the form of 7.62 cm (3.0 in.) unidirectional prepreg tapes.

Laminate Pattern Selection

Three fiber patterns were selected for this program. Six laminates were fabricated since each pattern was used in both the all-graphite and mixed graphite-glass composites. The fiber patterns and layup sequences are identified in table I. The layup sequences were selected to intersperse the ply orientations as thoroughly as possible so as to minimize the number of parallel adjacent plies and, thereby, to minimize the matrix stresses.

The three fiber patterns were selected on the basis of a previously unpublished investigation by the contractor. The results of that investigation are reported in this paper. In that systematic survey of the bearing and shear-out strengths of bolted joints, it was found that the optimum fiber patterns grouped about the quasi-isotropic combination.

Fabrication Procedures

The method of fabrication was as follows. Large flat panels were laid up for each fiber pattern and laminate thickness. The composites were cured conventionally in an autoclave. These panels were cut into several smaller pieces, one for each specimen configuration. Each of these pieces then had the aluminum doublers bonded to it in long continuous strips. The adhesive used was either FM-73 or EA9309. These pieces were then cut to the correct specimen length and slit to the appropriate widths, using a diamond-coated slitting wheel. Except for the bolt holes drilled at the NASA Langley Research Center (see fig. 1), all bolt holes were drilled by the contractor with carbide-tipped drills, drilling through part of the way from one side and then coming back from the other to minimize breakout. The holes which were drilled at NASA Langley were made with a diamond core drill using ultrasonic excitation. While all of the holes were satisfactory, and the test results do not favor one method over the other, the diamond-drilled holes were slightly cleaner when inspected visually. The techniques to ensure that the holes were properly located was to establish fixed index blocks on the drilling machine so that the holes were always located identically with respect to the ends and sides of the specimens. Each setup

was checked on scrap material before the specimens were drilled. Those specimens with bonded aluminum doublers were set up in a milling machine to trim the metal doublers with a fly-cutter so that they were parallel to the opposite face of the composite laminate and so that the composite laminate was located centrally within the doublers. This machining was done to ensure that the loads were applied properly.

Configurations

The test specimens and fixtures used in this program are shown in figures 1 to 13. Each test specimen is explained below. Bolts of 6.35 mm (0.25 in.) were used throughout the tests.

Net-tension specimens.- The test specimens illustrated in figures 1, 7 and 8 were proportioned to induce failure by tension through the bolt hole. A range of values of each of the geometric ratios d/w and e/w was covered with the objective of testing at a variety of stress concentration factors. Specimens of three widths (3, 4 and 6 times the bolt diameter), each having two or three edge distances were tested for each of the six laminates. The bolts were loaded in double shear. A total of 36 specimens was tested in this part of the investigation, with each specimen providing four or six data points.

Bearing and shearout specimens.- The test specimens shown in figures 2 and 9 were of sufficient width (10 bolt diameters) to preclude tension failures for the laminate patterns tested. Double-shear tests were performed at edge distances of two, four, six and eight bolt diameters to encompass both shearout failures, in which the proximity of the end of the specimen was sufficient to limit the joint strength, and bearing failures, in which all boundaries of the specimen were sufficiently far removed to permit the maximum strength possible to be developed. Twelve specimens, each with four test holes, were used to assess the resistance to shearout and bearing under tension loads.

Figures 3 and 11 depict the specimen and test fixture used for applying a compressive bearing load. Twelve of these specimens were tested. The bolts were loaded in double shear.

Open-hole specimens.- Figures 4 and 11 show the test specimens which were used to measure the strengths of each laminate in a strip containing an open

hole. The strip width was four times the bolt diameter. Twelve of these specimens were tested, each having the same geometry and providing two data points per specimen.

Multi-bolt interaction specimens.- Figures 5 and 10 show the two-row bolted joint specimens employed to investigate the interaction between stress concentrations when some of the total load is reacted by any given bolt while the remainder of the load passes by to be reacted at the other bolt hole(s). Both tensile and compressive loads were applied. Forty eight such specimens were tested, twenty four each in tension and compression. The selection of two bolts and uniformly thick laminates in this specimen was to ensure that the load reacted at each bolt would be known even though the load paths were redundant. With this design, the load must be shared equally between the two bolts. The bolt holes were drilled right through the three laminates simultaneously to ensure that the bolts were a precision fit in the holes. Indeed, the bolts were selected on a hole-by-hole basis to improve the fit. Figures 12 and 13 illustrate the fixtures employed to load these specimens in compression. The fixture in figure 13 provided lateral support for the compression specimens.

Pin-joint specimens.- Two quasi-isotropic specimens of the type shown for bearing and shearout in figure 2 were tested with the load transferred by a simple pin, instead of the conventional mechanical fasteners, to quantify just how much additional load transfer is accomplished because of the bolt head and nut.

Single-lap shear specimens.- Four quasi-isotropic all-graphite specimens were made and tested in tension as shown in figure 7. The special test fixture was designed to eliminate the laminate bending usually associated with single-shear single-row bolted joints.

Test Procedures

The bolts used throughout the tests were NAS 464-4 6.35 mm (0.25 in.) titanium alloy heat treated to 1100-1240 MPascal (160-180 ksi). New bolts were used for each test to preclude the possibility of accumulated bolt distortion affecting the results. The bolts were torqued to 2.8 N.m (25 in-lb), which is the normal tightening torque for such bolts in composite applications.

The method for testing those specimens containing two or more bolt holes at each end of the specimen was as follows. The load was always reacted at the central bolt hole through the doublers. The outermost holes were tested first and the specimens were then cut back as shown in figures 1 and 2 for the succeeding tests. The testing of the open-hole specimens in figure 4 was accomplished by pulling between each adjacent pair of large holes in turn. The method of introducing and reacting the load for the compression bearing specimens is evident from the test fixture illustrated in figure 3. Likewise, the loading of the single-lap joint specimens is explained in figure 6.

The testing of the tension interaction specimens posed no special problems. The fixture in figure 12 was used to load the compression interaction specimens. The load-introduction members contain a threaded hole, in the middle of their round bases, which was used to locate the fixtures correctly with respect to the loading platens of the test machine. The lateral-support fixture shown in figure 13 rode on the specimen itself.

Failure Modes for Bolted Joints in Composites

Figure 14 illustrates characteristic modes of failure for bolted joints in advanced filamentary composites. The basic modes of tension through the net section, shearout, cleavage, and bearing are governed by both geometric and material parameters. It is necessary to consider each of these failure modes in interpreting test data and in evaluating designs. In many instances a failure can occur in a combination of modes rather than in a single form.

TEST RESULTS AND DISCUSSION

The results of the specimen tests are reported in tables II to XIX. These various tables include both raw data and derived data as well as an identification of the mode of failure. The following observations are made on the data from the present investigation.

Net-tension specimens (tables II to VII).- The net section (tension-through-the-hole) stresses are significantly less than the ultimate laminate stresses, indicating the presence of stress concentration factors at failure. The failure loads and net-section stresses are functions of the geometric parameters d/w and e/w. The joint strengths do not vary much between any of

these fiber pattern and material combinations tested, but the modes of failure did vary. The widest (six bolt diameters) of the all-graphite laminates all failed in bearing, regardless of the edge distance, while the two narrower sets of such specimens (three and four bolt diameters) nearly all failed in tension, with a few bearing failures at large edge distances. In contrast with this behavior, the graphite-glass epoxy laminates exhibited no tension failures at all. This latter group failed predominantly by bearing for the larger edge distances and by shearout when the bolt was installed close to the end of the specimen (at two bolt diameters from the edge).

Bearing and shearout specimens (tables VIII to XI).- The bearing stresses at failure were typically of the order of 830 MPascal (120 ksi) regardless of fiber pattern or material. Most results were scattered throughout the range 690 to 970 MPascal (100 to 140 ksi). These results show that the fiber patterns tested represent a strength plateau which is insensitive to minor fiber pattern changes. The use of the softer glass plies in the longitudinal direction does not impose any loss in either bearing or tension strength but does tend to ensure that any failures at stress concentrations in such laminates will be local rather than potentially widespread and catastrophic due to a tension crack in an all-graphite laminate. The influence of shearout as a distinct mode other than a bearing failure is slight, being evident only for the orthotropic all-graphite laminates at the shortest edge distance tested, namely two bolt diameters. All other failures in this series of tests were by bearing.

The bearing strengths under compression were only slightly higher than for tensile bearing (despite the grossly different stress trajectories) for the all-graphite epoxy laminates but the strengths for the graphite-glass epoxy laminates under compressive bearing showed about a 20 per cent improvement with respect to tensile bearing.

Open-hole specimens (tables XII and XIII).- The graphite-glass epoxy laminates were consistently about 25 per cent stronger than the equivalent all-graphite epoxy specimen of the same fiber pattern. The net-section strengths for these 4d wide strips were about twice as high as those strips of the same width containing a loaded bolt hole. This result was expected because the stress concentration factors at loaded holes are typically much more severe than for unloaded holes. The fiber pattern had a measurable influence on the

strength attained, pattern 3 being slightly stronger than pattern 2 which was stronger than pattern 1. The patterns 6, 5 and 4 were ranked similarly. The holes caused failures at stresses significantly below the ultimate laminate strengths for each pattern and material combination.

Multi-bolt interaction specimens (tables XIV to XVII).- The most significant finding of the investigation of the two-row bolted joints is that the strengths were not very much higher than those of a single-row joint in an all-graphite specimen of the same width (four bolt diameters). The failure mode, net tension, was the same in each case. This similarity of failure loads means that the combination of the stress concentration induced by the load to the second bolt bypassing the first bolt and the stress concentration caused by the load in the first bolt itself is nearly as bad as that induced by reacting the entire load at a single bolt hole. The two-hole graphite-glass epoxy specimens exhibited higher strengths than for the single-hole specimens by as much as fifty percent, demonstrating again an advantage for the graphite-glass combination over the all-graphite reinforced composite. The compression loads sustained by these interaction specimens were consistently higher than for tensile loading.

Pin-connection test specimens (table XVIII).- The bearing strengths developed by pin loading of the holes in the quasi-isotropic all-graphite laminates were only about half as high as for the same specimens with conventional bolts.

Single-lap test specimens (table XIX).- The bearing strengths at failure with single shear bolts were about 690 MPascal (100 ksi) or about twenty percent lower than for double shear. This results applies when the bolt is able to deflect due to the local eccentricity in load path but the basic laminate is relieved from the gross bending moment usually associated with single-lap joints by the special fixture shown in figure 6.

DATA INTERPRETATION AND ANALYSIS METHODS

This section of the report begins with a listing of the basic laminate strengths which have been computed to serve as a basis for the establishment of stress concentration factors at failure. The purpose of the succeeding analyses for each of the characteristic failure modes is to generate methods

and understanding which will permit the generalization of specific test data to joint geometries for which test data are not available. Each of the basic failure modes (tension-through-the-hole, shearout, and bearing) is then assessed in turn. The test data from the present investigation are supplemented where appropriate by other results, given in the appendices where the source references are identified. The analysis for tension failures is in two parts. The first is for the elastic isotropic stress concentration factors and serves as the basis for all such analyses. Correlation factors between such elastic isotropic stress concentration factors and those observed at failure in composites are then established from test data. An isotropic elastic stress concentration reference is used for both quasi-isotropic laminates and orthotropic laminates in which the material axes coincide with the load and geometric axes because, for the specific area of interest, such orthotropy could be represented by a proportionality constant. The values of such correlation factors between the stress concentration factors are found to depend on both the composite material and the fiber pattern. The joint geometries at which transitions between failure modes occur are, likewise, found to be a function of both the composite material and fiber pattern. The various analyses for each individual failure mode for single bolted joints are then integrated into a method for preparing design charts covering the entire range of possible geometries and depicting over which regime each mode of failure prevails.

The data interpretation and analysis section then proceeds to address the problem of load sharing at multi-row bolted joints. The test data generated on two-row bolted joints are combined with those for single-row bolted joints and open holes, for each of the six laminates, to explain a linear interaction theory for those cases in which the failure mode is net tension. For wider bolt spacings, the failure can be bearing. A technique is proposed for accounting for a transition between bearing and tension failures in such cases.

BASIC LAMINATE STRENGTHS

The basic laminate strengths for the materials tested in this investigation have been computed using the monolayer data in table XX. The computer program used to compute laminate properties in terms of such experimentally

derived monolayer data employs a modified Hill's criterion to establish the load level at which some ply first becomes critical. Because of the much higher elongation of the glass fibers than the graphite fibers, an initial failure in a cross ply need not denote the maximum load capacity of the laminate. Indeed, the original computations for the strength of the hybrid graphite-glass/epoxy laminates predicted failures at lower loads than the 0 (0°) glass fibers alone could carry. Therefore, the program was modified to predict failure at the second fiber failure instead of the first in the event that, after the cross plies ($\pm\pi/4$) ($\pm45°$) had failed, the remaining fibers could withstand a higher load than that at which the initial failure was predicted. (It is believed that the failure of the $\pm\pi/4$ ($\pm45°$) graphite fibers prior to the failure of the 0 (0°) glass fibers is responsible for the preponderance of bearing failures for the hybrid laminates rather than the tension failures demonstrated by the all-graphite laminates having the same joint geometries).

The average failure strengths and moduli predicted for each of the six laminates used in this program are given in table XXI. These strengths serve as the basis for the calculated stress concentration factors in composites at failure.

ELASTIC ISOTROPIC STRESS CONCENTRATION FACTORS

a. Loaded Bolt Holes

The experimental data of Frocht and Hill (ref. 2), along with the theoretical investigations cited below, provide a means of establishing an empirical equation for the stress concentrations at lightly loaded bolt holes. Such an equation applies within the elastic regime for isotropic materials. At higher load levels the ductile materials, such as aluminum alloys, yield locally to reduce the stress concentrations at bolt holes. Composites, likewise, exhibit lower stress concentrations at failure than would be predicted from linear elastic theory. However, because of the more limited extensibility of composites in comparison with that of ductile metals, the stress concentration factors at failure for composites are much higher than for ductile metals. Consequently it is incorrect to perform stress analyses on bolted joints in fiber-reinforced composites by assuming that the net sections of the members being joined are

uniformly stressed at the yield stress (or at any other uniform stress, for that matter), as is commonly assumed for metal practice. The objective of this section is to develop the basis of analyses for bolted joints in graphite-epoxy composite laminates in such a form that the stress concentration factors at failure can be accounted for.

The elastic isotropic stress concentration factor at a loaded bolt hole is given here by the equation

$$k_{te} = 2 + \left(\frac{w}{d} - 1\right) - 1.5\,\frac{(w/d - 1)}{(w/d + 1)}\,\Theta \tag{1}$$

in which the parameter Θ is defined as

$$\begin{aligned} \Theta &= 1.5 - 0.5/(e/w) \quad \text{for} \quad e/w \leq 1 \\ \Theta &= 1 \qquad\qquad\qquad\quad \text{for} \quad e/w \geq 1 \end{aligned} \tag{2}$$

The various geometric parameters are identified in figure 15. The maximum stress in the plate, adjacent to the bolt hole on the diameter perpendicular to the load direction, is given by

$$\sigma_{max} = k_{te}\,\frac{P}{t(w - d)} \tag{3}$$

In this and all other mention of stress concentration factors in this report, the stress concentration factor is evaluated with respect to the net rather than gross section. Equations (1) and (2) lose their physical significance for $d \to w$ and for $e \to d/2$. For values of e not much greater than d/2 the critical stress condition is one of shearout or cleavage rather than of tension through the hole and it is necessary to account for these different failure modes separately to identify which is more critical for a particular geometry. For the limiting case in which $d/w \to 0$ (and e is not so small as to make shearout or cleavage critical) the failure mode will be in bearing but, even so, equation (1) correctly characterizes the tension stress in the laminate next to the loaded bolt hole.

Equation (1) above can be re-expressed with respect to the bearing area, instead of the net tension area, so that

$$k_{be} = \frac{\sigma_{max}}{P/td} = \frac{k_{te}}{(w/d - 1)} = 1 + \frac{2}{(w/d - 1)} - \frac{1.5\,\Theta}{(w/d + 1)} \tag{4}$$

Equations (1) and (4) are derived as follows. The limiting value of unity for k_{be} in an infinite plate is adopted from figure 7 of reference 2 in which it is attributed to theoretical investigations by Bickley (ref. 3) and by Knight (ref. 4). The limiting value $k_{te} = 2$ as the hole diameter approaches the width of a finite strip is also based on theory. Koiter (ref. 5) computed this limiting value for a large open hole in a narrow strip. Since there is no contact on the sides of a loose or net fit bolt hole, nothing in his analysis would be changed by reacting the load at one end by a bolt instead of the entire section. Therefore the same value should apply here also. The equations were also made to produce values of $k_{te} = k_{be} = 2.5$ for $d/w = 0.5$ and $e/w \geq 1$ to comply with the other of Knight's theoretical computations. In addition to these discrete points, the equations were selected to conform with the general trend of the experimental data of Frocht and Hill in figures 5 to 7 of reference 2. The final constraints imposed on equations (1) and (4) are the physically necessary ones that k_{be} is a monotonically increasing function of d/w and that $d(k_{be})/d(d/w) = 0$ as $d/w \to 0$. Likewise, k_{te} is a monotonically decreasing function of d/w. The form of the function Θ in equation (2) is such that, for an infinitely wide plate containing a loaded bolt hole within a finite distance of the edge of the plate,

$$k_{be} \to 1 + \frac{3}{4}\Big/\left(\frac{e}{d}\right) \qquad \text{as} \quad \frac{d}{w} \to 0 \tag{5}$$

This relation satisfies the obvious requirements that $k_{be} \to \infty$ for $e/d \to 0$ because the bolt would pull straight out of the half hole at the end of the laminate with no resistance and that the effect of the e/d ratio should become increasingly small as the value of that ratio becomes progressively larger. This constant 3/4 was deduced here largely by curve fitting the Frocht and Hill data (ref. 2) for $e/w \approx 1/3$ and $e/w \approx 1/2$ for moderate rather than small values of d/w because no more appropriate data is yet available.

Figures 16 and 17 depict equations (1) and (4). The experimental data of, and reported by, Frocht and Hill (ref. 2) are included in these figures. The dominant influence is clearly the d/w term in both equations while the e/w or e/d term has but a minor influence.

In order to adapt the equations above for single loaded bolt holes to the situation prevailing at multi-row bolted joints, it is necessary to understand

the stress trajectories in the immediate vicinity of the bolt hole. Bickley (ref. 3) has performed analytical studies on the elastic isotropic stress concentrations around loaded bolt holes. These investigations have established that the hoop tension stress adjacent to the bearing perimeter of the bolt is of the order of the average bolt bearing stress P/dt from a to c and on to the mirror image of a on diameter bb in figure 15. The bearing stress varies from about 2P/dt in the middle of the contact area (point c in figure 15) to zero on the edges (point a and opposite) for a loose or net fit bolt.

In order to derive expressions for the ratio of the strengths of bolted joints to the strength of the basic laminate containing the joint, it is necessary to rearrange equation (1) to read

$$P = \frac{\sigma_{max} tw}{\frac{2}{\left(1 - \frac{d}{w}\right)} + \frac{1}{\left(\frac{d}{w}\right)} - \frac{1.5\Theta}{\left(1 + \frac{d}{w}\right)}} \tag{6}$$

Equation (6) permits an assessment of the influence of the joint geometry on the joint strength and is plotted nondimensionally in figure 18. It can be seen that, for a given maximum stress in the plate, the load carried is maximized when

$$d/w = 0.40 \tag{7}$$

This corresponds with a bolt pitch of approximately 2.5 bolt diameters which, on the basis of this interpretation of the stress concentrations at loaded bolt holes in elastic isotropic materials, would appear to be the optimum bolt pitch. (The customary bolt pitch of 4d established for ductile metals has been established largely on the basis of ultimate static strength). Figure 18 indicates that the bolted joint strength is fairly insensitive to minor variations about the optimum location and that the maximum possible joint efficiency for a brittle elastic isotropic material barely exceeds 20 per cent.

b. Open Holes

The stress concentration factor at the net section of a strip containing an unloaded hole is needed for the assessment of the interaction of stress concentrations at multi-row bolted joints in loaded plates. The equation proposed here for a hole in a strip is

$$k_{te} = 2 + \left(1 - \frac{d}{w}\right)^3 \tag{8}$$

Corresponding with this, one can compute the net section strengths as a function of the hole diameter to width ratio. The strength of the net section can be non-dimensionalized to read

$$\frac{P}{\sigma_{max} wt} = \frac{\left(1 - \frac{d}{w}\right)}{k_{te}} = \frac{\left(1 - \frac{d}{w}\right)}{2 + \left(1 - \frac{d}{w}\right)^3} \tag{9}$$

Equation (8) was derived as follows. An obvious constraint is the classical solution that $k_{te} = 3$ as $d/w \to 0$, which is attributed to Kirsch in 1898 by Timoshenko (ref. 6). Another constraint is the theoretical value of $k_{te} \to 2$ as $d/w \to 1$ deduced by Koiter (ref. 5). (This value has been confirmed experimentally by Wahl and Beeuwkes (ref. 7)). A third constraint is not evident from equation (8) and requires an assessment of equation (9). On physical grounds one should assume both that P is greater for $d/w \to 0$ than for any greater value of d/w and that $d(P)/d(d/w)$ is zero as $d/w \to 0$. Equation (9) satisfies all of these constraints and, thereby, lends confidence to the simple equation (8).

Equations (8) and (9) are plotted in figures 19 and 20, along with largely photoelastic data from references 7 and 8.

STRESS CONCENTRATION FACTORS FOR COMPOSITES

a. Loaded Bolt Holes

Narrow composite strips and wide panels with relatively close bolt pitches tend to fail under load by tension of the net section through the bolt hole(s) (see fig. 14). The failure stresses are usually considerably less than the basic laminate strengths and the reason for this is the limited stress concentration relief associated with advanced composite materials. Consequently, the tension failure stress for composites is a function of the local stress concentration, and hence of the joint geometry, as well as of the material and fiber pattern. Some of the early investigations into bolted joints in advanced filamentary composites are still reported in reference 9 (Volume II, Analysis,

figures 2.4.2-15 to -17) in terms of an "allowable" net-section design strength supposedly applicable for all joint geometries. It is suggested here that the considerable scatter shown in those diagrams should be explained in terms of the influence of joint geometry on the net-section failure stress. Otherwise, the use of those data in the form presented in reference 9 will lead to some designs which are excessively conservative and to others which are dangerously unconservative.

In references 10 and 11 it is suggested that a linear relationship exists between the elastic isotropic stress concentration factors for low load levels and the stress concentrations at failure of bolted composite joints of the same geometry. The basis of this linear relationship is illustrated in figures 21 and 22 which have been replotted from reference 12 using the stress concentration equations (1) and (2). The stress concentration factors k_{tc} were evaluated with respect to experimentally determined laminate strengths. The straight lines have been constrained to pass through the point (1,1), for which there is no stress concentration at any load level, with a slope evaluated by minimization of the squares of the deviations between individual points and the lines. A straight line is employed because the degree of scatter does not justify any more complex representation. The test data on which figures 21 and 22 are based are recorded in tables XXII to XXV of the appendix.

The open-hole data have been included with the loaded-hole data to show that, at least as far as the net section through the bolt hole is concerned, the origin of the stress concentration is not important. Much the same proportional reduction in stress concentration at failure of the composite is shown for both the loaded and unloaded holes. Therefore, it is reasonable to assume that two bolted joints having different geometries but the same elastic isotropic stress concentrations (by compensating differences in the d/w and e/w ratios) would experience similar stress concentrations at failure also.

The justification offered for plotting measured orthotropic stress concentration factors at failure of the non-isotropic material in figure 22 against calculated elastic isotropic stress concentration factors is as follows. When attention is confined to only the net section through the bolt hole perpendicular to the load direction and the axes of material orthotropy are the same as the geometric axes of the joint (length and width), the difference between the

elastic isotropic stress concentration factors and the corresponding elastic orthotropic stress concentration factors is merely a proportionality constant. This constant can be just as conveniently accounted for in the slope of the line in figure 22, without having to evaluate the constant, as by determining its value and rescaling the abscissa of such a figure.

Test data for the present program, from tables II to IV, are depicted in figures 23 and 24, showing how the stress concentrations at failure compare with the calculated elastic isotropic stress concentrations. The equations used to characterize the stress concentrations are as follows:

Quasi-isotropic Thornel 300 / Narmco 5208 $(0, \pi/4, \pi/2, -\pi/4)_s$

$$k_{tc} = 0.73 + 0.27\, k_{te} \tag{10}$$

Orthotropic Thornel 300 / Narmco 5208

$(0, \pi/4, \pi/2, 0, -\pi/4, \pi/2, 0, \pi/4)_s$ & $(0, \pi/4, 0, -\pi/4, \pi/2, \pi/4, 0, -\pi/4)_s$

$$k_{tc} = 0.60 + 0.41\, k_{te} \tag{11}$$

The similarity of the results for patterns 2 and 3 results from the similar elastic moduli and strengths (see table XXI). The hybrid glass-graphite/epoxy laminates did not fail in tension for this program so no stress concentration values could be calculated. The equations corresponding with equations (10) and (11) for the Morganite II / Narmco 1004 system, for which the results are presented in figures 21 and 22 are as follows:

Quasi-isotropic Morganite II / Narmco 1004 $(0, \pi/4, \pi/2, -\pi/4)_s$

$$k_{tc} = 0.75 + 0.25\, k_{te} \tag{12}$$

Orthotropic Morganite II / Narmco 1004 $(0, \pi/4, 0, -\pi/4)_s$

$$k_{tc} = 0.54 + 0.46\, k_{te} \tag{13}$$

These equations (12) and (13) should not be expected to apply also to the similar Modmor II / Narmco 1004 graphite epoxy (Narmco 5206) material because of a significant change in interlaminar shear strength between the two systems.

Figures 23 and 24 include test data for bearing failures as well as the tension failures respresented by equations (10) and (11). The reason why these data contribute confidence to the coefficients in equations (10) and (11) is as

follows. If a joint specimen fails in bearing rather than tension, the computed value of k_{tc} would necessarily be higher than that which would have been exhibited during a tension failure. Therefore, those data in figures 23 and 24 pertaining to bearing failures should lie consistently above the lines denoting equations (10) and (11). This is seen to be so. Furthermore, an examination of figures 23 and 24 shows that the transition between tension and bearing failures for these composite laminates occurs for joint geometries having k_{te} values of about 5.5 and that the bearing data diverge progressively more from the lines plotted for tension failures with still greater values of the stress concentration factor k_{te}. (The data plotted in figures 21 and 22 are complete. Bearing and tension results for that investigation were indistinguishible).

In equations (10) to (13) the net-section strength is related to the material and geometric properties of the joint in terms of the equation

$$P = \frac{(w - d)tF_{tu}}{k_{tc}} \tag{14}$$

The application of the concepts described above is explained as follows. An elastic isotropic stress concentration factor is evaluated for any specific geometry under consideration, using equations (1) and (2). Then, for the particular material system being assessed, the corresponding stress-concentration factor in the composite laminate at failure is evaluated by means of an equation such as equation (10). This design method does not require the testing of each and every joint geometry being assessed. The test data from selected geometries can thus be generalized to other geometries, which were not tested, by working in terms of the stress concentrations. As more data become available, the coefficients in equations (10) to (13) and the like can be expanded to account for such effects as different environments and different bolt diameters.

Composite materials have been shown in figures 21 and 23 to exhibit lower stress concentrations at failure than linear elastic theory would predict. Therefore, it is appropriate to redefine equation (6) as follows, for composite materials.

$$\frac{P}{F_{tu}tw} = \left(1 - \frac{d}{w}\right) \Big/ k_{tc} \tag{15}$$

Equation (15) is plotted in figure 25, in which the relationship between k_{tc} and k_{te} is of the form

$$(k_{tc} - 1) = \text{CONSTANT} \times (k_{te} - 1) \qquad (16)$$

The values of the constant shown in figure 25 are 0, 0.1, 0.2, 0.4, 0.6, 0.8, and 1. Three features in figure 25 are noted. The first is that the smaller values of the constant are associated with higher joint strengths for a given common laminate strength F_{tu} because k_{tc} is less than k_{te}. The second feature is that the optimum value of d/w changes as the stress concentrations decrease close to the limiting fully-plastic case. Whereas the optimum d/w ratio is 0.40 for a perfectly-elastic isotropic material, that optimum is closer to 0.30 for the quasi-isotropic composites tested in this program since the constant in equation (16) is, in that case, given by equation (8) as 0.27. The optimum for the two orthotropic laminate patterns tested in the present program is, likewise, found to be at d/w ≈ 0.35. This shows that the optimum joint geometry (dominated by the d/w ratio) is a function of both the material system and fiber pattern. The third feature of figure 25 is that the stress concentration relief exhibited by the graphite-epoxy laminates is sufficient to double the optimum bolted joint strength for the quasi-isotropic laminates tested (with respect to predictions for a brittle elastic isotropic material) from just over 20 percent of the basic material strength to 42 percent. The radial lines from the origin in figure 25 denote lines of constant bearing strength F_{br}. The predominant failure mode for small d/w ratios is usually bearing, rather than tension, so the tension strengths predicted in that portion of figure 25 can not usually be realized. (Bearing failures are discussed in a later section of this report). Because figure 25 is plotted in non-dimensionalized form, it does not provide a convenient quantitative comparison between the potential strengths of the different laminate patterns tested during the present program. Figures 26 have been prepared to afford such a comparison, taking into account the different basic laminate strengths for the all-graphite composites.

b. Open Holes

The test data from the present investigation, pertaining to tension failures at unloaded holes, are recorded in tables XII and XIII and are illustrated in figure 27. The results for the all-graphite laminates all represent tension-

through-the-hole failures. However, none of those coupons with glass fibers show any evidence of tension failure. All of this latter group show classical shearout failues in the 0 (0°) direction originating at the sides of the holes. It is not possible to make deductions about the tensile failure of graphite-glass hybrid laminates at stress concentrations on the basis of these data. The stress concentration factors for the present all-graphite specimens have been calculated to lie in the range 1.5 to 2.0 at failure and are significantly lower than the stress concentration factors calculated for loaded bolt holes in equivalent specimens. These results are shown in the lower left corners of figures 23 and 24, using equation (8) to compute the elastic isotropic stress concentration factors k_{te}. Figure 21, likewise, includes open-hole results in the lower left corner and these are seen to be compatible with the line plotted to fit the loaded hole results.

The results of the present investigation are supplemented by some previously unpublished tests on filled (but unloaded) holes in the Modmor II / Narmco 1004 graphite-epoxy encompassing a far wider range of fiber patterns than was tested here. These results (see tables XXVI to XXVIII of this report), obtained by the contractor, are illustrated in figures 28 to 30 to show the influence of fiber pattern, hole size, and direction of loading (tension or compression) on the strength of graphite-epoxy laminates. The test specimen used for both the specimens with the holes and the basic laminate control specimens was a honeycomb sandwich beam under four-point loading. The holes tested were of 6.35 mm (0.25 in.) diameter in 38.1 mm (1.5 in.) wide strips and 25.4 mm (1.0 in.) diameter in 50.8 mm (2.0 in.). The holes were filled with net-fit pins. Figure 28 presents the tensile test results for both size holes plotted in terms of the ratio of the stress concentration factors observed at failure to the elastic orthotropic stress concentration factors as calculated using equations from reference 9. It is clear both that there is significant stress concentration relief, between low stresses and failure, in all cases and that the larger holes are associated with consistently greater stress concentrations at failure. There is also a clear indication that the maximum relief is achieved with laminates which contain either few or many 0 (0°) plies. Figure 28 cannot be used to determine the absolute strength of a laminate with a hole in it because of the variable orthotropic reference strengths. This limitation is overcome in

figure 29, in which the net-section strength for the 6.35 mm (0.25 in.) holes is depicted on an absolute basis. The strength increases essentially monotonically with the percentage of 0 (0°) plies. Figure 30 presents the corresponding data for compressive instead of tensile load. The test specimens were honeycomb sandwich beams with 6.35 mm (0.25 in.) holes in the 38.1 mm (1.5 in.) wide facings, just as for the tensile tests. An examination of figures 29, for tensile loading, and 30, for compressive loading, shows that the strength of laminates with unloaded filled holes is lower when loaded in compression than in tension. Since the pins filling the holes were not an interference fit, one should assume that the same results would apply also for open holes. Compressive tests were not conducted for the 25.4 mm (1.0 in.) holes.

A direct comparison between the present and prior test results is possible only for the quasi-isotropic all-graphite pattern. In this case, the present stress concentration factors ranged from 1.5 to 1.7 while, in the prior tests, the factors ranged from 1.5 to 1.6. The results are thus seen to be comparable, with the small difference possibly attributable to the different tests specimen geometries. Test data from the present program are included in figure 29.

SHEAROUT STRESS CONTOURS

When the edge distance between a loaded bolt and the edge of a composite laminate is small, or the fiber pattern is deficient in cross plies ($\pm\pi/4$ and/or $\pi/2$ ($\pm45°$ and/or 90°)), the predominant mode of failure is either shearout or cleavage (fig. 14). Just as in the preceding case of tension through-the-hole failures, the characteristic shearout and cleavage modes of failure are strongly influenced by the joint geometry, fiber pattern, and composite material of which the joint is made.

Figure 31 shows previously unpublished shearout stress contours, as a function of fiber pattern, which were obtained during an earlier investigation, by the contractor, on Modmor II / Narmco 1004 graphite-epoxy laminates. These data are given in tables XXIX to XXXII of this report. All such specimens tested had 6.35 mm (0.25 in.) diameter bolts, an edge distance of 12.7 mm (0.5 in.), and a width at least as great as 38.5 mm (2.5 in.). That geometry had been selected in anticipation of consistent shearout or cleavage failures. Yet,

despite an edge distance ratio e/d (fig. 15) as low as 2 and a w/d ratio at least as great as 10, all of those fiber patterns containing less than 50 percent 0 (0°) plies failed consistently in tension through-the-hole rather than by shearout. Failures were by shearout in the upper portion of the triangle, and it can be seen that the reduction of cross plies is associated with a consistent loss of shearout strength.

Figure 32 illustrates the corresponding shearout stress contours for mixed graphite-epoxy laminates. These laminates were made from Modmor II fibers in the 0 (0°) and $\pi/2$ (90°) directions, and Thornel 75S fibers in the $\pm\pi/4$ ($\pm$45°) directions, with Narmco 1004 epoxy. The results share one characteristic with those in figure 31 inasmuch as the highest shearout strength is demonstrated for intermediate amounts of $\pm\pi/4$ ($\pm$45°) fibers, with lower strengths for those laminates containing either few or many such fibers. The major difference between figures 31 and 32 is that, in the latter, all failures were in shearout. This difference between figures 31 and 32 illustrates the sensitivity of the strength and behavior of bolted joints in composites to the particular composite material as well as to the joint geometry and fiber pattern. The data from which figure 32 was prepared are recorded in reference 13.

Figure 33, replotted from reference 13, presents the corresponding shearout stress contours for AVCO 5505 boron-epoxy, 0.1 mm (0.004 in.) fibers. This diagram is included in a report on graphite-epoxy to emphasize the point that the nature of the data presented in figures 31 and 32 is characteristic of the particular materials system being assessed. In comparison with figures 31 and 32 for graphite-epoxies, the boron-epoxy data shares the characteristic of lower strengths for few and many $\pm\pi/4$ ($\pm$45°) fibers. There is a transition between shearout and tension failures, but at a different location than in figure 31. The The data for these tests are recorded in reference 13.

The "shearout stresses" in figures 31 to 33 were calculated by the customary formula

$$\tau_s = P \; / \; [2t(e - \tfrac{d}{2})] \qquad (17)$$

The value so calculated is not, in general, a material property alone since it is known from prior testing to be a function of the e/d ratio (ref. 14) and possibly the w/d ratio also. Such shearout stresses are meaningful as a measure

of joint strength, even if the failure mode is in bearing or tension (as is the case for many of the failures of the specimens tested to produce figures 31 to 33), provided that the specimen geometry is identified to prevent unwarranted extrapolation. In every test on which figures 31 to 33 are based, the w/d ratio was at least eight and sometimes as high as twelve to eliminate any influence from that parameter.

The shearout test data for the present investigation are reported in tables VIII and IX. Equation (17) was used to compute the "shearout stresses". The value of w/d used for these specimens was sufficiently high that its value should have very little effect on the results. It should be noted that, in tables VIII and IX, shearout failure occurred only for e/d values as low as two. For greater edge distances, the failure was always bearing and occurred at a higher load.

The shearout stresses developed in this test program for e/d ratios of the order of two are either as good as or better than those which have been attained in prior investigations (compare, for example, tables VIII and IX with figure 31). The stresses are, however, significantly less than the in-plane shear strengths of the laminates tested (see table XXI). This confirms the presence of significant stress concentrations in the shear distribution reacting the bolt load, as has been observed in prior investigations.

In concluding this section, it should be noted that very few shearout failures were experienced during this program. This is the result of consciously restricting the fiber patterns to be favorable for efficient bolted joints and essentially free from premature failure by shearout (see figure 31). This investigation confirmed that earlier assessment. Shearout failures at large edge distances in composite laminates are associated with unsuitable fiber patterns for bolted joints. The failure loads of bolted composite joints failing in shearout has been found by prior testing to be either independent of, or only weakly dependent upon, the e/d ratio (see ref. 14).

BEARING STRESS CONTOURS

In most cases in which both the edge distance and panel width (or bolt

pitch) are large in comparison with the bolt diameter, the dominant failure mode is bearing. Such damage is localized and is usually not associated with catastrophic failure of a composite structure. The initiation of such a failure may be caused by compressive bearing at the base of the bolt hole or by tension or shearout at the sides of the hole.

Figure 34 presents some previously unpublished test results from a systematic survey of the bearing strength of Modmor II / Narmco 1004 graphite-epoxy laminates of various fiber patterns. These data were obtained from the same test specimens as used for the shearout tests shown in figure 31, but with a greater edge distance. Two important features are evident in figure 34. The first is the large plateau at the peak bearing stress in the vicinity of the quasi-isotropic pattern (25% 0, 50% $\pm\pi/4$, 25% $\pi/2$). The second important feature in figure 34 is the change in failure mode from bearing to shearout, in spite of the large edge distances and widths, for those laminate patterns containing more than about fifty to sixty percent of 0 (0°) plies. Figures 35 and 36 (replotted from reference 13) contain bearing data corresponding with the shearout data for the mixed-graphite and boron/epoxy laminates for which the shearout results are presented in figures 32 and 33. The shape and location of the transitions in failure modes differs between each of figures 34 to 36 and, therefore, such behavior cannot be projected from one material for which test data exist to another for which they do not. Joint geometries known to be associated with bearing failures for one composite material are sometimes associated with tension or shearout failures for other composites, even if the joint geometries are identical. The test data from which figure 34 has been prepared are recorded in tables XXIX to XXXII of this report.

The test data from the present investigation are reported in tables VIII and IX and illustrated in figures 37 and 38. A photograph of typical failure modes is provided in figure 39. An edge distance ratio e/d as great as four is necessary to develop the full bearing strength of these laminates. The solid symbols in figures 37 and 38 denote bearing failures, while the open symbols signify tension failures, at less than the potential bearing strength. The solid lines show average strengths of bearing failures for the range of e/d ratios over which each line extends. The chain lines refer to the predictions of equation (5).

In comparing the data in figures 37 and 38 with those shown in figure 34, two things are clear. First, the present data are consistent with the existence of a plateau of maximum bearing strength for the same fiber pattern domain as was demonstrated in figure 34. However, the strengths of the laminates tested during the present investigation [891-908 MPascal (129-131 ksi) for the all-graphite laminates and 834-850 MPascal (119-122 ksi) for the graphite-glass hybrid laminates] are significantly lower than those shown in figure 34 [965-1000 MPascal (140-145 ksi)] and considerably lower than those bearing stresses [1172-1241 MPascal (170-180 ksi)] associated with the net-tension failures in the tests on which figures 21 and 22 are based (see tables XXII to XXV of this report). Second, the data in figures 37 and 38 suggest that, for all practical purposes, the same maximum bearing strength was developed for both material systems and all three fiber patterns tested in the present program. These results highlight the need for data generated specifically for the composite material of interest.

COMPRESSION BEARING

Tables X and XI record the measurements made on compression bearing specimens during the present investigation. The results are summarized in figure 40, showing average bearing strengths of 866 MPascal (126 ksi) for the all-graphite laminates and 1209 MPascal (175 ksi) for the hybrid graphite-glass laminates. In comparison with tension bearing (see figures 37 and 38), it is apparent that there is a slight increase in bearing strength for the all-graphite laminates when the bolt load is reacted by compression rather than by tension, but for the hybrid laminates, there is a pronounced increase in bearing strength.

Figure 41 illustrates sample compression bearing failure modes and it is evident that these look very similar to those in figure 39 for tension bearing. The logitudinal stresses in the fibers adjacent to the hole diameter perpendicular to the load changes sign between tensile and compressive bearing, yet the failure modes and loads exhibited are much the same for both cases. Therefore, it is concluded that the longitudinal stress did not play a major role in the bearing failures observed during the present investigation. With the elimin-

ation of this factor and the similarity of the shear fracture lines in figures 39 and 41, it is evident that the in-plane shear dominated the bearing failures for this program.

STRENGTH OF SINGLE HOLE (ROW) BOLTED JOINTS

The analyses above for tension, shearout, and bearing failures each govern a range of joint geometry which cannot be defined a priori for any given combination of material and laminate pattern until the various interactions have been established. The purpose of this section is to integrate these three analyses and to show, thereby, how to compute the strength and governing failure mode. The method applies to a single bolt or to individual bolts out of a single row. The basis of the method is the stress concentration equations (1) to (16), together with figure 17 when replotted in terms of stress concentration factors at failure of the composites.

The derivation of the equations governing the transition between tension and bearing failures is as follows. From equation (15), the joint strength for a tensile failure is given by

$$P = F_{tu}\, w\, t \left(1 - \frac{d}{w}\right) \Big/ k_{tc} \tag{18}$$

while, for a bearing failure

$$P = F_{br}\, d\, t \tag{19}$$

Now the stress concentration factor in the composite at failure is expressible with respect to either the net section or the bearing area and these factors are related, as in equation (4), by

$$k_{bc} = k_{tc} \Big/ \left(\frac{w}{d} - 1\right) \tag{20}$$

At the transition between tension and bearing failures, then,

$$P = F_{tu}\, d\, t \Big/ k_{bc} = F_{br}\, d\, t \tag{21}$$

whence

$$k_{bc} = F_{tu} \Big/ F_{br} \tag{22}$$

If, for sufficiently small values of d/w, the net-tension analysis were to predict lower stress concentration factors than given by equation (22), these lower values could not be realized because of a failure in bearing. This failure mode transition is shown in figure 42, based on experimental data, where bearing failures dominate up to some value of d/w, with tension failures for greater values of d/w. Instead of k_{bc} continuing to decrease with decreasing d/w according to a tension calculation, k_{bc} is not permitted to decrease below the value calculated using equation (22) for bearing failures. Figure 43 presents strengths for the three patterns of Thornel 300 / Narmco 5208 graphite-epoxy composite using data generated in the present investigation and for the two patterns of Morganite II / Narmco 1004 graphite-epoxy composite. All such data are recorded in the tables of this report and the specific locations are cited in the text above for each failure mode. The composite stress concentration factors at failure are computed as follows. From equation (16),

$$k_{tc} = 1 + C\ (k_{te} - 1) \tag{23}$$

and, from equation (19),

$$k_{bc} = k_{tc} \Big/ \left(\frac{w}{d} - 1\right) \tag{24}$$

while, from equations (1) and (2),

$$k_{te} = 2 + \frac{w}{d} - 1 \ - 1.5\ \Theta \left(\frac{w}{d} - 1\right) \Big/ \left(\frac{w}{d} + 1\right) \tag{25}$$

These equations enable the stress concentration factor

$$k_{bc} = f\left(\frac{d}{w},\ C,\ \frac{e}{w}\right) \tag{26}$$

to be evaluated and it is these computations which are shown in figures 42 and 43, using the values of C given by equations (10) to (13). Figures 42 and 43 apply only for $e/w \geq 1$.

Figures 44 and 45 show the relationship between joint strength and laminate width to bolt diameter ratio, for all six laminate patterns in the present investigation and the two laminate patterns for the other graphite-epoxy identified above. The experimental data are included on these plots. No tension failures were observed for the glass-graphite fiber reinforced laminates tested in this program, so the transitions between bearing and tension failures cannot

be located. All the plots in figures 44 and 45 are dimensional to permit a one-to-one comparison between bolted joint strengths of laminates containing the same total number of plies. (The format of figure 43 lends itself more to an assessment of the joint efficiency of any particular laminate by relating the joint strength to the laminate strength away from the joint). The important conclusions to be drawn from figures 44 and 45 are: (1) that such plots provide a meaningful assessment of joint strength and serve as a basis of comparison between different composite materials and fiber patterns, (2) that the maximum joint strength, for a given laminate width, is attained with a d/w ratio close to that at the transition between bearing and tension failures, (3) that the load capacity per unit width decreases rapidly for geometries far removed from the transitional configurations, (4) that the orthotropic fiber patterns permit closer bolt spacings without the risk of catastrophic tension failures than the quasi-isotropic patterns allow, and (5) that the use of glass longitudinal fibers rather than graphite appears to reduce the stress concentrations in tension at the net section through the bolt(s).

Figures 42 to 45 do not address the influence of the e/d ratio on the joint strength. Figure 46 is a qualitative generalization for a range of e/d values, of one of the lines in figure 43. The shearout failure zone lies below those for bearing and tension. It is important to note that, for some fiber pattern / material combinations, the bearing zone may disappear completely and that, for others, either the tension or shearout and cleavage zones may be forced outside the range of geometries of practical interest. Nevertheless, the general form of figure 46 would hold.

STRESS CONCENTRATION INTERACTION (MULTI-ROW) BOLTED JOINTS

The preceding sections have dealt with either single-bolt joints or with individual bolts isolated out of a single row by representing the latter as a single bolt in a strip of a width equal to the bolt pitch. In such cases, the failure can be defined uniquely in terms of the bolt load alone. In most applications, however, this is not the case because the load is frequently transferred in multi-row fastener patterns (as at a chordwise splice in a wing

skin, for example) or along a bolt seam aligned with the dominant load (as at a wing spar cap, for instance). In such more complex load situations, it is necessary to characterize both the bolt load and also the general stress field in which the particular bolt under consideration is located. The stress concentrations from each source will obviously interact and "analyses" which do not take this into account would not be meaningful. The first interaction data for bolted joints in composites appear in reference 15. The first attempt to explain such interactions analytically, and to account for them during design, is in reference 16. Additional experimental work is reported in reference 17, using essentially the same two-bolt interaction specimen as used in the present investigation. However, the laminate patterns in reference 17 are different from those used in the present investigation, so a comparison is not possible.

The interpretation (ref. 16) of the original data (ref. 15) suggested a linear interaction between tension and bearing stresses of the form

$$\sigma_{max} = k_b \sigma_b + k_t \sigma_t \leq F_{tu} \qquad (27)$$

in which F_{tu} was the basic laminate strength, σ_b the bolt bearing stress at the hole under consideration, and σ_t the net-section tension stress caused by the remainder of the load (not reacted at that bolt). The proportionality constants k_b and k_t account for both the specimen geometry and any stress concentration relief of which the material is capable. This summation may be looked upon as the sum of the contribution due to the load reacted at a bolt hole and that due to the portion of the total load running by that hole and reacted elsewhere. The data generated during the present investigation confirm the validity of equation (27) for the all-graphite laminates subject to tension loads, for which the failures were in net-section tension. For the hybrid glass-graphite laminates, the failure mode changed from tension to bearing and this requires that the interaction (27) appears to be subject to the same cut-off as defined in equation (22) for single-row bolted joints. Thus, equation (27) should be re-arranged to read

$$\sigma_b = (F_{tu} - k_t \sigma_t) / k_b \leq F_{br} \qquad (28)$$

to cover both tensile and bearing failures.

Before proceeding with the discussion of the present test results on this

topic, it is appropriate to demonstrate what can be predicted on the basis of the single-hole equations, developed above, when used in conjunction with equation (27) or (28). The expressions for k_b at a loaded bolt hole and k_t at an unloaded hole can be evaluated in terms of the elastic isotropic factors, k_{be} and k_{te} and the correlation factor C between stress concentration factors observed in composites at failure and those in truly isotropic elastic material specimens of the same geometry. Equation (16) reads

$$k_{tc} = 1 + C\ (k_{te} - 1) \tag{29}$$

in which, for a loaded hole, equation (1) reads

$$k_{te} = 2 + \left(\frac{w}{d} - 1\right) - 1.5\ \frac{(w/d - 1)}{(w/d + 1)}\ \Theta \tag{30}$$

(in which Θ is defined in equation (2) and usually has the value unity) and, for an unloaded hole, equation (8) reads

$$k_{te} = 2 + \left(1 - \frac{d}{w}\right)^3 \tag{31}$$

Now, from equation (4),

$$k_{be} = k_{te} \Big/ \left(\frac{w}{d} - 1\right) \quad \text{and} \quad k_{bc} = k_{tc} \Big/ \left(\frac{w}{d} - 1\right)$$

so that equation (26) takes on the form given by

$$k_b = \frac{1}{(w/d - 1)}\left[1 + C\left(\frac{w}{d} - 1.5\ \frac{(w/d - 1)}{(w/d + 1)}\ \Theta\right)\right] \tag{32}$$

$$k_t = 1 + C\left[1 + (1 - \frac{d}{w})^3\right] \tag{33}$$

Figure 47 illustrates some predictions using these coefficients, plotted in non-dimensional form, for several different values of d/w, for the quasi-isotropic graphite-epoxy laminates tested in this program, for which equation (10) gives C = 0.269. The value of Θ is set at unity to isolate end effects. The horizontal cut-off denotes bearing failures, while the sloping lines signify tension failures. On the basis of these predictions, one could anticipate that, for the w/d = 4 set of interaction specimens tested for this investigation, the failures would all be in tension for the single hole both loaded and unloaded as well as for the two-hole specimens. The linear equation (26) should hold

for that case. This, indeed, was observed to be so. For wider strips and the same bolt diameter, figure 47 would suggest a non-linear interaction with bearing failures for relatively light tension loads. This figure indicates that, for single loaded bolt holes, bearing failures will occur for $w/d \geq 5$. This is consistent with the present investigation of tension through-the-hole failures, in which it was seen that bearing failures occurred for $w/d \geq 6$ while tension failures occurred for $w/d \leq 4$, for the quasi-isotropic graphite epoxy. The transitional value of w/d at which bearing failures first occur, and the value of the bearing cut-off F_{br}/F_{tu} are both functions of the composite material and fiber pattern. Plots of the type of figure 47 for multi-row bolted joints could be prepared similarly from single-hole data for any composite material for which tests had established the values of C and F_{br}/F_{tu}.

The interaction test data generated during this program are recorded in tables XIV to XVII and shown in figures 48 to 59. The linear interaction for tensile loading of the all-graphite laminates is particularly clear for all three patterns (see figs. 48 to 50). The graphite-glass hybrid laminates exhibit a non-linear interaction in the manner that follows from figure 47 because, for such laminates in a joint geometry for which $w/d = 4$, the failure of single loaded holes was observed to be in bearing rather than tension. The diagrams for the all-graphite laminates, figures 48 to 50, contain also the theoretical predictions based on the single-hole data discussed above. It is evident that the agreement is good but could be improved by a higher value of k_t in equation (26). The reason for this is apparent from figures 23 and 24 which show that the mean theoretical values for k_{tc} (given by equations (10) and (11)) are significantly less than those observed experimentally for open holes. The use of an upper bound estimate for k_{tc} instead of a linear mean value constrained to pass through the points (1,1) in figures 23 and 24 would permit an improvement in predicting the test data in figures 48 to 50. The corresponding lines in figures 51 to 53 permit the use of equations (26) to (33) in reverse to compute values of C in equation (29) for the graphite/glass hybrid laminates. The values so computed are as follows:

Pattern 4: $C = 0.51$, Pattern 5: $C = 0.48$, Pattern 6: $C = 0.61$ (34)

The actual computation of these values was performed as follows, using the two-

row loaded hole data. For w/d = 4, equation (31) gives $k_{te} = 2.42$ for an open hole, while equation (30) gives $k_{te} = 4.10$ for a loaded hole. Since the failures were in tension and each bolt accepts an equal load, the failure condition can be expressed in the form

$$F_{tu} = (1 + 3.10C)\left(\frac{d}{w - d}\right)\sigma_{br} + (1 + 1.42C)\sigma_t \qquad (35)$$

from which C can be determined. (The quantity σ_{br} d / (w - d) is equal to the net-section tension stress at the bolt hole, due to the bearing load).

A point of special significance about the tension/bearing interaction test results is that, for the all-graphite laminates tested, the use of two bolts in series did not increase the load carried much above that which a single bolt alone would be expected to have carried in a laminate of that thickness (twice that on which the single-bolt tests were performed). That this should be so can be deduced from figures 48 to 50, regardless of the relative proportion of bearing and tension loads, provided that the linear interaction for tension failures applies. For the quasi-isotropic pattern, with w/d = 4, the tension load capacity of the net section is practically identical with the bearing load capacity on a single bolt. Therefore, any ratio of loads shared between bearing and tension in a multi-row joint of that w/d ratio made from that composite material and laminate must inevitably be associated with essentially the same total load capacity per unit laminate thickness. The orthotropic patterns 2 and 3 carry slightly more load in net tension for w/d = 4 than in bearing, so the mult-row bolted joints would be slightly stronger than a single-row for those materials, fiber pattern and geometry combinations. Figure 47 suggests that, even for other w/d ratios, provided that the failures are by tension at the net section, the use of multi-row bolted joints offers no significant strength increase over a single-row joint of the same material and geometry. Only in that regime of joint geometries as is associated with bearing failures for single-row bolted joints is there to be found any major increase in joint strength by the use of multi-row bolt patterns. Furthermore, even in such cases, it appears that still higher strengths could be attained by a single row of bolts closer together. However, this latter approach would mean accepting potentially catastrophic tension failures in conjunction with such higher loads. The analysis methods developed in this section permit a rational investigation

of alternative joint design configurations without an extensive test program. These methods can establish whether or not a candidate design is either suitable or optimum for a given requirement and can minimize the amount of any testing necessary.

The interaction between compression and bearing in mult-row bolted joints depends on a fundamentally different mechanism than that discussed above for tensile loading. In the case of the compression of a laminate containing an unfilled hole, there is a stress concentration just as with tensile loading of the same specimen. When the hole is filled with a net-fit bolt, however, the picture is changed completely. The compression load need no longer be diverted around the hole; it can be transmitted straight across by bearing on both sides of the bolt. In this situation, the superposition of laminate compression to compressive bearing is simply additive with respect to bearing stress. Thus,

$$\sigma_b + \sigma_c \leq F_{br} \tag{36}$$

The test data in figures 54 to 56 for compressive loading of the all-graphite laminates support this superposition for filled holes. The corresponding test data in figures 57 to 59 for the graphite/glass hybrid laminates are influenced by buckling, inasmuch as the drop off in bearing capacity is greater than equation (36) would predict. Figures 54 to 59 contain also a probable vertical cut-off line for loose fit bolts which are sufficiently sloppy to prevent the reaction of the compressive laminate stress by bearing on the bolt and cause the diversion of the load around the hole. Open-hole compression tests were not run in this program, so these cut-offs have been estimated in terms of calculated laminate strengths in compression and stress concentration factors deduced for tensile loading of laminates containing open holes.

DIFFERENCES BETWEEN PROTRUDING HEAD FASTENERS AND PIN CONNECTIONS

Figure 60 shows the data, recorded in table XVIII, for pin-loaded holes and the comparison with the higher strengths exhibited by regular hexagon-head bolts with nuts. These tests were performed for the quasi-isotropic pattern 1 in the all-graphite material and showed a nearly two-to-one increase in strength between pins and bolts. The difference in test technique between the two sets

of test results in figure 60 is that, in the case of the pin tests, the nuts were not in contact with the clevis plates. Otherwise, the test setup is like that shown in figure 1.

The explanation offered here to explain the differences in figure 60 is as follows. The basis of the greater strength for protruding head fasteners with respect to pin connections (which can develop no tensile load) is the appreciable differences between the initial and ultimate failures of bolted joints in composite laminates, particularly if the initially damaged area is constrained so that the broken material cannot be displaced. Figure 61 is a photo of relatively modest damage sustained at bolt holes without any reduction in load capacity during an earlier previously unreported test by the contractor on Modmor II / Narmco 1004 graphite epoxy. In this specimen, the bolt was dragged about three diameters by the load. The broken composite material re remained constrained by the bolt, the steel clevis plates and the as yet undamaged composite. Since there was nowhere to which the damaged composite material could be displaced, and the mode of failure for that and many other fiber patterns is of a local nature, the bolt maintained its load and would continue to do so as long as the load direction was not reversed.

COMPARISON BETWEEN SINGLE-LAP AND DOUBLE-LAP JOINTS

Despite the care taken to eliminate or minimize the effects of bending and eccentricity by the special fixture in figure 6, figure 62 shows how the test results from the present investigation, recorded in table XIX, still show about a twently percent drop with respect to double-shear strengths. Therefore, due account should be taken of the differences between single- and double-shear bolted joints in the analysis of practical areospace structures.

CONCLUDING REMARKS

The following conclusions were made from this investigation.

The fiber patterns tested were well chosen and their performance is representative of other patterns containing similar percentages in each of the $(0, \pm\pi/4, \pi/2)$ directions because the three patterns tested lie on what can be

thought of as a strength plateau. The choice of fiber pattern in the joint area, for any given application, is influenced by the laminate outside the joint area and the desired mode of failure at the joint.

The multi-test (multiple-hole) test specimens were found to offer significant economy in specimen fabrication costs, when evaluated on a per test basis, without causing any interaction between the individual test results and without adding unduly to the complexity of the tests.

The use of glass fibers was beneficial in nearly every case. The exception was that, because of a lower modulus for the glass fibers with respect to the graphite fibers, the stabilization of compressively loaded joint specimens was a problem. Those specimens containing longitudinal glass fibers which were loaded in tension were consistently as strong or stronger than the equivalent all-graphite specimens. The glass/graphite hybrids were almost exclusively associated with local bearing failures rather than the potentially catastrophic tension-through-the-hole failures which prevailed for many of the all-graphite specimens.

The materials behaved in a predictable manner inasmuch as the empirical analysis methods devéloped from single-hole data were shown to be consistent with the observations on two-row bolted joint tests. The key to the analysis method is the analysis for tension failures, to which an experimentally derived cut-off for bearing failures is applied to prevent misapplication of the tension analysis to joint geometries for which it does not hold. Elastic isotropic stress concentration factors are computed for any given joint geometry by new equations presented in this report. The corresponding stress concentration factor to be anticipated in the composite at failure is then computed from the elastic isotropic value and an experimentally derived correlation factor for that particular composite material. The experimental testing need not include the geometry being analyzed so these methods serve to generalize existing test data beyond those specific geometries already tested.

The testing on two-row bolted joints is representative of multi-row bolted joints. The key result is that, for those joint geometries producing tension failures for a single bolt, the addition of further rows of bolts will generally increase the joint strength very little. Only when bearing failures

occur do multi-row bolt patterns increase the joint strength significantly above the strength of a single bolt row. From the present testing, the orthotropic patterns are slightly superior to the quasi-isotropic pattern and those laminates containing the longitudinal glass fibers were distinctly superior to the all-graphite laminates with regard to their suitability for multi-row bolt patterns. The transition between tension and bearing failures occurs in the range of a strip width (or bolt pitch) of between four and six diameters for the all-graphite laminates but at a width less than three diameters for the glass/graphite hybrid laminates. Since the bearing strengths for all laminates tested were similar, it would be possible to use more bolts per unit width in laminates having longitudinal glass plies, thereby making stronger joints.

In most cases, the maximum obtainable bolted joint strength for a given width of composite laminate is associated with a w/d ratio slightly less than those for which bearing failures occur. In some of the orthotropic pattern cases, the maximum strength is developed when the w/d ratio is at the transition between bearing and tension failures.

Neither perfectly elastic nor fully-plastic theories are capable of explaining the test results. The strength loss in the best designed single-row bolted joints, with respect to the basic laminate strength, is of the order of a factor of two or slightly higher.

The highest possible joint strengths for graphite-epoxy composites have been found not to exceed about forty to fifty percent of the basic laminate strength, even for the ideal combination of joint dimensions. The d/w ratio dominates the joint strength (with the e/w ratio having only a minor effect) and the maximum joint strengths are developed only throughout a small range of d/w values (typically from about 0.25 to 0.4). The strongest joints are associated with the joint geometry at the transition between bearing and tension failures or with a tension failure for slightly greater d/w values.

There were no significant differences between the performance of bolt holes drilled with carbide tipped drills or ultrasonically excited diamond core drills. The latter holes were visibly cleaner, however.

Joints with regular bolts having protruding heads are about twice as

strong as those loaded only by a simple pin for those cases in which the failure mode is bearing. The mechanism of this strength gain appears to be one of damage confinement rather than additional load transfer through friction.

The significance of the findings of the present investigation are twofold. This is the first systematic test program encompassing a wider range of joint geometries than have been investigated before in programs more closely tied to specific composite hardware. Therefore the basic governing phenomena have been explored more thoroughly. Second, the empirical analysis methods developed provide a capability for the rational analysis and design of bolted joints in graphite-epoxy composites.

Further tests are recommended in three areas. The first is that of larger bolt diameters because of differentes observed in other programs between joint strengths and stress concentrations at different size holes. The second is the testing of mult-row bolted joints in strips sufficiently wide to enforce bearing failures rather than the tension failures which occurred during the present program, in order to confirm the validity of the present theoretical projections in this area and to thereby assist in the oprimization of joint proportions. The third series of tests should account for environmental effects such as reduced and elevated temperatures because the matrix resin properties are sensitive to environmental effects.

REFERENCES

1. Mechtly, E. A.: The International System of Units — Physical Constants and Conversion Factors. NASA SP-7012, 1973.

2. Frocht, M. M. and Hill, H. N.: Stress Concentration Factors Around a Central Circular Hole in a Plate Loaded Through Pin in the Hole. Journal of Applied Mechanics, Volume 7, pp. A5-A9, March 1940.

3. Bickley, W. G.: The Distribution of Stress Round a Circular Hole in a Plate. Philosophical Transactions of the Royal Society (London), Series A, Volume 227, pp. 383-415, 1928.

4. Knight, R. C.: Action of a Rivet in a Plate of Finite Breadth. Philosophical Magazine, Series 7, Volume 19, pp. 517-540, March 1935.

5. Koiter, W. T.: An Elementary Solution of Two Stress Concentration Problems in the Neighbourhood of a Hole. Journal of Applied Mathematics, Volume XV, Number 3, pp. 303-308, 1957.

6. Timoshenko, S. and Goodier, J. N.: Theory of Elasticity. Second edition, McGraw-Hill Book Co., Inc., p. 80, 1951.

7. Wahl, A. M. and Beeuwkes, R.: Stress Concentration Produced by Holes and Notches. American Society of Mechanical Engineers Transactions, Volume 56, pp. 617-636, 1934.

8. Seely, F. B. and Smith, J. O.: Advanced Mechanics of Materials. Second edition. John Wiley & Sons, Inc., p. 394, 1952.

9. Anon.: Advanced Composites Design Guide. North American Rockwell, USAF Contract Report, Third edition, January 1973.

10. Thompson, C. E. and Hart-Smith, L. J.: Composite Material Structures — Joints. Douglas Aircraft Company, Technical Report MDC-J0638, July 1971.

11. Lehman, G. M.: Development of a Graphite Horizontal Stabilizer. Douglas Aircraft Company, NADC Contract Report MDC-J0945, December 1970.

12. Lehman, G. M.: Development of a Graphite Horizontal Stabilizer. Douglas Aircraft Company, NADC Contract Report MDC-J1435, June 1970.

13. Nelson, W. D.: Composite Wing Conceptual Design. Douglas Aircraft Company,

USAF Contract Report MDC-J4110, November 1971.

14. Nelson, W. D.: Composite Wing Conceptual Design. Douglas Aircraft Company, USAF Contract Report MDC-J4140, August 1971.

15. Leonhardt, J. L., Shockey, P. D. and Studer, V. J.: Advanced Development of Boron Composite Wing Structural Components. Convair / General Dynamics, USAF Contract Report AFML-TR-70-261, December 1970.

16. Nelson, W. D.: Composite Wing Conceptual Design. Douglas Aircraft Company, USAF Contract Report MDC-J4129, May 1971.

17. Fant, J. A., Olson, F. O. and Roberts, R. H.: Advanced Composite Technology Fuselage Program. Convair / General Dynamics, USAF Contract Report AFML-TR-71-41, Volume VI, October 1973.

TABLE I

LAMINATE PATTERNS AND LAYUP SEQUENCES

LAMINATE PATTERN NUMBER	MATERIAL	PLY PERCENTAGES		
		0 (0°)	$\pm\pi/4$ ($\pm 45°$)	$\pi/2$ (90°)
1	GRAPHITE-EPOXY (QUASI-ISOTROPIC)	25	50	25
2	GRAPHITE-EPOXY	37.5	37.5	25
3	GRAPHITE-EPOXY	37.5	50	12.5
4	GRAPHITE-GLASS-EPOXY	25*	50	25
5	GRAPHITE-GLASS-EPOXY	37.5*	37.5	25
6	GRAPHITE-GLASS-EPOXY	37.5*	50	12.5

* GLASS FIBERS — ALL OTHERS GRAPHITE

LAMINATE PATTERN NUMBER	LAYUP SEQUENCE FOR 16-PLY LAMINATE	LAYUP SEQUENCE FOR 32-PLY LAMINATE
1 , 4	$[(0/\frac{\pi}{4}/\frac{\pi}{2}/-\frac{\pi}{4})_2]_s$	$[(0/\frac{\pi}{4}/\frac{\pi}{2}/-\frac{\pi}{4})_4]_s$
2 , 5	$(0/\frac{\pi}{4}/\frac{\pi}{2}/0/-\frac{\pi}{4}/\frac{\pi}{2}/0/\frac{\pi}{4}/-\frac{\pi}{4}/0/\frac{\pi}{2}/-\frac{\pi}{4}/0/\frac{\pi}{2}/\frac{\pi}{4}/0)$	$(0/\frac{\pi}{4}/\frac{\pi}{2}/0/-\frac{\pi}{4}/\frac{\pi}{2}/0/\frac{\pi}{4}/-\frac{\pi}{4}/0/\frac{\pi}{2}/-\frac{\pi}{4}/0/\frac{\pi}{2}/\frac{\pi}{4}/0)_s$
3 , 6	$(0/\frac{\pi}{4}/0/-\frac{\pi}{4}/\frac{\pi}{2}/\frac{\pi}{4}/0/-\frac{\pi}{4})_s$	$[(0/\frac{\pi}{4}/0/-\frac{\pi}{4}/\frac{\pi}{2}/\frac{\pi}{4}/0/-\frac{\pi}{4})_2]_s$

TABLE IIA

TENSION THROUGH-THE-HOLE SPECIMENS

ALL GRAPHITE FIBERS, EPOXY RESIN
FIBER PATTERN - 25 PCT 0, 50 PCT ±π/4, 25 PCT π/2

SI UNITS

SPECIMEN ID	HOLE ID	HOLE DIAM MM	BOLT DIAM MM	PANEL WIDTH MM	EDGE DIST. MM	PANEL THICK. MM	FAILURE LOAD KNEWTON	FAILURE MODE	BEARING STRENGTH MPASCAL	TENSION STRENGTH MPASCAL	SHEAROUT STRENGTH MPASCAL
THS-1-1	A	6.477	6.340	38.19	19.25	2.294	9.2968	BRG	639.3	127.8	126.6
THS-1-1	B	6.454	6.340	38.17	38.41	2.304	14.3233	BRG	980.7	196.0	88.4
THS-1-1	C	6.457	6.340	38.17	38.45	2.456	14.5679	BRG	935.5	187.0	84.2
THS-1-1	D	6.358	6.340	38.22	18.89	2.494	12.0324	BRG	760.9	151.4	153.5
THS-1-2	A	6.350	6.340	38.35	19.00	2.332	11.6543	BRG	788.4	156.2	157.9
THS-1-2	B	6.464	6.340	38.29	38.41	2.349	13.9007	BRG	933.2	185.9	84.1
THS-1-2	C	6.449	6.340	38.32	38.40	2.306	13.2112	BRG	903.5	179.8	81.4
THS-1-2	D	6.530	6.340	38.35	19.19	2.304	11.1206	BRG	761.4	151.7	151.5
THS-1-3	A	6.413	6.325	25.50	12.55	2.207	9.7861	TENS	701.0	232.3	237.3
THS-1-3	B'	6.337	6.337	25.43	19.43	2.235	10.9426	TENS	772.5	256.4	150.6
THS-1-3	B	6.403	6.340	25.47	25.52	2.222	11.4542	TENS	812.9	270.4	115.4
THS-1-3	C	6.375	6.340	25.24	25.50	2.268	11.3652	TENS	790.3	265.6	112.3
THS-1-3	C'	6.378	6.337	25.22	19.54	2.278	11.4319	TENS	791.8	266.2	153.4
THS-1-3	D	6.424	6.325	25.26	12.57	2.261	9.8973	TENS	692.2	232.5	234.0
THS-1-4	A	6.403	6.325	25.58	12.53	2.342	10.3866	TENS	701.3	231.3	237.7
THS-1-4	B'	6.312	6.337	25.54	19.72	2.360	11.7211	TENS	783.8	258.3	150.0
THS-1-4	B	6.406	6.340	25.56	25.55	2.352	11.5876	TENS	777.1	257.2	110.2
THS-1-4	C	6.375	6.340	25.52	25.55	2.276	11.4764	TENS	795.4	263.3	112.7
THS-1-4	C'	6.149	6.337	25.52	19.36	2.283	11.7656	TENS	813.0	265.9	158.2
THS-1-4	D	6.398	6.325	25.52	12.60	2.268	9.5637	TENS	666.7	220.5	224.2
THS-1-5	A	6.360	6.325	19.12	12.47	2.339	7.5397	TENS	509.6	252.7	173.4
THS-1-5	B'	6.246	6.337	19.12	19.69	2.314	8.1803	TENS	557.8	274.5	106.7
THS-1-5	B	6.431	6.314	19.12	25.55	2.327	8.3627	TENS	569.2	283.2	80.4
THS-1-5	C	6.406	6.314	19.20	25.55	2.296	8.9632	TENS	618.2	305.0	87.3
THS-1-5	C'	6.223	6.337	19.14	19.75	2.311	8.5851	TENS	586.1	287.5	111.6
THS-1-5	D	6.360	6.325	19.26	12.46	2.281	8.6296	TENS	598.2	293.2	203.9
THS-1-6	A	6.350	6.325	19.31	12.45	2.271	8.4294	TENS	586.9	286.5	200.2
THS-1-6	B'	6.429	6.337	19.30	19.90	2.327	8.6740	TENS	588.3	289.7	111.7
THS-1-6	B	6.398	6.340	19.30	25.54	2.299	8.8964	TENS	610.5	299.9	86.6
THS-1-6	C	6.403	6.340	19.34	25.54	2.309	8.9632	TENS	612.3	300.0	86.9
THS-1-6	C'	6.350	6.337	19.32	19.86	2.322	8.5851	TENS	583.5	285.1	110.8
THS-1-6	D	6.360	6.325	19.37	12.45	2.306	9.1856	TENS	629.7	306.2	214.7

TABLE IIB

TENSION THROUGH-THE-HOLE SPECIMENS

ALL GRAPHITE FIBERS, EPOXY RESIN
FIBER PATTERN - 25 PCT 0 DEG., 50 PCT ±45 DEG., 25 PCT 90 DEG.

US CUSTOMARY UNITS

SPECIMEN ID	HOLE ID	HOLE DIAM IN.	BOLT DIAM IN.	PANEL WIDTH IN.	EDGE DIST. IN.	PANEL THICK. IN.	FAILURE LOAD LB	FAILURE MODE	BEARING STRENGTH KSI	TENSION STRENGTH KSI	SHEAROUT STRENGTH KSI
THS-1-1	A	.2550	.2496	1.504	.758	.0903	2090.0	BRG	92.7	18.5	18.4
THS-1-1	B	.2541	.2496	1.503	1.512	.0907	3220.0	BRG	142.2	28.4	12.8
THS-1-1	C	.2542	.2496	1.503	1.514	.0967	3275.0	BRG	135.7	27.1	12.2
THS-1-1	D	.2503	.2496	1.505	.744	.0982	2705.0	BRG	110.4	22.0	22.3
THS-1-2	A	.2500	.2496	1.510	.748	.0918	2620.0	BRG	114.3	22.7	22.9
THS-1-2	B	.2545	.2496	1.507	1.512	.0925	3125.0	BRG	135.4	27.0	12.2
THS-1-2	C	.2539	.2496	1.509	1.512	.0908	2970.0	BRG	131.0	26.1	11.8
THS-1-2	D	.2571	.2496	1.510	.756	.0907	2500.0	BRG	110.4	22.0	22.0
THS-1-3	A	.2525	.2490	1.004	.494	.0869	2200.0	TENS	101.7	33.7	34.4
THS-1-3	B'	.2495	.2495	1.001	.765	.0880	2460.0	TENS	112.0	37.2	21.8
THS-1-3	B	.2521	.2496	1.003	1.005	.0875	2575.0	TENS	117.9	39.2	16.7
THS-1-3	C	.2510	.2496	.994	1.004	.0893	2555.0	TENS	114.6	38.5	16.3
THS-1-3	C'	.2511	.2495	.993	.769	.0897	2570.0	TENS	114.8	38.6	22.3
THS-1-3	D	.2529	.2490	.994	.495	.0890	2225.0	TENS	100.4	33.7	33.9
THS-1-4	A	.2521	.2490	1.007	.493	.0922	2335.0	TENS	101.7	33.5	34.5
THS-1-4	B'	.2485	.2495	1.005	.776	.0929	2635.0	TENS	113.7	37.5	21.8
THS-1-4	B	.2522	.2496	1.006	1.006	.0926	2605.0	TENS	112.7	37.3	16.0
THS-1-4	C	.2510	.2496	1.005	1.006	.0896	2580.0	TENS	115.4	38.2	16.4
THS-1-4	C'	.2421	.2495	1.005	.762	.0899	2645.0	TENS	117.9	38.6	22.9
THS-1-4	D	.2519	.2490	1.005	.496	.0893	2150.0	TENS	96.7	32.0	32.5
THS-1-5	A	.2504	.2490	.753	.491	.0921	1695.0	TENS	73.9	36.6	25.1
THS-1-5	B'	.2459	.2495	.753	.775	.0911	1839.0	TENS	80.9	39.8	15.5
THS-1-5	B	.2532	.2486	.753	1.006	.0916	1880.0	TENS	82.6	41.1	11.7
THS-1-5	C	.2522	.2486	.756	1.006	.0904	2015.0	TENS	89.7	44.2	12.7
THS-1-5	C'	.2450	.2495	.754	.777	.0910	1930.0	TENS	85.0	41.7	16.2
THS-1-5	D	.2504	.2490	.758	.490	.0898	1940.0	TENS	86.8	42.5	29.6
THS-1-6	A	.2509	.2490	.760	.490	.0894	1895.0	TENS	85.1	41.5	29.0
THS-1-6	B'	.2531	.2495	.760	.784	.0916	1950.0	TENS	85.3	42.0	16.2
THS-1-6	B	.2519	.2496	.760	1.005	.0905	2000.0	TENS	88.5	43.5	12.6
THS-1-6	C	.2521	.2496	.762	1.005	.0909	2015.0	TENS	88.8	43.5	12.6
THS-1-6	C'	.2500	.2495	.761	.782	.0914	1930.0	TENS	84.6	41.4	16.1
THS-1-6	D	.2504	.2490	.762	.490	.0908	2065.0	TENS	91.3	44.4	31.1

TABLE IIIA

TENSION THROUGH-THE-HOLE SPECIMENS

ALL GRAPHITE FIBERS, EPOXY RESIN
FIBER PATTERN - 37.5 PCT 0, 37.5 PCT ±π/4, 25 PCT π/2

SI UNITS

SPECIMEN ID	HOLE ID	HOLE DIAM MM	BOLT DIAM MM	PANEL WIDTH MM	EDGE DIST. MM	PANEL THICK. MM	FAILURE LOAD KNEWTON	FAILURE MODE	BEARING STRENGTH MPASCAL	TENSION STRENGTH MPASCAL	SHEAROUT STRENGTH MPASCAL
THS-2-1	A	6.426	6.340	38.19	19.21	2.311	11.0538	BRG	754.3	150.6	149.5
THS-2-1	B	6.452	6.340	38.17	38.42	2.228	14.4567	BRG	1023.7	204.6	92.2
THS-2-1	C	6.452	6.340	38.17	38.46	2.240	14.5457	BRG	1024.1	204.7	92.1
THS-2-1	D	6.490	6.340	38.22	19.20	2.304	10.9426	BRG	749.2	149.7	148.9
THS-2-2	A	6.350	6.340	38.35	19.44	2.482	11.4764	BRG	729.5	144.5	142.2
THS-2-2	B	6.452	6.340	38.29	38.40	2.494	13.5226	BRG	855.1	170.3	77.1
THS-2-2	C	6.474	6.340	38.32	38.47	2.489	15.2129	BRG	964.0	191.9	86.7
THS-2-2	D	6.426	6.340	38.35	19.17	2.464	9.4302	BRG	603.7	119.9	119.9
THS-2-3	A	6.421	6.325	25.44	12.64	2.327	9.4080	TENS	639.3	212.6	214.4
THS-2-3	B'	6.325	6.337	25.38	19.48	2.352	12.1659	TENS	816.2	271.4	158.5
THS-2-3	B	6.383	6.340	25.41	25.51	2.339	12.3438	TENS	832.3	277.3	118.2
THS-2-3	C	6.378	6.340	25.50	25.49	2.337	13.3447	TENS	900.8	298.6	128.0
THS-2-3	C'	6.370	6.337	25.46	19.70	2.372	12.9221	TENS	859.5	285.3	165.0
THS-2-3	D	6.406	6.325	25.57	12.56	2.299	9.6749	TENS	665.5	219.7	225.0
THS-2-4	A	6.413	6.325	25.54	12.55	2.322	9.7861	TENS	666.5	220.4	225.6
THS-2-4	B'	6.276	6.337	25.46	19.31	2.357	12.3216	TENS	824.9	272.5	161.7
THS-2-4	B	6.401	6.340	25.48	25.58	2.357	12.4995	TENS	836.4	277.9	118.5
THS-2-4	C	6.413	6.340	25.50	25.55	2.339	12.4550	TENS	839.8	279.0	119.1
THS-2-4	C'	6.337	6.337	25.46	19.55	2.332	12.2771	TENS	830.8	275.4	160.7
THS-2-4	D	6.421	6.325	25.50	12.55	2.383	10.3644	TENS	687.8	228.0	232.8
THS-2-5	A	6.347	6.325	19.36	12.47	2.306	9.8306	TENS	673.9	327.4	229.2
THS-2-5	B'	6.345	6.337	19.31	19.76	2.370	9.7861	TENS	651.6	318.6	124.5
THS-2-5	B	6.401	6.340	19.34	25.53	2.339	10.2532	TENS	691.3	338.8	98.2
THS-2-5	C	6.452	6.340	19.25	25.57	2.337	9.6304	TENS	650.0	322.1	92.2
THS-2-5	C'	6.302	6.337	19.23	19.32	2.286	9.5192	TENS	657.1	322.0	128.7
THS-2-5	D	6.314	6.325	19.26	12.45	2.388	9.3858	TENS	621.5	303.7	211.4
THS-2-6	A	6.350	6.325	19.25	12.47	2.334	9.0077	TENS	610.1	299.2	207.6
THS-2-6	B'	6.269	6.337	19.22	19.72	2.349	9.5637	TENS	642.3	314.4	122.7
THS-2-6	B	6.408	6.340	19.23	25.55	2.342	9.3190	TENS	627.7	310.3	89.0
THS-2-6	C	6.431	6.340	19.27	25.57	2.349	9.8973	TENS	664.5	328.1	94.2
THS-2-6	C'	6.373	6.337	19.24	19.85	2.357	10.0752	TENS	674.5	332.2	128.3
THS-2-6	D	6.378	6.325	19.30	12.48	2.339	9.1189	TENS	616.3	301.7	209.7

TABLE IIIB

TENSION THROUGH-THE-HOLE SPECIMENS

ALL GRAPHITE FIBERS, EPOXY RESIN
FIBER PATTERN - 37.5 PCT 0 DEG., 37.5 PCT ±45 DEG., 25 PCT 90 DEG.

US CUSTOMARY UNITS

SPECIMEN ID	HOLE ID	HOLE DIAM IN.	BOLT DIAM IN.	PANEL WIDTH IN.	EDGE DIST. IN.	PANEL THICK. IN.	FAILURE LOAD LB	FAILURE MODE	BEARING STRENGTH KSI	TENSION STRENGTH KSI	SHEAROUT STRENGTH KSI
THS-2-1	A	.2530	.2496	1.504	.756	.0910	2485.0	BRG	109.4	21.8	21.7
THS-2-1	B	.2540	.2496	1.503	1.513	.0877	3250.0	BRG	148.5	29.7	13.4
THS-2-1	C	.2540	.2496	1.503	1.514	.0882	3270.0	BRG	148.5	29.7	13.4
THS-2-1	D	.2555	.2496	1.505	.756	.0907	2460.0	BRG	108.7	21.7	21.6
THS-2-2	A	.2500	.2496	1.510	.765	.0977	2580.0	BRG	105.8	21.0	20.6
THS-2-2	B	.2540	.2496	1.507	1.512	.0982	3040.0	BRG	124.0	24.7	11.2
THS-2-2	C	.2549	.2496	1.509	1.515	.0980	3420.0	BRG	139.8	27.8	12.6
THS-2-2	D	.2530	.2496	1.510	.755	.0970	2120.0	BRG	87.6	17.4	17.4
THS-2-3	A	.2528	.2490	1.002	.498	.0916	2115.0	TENS	92.7	30.8	31.1
THS-2-3	B'	.2490	.2495	.999	.767	.0926	2735.0	TENS	118.4	39.4	23.0
THS-2-3	B	.2513	.2496	1.000	1.004	.0921	2775.0	TENS	120.7	40.2	17.1
THS-2-3	C	.2511	.2496	1.004	1.003	.0920	3000.0	TENS	130.6	43.3	18.6
THS-2-3	C'	.2508	.2495	1.002	.775	.0934	2905.0	TENS	124.7	41.4	23.9
THS-2-3	D	.2522	.2490	1.007	.494	.0905	2175.0	TENS	96.5	31.9	32.6
THS-2-4	A	.2525	.2490	1.005	.494	.0914	2200.0	TENS	96.7	32.0	32.7
THS-2-4	B'	.2471	.2495	1.002	.760	.0928	2770.0	TENS	119.6	39.5	23.4
THS-2-4	B	.2520	.2496	1.003	1.007	.0928	2810.0	TENS	121.3	40.3	17.2
THS-2-4	C	.2525	.2496	1.004	1.006	.0921	2800.0	TENS	121.8	40.5	17.3
THS-2-4	C'	.2495	.2495	1.002	.770	.0918	2760.0	TENS	120.5	39.9	23.3
THS-2-4	D	.2528	.2490	1.004	.494	.0938	2330.0	TENS	99.8	33.1	33.8
THS-2-5	A	.2499	.2490	.762	.491	.0908	2210.0	TENS	97.7	47.5	33.2
THS-2-5	B'	.2498	.2495	.760	.778	.0933	2200.0	TENS	94.5	46.2	18.1
THS-2-5	B	.2520	.2496	.761	1.005	.0921	2305.0	TENS	100.3	49.1	14.2
THS-2-5	C	.2540	.2496	.758	1.007	.0920	2165.0	TENS	94.3	46.7	13.4
THS-2-5	C'	.2481	.2495	.757	.761	.0900	2140.0	TENS	95.3	46.7	18.7
THS-2-5	D	.2486	.2490	.758	.490	.0940	2110.0	TENS	90.1	44.0	30.7
THS-2-6	A	.2500	.2490	.758	.491	.0919	2025.0	TENS	88.5	43.4	30.1
THS-2-6	B'	.2468	.2495	.757	.776	.0925	2150.0	TENS	93.2	45.6	17.8
THS-2-6	B	.2523	.2496	.757	1.006	.0922	2095.0	TENS	91.0	45.0	12.9
THS-2-6	C	.2532	.2496	.759	1.007	.0925	2225.0	TENS	96.4	47.6	13.7
THS-2-6	C'	.2509	.2495	.757	.781	.0928	2265.0	TENS	97.8	48.2	18.6
THS-2-6	D	.2511	.2490	.760	.491	.0921	2050.0	TENS	89.4	43.8	30.4

TABLE IVA

TENSION THROUGH-THE-HOLE SPECIMENS

ALL GRAPHITE FIBERS, EPOXY RESIN
FIBER PATTERN - 37.5 PCT 0, 50 PCT ±π/4, 12.5 PCT π/2

SI UNITS

SPECIMEN ID	HOLE ID	HOLE DIAM MM	BOLT DIAM MM	PANEL WIDTH MM	EDGE DIST. MM	PANEL THICK. MM	FAILURE LOAD KNEWTON	FAILURE MODE	BEARING STRENGTH MPASCAL	TENSION STRENGTH MPASCAL	SHEAROUT STRENGTH MPASCAL
THS-3-1	A	6.383	6.340	37.92	19.04	2.314	11.6543	BRG	794.4	159.7	158.9
THS-3-1	B	6.452	6.340	37.88	38.43	2.327	13.9674	BRG	946.9	191.0	85.3
THS-3-1	C	6.467	6.340	37.68	38.46	2.215	13.3447	BRG	950.3	193.0	85.5
THS-3-1	D	6.477	6.340	37.79	19.11	2.200	12.5662	BRG	901.1	182.4	180.0
THS-3-2	A	6.358	6.340	37.94	19.20	2.337	12.5440	BRG	846.7	170.0	167.5
THS-3-2	B	6.474	6.340	37.49	38.47	2.253	13.1890	BRG	923.4	188.7	83.1
THS-3-2	C	6.447	6.340	38.08	38.41	2.337	14.1676	BRG	956.3	191.6	86.1
THS-3-2	D	6.441	6.340	39.00	19.18	2.281	11.4097	BRG	789.0	153.7	156.7
THS-3-3	A	6.408	6.325	25.49	12.57	2.344	10.4533	TENS	705.0	233.7	238.0
THS-3-3	B'	6.350	6.337	25.26	19.43	2.357	11.9880	BRG	802.5	269.0	156.4
THS-3-3	B	6.401	6.340	25.37	25.51	2.352	13.1223	BRG	880.0	294.1	125.0
THS-3-3	C	6.401	6.340	25.42	25.55	2.327	12.9888	BRG	880.6	293.5	124.9
THS-3-3	C'	6.325	6.337	25.31	19.55	2.306	13.4114	TENS	917.6	306.3	177.5
THS-3-3	D	6.431	6.325	25.53	12.56	2.349	10.7425	TENS	722.9	239.3	244.6
THS-3-4	A	6.408	6.325	25.55	12.50	2.383	10.8092	TENS	717.3	237.0	243.9
THS-3-4	B'	6.370	6.337	25.49	19.42	2.380	11.4097	BRG	756.5	250.7	147.6
THS-3-4	B	6.375	6.340	25.52	25.63	2.383	13.2112	BRG	874.6	289.6	123.6
THS-3-4	C	6.370	6.340	25.44	25.58	2.339	14.8571	BRG	1001.8	333.0	141.8
THS-3-4	C'	6.380	6.337	25.41	19.62	2.360	12.0769	BRG	807.6	269.0	155.7
THS-3-4	D	6.393	6.325	25.47	12.58	2.319	10.3644	TENS	706.6	234.3	238.3
THS-3-5	A	6.368	6.325	19.33	12.43	2.324	9.2301	TENS	627.9	306.4	214.7
THS-3-5	B'	6.236	6.337	19.37	19.72	2.360	10.4533	TENS	699.0	337.2	133.4
THS-3-5	B	6.413	6.340	19.35	25.57	2.342	10.6757	TENS	719.0	352.3	101.9
THS-3-5	C	6.424	6.340	19.23	25.59	2.362	10.4088	TENS	695.0	344.1	98.5
THS-3-5	C'	6.299	6.337	19.15	19.77	2.327	11.5876	TENS	785.9	387.6	149.8
THS-3-5	D	6.375	6.325	19.30	12.43	2.395	9.8083	TENS	647.5	316.7	221.6
THS-3-6	A	6.368	6.325	19.10	12.51	2.385	9.9195	TENS	657.6	326.6	223.1
THS-3-6	B'	6.454	6.337	19.28	19.77	2.344	11.2540	TENS	757.5	374.2	145.1
THS-3-6	B	6.424	6.340	19.19	25.59	2.365	10.5423	TENS	703.2	349.1	99.6
THS-3-6	C	6.413	6.340	19.27	25.57	2.327	11.5654	TENS	784.1	386.7	111.1
THS-3-6	C'	6.401	6.337	19.25	19.76	2.339	10.9871	TENS	741.1	365.5	141.8
THS-3-6	D	6.358	6.325	19.29	12.50	2.314	10.4311	TENS	712.8	348.7	241.8

TABLE IV8

TENSION THROUGH-THE-HOLE SPECIMENS

ALL GRAPHITE FIBERS, EPOXY RESIN
FIBER PATTERN - 37.5 PCT 0 DEG., 50 PCT ±45 DEG., 12.5 PCT 90 DEG.

US CUSTOMARY UNITS

SPECIMEN ID	HOLE ID	HOLE DIAM IN.	BOLT DIAM IN.	PANEL WIDTH IN.	EDGE DIST. IN.	PANEL THICK. IN.	FAILURE LOAD LB	FAILURE MODE	BEARING STRENGTH KSI	TENSION STRENGTH KSI	SHEAROUT STRENGTH KSI
THS-3-1	A	.2513	.2496	1.493	.749	.0911	2620.0	BRG	115.2	23.2	23.1
THS-3-1	B	.2540	.2496	1.491	1.513	.0916	3140.0	BRG	137.3	27.7	12.4
THS-3-1	C	.2546	.2496	1.483	1.514	.0872	3000.0	BRG	137.8	28.0	12.4
THS-3-1	D	.2550	.2496	1.488	.752	.0866	2825.0	BRG	130.7	26.5	26.1
THS-3-2	A	.2503	.2496	1.494	.756	.0920	2820.0	BRG	122.8	24.7	24.3
THS-3-2	B	.2549	.2496	1.476	1.514	.0887	2965.0	BRG	133.9	27.4	12.0
THS-3-2	C	.2538	.2496	1.499	1.512	.0920	3185.0	BRG	138.7	27.8	12.5
THS-3-2	D	.2536	.2496	1.535	.755	.0898	2565.0	BRG	114.4	22.3	22.7
THS-3-3	A	.2523	.2490	1.003	.495	.0923	2350.0	TENS	102.3	33.9	34.5
THS-3-3	B'	.2500	.2495	.994	.765	.0928	2695.0	BRG	116.4	39.0	22.7
THS-3-3	B	.2520	.2496	.999	1.005	.0926	2950.0	BRG	127.6	42.7	18.1
THS-3-3	C	.2520	.2496	1.001	1.006	.0916	2920.0	BRG	127.7	42.6	18.1
THS-3-3	C'	.2490	.2495	.996	.770	.0908	3015.0	TENS	133.1	44.4	25.7
THS-3-3	D	.2532	.2490	1.005	.495	.0925	2415.0	TENS	104.9	34.7	35.5
THS-3-4	A	.2523	.2490	1.006	.492	.0938	2430.0	TENS	104.0	34.4	35.4
THS-3-4	B'	.2508	.2495	1.004	.765	.0937	2565.0	BRG	109.7	36.4	21.4
THS-3-4	B	.2510	.2496	1.005	1.009	.0938	2970.0	BRG	126.9	42.0	17.9
THS-3-4	C	.2508	.2496	1.002	1.007	.0921	3340.0	BRG	145.3	48.3	20.6
THS-3-4	C'	.2512	.2495	1.000	.773	.0929	2715.0	BRG	117.1	39.0	22.6
THS-3-4	D	.2517	.2490	1.003	.495	.0913	2330.0	TENS	102.5	34.0	34.6
THS-3-5	A	.2507	.2490	.761	.489	.0915	2075.0	TENS	91.1	44.4	31.1
THS-3-5	B'	.2455	.2495	.763	.776	.0929	2350.0	TENS	101.4	48.9	19.3
THS-3-5	B	.2525	.2496	.762	1.007	.0922	2400.0	TENS	104.3	51.1	14.8
THS-3-5	C	.2529	.2496	.757	1.007	.0930	2340.0	TENS	100.8	49.9	14.3
THS-3-5	C'	.2480	.2495	.754	.779	.0916	2605.0	TENS	114.0	56.2	21.7
THS-3-5	D	.2510	.2490	.760	.489	.0943	2205.0	TENS	93.9	45.9	32.1
THS-3-6	A	.2507	.2490	.752	.492	.0939	2230.0	TENS	95.4	47.4	32.4
THS-3-6	B'	.2541	.2495	.759	.778	.0923	2530.0	TENS	109.9	54.3	21.0
THS-3-6	B	.2529	.2496	.756	1.007	.0931	2370.0	TENS	102.0	50.6	14.4
THS-3-6	C	.2525	.2496	.759	1.007	.0916	2600.0	TENS	113.7	56.1	16.1
THS-3-6	C'	.2520	.2495	.758	.778	.0921	2470.0	TENS	107.5	53.0	20.6
THS-3-6	D	.2503	.2490	.759	.492	.0911	2345.0	TENS	103.4	50.6	35.1

TABLE VA

TENSION THROUGH-THE-HOLE SPECIMENS

S-GLASS LONGITUDINAL PLIES, GRAPHITE CROSS PLIES, EPOXY RESIN
FIBER PATTERN - 25 PCT 0, 50 PCT ±π/4, 25 PCT π/2

SI UNITS

SPECIMEN ID	HOLE ID	HOLE DIAM MM	BOLT DIAM MM	PANEL WIDTH MM	EDGE DIST. MM	PANEL THICK. MM	FAILURE LOAD KNEWTON	FAILURE MODE	BEARING STRENGTH MPASCAL	TENSION STRENGTH MPASCAL	SHEAROUT STRENGTH MPASCAL
THS-4-1	A	6.375	6.340	38.12	18.30	2.263	11.7656	SHR	820.0	163.8	172.1
THS-4-1	B	6.449	6.340	38.01	38.36	2.261	14.0341	BRG	979.2	196.7	88.4
THS-4-1	C	6.419	6.340	37.73	38.34	2.296	13.5226	BRG	928.9	188.1	83.8
THS-4-1	D	6.495	6.340	37.72	19.23	2.271	11.9212	SHR	828.1	168.1	164.3
THS-4-2	A	6.391	6.340	38.03	18.03	2.210	10.3644	SHR	739.8	148.3	158.1
THS-4-2	B	6.419	6.340	37.68	38.07	2.286	14.4567	BRG	997.5	202.3	90.7
THS-4-2	C	6.434	6.340	38.03	38.17	2.273	13.5004	BRG	936.7	187.9	85.0
THS-4-2	D	6.502	6.340	37.58	19.20	2.261	9.5192	SHR	664.2	135.5	132.0
THS-4-3	A	6.421	6.325	25.52	12.53	2.306	10.7202	SHR	734.9	243.3	249.3
THS-4-3	B'	6.347	6.337	25.42	19.60	2.278	12.5885	BRG	871.9	289.6	168.1
THS-4-3	B	6.408	6.340	25.47	25.56	2.294	12.3661	BRG	850.4	282.8	120.6
THS-4-3	C	6.408	6.340	25.43	25.58	2.266	11.9880	BRG	834.6	278.2	118.2
THS-4-3	C'	6.350	6.337	25.42	19.63	2.281	12.0547	BRG	834.0	277.1	160.6
THS-4-3	D	6.424	6.325	25.44	12.55	2.250	9.9195	SHR	696.9	231.8	235.9
THS-4-4	A	6.408	6.325	25.60	12.54	2.283	10.7202	SHR	742.3	244.7	251.5
THS-4-4	B'	6.325	6.337	25.52	19.46	2.296	13.2335	BRG	909.4	300.2	176.8
THS-4-4	B	6.373	6.340	25.56	25.55	2.291	12.1214	BRG	834.5	275.7	118.3
THS-4-4	C	6.411	6.340	25.43	25.59	2.261	12.0102	BRG	838.0	279.3	118.7
THS-4-4	C'	6.271	6.337	25.38	19.54	2.250	11.9657	BRG	839.0	278.2	162.1
THS-4-4	D	6.431	6.325	25.47	12.55	2.268	10.2754	SHR	716.3	237.9	242.6
THS-4-5	A	6.383	6.325	19.17	12.46	2.266	10.0752	BRG	703.1	347.6	239.8
THS-4-5	B'	6.350	6.337	19.17	19.79	2.278	10.4756	BRG	725.5	358.7	138.4
THS-4-5	B	6.429	6.340	19.17	25.58	2.273	10.8314	BRG	751.5	373.9	106.5
THS-4-5	C	6.441	6.340	19.34	25.56	2.278	10.2309	BRG	708.3	348.1	100.5
THS-4-5	C'	6.325	6.337	19.29	19.98	2.268	10.4978	BRG	730.3	357.1	137.6
THS-4-5	D	6.370	6.325	19.40	12.51	2.289	10.1419	BRG	700.7	340.2	237.6
THS-4-6	A	6.375	6.325	19.37	12.46	2.329	10.0085	BRG	679.4	330.6	231.8
THS-4-6	B'	6.353	6.337	19.30	19.62	2.289	10.5200	BRG	725.4	355.0	139.7
THS-4-6	B	6.434	6.340	19.34	25.62	2.309	11.0538	BRG	755.2	371.0	106.9
THS-4-6	C	6.474	6.340	19.44	25.62	2.314	11.1428	BRG	759.6	371.3	107.6
THS-4-6	C'	6.350	6.337	19.45	19.98	2.311	10.4311	BRG	712.1	344.5	134.2
THS-4-6	D	6.380	6.325	19.44	12.44	2.314	8.6963	SHR	594.2	287.9	203.1

TABLE V8

TENSION THROUGH-THE-HOLE SPECIMENS

S-GLASS LONGITUDINAL PLIES, GRAPHITE CROSS PLIES, EPOXY RESIN
FIBER PATTERN - 25 PCT 0 DEG., 50 PCT ±45 DEG., 25 PCT 90 DEG.

US CUSTOMARY UNITS

SPECIMEN ID	HOLE ID	HOLE DIAM IN.	BOLT DIAM IN.	PANEL WIDTH IN.	EDGE DIST. IN.	PANEL THICK. IN.	FAILURE LOAD LB	FAILURE MODE	BEARING STRENGTH KSI	TENSION STRENGTH KSI	SHEAROUT STRENGTH KSI
THS-4-1	A	.2510	.2496	1.501	.720	.0891	2645.0	SHR	118.9	23.8	25.0
THS-4-1	B	.2539	.2496	1.497	1.510	.0890	3155.0	BRG	142.0	28.5	12.8
THS-4-1	C	.2527	.2496	1.486	1.509	.0904	3040.0	BRG	134.7	27.3	12.2
THS-4-1	D	.2557	.2496	1.485	.757	.0894	2680.0	SHR	120.1	24.4	23.8
THS-4-2	A	.2516	.2496	1.497	.710	.0870	2330.0	SHR	107.3	21.5	22.9
THS-4-2	B	.2527	.2496	1.483	1.499	.0900	3250.0	BRG	144.7	29.3	13.2
THS-4-2	C	.2533	.2496	1.497	1.503	.0895	3035.0	BRG	135.9	27.3	12.3
THS-4-2	D	.2560	.2496	1.480	.756	.0890	2140.0	SHR	96.3	19.6	19.1
THS-4-3	A	.2528	.2490	1.005	.493	.0908	2410.0	SHR	106.6	35.3	36.2
THS-4-3	B'	.2499	.2495	1.001	.772	.0897	2830.0	BRG	126.5	42.0	24.4
THS-4-3	B	.2523	.2496	1.003	1.006	.0903	2780.0	BRG	123.3	41.0	17.5
THS-4-3	C	.2523	.2496	1.001	1.007	.0892	2695.0	BRG	121.0	40.3	17.1
THS-4-3	C'	.2500	.2495	1.001	.773	.0898	2710.0	BRG	121.0	40.2	23.3
THS-4-3	D	.2529	.2490	1.001	.494	.0886	2230.0	SHR	101.1	33.6	34.2
THS-4-4	A	.2523	.2490	1.008	.494	.0899	2410.0	SHR	107.7	35.5	36.5
THS-4-4	B'	.2490	.2495	1.005	.766	.0904	2975.0	BRG	131.9	43.5	25.6
THS-4-4	B	.2509	.2496	1.006	1.006	.0902	2725.0	BRG	121.0	40.0	17.2
THS-4-4	C	.2524	.2496	1.001	1.007	.0890	2700.0	BRG	121.5	40.5	17.2
THS-4-4	C'	.2469	.2495	.999	.769	.0886	2690.0	BRG	121.7	40.3	23.5
THS-4-4	D	.2532	.2490	1.003	.494	.0893	2310.0	SHR	103.9	34.5	35.2
THS-4-5	A	.2513	.2490	.755	.491	.0892	2265.0	BRG	102.0	50.4	34.8
THS-4-5	B'	.2500	.2495	.755	.779	.0897	2355.0	BRG	105.2	52.0	20.1
THS-4-5	B	.2531	.2496	.755	1.007	.0895	2435.0	BRG	109.0	54.2	15.4
THS-4-5	C	.2536	.2496	.762	1.006	.0897	2300.0	BRG	102.7	50.5	14.6
THS-4-5	C'	.2490	.2495	.759	.787	.0893	2360.0	BRG	105.9	51.8	20.0
THS-4-5	D	.2508	.2490	.764	.493	.0901	2280.0	BRG	101.6	49.3	34.5
THS-4-6	A	.2510	.2490	.763	.490	.0917	2250.0	BRG	98.5	48.0	33.6
THS-4-6	B'	.2501	.2495	.760	.773	.0901	2365.0	BRG	105.2	51.5	20.3
THS-4-6	B	.2533	.2496	.761	1.009	.0909	2485.0	BRG	109.5	53.8	15.5
THS-4-6	C	.2549	.2496	.766	1.009	.0911	2505.0	BRG	110.2	53.9	15.6
THS-4-6	C'	.2500	.2495	.766	.787	.0910	2345.0	BRG	103.3	50.0	19.5
THS-4-6	D	.2512	.2490	.765	.490	.0911	1955.0	SHR	86.2	41.8	29.5

TABLE VIA

TENSION THROUGH-THE-HOLE SPECIMENS

S-GLASS LONGITUDINAL PLIES, GRAPHITE CROSS PLIES, EPOXY RESIN
FIBER PATTERN - 37.5 PCT 0, 37.5 PCT ±π/4, 25 PCT π/2

SI UNITS

SPECIMEN ID	HOLE ID	HOLE DIAM MM	BOLT DIAM MM	PANEL WIDTH MM	EDGE DIST. MM	PANEL THICK. MM	FAILURE LOAD KNEWTON	FAILURE MODE	BEARING STRENGTH MPASCAL	TENSION STRENGTH MPASCAL	SHEAROUT STRENGTH MPASCAL
THS-5-1	A	6.368	6.340	37.86	18.48	2.184	10.5868	SHR	764.5	153.9	158.4
THS-5-1	B	6.459	6.340	37.93	38.28	2.225	12.7442	BRG	903.4	182.0	81.7
THS-5-1	C	6.477	6.340	38.10	38.31	2.177	11.0094	BRG	797.8	159.9	72.1
THS-5-1	D	6.497	6.340	38.30	18.55	2.179	10.2976	SHR	745.3	148.6	154.4
THS-5-2	A	6.365	6.340	38.01	18.64	2.187	11.0094	SHR	794.0	159.1	162.8
THS-5-2	B	6.472	6.340	37.95	38.25	2.202	11.6988	BRG	837.9	168.8	75.9
THS-5-2	C	6.429	6.340	38.13	38.23	2.184	12.3438	BRG	891.3	178.3	80.7
THS-5-2	D	6.500	6.340	38.32	19.05	2.189	11.0983	SHR	799.5	159.3	160.4
THS-5-3	A	6.424	6.325	25.14	12.53	2.240	9.4302	SHR	665.6	224.9	225.9
THS-5-3	B'	6.396	6.337	24.93	19.53	2.258	11.7878	BRG	823.7	281.6	159.8
THS-5-3	B	6.419	6.340	25.04	25.66	2.250	12.8998	BRG	904.1	307.8	127.7
THS-5-3	C	6.401	6.340	25.54	25.58	2.268	12.0769	BRG	839.8	278.2	119.0
THS-5-3	C'	6.429	6.337	25.45	19.51	2.281	11.2762	BRG	780.1	259.9	151.7
THS-5-3	D	6.413	6.325	25.62	12.59	2.256	9.3858	SHR	657.9	216.6	221.8
THS-5-4	A	6.431	6.325	25.41	12.58	2.073	9.9195	SHR	756.7	252.2	255.6
THS-5-4	B'	6.388	6.337	25.37	19.48	2.253	12.6774	BRG	887.9	296.4	172.7
THS-5-4	B	6.424	6.340	25.39	25.61	2.164	11.5876	BRG	844.6	282.4	119.5
THS-5-4	C	6.426	6.340	25.52	25.59	2.256	12.5440	BRG	877.2	291.2	124.3
THS-5-4	C'	6.327	6.337	25.52	19.57	2.258	11.2095	BRG	783.3	258.6	151.3
THS-5-4	D	6.416	6.325	25.52	12.51	2.253	10.1419	SHR	711.8	235.6	242.0
THS-5-5	A	6.391	6.325	19.28	12.50	2.230	9.0744	BRG	643.4	315.8	218.5
THS-5-5	B'	6.325	6.337	19.19	19.95	2.240	10.8314	BRG	762.9	375.7	144.0
THS-5-5	B	6.462	6.340	19.24	25.58	2.235	11.7211	BRG	827.1	410.5	117.3
THS-5-5	C	6.462	6.340	19.27	25.62	2.273	11.8545	BRG	822.5	407.1	116.5
THS-5-5	C'	6.327	6.337	19.24	19.72	2.268	11.0316	BRG	767.4	376.6	146.9
THS-5-5	D	6.365	6.325	19.32	12.46	2.281	8.9187	BRG	618.2	301.8	210.7
THS-5-6	A	6.388	6.325	19.16	12.52	2.197	9.8528	SHR	709.1	351.0	240.5
THS-5-6	B'	6.271	6.337	19.09	19.78	2.184	11.2985	BRG	816.2	403.4	155.4
THS-5-6	B	6.434	6.340	19.13	25.49	2.192	11.2762	BRG	811.4	405.2	115.5
THS-5-6	C	6.434	6.340	19.25	25.55	2.212	11.4319	BRG	815.1	403.2	115.7
THS-5-6	C'	6.358	6.337	19.22	19.64	2.230	11.7211	BRG	829.3	408.7	159.6
THS-5-6	D	6.383	6.325	19.28	12.48	2.195	9.3635	SHR	674.6	330.9	229.7

TABLE VIB

TENSION THROUGH-THE-HOLE SPECIMENS

S-GLASS LONGITUDINAL PLIES, GRAPHITE CROSS PLIES, EPOXY RESIN
FIBER PATTERN - 37.5 PCT 0 DEG., 37.5 PCT ±45 DEG., 25 PCT 90 DEG.

US CUSTOMARY UNITS

SPECIMEN ID	HOLE ID	HOLE DIAM IN.	BOLT DIAM IN.	PANEL WIDTH IN.	EDGE DIST. IN.	PANEL THICK. IN.	FAILURE LOAD LB	FAILURE MODE	BEARING STRENGTH KSI	TENSION STRENGTH KSI	SHEAROUT STRENGTH KSI
THS-5-1	A	.2507	.2496	1.490	.728	.0860	2380.0	SHR	110.9	22.3	23.0
THS-5-1	B	.2543	.2496	1.493	1.507	.0876	2865.0	BRG	131.0	26.4	11.9
THS-5-1	C	.2550	.2496	1.500	1.508	.0857	2475.0	BRG	115.7	23.2	10.5
THS-5-1	D	.2558	.2496	1.508	.730	.0858	2315.0	SHR	108.1	21.5	22.4
THS-5-2	A	.2506	.2496	1.497	.734	.0861	2475.0	SHR	115.2	23.1	23.6
THS-5-2	B	.2548	.2496	1.494	1.506	.0867	2630.0	BRG	121.5	24.5	11.0
THS-5-2	C	.2531	.2496	1.501	1.505	.0860	2775.0	BRG	129.3	25.9	11.7
THS-5-2	D	.2559	.2496	1.509	.750	.0862	2495.0	SHR	116.0	23.1	23.3
THS-5-3	A	.2529	.2490	.990	.493	.0882	2120.0	SHR	96.5	32.6	32.8
THS-5-3	B'	.2518	.2495	.982	.769	.0889	2650.0	BRG	119.5	40.8	23.2
THS-5-3	B	.2527	.2496	.986	1.010	.0886	2900.0	BRG	131.1	44.6	18.5
THS-5-3	C	.2520	.2496	1.005	1.007	.0893	2715.0	BRG	121.8	40.3	17.3
THS-5-3	C'	.2531	.2495	1.002	.768	.0898	2535.0	BRG	113.1	37.7	22.0
THS-5-3	D	.2525	.2490	1.009	.496	.0888	2110.0	SHR	95.4	31.4	32.2
THS-5-4	A	.2532	.2490	1.000	.495	.0816	2230.0	SHR	109.8	36.6	37.1
THS-5-4	B'	.2515	.2495	.999	.767	.0887	2850.0	BRG	128.8	43.0	25.1
THS-5-4	B	.2529	.2496	.999	1.008	.0852	2605.0	BRG	122.5	41.0	17.3
THS-5-4	C	.2530	.2496	1.005	1.008	.0888	2820.0	BRG	127.2	42.2	18.0
THS-5-4	C'	.2491	.2495	1.005	.771	.0889	2520.0	BRG	113.6	37.5	21.9
THS-5-4	D	.2526	.2490	1.005	.493	.0887	2280.0	SHR	103.2	34.2	35.1
THS-5-5	A	.2516	.2490	.759	.492	.0878	2040.0	BRG	93.3	45.8	31.7
THS-5-5	B'	.2490	.2495	.756	.786	.0882	2435.0	BRG	110.7	54.5	20.9
THS-5-5	B	.2544	.2496	.757	1.007	.0880	2635.0	BRG	120.0	59.5	17.0
THS-5-5	C	.2544	.2496	.759	1.009	.0895	2665.0	BRG	119.3	59.0	16.9
THS-5-5	C'	.2491	.2495	.758	.776	.0893	2480.0	BRG	111.3	54.6	21.3
THS-5-5	D	.2506	.2490	.761	.491	.0898	2005.0	BRG	89.7	43.8	30.6
THS-5-6	A	.2515	.2490	.754	.493	.0865	2215.0	SHR	102.8	50.9	34.9
THS-5-6	B'	.2469	.2495	.752	.779	.0860	2540.0	BRG	118.4	58.5	22.5
THS-5-6	B	.2533	.2496	.753	1.004	.0863	2535.0	BRG	117.7	58.8	16.7
THS-5-6	C	.2533	.2496	.758	1.006	.0871	2570.0	BRG	118.2	58.5	16.8
THS-5-6	C'	.2503	.2495	.757	.773	.0878	2635.0	BRG	120.3	59.3	23.2
THS-5-6	D	.2513	.2490	.759	.491	.0864	2105.0	SHR	97.8	48.0	33.3

TABLE VIIA

TENSION THROUGH-THE-HOLE SPECIMENS

S-GLASS LONGITUDINAL PLIES, GRAPHITE CROSS PLIES, EPOXY RESIN
FIBER PATTERN - 37.5 PCT 0, 50 PCT ±π/4, 12.5 PCT π/2

SI UNITS

SPECIMEN ID	HOLE ID	HOLE DIAM MM	BOLT DIAM MM	PANEL WIDTH MM	EDGE DIST. MM	PANEL THICK. MM	FAILURE LOAD KNEWTON	FAILURE MODE	BEARING STRENGTH MPASCAL	TENSION STRENGTH MPASCAL	SHEAROUT STRENGTH MPASCAL
THS-6-1	A	6.482	6.340	37.99	19.24	2.217	10.7869	SHR	767.3	154.4	152.0
THS-6-1	B	6.429	6.340	38.05	38.38	2.212	12.1437	BRG	865.8	173.6	78.0
THS-6-1	C	6.449	6.340	37.98	38.35	2.217	13.3669	BRG	950.8	191.2	85.8
THS-6-1	D	6.378	6.340	38.04	19.18	2.172	11.0538	SHR	802.8	160.8	159.1
THS-6-2	A	6.485	6.340	38.01	18.98	2.222	9.8973	SHR	702.4	141.3	141.5
THS-6-2	B	6.464	6.340	37.96	38.36	2.215	13.4559	BRG	958.3	192.9	86.5
THS-6-2	C	6.472	6.340	38.11	38.38	2.151	13.6783	BRG	1002.9	200.9	90.5
THS-6-2	D	6.383	6.340	38.05	18.85	2.169	11.1873	SHR	813.5	162.8	164.7
THS-6-3	A	6.408	6.325	25.65	12.50	2.222	10.4533	SHR	743.7	244.5	253.0
THS-6-3	B'	6.299	6.337	25.48	18.90	2.083	11.0094	BRG	834.1	275.6	167.8
THS-6-3	B	6.416	6.340	25.57	25.62	2.154	11.0983	BRG	812.7	269.1	114.9
THS-6-3	C	6.441	6.340	25.27	25.62	2.187	12.4550	BRG	898.3	302.5	127.1
THS-6-3	C'	6.391	6.337	25.25	19.40	2.222	12.5440	BRG	890.6	299.4	174.2
THS-6-3	D	6.431	6.325	25.29	12.53	2.151	10.0752	SHR	740.5	248.3	251.3
THS-6-4	A	6.441	6.325	25.54	12.50	2.159	10.1419	SHR	742.7	245.9	253.2
THS-6-4	B'	6.431	6.337	25.46	19.52	2.197	11.3652	BRG	816.2	271.9	158.6
THS-6-4	B	6.398	6.340	25.50	25.58	2.179	12.0547	BRG	872.5	289.6	123.6
THS-6-4	C	6.408	6.340	25.34	25.65	2.184	12.0324	BRG	868.8	290.9	122.7
THS-6-4	C'	6.378	6.337	25.31	19.52	2.184	11.5654	BRG	835.5	279.7	162.1
THS-6-4	D	6.429	6.325	25.38	12.57	2.182	10.2754	SHR	744.6	248.5	251.7
THS-6-5	A	6.398	6.325	19.28	12.50	2.192	10.4756	SHR	755.6	371.1	256.9
THS-6-5	B'	6.223	6.337	19.26	19.58	2.189	11.5654	BRG	833.5	405.1	160.3
THS-6-5	B	6.454	6.340	19.30	25.58	2.192	10.5645	BRG	760.2	375.3	107.8
THS-6-5	C	6.444	6.340	19.31	25.58	2.197	11.5209	BRG	827.1	407.4	117.3
THS-6-5	C'	6.325	6.337	19.27	19.59	2.164	11.2762	BRG	822.2	402.6	158.6
THS-6-5	D	6.383	6.325	19.36	12.47	2.230	10.5423	SHR	747.4	364.4	254.6
THS-6-6	A	6.378	6.325	19.28	12.48	2.121	9.9640	SHR	742.8	364.2	252.8
THS-6-6	B'	6.350	6.337	19.21	19.79	2.182	10.6090	BRG	767.3	378.1	146.3
THS-6-6	B	6.454	6.340	19.24	25.58	2.151	11.2318	BRG	823.5	408.2	116.8
THS-6-6	C	6.477	6.340	19.15	25.58	2.200	11.0094	BRG	789.5	394.9	112.0
THS-6-6	C'	6.325	6.337	19.14	19.80	2.195	10.0752	BRG	724.4	358.3	138.0
THS-6-6	D	6.380	6.325	19.16	12.46	2.202	10.5868	SHR	760.1	376.1	259.4

TABLE VIIB

TENSION THROUGH-THE-HOLE SPECIMENS

S-GLASS LONGITUDINAL PLIES, GRAPHITE CROSS PLIES, EPOXY RESIN
FIBER PATTERN - 37.5 PCT 0 DEG., 50 PCT ±45 DEG., 12.5 PCT 90 DEG.

US CUSTOMARY UNITS

SPECIMEN ID	HOLE ID	HOLE DIAM IN.	BOLT DIAM IN.	PANEL WIDTH IN.	EDGE DIST. IN.	PANEL THICK. IN.	FAILURE LOAD LB	FAILURE MODE	BEARING STRENGTH KSI	TENSION STRENGTH KSI	SHEAROUT STRENGTH KSI
THS-6-1	A	.2552	.2496	1.496	.757	.0873	2425.0	SHR	111.3	22.4	22.0
THS-6-1	B	.2531	.2496	1.498	1.511	.0871	2730.0	BRG	125.6	25.2	11.3
THS-6-1	C	.2539	.2496	1.495	1.510	.0873	3005.0	BRG	137.9	27.7	12.4
THS-6-1	D	.2511	.2496	1.498	.755	.0855	2485.0	SHR	116.4	23.3	23.1
THS-6-2	A	.2553	.2496	1.496	.747	.0875	2225.0	SHR	101.9	20.5	20.5
THS-6-2	B	.2545	.2496	1.495	1.510	.0872	3025.0	BRG	139.0	28.0	12.5
THS-6-2	C	.2548	.2496	1.500	1.511	.0847	3075.0	BRG	145.5	29.1	13.1
THS-6-2	D	.2513	.2496	1.498	.742	.0854	2515.0	SHR	118.0	23.6	23.9
THS-6-3	A	.2523	.2490	1.010	.492	.0875	2350.0	SHR	107.9	35.5	36.7
THS-6-3	B'	.2480	.2495	1.003	.744	.0820	2475.0	BRG	121.0	40.0	24.3
THS-6-3	B	.2526	.2496	1.007	1.009	.0848	2495.0	BRG	117.9	39.0	16.7
THS-6-3	C	.2536	.2496	.995	1.009	.0861	2800.0	BRG	130.3	43.9	18.4
THS-6-3	C'	.2516	.2495	.994	.764	.0875	2820.0	BRG	129.2	43.4	25.3
THS-6-3	D	.2532	.2490	.996	.493	.0847	2265.0	SHR	107.4	36.0	36.4
THS-6-4	A	.2536	.2490	1.006	.492	.0850	2280.0	SHR	107.7	35.7	36.7
THS-6-4	B'	.2532	.2495	1.002	.769	.0865	2555.0	BRG	118.4	39.4	23.0
THS-6-4	B	.2519	.2496	1.004	1.007	.0858	2710.0	BRG	126.5	42.0	17.9
THS-6-4	C	.2523	.2496	.998	1.010	.0860	2705.0	BRG	126.0	42.2	17.8
THS-6-4	C'	.2511	.2495	.996	.768	.0860	2600.0	BRG	121.2	40.6	23.5
THS-6-4	D	.2531	.2490	.999	.495	.0859	2310.0	SHR	108.0	36.0	36.5
THS-6-5	A	.2519	.2490	.759	.492	.0863	2355.0	SHR	109.6	53.8	37.3
THS-6-5	B'	.2450	.2495	.758	.771	.0862	2600.0	BRG	120.9	58.8	23.3
THS-6-5	B	.2541	.2496	.760	1.007	.0863	2375.0	BRG	110.3	54.4	15.6
THS-6-5	C	.2537	.2496	.760	1.007	.0865	2590.0	BRG	120.0	59.1	17.0
THS-6-5	C'	.2490	.2495	.759	.771	.0852	2535.0	BRG	119.3	58.4	23.0
THS-6-5	D	.2513	.2490	.762	.491	.0878	2370.0	SHR	108.4	52.8	36.9
THS-6-6	A	.2511	.2490	.759	.491	.0835	2240.0	SHR	107.7	52.8	36.7
THS-6-6	B'	.2500	.2495	.756	.779	.0859	2385.0	BRG	111.3	54.8	21.2
THS-6-6	B	.2541	.2496	.758	1.007	.0847	2525.0	BRG	119.4	59.2	16.9
THS-6-6	C	.2550	.2496	.754	1.007	.0866	2475.0	BRG	114.5	57.3	16.2
THS-6-6	C'	.2490	.2495	.753	.780	.0864	2265.0	BRG	105.1	52.0	20.0
THS-6-6	D	.2512	.2490	.754	.490	.0867	2380.0	SHR	110.2	54.6	37.6

TABLE VIIIA

BEARING AND SHEAROUT SPECIMENS
(TENSILE LOADING)

ALL GRAPHITE FIBERS, EPOXY RESIN

SI UNITS

SPECIMEN ID	HOLE ID	HOLE DIAM MM	BOLT DIAM MM	PANEL WIDTH MM	EDGE DIST. MM	PANEL THICK. MM	FAILURE LOAD KNEWTON	FAILURE MODE	BEARING STRENGTH MPASCAL	TENSION STRENGTH MPASCAL	SHEAROUT STRENGTH MPASCAL
FIBER PATTERN - 25 PCT 0, 50 PCT ±π/4, 25 PCT π/2											
BSS-1-1	A	6.360	6.325	63.55	12.81	2.294	10.8981	BRG	751.3	83.1	246.7
BSS-1-1	B	6.360	6.325	63.38	37.80	2.342	11.8100	BRG	797.4	88.4	72.8
BSS-1-1	C	6.365	6.325	63.53	50.88	2.281	11.8323	BRG	820.2	90.7	54.4
BSS-1-1	D	6.373	6.325	63.70	25.63	2.273	13.1223	BRG	912.7	100.7	128.6
BSS-1-2	A	6.355	6.325	63.61	12.79	2.332	10.6980	BRG	725.4	80.1	238.6
BSS-1-2	B	6.370	6.325	63.66	37.77	2.332	12.8554	BRG	871.7	96.2	79.7
BSS-1-2	C	6.373	6.325	63.96	50.94	2.304	12.4995	BRG	857.9	94.2	56.8
BSS-1-2	D	6.370	6.325	63.53	25.88	2.283	12.9888	BRG	899.4	99.5	125.3
FIBER PATTERN - 37.5 PCT 0, 37.5 PCT ±π/4, 25 PCT π/2											
BSS-2-1	A	6.358	6.337	63.60	12.77	2.329	9.8973	BRG	670.5	74.2	221.6
BSS-2-1	B	6.355	6.337	63.44	37.83	2.342	10.7425	BRG	723.8	80.4	66.2
BSS-2-1	C	6.365	6.337	63.47	50.89	2.352	12.8109	BRG	859.5	95.4	57.1
BSS-2-1	D	6.368	6.337	63.70	25.96	2.316	13.2779	BRG	904.5	100.0	125.8
BSS-2-2	A	6.373	6.337	63.70	12.80	2.367	10.2754	BRG	684.9	75.7	225.7
BSS-2-2	B	6.358	6.337	63.64	37.90	2.316	13.8340	BRG	942.4	104.2	86.0
BSS-2-2	C	6.368	6.337	63.67	50.94	2.355	14.1009	BRG	945.0	104.5	62.7
BSS-2-2	D	6.373	6.337	63.66	25.21	2.377	12.5885	BRG	835.5	92.4	120.2
FIBER PATTERN - 37.5 PCT 0, 50 PCT ±π/4, 12.5 PCT π/2											
BSS-3-1	A	6.332	6.325	63.76	12.79	2.322	10.2976	BRG	701.3	77.2	230.5
BSS-3-1	B	6.347	6.325	63.67	37.75	2.332	12.3216	BRG	835.5	92.2	76.4
BSS-3-1	C	6.337	6.325	63.83	51.00	2.294	11.7878	BRG	812.6	89.4	53.7
BSS-3-1	D	6.350	6.325	63.93	25.52	2.286	13.1223	BRG	907.6	99.7	128.4
BSS-3-2	A	6.370	6.325	63.60	12.82	2.238	10.5868	BRG	748.0	82.7	245.4
BSS-3-2	B	6.358	6.325	63.66	37.78	2.283	12.1881	BRG	843.9	93.2	77.1
BSS-3-2	C	6.370	6.325	63.83	50.91	2.291	13.5671	BRG	936.3	103.1	62.0
BSS-3-2	D	6.360	6.325	63.93	25.54	2.286	13.4336	BRG	929.1	102.1	131.4

TABLE VIIIB

BEARING AND SHEAROUT SPECIMENS
(TENSILE LOADING)

ALL GRAPHITE FIBERS, EPOXY RESIN

US CUSTOMARY UNITS

SPECIMEN ID	HOLE ID	HOLE DIAM IN.	BOLT DIAM IN.	PANEL WIDTH IN.	EDGE DIST. IN.	PANEL THICK. IN.	FAILURE LOAD LB	FAILURE MODE	BEARING STRENGTH KSI	TENSION STRENGTH KSI	SHEAROUT STRENGTH KSI
FIBER PATTERN - 25 PCT 0 DEG., 50 PCT ±45 DEG., 25 PCT 90 DEG.											
BSS-1-1	A	.2504	.2490	2.502	.504	.0903	2450.0	BRG	109.0	12.1	35.8
BSS-1-1	B	.2504	.2490	2.495	1.488	.0922	2655.0	BRG	115.6	12.8	10.6
BSS-1-1	C	.2506	.2490	2.501	2.003	.0898	2660.0	BRG	119.0	13.2	7.9
BSS-1-1	D	.2509	.2490	2.508	1.009	.0895	2950.0	BRG	132.4	14.6	18.7
BSS-1-2	A	.2502	.2490	2.504	.504	.0918	2405.0	BRG	105.2	11.6	34.6
BSS-1-2	B	.2508	.2490	2.506	1.487	.0918	2890.0	BRG	126.4	14.0	11.6
BSS-1-2	C	.2509	.2490	2.518	2.005	.0907	2810.0	BRG	124.4	13.7	8.2
BSS-1-2	D	.2508	.2490	2.501	1.019	.0899	2920.0	BRG	130.4	14.4	18.2
FIBER PATTERN - 37.5 PCT 0 DEG., 37.5 PCT ±45 DEG., 25 PCT 90 DEG.											
BSS-2-1	A	.2503	.2495	2.504	.503	.0917	2225.0	BRG	97.3	10.8	32.1
BSS-2-1	B	.2502	.2495	2.498	1.489	.0922	2415.0	BRG	105.0	11.7	9.6
BSS-2-1	C	.2506	.2495	2.499	2.003	.0926	2880.0	BRG	124.7	13.8	8.3
BSS-2-1	D	.2507	.2495	2.508	1.022	.0912	2985.0	BRG	131.2	14.5	18.2
BSS-2-2	A	.2509	.2495	2.508	.504	.0932	2310.0	BRG	99.3	11.0	32.7
BSS-2-2	B	.2503	.2495	2.506	1.492	.0912	3110.0	BRG	136.7	15.1	12.5
BSS-2-2	C	.2507	.2495	2.507	2.005	.0927	3170.0	BRG	137.1	15.2	9.1
BSS-2-2	D	.2509	.2495	2.506	.993	.0936	2830.0	BRG	121.2	13.4	17.4
FIBER PATTERN - 37.5 PCT 0 DEG., 50 PCT ±45 DEG., 12.5 PCT 90 DEG.											
BSS-3-1	A	.2493	.2490	2.510	.503	.0914	2315.0	BRG	101.7	11.2	33.4
BSS-3-1	B	.2499	.2490	2.507	1.486	.0918	2770.0	BRG	121.2	13.4	11.1
BSS-3-1	C	.2495	.2490	2.513	2.008	.0903	2650.0	BRG	117.9	13.0	7.8
BSS-3-1	D	.2500	.2490	2.517	1.005	.0900	2950.0	BRG	131.6	14.5	18.6
BSS-3-2	A	.2508	.2490	2.504	.505	.0881	2380.0	BRG	108.5	12.0	35.6
BSS-3-2	B	.2503	.2490	2.506	1.487	.0899	2740.0	BRG	122.4	13.5	11.2
BSS-3-2	C	.2508	.2490	2.513	2.004	.0902	3050.0	BRG	135.8	14.9	9.0
BSS-3-2	D	.2504	.2490	2.517	1.006	.0900	3020.0	BRG	134.8	14.8	19.1

TABLE IXA

BEARING AND SHEAROUT SPECIMENS
(TENSILE LOADING)

S-GLASS LONGITUDINAL PLIES, GRAPHITE CROSS PLIES, EPOXY RESIN

SI UNITS

SPECIMEN ID	HOLE ID	HOLE DIAM MM	BOLT DIAM MM	PANEL WIDTH MM	EDGE DIST. MM	PANEL THICK. MM	FAILURE LOAD KNEWTON	FAILURE MODE	BEARING STRENGTH MPASCAL	TENSION STRENGTH MPASCAL	SHEAROUT STRENGTH MPASCAL
FIBER PATTERN - 25 PCT 0, 50 PCT ±π/4, 25 PCT π/2											
BSS-4-1	A	6.347	6.325	63.67	12.80	2.314	10.2309	SHR	699.1	77.1	229.7
BSS-4-1	B	6.350	6.325	63.61	37.88	2.324	12.9888	BRG	883.7	97.6	80.5
BSS-4-1	C	6.302	6.325	63.63	50.81	2.314	12.7219	BRG	869.3	95.9	57.7
BSS-4-1	D	6.337	6.325	63.67	25.22	2.311	12.1214	BRG	829.2	91.5	118.9
FIBER PATTERN - 37.5 PCT 0, 37.5 PCT ±π/4, 25 PCT π/2											
BSS-5-1	A	6.342	6.325	63.69	12.80	2.215	9.4080	SHR	671.6	74.1	220.6
BSS-5-1	B	6.353	6.325	63.69	37.76	2.215	11.6543	BRG	832.0	91.8	76.1
BSS-5-1	C	6.330	6.325	63.65	50.85	2.235	12.5662	BRG	888.9	98.1	58.9
BSS-5-1	D	6.307	6.325	63.72	25.36	2.222	11.7211	BRG	833.9	91.9	118.8
BSS-5-2	A	6.325	6.325	63.73	12.83	2.210	9.6526	SHR	690.7	76.1	225.9
BSS-5-2	B	6.353	6.325	63.86	37.85	2.248	12.5440	BRG	882.3	97.0	80.5
BSS-5-2	C	6.353	6.325	63.81	50.90	2.243	13.7450	BRG	969.0	106.7	64.2
BSS-5-2	D	6.368	6.325	63.82	25.05	2.233	13.4114	BRG	949.8	104.6	137.4
FIBER PATTERN - 37.5 PCT 0, 50 PCT ±π/4, 12.5 PCT π/2											
BSS-6-1	A	6.340	6.325	63.65	12.94	2.090	10.1642	SHR	768.8	84.8	248.9
BSS-6-1	B	6.350	6.325	63.65	37.97	2.228	12.0102	BRG	852.5	94.1	77.5
BSS-6-1	C	6.337	6.325	63.69	50.84	2.192	11.0761	BRG	798.9	88.1	53.0
BSS-6-1	D	6.528	6.325	63.55	25.23	2.235	12.5440	SHR	887.3	98.4	127.7
BSS-6-2	A	6.373	6.325	63.86	12.83	2.245	10.5868	SHR	745.5	82.0	244.3
BSS-6-2	B	6.345	6.325	63.81	37.90	2.164	12.2326	BRG	893.7	98.4	81.4
BSS-6-2	C	6.350	6.325	63.70	50.85	2.164	12.0992	BRG	884.0	97.5	58.6
BSS-6-2	D	6.500	6.325	63.72	25.14	2.197	11.9435	BRG	859.5	95.0	124.1

TABLE IXB

BEARING AND SHEAROUT SPECIMENS
(TENSILE LOADING)

S-GLASS LONGITUDINAL PLIES, GRAPHITE CROSS PLIES, EPOXY RESIN

US CUSTOMARY UNITS

SPECIMEN ID	HOLE ID	HOLE DIAM IN.	BOLT DIAM IN.	PANEL WIDTH IN.	EDGE DIST. IN.	PANEL THICK. IN.	FAILURE LOAD LB	FAILURE MODE	BEARING STRENGTH KSI	TENSION STRENGTH KSI	SHEAROUT STRENGTH KSI
FIBER PATTERN - 25 PCT 0 DEG., 50 PCT ±45 DEG., 25 PCT 90 DEG.											
BSS-4-1	A	.2499	.2490	2.507	.504	.0911	2300.0	SHR	101.4	11.2	33.3
BSS-4-1	B	.2500	.2490	2.504	1.491	.0915	2920.0	BRG	128.2	14.2	11.7
BSS-4-1	C	.2481	.2490	2.505	2.000	.0911	2860.0	BRG	126.1	13.9	8.4
BSS-4-1	D	.2495	.2490	2.507	.993	.0910	2725.0	BRG	120.3	13.3	17.2
FIBER PATTERN - 37.5 PCT 0 DEG., 37.5 PCT ±45 DEG., 25 PCT 90 DEG.											
BSS-5-1	A	.2497	.2490	2.507	.504	.0872	2115.0	SHR	97.4	10.7	32.0
BSS-5-1	B	.2501	.2490	2.507	1.487	.0872	2620.0	BRG	120.7	13.3	11.0
BSS-5-1	C	.2492	.2490	2.506	2.002	.0880	2825.0	BRG	128.9	14.2	8.5
BSS-5-1	D	.2483	.2490	2.509	.998	.0875	2635.0	BRG	120.9	13.3	17.2
BSS-5-2	A	.2490	.2490	2.509	.505	.0870	2170.0	SHR	100.2	11.0	32.8
BSS-5-2	B	.2501	.2490	2.514	1.490	.0885	2820.0	BRG	128.0	14.1	11.7
BSS-5-2	C	.2501	.2490	2.512	2.004	.0883	3090.0	BRG	140.5	15.5	9.3
BSS-5-2	D	.2507	.2490	2.513	.986	.0879	3015.0	BRG	137.8	15.2	19.9
FIBER PATTERN - 37.5 PCT 0 DEG., 50 PCT ±45 DEG., 12.5 PCT 90 DEG.											
BSS-6-1	A	.2496	.2490	2.506	.509	.0823	2285.0	SHR	111.5	12.3	36.1
BSS-6-1	B	.2500	.2490	2.506	1.495	.0877	2700.0	BRG	123.6	13.6	11.2
BSS-6-1	C	.2495	.2490	2.507	2.002	.0863	2490.0	BRG	115.9	12.8	7.7
BSS-6-1	D	.2570	.2490	2.502	.993	.0880	2820.0	SHR	128.7	14.3	18.5
BSS-6-2	A	.2509	.2490	2.514	.505	.0884	2380.0	SHR	108.1	11.9	35.4
BSS-6-2	B	.2498	.2490	2.512	1.492	.0852	2750.0	BRG	129.6	14.3	11.8
BSS-6-2	C	.2500	.2490	2.508	2.002	.0852	2720.0	BRG	128.2	14.1	8.5
BSS-6-2	D	.2559	.2490	2.509	.990	.0865	2685.0	BRG	124.7	13.8	18.0

TABLE XA

BEARING AND SHEAROUT SPECIMENS
(COMPRESSIVE LOADING)

ALL GRAPHITE FIBERS, EPOXY RESIN

SI UNITS

SPECIMEN ID	HOLE ID	HOLE DIAM MM	BOLT DIAM MM	PANEL WIDTH MM	EDGE DIST. MM	PANEL THICK. MM	FAILURE LOAD KNEWTON	FAILURE MODE	BEARING STRENGTH MPASCAL	COMPR. STRENGTH MPASCAL	SHEAROUT STRENGTH MPASCAL
FIBER PATTERN - 25 PCT 0, 50 PCT ±π/4, 25 PCT π/2											
BSS-1-4	A	6.419	6.276	50.64	25.40	2.324	12.7219	BRG	872.1	123.8	123.3
BSS-1-4	B	6.495	6.495	50.31	25.66	2.329	12.7219	BRG	841.0	124.7	121.9
BSS-1-5	A	6.419	6.269	51.43	25.59	2.304	13.6560	BRG	945.6	131.7	132.4
BSS-1-5	B	6.457	6.264	51.41	25.62	2.337	12.3216	BRG	841.8	117.3	117.7
FIBER PATTERN - 37.5 PCT 0, 37.5 PCT ±π/4, 25 PCT π/2											
BSS-2-4	A	6.386	6.292	51.04	25.34	2.367	12.1437	BRG	815.3	114.9	115.8
BSS-2-4	B	6.480	6.276	51.16	25.61	2.362	11.7211	BRG	790.6	111.1	110.9
BSS-2-5	A	6.528	6.292	50.81	25.57	2.329	13.9897	BRG	954.6	135.7	134.6
BSS-2-5	B	6.403	6.274	50.77	25.25	2.360	12.1437	BRG	820.3	116.0	116.7
FIBER PATTERN - 37.5 PCT 0, 50 PCT ±π/4, 12.5 PCT π/2											
BSS-3-4	A	6.444	6.292	51.81	25.68	2.299	13.1000	BRG	905.8	125.6	126.9
BSS-3-4	B	6.502	6.276	50.81	25.60	2.329	12.7219	BRG	870.2	123.3	122.2

TABLE XB

BEARING AND SHEAROUT SPECIMENS
(COMPRESSIVE LOADING)

ALL GRAPHITE FIBERS, EPOXY RESIN

US CUSTOMARY UNITS

SPECIMEN ID	HOLE ID	HOLE DIAM IN.	BOLT DIAM IN.	PANEL WIDTH IN.	EDGE DIST. IN.	PANEL THICK. IN.	FAILURE LOAD LB	FAILURE MODE	BEARING STRENGTH KSI	COMPR. STRENGTH KSI	SHEAROUT STRENGTH KSI
FIBER PATTERN - 25 PCT 0 DEG., 50 PCT ±45 DEG., 25 PCT 90 DEG.											
BSS-1-4	A	.2527	.2471	1.994	1.000	.0915	2860.0	BRG	126.5	18.0	17.9
BSS-1-4	B	.2557	.2557	1.981	1.010	.0917	2860.0	BRG	122.0	18.1	17.7
BSS-1-5	A	.2527	.2468	2.025	1.007	.0907	3070.0	BRG	137.1	19.1	19.2
BSS-1-5	B	.2542	.2466	2.024	1.009	.0920	2770.0	BRG	122.1	17.0	17.1
FIBER PATTERN - 37.5 PCT 0 DEG., 37.5 PCT ±45 DEG., 25 PCT 90 DEG.											
BSS-2-4	A	.2514	.2477	2.010	.998	.0932	2730.0	BRG	118.3	16.7	16.8
BSS-2-4	B	.2551	.2471	2.014	1.008	.0930	2635.0	BRG	114.7	16.1	16.1
BSS-2-5	A	.2570	.2477	2.000	1.007	.0917	3145.0	BRG	138.5	19.7	19.5
BSS-2-5	B	.2521	.2470	1.999	.994	.0929	2730.0	BRG	119.0	16.8	16.9
FIBER PATTERN - 37.5 PCT 0 DEG., 50 PCT ±45 DEG., 12.5 PCT 90 DEG.											
BSS-3-4	A	.2537	.2477	2.040	1.011	.0905	2945.0	BRG	131.4	18.2	18.4
BSS-3-4	B	.2560	.2471	2.000	1.008	.0917	2860.0	BRG	126.2	17.9	17.7

TABLE XIA

BEARING AND SHEAROUT SPECIMENS
(COMPRESSIVE LOADING)

S-GLASS LONGITUDINAL PLIES, GRAPHITE CROSS PLIES, EPOXY RESIN

SI UNITS

SPECIMEN ID	HOLE ID	HOLE DIAM MM	BOLT DIAM MM	PANEL WIDTH MM	EDGE DIST. MM	PANEL THICK. MM	FAILURE LOAD KNEWTON	FAILURE MODE	BEARING STRENGTH MPASCAL	COMPR. STRENGTH MPASCAL	SHEAROUT STRENGTH MPASCAL
FIBER PATTERN - 25 PCT 0, 50 PCT ±π/4, 25 PCT π/2											
BSS-4-4	A	6.408	6.284	50.87	25.09	2.273	10.6757	BRG	747.3	105.6	107.3
BSS-4-4	B	6.507	6.281	51.10	25.60	2.266	14.7681	BRG	1037.7	146.2	145.8
BSS-4-5	A	6.403	6.274	50.80	25.60	2.273	15.3464	BRG	1076.0	152.0	150.7
BSS-4-5	B	6.520	6.281	51.28	25.64	2.271	14.8126	BRG	1038.5	145.7	145.8
FIBER PATTERN - 37.5 PCT 0, 37.5 PCT ±π/4, 25 PCT π/2											
BSS-5-4	A	6.441	6.266	51.15	25.85	2.169	12.6774	BRG	932.7	130.7	129.2
BSS-5-4	B	6.533	6.266	51.02	25.64	2.200	13.1445	BRG	953.7	134.3	133.5
BSS-5-5	A	6.431	6.281	51.42	25.63	2.187	15.3464	BRG	1117.1	156.0	156.5
BSS-5-5	B	6.566	6.266	51.15	25.66	2.243	15.1684	BRG	1079.3	151.7	151.1
FIBER PATTERN - 37.5 PCT 0, 50 PCT ±π/4, 12.5 PCT π/2											
BSS-6-4	A	6.429	6.266	50.79	25.79	2.189	14.9238	BRG	1087.8	153.7	151.0
BSS-6-4	B	6.396	6.276	50.91	25.59	2.212	12.8554	BRG	925.8	130.5	129.7
BSS-6-5	A	6.424	6.264	50.92	25.40	2.250	14.6347	BRG	1038.2	146.1	146.5
BSS-6-5	B	6.551	6.284	50.86	25.58	2.197	14.5679	BRG	1055.2	149.6	148.7

TABLE XIB

BEARING AND SHEAROUT SPECIMENS
(COMPRESSIVE LOADING)

S-GLASS LONGITUDINAL PLIES, GRAPHITE CROSS PLIES, EPOXY RESIN

US CUSTOMARY UNITS

SPECIMEN ID	HOLE ID	HOLE DIAM IN.	BOLT DIAM IN.	PANEL WIDTH IN.	EDGE DIST. IN.	PANEL THICK. IN.	FAILURE LOAD LB	FAILURE MODE	BEARING STRENGTH KSI	COMPR. STRENGTH KSI	SHEAROUT STRENGTH KSI
FIBER PATTERN - 25 PCT 0 DEG., 50 PCT ±45 DEG., 25 PCT 90 DEG.											
BSS-4-4	A	.2523	.2474	2.003	.988	.0895	2400.0	BRG	108.4	15.3	15.6
BSS-4-4	B	.2562	.2473	2.012	1.008	.0892	3320.0	BRG	150.5	21.2	21.1
BSS-4-5	A	.2521	.2470	2.000	1.008	.0895	3450.0	BRG	156.1	22.1	21.9
BSS-4-5	B	.2567	.2473	2.019	1.009	.0894	3330.0	BRG	150.6	21.1	21.1
FIBER PATTERN - 37.5 PCT 0 DEG., 37.5 PCT ±45 DEG., 25 PCT 90 DEG.											
BSS-5-4	A	.2536	.2467	2.014	1.018	.0854	2850.0	BRG	135.3	19.0	18.7
BSS-5-4	B	.2572	.2467	2.009	1.009	.0866	2955.0	BRG	138.3	19.5	19.4
BSS-5-5	A	.2532	.2473	2.024	1.009	.0861	3450.0	BRG	162.0	22.6	22.7
BSS-5-5	B	.2585	.2467	2.014	1.010	.0883	3410.0	BRG	156.5	22.0	21.9
FIBER PATTERN - 37.5 PCT 0 DEG., 50 PCT ±45 DEG., 12.5 PCT 90 DEG.											
BSS-6-4	A	.2531	.2467	2.000	1.015	.0862	3355.0	BRG	157.8	22.3	21.9
BSS-6-4	B	.2518	.2471	2.004	1.007	.0871	2890.0	BRG	134.3	18.9	18.8
BSS-6-5	A	.2529	.2466	2.005	1.000	.0886	3290.0	BRG	150.6	21.2	21.3
BSS-6-5	B	.2579	.2474	2.002	1.007	.0865	3275.0	BRG	153.0	21.7	21.6

TABLE XIIA

OPEN-HOLE SPECIMENS

ALL GRAPHITE FIBERS, EPOXY RESIN

SI UNITS

SPECIMEN ID	HOLE ID	HOLE DIAM MM	BOLT DIAM MM	PANEL WIDTH MM	EDGE DIST. MM	PANEL THICK. MM	FAILURE LOAD KNEWTON	FAILURE MODE	TENSION STRENGTH MPASCAL
FIBER PATTERN - 25 PCT 0, 50 PCT ±π/4, 25 PCT π/2									
OHS-1-1	A	6.350	6.325	25.28	50.80	2.400	13.5893	TENS	299.1
OHS-1-1	B	6.452	6.325	25.27	50.80	2.367	12.5440	TENS	281.6
OHS-1-2	A	6.373	6.325	25.16	50.80	2.410	13.2779	TENS	293.1
OHS-1-2	B	6.452	6.325	25.20	50.80	2.332	13.7895	TENS	315.4
FIBER PATTERN - 37.5 PCT 0, 37.5 PCT ±π/4, 25 PCT π/2									
OHS-2-1	A	6.416	6.337	25.15	50.80	2.451	16.2583	TENS	354.1
OHS-2-1	B	6.419	6.337	25.25	50.80	2.487	16.4139	TENS	350.5
OHS-2-2	A	6.375	6.337	25.28	50.80	2.550	15.6577	TENS	324.8
OHS-2-2	B	6.411	6.337	25.26	50.80	2.492	14.9460	TENS	318.2
FIBER PATTERN - 37.5 PCT 0, 50 PCT ±π/4, 12.5 PCT π/2									
OHS-3-1	A	6.398	6.337	25.30	50.80	2.537	15.7245	TENS	327.9
OHS-3-1	B	6.452	6.337	25.27	50.80	2.540	16.5696	TENS	346.7
OHS-3-2	A	6.408	6.337	25.28	50.80	2.637	17.2146	TENS	346.0
OHS-3-2	B	6.454	6.337	25.29	50.80	2.639	17.8596	TENS	359.2

TABLE XIIB

OPEN-HOLE SPECIMENS

ALL GRAPHITE FIBERS, EPOXY RESIN

US CUSTOMARY UNITS

SPECIMEN ID	HOLE ID	HOLE DIAM IN.	BOLT DIAM IN.	PANEL WIDTH IN.	EDGE DIST. IN.	PANEL THICK. IN.	FAILURE LOAD LB	FAILURE MODE	TENSION STRENGTH KSI
FIBER PATTERN - 25 PCT 0 DEG., 50 PCT ±45 DEG., 25 PCT 90 DEG.									
OHS-1-1	A	.2500	.2490	.995	2.000	.0945	3055.0	TENS	43.4
OHS-1-1	B	.2540	.2490	.995	2.000	.0932	2820.0	TENS	40.8
OHS-1-2	A	.2509	.2490	.991	2.000	.0949	2985.0	TENS	42.5
OHS-1-2	B	.2540	.2490	.992	2.000	.0918	3100.0	TENS	45.7
FIBER PATTERN - 37.5 PCT 0 DEG., 37.5 PCT ±45 DEG., 25 PCT 90 DEG.									
OHS-2-1	A	.2526	.2495	.990	2.000	.0965	3655.0	TENS	51.4
OHS-2-1	B	.2527	.2495	.994	2.000	.0979	3690.0	TENS	50.8
OHS-2-2	A	.2510	.2495	.995	2.000	.1004	3520.0	TENS	47.1
OHS-2-2	B	.2524	.2495	.994	2.000	.0981	3360.0	TENS	46.2
FIBER PATTERN - 37.5 PCT 0 DEG., 50 PCT ±45 DEG., 12.5 PCT 90 DEG.									
OHS-3-1	A	.2519	.2495	.996	2.000	.0999	3535.0	TENS	47.6
OHS-3-1	B	.2540	.2495	.995	2.000	.1000	3725.0	TENS	50.3
OHS-3-2	A	.2523	.2495	.995	2.000	.1038	3870.0	TENS	50.2
OHS-3-2	B	.2541	.2495	.996	2.000	.1039	4015.0	TENS	52.1

TABLE XIIIA

OPEN-HOLE SPECIMENS

S-GLASS LONGITUDINAL PLIES, GRAPHITE CROSS PLIES, EPOXY RESIN

SI UNITS

SPECIMEN ID	HOLE ID	HOLE DIAM MM	BOLT DIAM MM	PANEL WIDTH MM	EDGE DIST. MM	PANEL THICK. MM	FAILURE LOAD KNEWTON	FAILURE MODE	TENSION STRENGTH MPASCAL
FIBER PATTERN - 25 PCT 0, 50 PCT ±π/4, 25 PCT π/2									
OHS-4-1	A	6.421	6.337	25.42	50.80	2.296	17.1701	DELAM	393.7
OHS-4-1	B	6.523	6.337	25.39	50.80	2.258	16.7476	DELAM	393.1
OHS-4-2	A	6.520	6.337	25.19	50.80	2.278	16.9922	DELAM	399.4
OHS-4-2	B	6.599	6.337	25.24	50.80	2.324	17.2591	DELAM	398.3
FIBER PATTERN - 37.5 PCT 0, 37.5 PCT ±π/4, 25 PCT π/2									
OHS-5-1	A	6.459	6.337	25.35	50.80	2.352	22.5080	DELAM	506.5
OHS-5-1	B	6.368	6.337	25.22	50.80	2.329	18.9939	DELAM	432.6
OHS-5-2	A	6.378	6.337	25.11	50.80	2.390	21.7296	DELAM	485.3
OHS-5-2	B	6.457	6.337	25.07	50.80	2.431	22.3301	DELAM	493.4
FIBER PATTERN - 37.5 PCT 0, 50 PCT ±π/4, 12.5 PCT π/2									
OHS-6-1	A	6.368	6.337	25.20	50.80	2.286	23.3532	DELAM	542.4
OHS-6-1	B	6.454	6.337	25.23	50.80	2.421	23.1975	DELAM	510.3
OHS-6-2	A	6.368	6.337	25.50	50.80	2.466	23.6201	DELAM	500.5
OHS-6-2	B	6.452	6.337	26.45	50.80	2.426	23.5756	DELAM	485.9

TABLE XIIIB

OPEN-HOLE SPECIMENS

S-GLASS LONGITUDINAL PLIES, GRAPHITE CROSS PLIES, EPOXY RESIN

US CUSTOMARY UNITS

SPECIMEN ID	HOLE ID	HOLE DIAM IN.	BOLT DIAM IN.	PANEL WIDTH IN.	EDGE DIST. IN.	PANEL THICK. IN.	FAILURE LOAD LB	FAILURE MODE	TENSION STRENGTH KSI
FIBER PATTERN - 25 PCT 0 DEG., 50 PCT ±45 DEG., 25 PCT 90 DEG.									
OHS-4-1	A	.2528	.2495	1.001	2.000	.0904	3860.0	DELAM	57.1
OHS-4-1	B	.2568	.2495	1.000	2.000	.0889	3765.0	DELAM	57.0
OHS-4-2	A	.2567	.2495	.992	2.000	.0897	3820.0	DELAM	57.9
OHS-4-2	B	.2598	.2495	.994	2.000	.0915	3880.0	DELAM	57.8
FIBER PATTERN - 37.5 PCT 0 DEG., 37.5 PCT ±45 DEG., 25 PCT 90 DEG.									
OHS-5-1	A	.2543	.2495	.998	2.000	.0926	5060.0	DELAM	73.5
OHS-5-1	B	.2507	.2495	.993	2.000	.0917	4270.0	DELAM	62.7
OHS-5-2	A	.2511	.2495	.989	2.000	.0941	4885.0	DELAM	70.4
OHS-5-2	B	.2542	.2495	.987	2.000	.0957	5020.0	DELAM	71.6
FIBER PATTERN - 37.5 PCT 0 DEG., 50 PCT ±45 DEG., 12.5 PCT 90 DEG.									
OHS-6-1	A	.2507	.2495	.992	2.000	.0900	5250.0	DELAM	78.7
OHS-6-1	B	.2541	.2495	.993	2.000	.0953	5215.0	DELAM	74.0
OHS-6-2	A	.2507	.2495	1.004	2.000	.0971	5310.0	DELAM	72.6
OHS-6-2	B	.2540	.2495	1.042	2.000	.0955	5300.0	DELAM	70.5

TABLE XIVA

INTERACTION SPECIMENS
(TENSILE LOADING)

ALL GRAPHITE FIBERS, EPOXY RESIN

SI UNITS

SPECIMEN ID	HOLE ID	HOLE DIAM MM	BOLT DIAM MM	PANEL WIDTH MM	EDGE DIST. MM	PANEL THICK. MM	FAILURE LOAD KNEWTON	FAILURE MODE	BEARING STRENGTH MPASCAL	TENSION STRENGTH MPASCAL	SHEAROUT STRENGTH MPASCAL
FIBER PATTERN - 25 PCT 0, 50 PCT ±π/4, 25 PCT π/2											
IS-1-1		6.431	6.431	25.19	25.40	4.597	22.4190	TENS	379.1	259.9	55.0
IS-1-2		6.515	6.515	25.50	25.40	4.610	23.5756	TENS	392.5	269.3	57.7
IS-1-3		6.457	6.457	25.53	25.40	4.615	23.0863	TENS	387.4	262.3	56.4
IS-1-4		6.525	6.525	25.43	25.40	4.638	23.0418	TENS	380.7	262.8	56.1
FIBER PATTERN - 37.5 PCT 0, 37.5 PCT ±π/4, 25 PCT π/2											
IS-2-1		6.365	6.365	25.63	25.40	4.615	26.7783	TENS	455.8	301.2	65.3
IS-2-2		6.436	6.436	25.65	25.40	4.719	28.5576	TENS	470.1	315.0	68.2
IS-2-3		6.383	6.383	25.59	25.40	4.549	27.6679	TENS	476.4	316.7	68.5
IS-2-4		6.380	6.380	25.51	25.40	4.648	25.5773	TENS	431.2	287.6	61.9
FIBER PATTERN - 37.5 PCT 0, 50 PCT ±π/4, 12.5 PCT π/2											
IS-3-1		6.406	6.406	25.44	25.40	4.257	28.0238	TENS	513.8	345.8	74.1
IS-3-2		6.391	6.391	25.42	25.40	4.321	27.4010	TENS	496.2	333.3	71.4
IS-3-3		6.365	6.365	25.39	25.40	4.321	27.8459	TENS	506.3	338.7	72.5
IS-3-4		6.520	6.520	25.57	25.40	4.735	26.4224	TENS	428.0	292.9	63.0

NOTE THAT TENSION STRENGTH REFERS TO ENTIRE LOAD AT NET SECTION

TABLE XIVB

INTERACTION SPECIMENS
(TENSILE LOADING)

ALL GRAPHITE FIBERS, EPOXY RESIN

US CUSTOMARY UNITS

SPECIMEN ID	HOLE ID	HOLE DIAM IN.	BOLT DIAM IN.	PANEL WIDTH IN.	EDGE DIST. IN.	PANEL THICK. IN.	FAILURE LOAD LB	FAILURE MODE	BEARING STRENGTH KSI	TENSION STRENGTH KSI	SHEAROUT STRENGTH KSI
FIBER PATTERN - 25 PCT 0 DEG., 50 PCT ±45 DEG., 25 PCT 90 DEG.											
IS-1-1		.2532	.2532	.992	1.000	.1810	5040.0	TENS	55.0	37.7	8.0
IS-1-2		.2565	.2565	1.004	1.000	.1815	5300.0	TENS	56.9	39.1	8.4
IS-1-3		.2542	.2542	1.005	1.000	.1817	5190.0	TENS	56.2	38.0	8.2
IS-1-4		.2569	.2569	1.001	1.000	.1826	5180.0	TENS	55.2	38.1	8.1
FIBER PATTERN - 37.5 PCT 0 DEG., 37.5 PCT ±45 DEG., 25 PCT 90 DEG.											
IS-2-1		.2506	.2506	1.009	1.000	.1817	6020.0	TENS	66.1	43.7	9.5
IS-2-2		.2534	.2534	1.010	1.000	.1858	6420.0	TENS	68.2	45.7	9.9
IS-2-3		.2513	.2513	1.007	1.000	.1791	6220.0	TENS	69.1	45.9	9.9
IS-2-4		.2512	.2512	1.005	1.000	.1830	5750.0	TENS	62.5	41.7	9.0
FIBER PATTERN - 37.5 PCT 0 DEG., 50 PCT ±45 DEG., 12.5 PCT 90 DEG.											
IS-3-1		.2522	.2522	1.002	1.000	.1676	6300.0	TENS	74.5	50.2	10.8
IS-3-2		.2516	.2516	1.001	1.000	.1701	6160.0	TENS	72.0	48.3	10.4
IS-3-3		.2506	.2506	1.000	1.000	.1701	6260.0	TENS	73.4	49.1	10.5
IS-3-4		.2567	.2567	1.007	1.000	.1864	5940.0	TENS	62.1	42.5	9.1

NOTE THAT TENSION STRENGTH REFERS TO ENTIRE LOAD AT NET SECTION

TABLE XVA

INTERACTION SPECIMENS
(TENSILE LOADING)

S-GLASS LONGITUDINAL PLIES, GRAPHITE CROSS PLIES, EPOXY RESIN

SI UNITS

SPECIMEN ID	HOLE ID	HOLE DIAM MM	BOLT DIAM MM	PANEL WIDTH MM	EDGE DIST. MM	PANEL THICK. MM	FAILURE LOAD KNEWTON	FAILURE MODE	BEARING STRENGTH MPASCAL	TENSION STRENGTH MPASCAL	SHEAROUT STRENGTH MPASCAL
FIBER PATTERN - 25 PCT 0, 50 PCT ±π/4, 25 PCT π/2											
IS-4-1		6.411	6.411	25.38	25.40	4.521	29.6696	BRG	511.8	345.9	73.9
IS-4-2		6.441	6.441	25.37	25.40	4.519	31.8938	TENS	547.9	372.9	79.6
IS-4-3		6.358	6.358	25.54	25.40	4.508	30.4258	TAB	530.7	351.8	75.9
IS-4-4		6.383	6.383	25.39	25.40	4.496	31.3155	BRG	545.6	366.4	78.4
FIBER PATTERN - 37.5 PCT 0, 37.5 PCT ±π/4, 25 PCT π/2											
IS-5-1		6.383	6.383	25.52	25.40	4.455	35.7637	BRG	628.8	419.5	90.4
IS-5-2		6.363	6.363	25.47	25.40	4.417	33.4951	BRG	595.9	396.8	85.3
IS-5-3		6.380	6.380	25.32	25.40	4.534	35.0075	BRG	605.1	407.7	86.9
IS-5-4		6.353	6.353	25.52	25.40	4.491	34.9630	BRG	612.8	406.2	87.6
FIBER PATTERN - 37.5 PCT 0, 50 PCT ±π/4, 12.5 PCT π/2											
IS-6-1		6.358	6.358	25.45	25.40	4.341	34.6072	BRG	627.0	417.6	89.7
IS-6-2		6.396	6.396	25.46	25.40	4.402	35.1410	BRG	624.1	418.8	89.9
IS-6-3		6.370	6.370	25.50	25.40	4.404	35.2744	BRG	628.6	418.6	90.1
IS-6-4		6.363	6.363	25.36	25.40	4.379	35.6747	BRG	640.2	428.9	91.7

NOTE THAT TENSION STRENGTH REFERS TO ENTIRE LOAD AT NET SECTION

TABLE XVB

INTERACTION SPECIMENS
(TENSILE LOADING)

S-GLASS LONGITUDINAL PLIES, GRAPHITE CROSS PLIES, EPOXY RESIN

US CUSTOMARY UNITS

SPECIMEN ID	HOLE ID	HOLE DIAM IN.	BOLT DIAM IN.	PANEL WIDTH IN.	EDGE DIST. IN.	PANEL THICK. IN.	FAILURE LOAD LB	FAILURE MODE	BEARING STRENGTH KSI	TENSION STRENGTH KSI	SHEAROUT STRENGTH KSI
FIBER PATTERN - 25 PCT 0 DEG., 50 PCT ±45 DEG., 25 PCT 90 DEG.											
IS-4-1		.2524	.2524	.999	1.000	.1780	6670.0	BRG	74.2	50.2	10.7
IS-4-2		.2536	.2536	.999	1.000	.1779	7170.0	TENS	79.5	54.1	11.5
IS-4-3		.2503	.2503	1.005	1.000	.1775	6840.0	TAB	77.0	51.0	11.0
IS-4-4		.2513	.2513	1.000	1.000	.1770	7040.0	BRG	79.1	53.1	11.4
FIBER PATTERN - 37.5 PCT 0 DEG., 37.5 PCT ±45 DEG., 25 PCT 90 DEG.											
IS-5-1		.2513	.2513	1.005	1.000	.1754	8040.0	BRG	91.2	60.8	13.1
IS-5-2		.2505	.2505	1.003	1.000	.1739	7530.0	BRG	86.4	57.6	12.4
IS-5-3		.2512	.2512	.997	1.000	.1785	7870.0	BRG	87.8	59.1	12.6
IS-5-4		.2501	.2501	1.005	1.000	.1768	7860.0	BRG	88.9	58.9	12.7
FIBER PATTERN - 37.5 PCT 0 DEG., 50 PCT ±45 DEG., 12.5 PCT 90 DEG.											
IS-6-1		.2503	.2503	1.002	1.000	.1709	7780.0	BRG	90.9	60.6	13.0
IS-6-2		.2518	.2518	1.002	1.000	.1733	7900.0	BRG	90.5	60.7	13.0
IS-6-3		.2508	.2508	1.004	1.000	.1734	7930.0	BRG	91.2	60.7	13.1
IS-6-4		.2505	.2505	.998	1.000	.1724	8020.0	BRG	92.9	62.2	13.3

NOTE THAT TENSION STRENGTH REFERS TO ENTIRE LOAD AT NET SECTION

TABLE XVIA

INTERACTION SPECIMENS
(COMPRESSIVE LOADING)

ALL GRAPHITE FIBERS, EPOXY RESIN

SI UNITS

SPECIMEN ID	HOLE ID	HOLE DIAM MM	BOLT DIAM MM	PANEL WIDTH MM	EDGE DIST. MM	PANEL THICK. MM	FAILURE LOAD KNEWTON	FAILUPE MODE	BEARING STRENGTH MPASCAL	COMPR. STRENGTH MPASCAL	SHEAROUT STRENGTH MPASCAL
FIBER PATTERN - 25 PCT 0, 50 PCT ±π/4, 25 PCT π/2											
IS-1-5		6.525	6.525	25.32	25.40	4.699	36.2530	BRG	591.2	410.5	87.1
IS-1-6		6.579	6.579	25.47	25.40	4.651	39.2556	BUCKL	641.5	446.9	95.4
IS-1-7		6.441	6.441	25.54	25.40	4.379	40.8792	BRG	724.6	488.9	105.2
IS-1-8		6.502	6.502	25.31	25.40	4.585	37.0092	BUCKL	620.7	429.1	91.1
FIBER PATTERN - 37.5 PCT 0, 37.5 PCT ±π/4, 25 PCT π/2											
IS-2-5		6.360	6.360	25.48	25.40	4.666	41.3462	BRG	696.6	463.4	99.7
IS-2-6		6.368	6.368	25.45	25.40	4.602	41.8133	BRG	713.4	476.1	102.2
IS-2-7		6.413	6.413	25.42	25.40	4.699	44.3933	BUCKL	736.5	497.0	106.4
IS-2-8		6.380	6.380	25.15	25.40	4.646	40.8347	BUCKL	688.8	468.3	98.9
FIBER PATTERN - 37.5 PCT 0, 50 PCT ±π/4, 12.5 PCT π/2											
IS-3-5		6.431	6.431	25.49	25.40	4.689	32.4276	BRG	537.7	362.8	77.9
IS-3-6		6.472	6.472	25.46	25.40	4.585	34.1624	BRG	575.7	392.4	84.0
IS-3-7		6.449	6.449	25.41	25.40	4.448	37.0092	BUCKL	645.2	439.0	93.8
IS-3-8		6.360	6.360	25.42	25.40	4.557	31.6713	BUCKL	546.4	364.6	78.2

NOTE THAT COMPP. STRENGTH REFERS TO ENTIRE COMPRESSIVE LOAD AT NET SECTION

TABLE XVIB

INTERACTION SPECIMENS
(COMPRESSIVE LOADING)

ALL GRAPHITE FIBERS, EPOXY RESIN

US CUSTOMARY UNITS

SPECIMEN ID	HOLE ID	HOLE DIAM IN.	BOLT DIAM IN.	PANEL WIDTH IN.	EDGE DIST. IN.	PANEL THICK. IN.	FAILURE LOAD LB	FAILURE MODE	BEARING STRENGTH KSI	COMPR. STRENGTH KSI	SHEAROUT STRENGTH KSI
FIBER PATTERN - 25 PCT 0 DEG., 50 PCT ±45 DEG., 25 PCT 90 DEG.											
IS-1-5		.2569	.2569	.997	1.000	.1850	8150.0	BRG	85.7	59.5	12.6
IS-1-6		.2590	.2590	1.003	1.000	.1831	8825.0	BUCKL	93.0	64.8	13.8
IS-1-7		.2536	.2536	1.005	1.000	.1724	9190.0	BRG	105.1	70.9	15.3
IS-1-8		.2560	.2560	.997	1.000	.1805	8320.0	BUCKL	90.0	62.2	13.2
FIBER PATTERN - 37.5 PCT 0 DEG., 37.5 PCT ±45 DEG., 25 PCT 90 DEG.											
IS-2-5		.2504	.2504	1.003	1.000	.1837	9295.0	BRG	101.0	67.2	14.5
IS-2-6		.2507	.2507	1.002	1.000	.1812	9400.0	BRG	103.5	69.0	14.8
IS-2-7		.2525	.2525	1.001	1.000	.1850	9980.0	BUCKL	106.8	72.1	15.4
IS-2-8		.2512	.2512	.990	1.000	.1829	9180.0	BUCKL	99.9	67.9	14.4
FIBER PATTERN - 37.5 PCT 0 DEG., 50 PCT ±45 DEG., 12.5 PCT 90 DEG.											
IS-3-5		.2532	.2532	1.004	1.000	.1846	7290.0	BRG	78.0	52.6	11.3
IS-3-6		.2548	.2548	1.002	1.000	.1805	7680.0	BRG	83.5	56.9	12.2
IS-3-7		.2539	.2539	1.000	1.000	.1751	8320.0	BUCKL	93.6	63.7	13.6
IS-3-8		.2504	.2504	1.001	1.000	.1794	7120.0	BUCKL	79.2	52.9	11.3

NOTE THAT COMPR. STRENGTH REFERS TO ENTIRE COMPRESSIVE LOAD AT NET SECTION

TABLE XVIIA

INTERACTION SPECIMENS
(COMPRESSIVE LOADING)

S-GLASS LONGITUDINAL PLIES, GRAPHITE CROSS PLIES, EPOXY RESIN

SI UNITS

SPECIMEN ID	HOLE ID	HOLE DIAM MM	BOLT DIAM MM	PANEL WIDTH MM	EDGE DIST. MM	PANEL THICK. MM	FAILURE LOAD KNEWTON	FAILURE MODE	BEARING STRENGTH MPASCAL	COMPR. STRENGTH MPASCAL	SHEAROUT STRENGTH MPASCAL
FIBER PATTERN - 25 PCT 0, 50 PCT ±π/4, 25 PCT π/2											
IS-4-5		6.396	6.396	25.52	25.40	4.562	31.5601	BUCKL	540.9	361.8	77.9
IS-4-6		6.408	6.408	25.54	25.40	4.539	32.5165	BUCKL	558.9	374.4	80.7
IS-4-7		6.411	6.411	25.51	25.40	4.582	34.8296	BUCKL	592.8	398.1	85.6
IS-4-8		6.383	6.383	25.38	25.40	4.605	32.7834	BUCKL	557.7	374.7	80.1
FIBER PATTERN - 37.5 PCT 0, 37.5 PCT ±π/4, 25 PCT π/2											
IS-5-5		6.436	6.436	25.53	25.40	4.448	29.3138	BUCKL	512.0	345.2	74.3
IS-5-6		6.447	6.447	25.26	25.40	4.404	30.6483	BUCKL	539.7	369.8	78.4
IS-5-7		6.355	6.355	25.52	25.40	4.463	38.0768	BUCKL	671.3	445.1	96.0
IS-5-8		6.406	6.406	25.37	25.40	4.432	33.9399	BUCKL	597.7	403.8	86.2
FIBER PATTERN - 37.5 PCT 0, 50 PCT ±π/4, 12.5 PCT π/2											
IS-6-5		6.368	6.368	25.48	25.40	4.381	34.2291	BUCKL	613.4	408.8	87.9
IS-6-6		6.353	6.353	25.53	25.40	4.430	34.1624	BUCKL	607.0	402.1	86.8
IS-6-7		6.363	6.363	25.27	25.40	4.392	36.4754	BUCKL	652.7	439.2	93.5
IS-6-8		6.434	6.434	25.26	25.40	4.346	34.8741	BUCKL	623.6	426.4	90.4

NOTE THAT COMPR. STRENGTH REFERS TO ENTIRE COMPRESSIVE LOAD AT NET SECTION

TABLE XVIIB

INTERACTION SPECIMENS
(COMPRESSIVE LOADING)

S-GLASS LONGITUDINAL PLIES, GRAPHITE CROSS PLIES, EPOXY RESIN

US CUSTOMARY UNITS

SPECIMEN ID	HOLE ID	HOLE DIAM IN.	BOLT DIAM IN.	PANEL WIDTH IN.	EDGE DIST. IN.	PANEL THICK. IN.	FAILURE LOAD LB	FAILURE MODE	BEARING STRENGTH KSI	COMPR. STRENGTH KSI	SHEAROUT STRENGTH KSI
FIBER PATTERN - 25 PCT 0 DEG., 50 PCT ±45 DEG., 25 PCT 90 DEG.											
IS-4-5		.2518	.2518	1.005	1.000	.1796	7095.0	BUCKL	78.4	52.5	11.3
IS-4-6		.2523	.2523	1.006	1.000	.1787	7310.0	BUCKL	81.1	54.3	11.7
IS-4-7		.2524	.2524	1.004	1.000	.1804	7830.0	BUCKL	86.0	57.7	12.4
IS-4-8		.2513	.2513	.999	1.000	.1813	7370.0	BUCKL	80.9	54.3	11.6
FIBER PATTERN - 37.5 PCT 0 DEG., 37.5 PCT ±45 DEG., 25 PCT 90 DEG.											
IS-5-5		.2534	.2534	1.005	1.000	.1751	6590.0	BUCKL	74.3	50.1	10.8
IS-5-6		.2538	.2538	.995	1.000	.1734	6890.0	BUCKL	78.3	53.6	11.4
IS-5-7		.2502	.2502	1.005	1.000	.1757	8560.0	BUCKL	97.4	64.6	13.9
IS-5-8		.2522	.2522	.999	1.000	.1745	7630.0	BUCKL	86.7	58.6	12.5
FIBER PATTERN - 37.5 PCT 0 DEG., 50 PCT ±45 DEG., 12.5 PCT 90 DEG.											
IS-6-5		.2507	.2507	1.003	1.000	.1725	7695.0	BUCKL	89.0	59.3	12.8
IS-6-6		.2501	.2501	1.005	1.000	.1744	7680.0	BUCKL	88.0	58.3	12.6
IS-6-7		.2505	.2505	.995	1.000	.1729	8200.0	BUCKL	94.7	63.7	13.6
IS-6-8		.2533	.2533	.994	1.000	.1711	7840.0	BUCKL	90.4	61.8	13.1

NOTE THAT COMPR. STRENGTH REFERS TO ENTIRE COMPRESSIVE LOAD AT NET SECTION

TABLE XVIIIA

PIN CONNECTION SPECIMENS

ALL GRAPHITE FIBERS, EPOXY RESIN
FIBER PATTERN - 25 PCT 0, 50 PCT ±π/4, 25 PCT π/2

SI UNITS

SPECIMEN ID	HOLE ID	HOLE DIAM MM	BOLT DIAM MM	PANEL WIDTH MM	EDGE DIST. MM	PANEL THICK. MM	FAILURE LOAD KNEWTON	FAILURE MODE	BEARING STRENGTH MPASCAL	TENSION STRENGTH MPASCAL	SHEAROUT STRENGTH MPASCAL
PC-1-1	A	6.449	6.337	63.69	12.54	2.306	6.8058	BRG	465.6	51.6	158.4
PC-1-1	B	6.444	6.337	63.85	37.97	2.322	6.6723	BRG	453.5	50.1	41.4
PC-1-1	C	6.429	6.337	64.16	50.89	2.296	5.9829	BRG	411.2	45.1	27.3
PC-1-1	D	6.429	6.337	64.41	25.59	2.306	6.5611	BRG	448.9	49.1	63.6
PC-1-2	A	6.454	6.337	64.02	12.55	2.304	6.6723	BRG	457.0	50.3	155.4
PC-1-2	B	6.447	6.337	63.94	37.82	2.324	4.9153	BRG	333.7	36.8	30.6
PC-1-2	C	6.434	6.337	63.91	50.95	2.294	5.7382	BRG	394.8	43.5	26.2
PC-1-2	D	6.413	6.337	63.99	25.59	2.309	6.4944	BRG	443.9	48.9	62.8

TABLE XVIIIB

PIN CONNECTION SPECIMENS

ALL GRAPHITE FIBERS, EPOXY RESIN
FIBER PATTERN - 25 PCT 0 DEG., 50 PCT ±45 DEG., 25 PCT 90 DEG.

US CUSTOMARY UNITS

SPECIMEN ID	HOLE ID	HOLE DIAM IN.	BOLT DIAM IN.	PANEL WIDTH IN.	EDGE DIST. IN.	PANEL THICK. IN.	FAILURE LOAD LB	FAILURE MODE	BEARING STRENGTH KSI	TENSION STRENGTH KSI	SHEAROUT STRENGTH KSI
PC-1-1	A	.2539	.2495	2.507	.494	.0908	1530.0	BRG	67.5	7.5	23.0
PC-1-1	B	.2537	.2495	2.514	1.495	.0914	1500.0	BRG	65.8	7.3	6.0
PC-1-1	C	.2531	.2495	2.526	2.003	.0904	1345.0	BRG	59.6	6.5	4.0
PC-1-1	D	.2531	.2495	2.536	1.007	.0908	1475.0	BRG	65.1	7.1	9.2
PC-1-2	A	.2541	.2495	2.521	.494	.0907	1500.0	BRG	66.3	7.3	22.5
PC-1-2	B	.2538	.2495	2.517	1.489	.0915	1105.0	BRG	48.4	5.3	4.4
PC-1-2	C	.2533	.2495	2.516	2.006	.0903	1290.0	BRG	57.3	6.3	3.8
PC-1-2	D	.2525	.2495	2.519	1.007	.0909	1460.0	BRG	64.4	7.1	9.1

TABLE XIXA

SINGLE-LAP SPECIMENS

ALL GRAPHITE FIBERS, EPOXY RESIN
FIBER PATTERN - 25 PCT 0, 50 PCT ±π/4, 25 PCT π/2

SI UNITS

SPECIMEN ID	HOLE ID	HOLE DIAM MM	BOLT DIAM MM	PANEL WIDTH MM	EDGE DIST. MM	PANEL THICK. MM	FAILURE LOAD KNEWTON	FAILURE MODE	BEARING STRENGTH MPASCAL	TENSION STRENGTH MPASCAL	SHEAROUT STRENGTH MPASCAL
SL-1-1		6.584	6.335	25.31	25.80	4.608	19.5277	TENS	669.0	226.3	94.1
SL-1-2		6.540	6.342	25.33	25.57	4.590	20.6620	TENS	709.8	239.6	101.0
SL-1-3		6.558	6.335	25.33	25.85	4.597	19.9280	TENS	684.3	231.0	96.0
SL-1-4		6.548	6.342	25.36	25.75	4.597	17.8819	BRG	613.3	206.7	86.5

TABLE XIXB

SINGLE-LAP SPECIMENS

ALL GRAPHITE FIBERS, EPOXY RESIN
FIBER PATTERN - 25 PCT 0 DEG., 50 PCT ±45 DEG., 25 PCT 90 DEG.

US CUSTOMARY UNITS

SPECIMEN ID	HOLE ID	HOLE DIAM IN.	BOLT DIAM IN.	PANEL WIDTH IN.	EDGE DIST. IN.	PANEL THICK. IN.	FAILURE LOAD LB	FAILURE MODE	BEARING STRENGTH KSI	TENSION STRENGTH KSI	SHEAROUT STRENGTH KSI
SL-1-1		.2592	.2494	.997	1.016	.1814	4390.0	TENS	97.0	32.8	13.7
SL-1-2		.2575	.2497	.997	1.007	.1807	4645.0	TENS	102.9	34.8	14.6
SL-1-3		.2582	.2494	.997	1.018	.1810	4480.0	TENS	99.2	33.5	13.9
SL-1-4		.2578	.2497	.998	1.014	.1810	4020.0	BRG	88.9	30.0	12.6

TABLE XX

MONOLAYER PROPERTIES

GRAPHITE-EPOXY	E_L = 134.0 GPascal (19.44×10^6 psi)	E_T = 11.54 GPascal (1.674×10^6 psi)
	G_{LT} = 6.18 GPascal (0.897×10^6 psi)	ν_{LT} = 0.3785
	t_{ply} = 0.14 mm (0.0057 in.)	
	$F_{L(TENS)}$ = 1404 MPascal (203.66 ksi)	$F_{L(COMP)}$ = 1359 MPascal (197.13 ksi)
	$F_{T(TENS)}$ = 40.8 MPascal (5.922 ksi)	$F_{T(COMP)}$ = 142.4 MPascal (20.65 ksi)
	F_{LT} = 92.0 MPascal (13.34 ksi)	
GLASS-EPOXY	E_L = 57.2 GPascal (8.3×10^6 psi)	E_T = 19.99 GPascal (2.9×10^6 psi)
	G_{LT} = 5.93 GPascal (0.86×10^6 psi)	ν_{LT} = 0.26
	t_{ply} = 0.13 mm (0.0051 in.)	
	$F_{L(TENS)}$ = 1993 MPascal (289.0 ksi)	$F_{L(COMP)}$ = 1172 MPascal (170.0 ksi)
	$F_{T(TENS)}$ = 75.8 MPascal (11.0 ksi)	$F_{T(COMP)}$ = 200.0 MPascal (29.0 ksi)
	F_{LT} = 62.1 MPascal (9.0 ksi)	

TABLE XXI

CALCULATED LAMINATE MATERIAL MECHANICAL PROPERTIES

PANEL No.	MATERIAL	PLY ORIENTATION (%)			F_x^{tu} MPascal (psi)	F_x^{cu} MPascal (psi)	F_{xy}^{su} MPascal (psi)	E_x GPascal (10^6 psi)
	FIBER/RESIN	0 (0°)	±π/4 (±45°)	π/2 (90°)				
1	T300/N5208 T300/N5208 T300/N5208	25	50	25	468 (67900)	453 (65720)	340 (49250)	53.62 (7.777)
2	T300/N5208 T300/N5208 T300/N5208	37.5	37.5	25	622 (90270)	602 (87370)	255 (36940)	66.66 (9.668)
3	T300/N5208 T300/N5208 T300/N5208	37.5	50	12.5	614 (89110)	595 (86240)	340 (49250)	67.07 (9.727)
4	S1014/N5208 T300/N5208 T300/N5208	25	50	25	774 (112200)	504 (73140)	349 (50580)	33.80 (4.903)
5	S1014/N5208 T300/N5208 T300/N5208	37.5	37.5	25	850 (123300)	604 (87680)	265 (38460)	37.00 (5.867)
6	S1014/N5208 T300/N5208 T300/N5208	37.5	50	12.5	1000 (145000)	588 (85270)	353 (51270)	37.65 (5.460)

TABLE XXIIA

TENSION THROUGH-THE-HOLE SPECIMENS

ALL GRAPHITE FIBERS, EPOXY RESIN
FIBER PATTERN - 25 PCT 0, 50 PCT ±π/4, 25 PCT π/2

SI UNITS

SPECIMEN ID	HOLE ID	HOLE DIAM MM	BOLT DIAM MM	PANEL WIDTH MM	EDGE DIST. MM	PANEL THICK. MM	FAILURE LOAD KNEWTON	FAILURE MODE	BEARING STRENGTH MPASCAL	TENSION STRENGTH MPASCAL	SHEAROUT STRENGTH MPASCAL
TH-529-1		6.350	6.350	31.78	19.18	2.395	15.3998	TENS	1012.5	252.9	200.9
TH-529-2		6.350	6.350	31.42	19.30	2.438	14.5412	TENS	939.1	237.9	184.9
TH-529-3		6.350	6.350	31.88	18.92	2.413	12.4016	TENS	809.4	201.3	163.2
TH-531-1		6.350	6.350	31.45	25.53	2.273	15.5643	TENS	1078.2	272.8	153.2
TH-531-2		6.350	6.350	31.88	25.78	2.311	14.8571	TENS	1012.2	251.8	142.2
TH-531-3		6.350	6.350	31.65	25.65	2.291	14.1676	TENS	973.8	244.4	137.5
TH-533-1		6.401	6.350	31.29	38.51	2.438	15.6088	TENS	1008.1	257.2	90.7
TH-533-2		6.350	6.350	31.98	38.23	2.489	16.9433	TENS	1071.9	265.6	97.1
TH-533-3		6.350	6.350	31.70	38.35	2.413	17.2146	TENS	1123.5	281.4	101.4
TH-541-1		6.350	6.350	31.90	19.18	3.200	18.3934	TENS	905.1	224.9	179.6
TH-541-2		6.350	6.350	31.93	18.92	3.226	21.1380	TENS	1031.9	256.2	208.1
TH-541-3		6.350	6.350	31.75	19.18	3.327	20.1060	TENS	951.6	237.9	188.8
TH-543-1		6.350	6.350	31.27	25.53	3.251	22.9884	TENS	1113.5	283.8	158.2
TH-543-2		6.350	6.350	31.29	25.25	3.277	21.9831	TENS	1056.6	269.0	152.0
TH-543-3		6.350	6.350	31.90	25.27	3.226	21.5783	TENS	1053.4	261.8	151.4
TH-545-1		6.350	6.350	31.14	38.35	3.429	22.8728	TENS	1050.5	269.1	94.8
TH-545-2		6.350	6.350	31.95	38.35	3.454	21.2847	TENS	970.3	240.7	87.6
TH-545-3		6.350	6.350	31.95	38.25	3.429	22.0632	TENS	1013.3	251.3	91.7

TABLE XXIIB

TENSION THROUGH-THE-HOLE SPECIMENS

ALL GRAPHITE FIBERS, EPOXY RESIN
FIBER PATTERN - 25 PCT 0 DEG., 50 PCT ±45 DEG., 25 PCT 90 DEG.

US CUSTOMARY UNITS

SPECIMEN ID	HOLE ID	HOLE DIAM IN.	BOLT DIAM IN.	PANEL WIDTH IN.	EDGE DIST. IN.	PANEL THICK. IN.	FAILURE LOAD LB	FAILURE MODE	BEARING STRENGTH KSI	TENSION STRENGTH KSI	SHEAROUT STRENGTH KSI
TH-529-1		.2500	.2500	1.251	.755	.0943	3462.0	TENS	146.9	36.7	29.1
TH-529-2		.2500	.2500	1.237	.760	.0960	3269.0	TENS	136.2	34.5	26.8
TH-529-3		.2500	.2500	1.255	.745	.0950	2788.0	TENS	117.4	29.2	23.7
TH-531-1		.2500	.2500	1.238	1.005	.0895	3499.0	TENS	156.4	39.6	22.2
TH-531-2		.2500	.2500	1.255	1.015	.0910	3340.0	TENS	146.8	36.5	20.6
TH-531-3		.2500	.2500	1.246	1.010	.0902	3185.0	TENS	141.2	35.5	19.9
TH-533-1		.2500	.2500	1.232	1.516	.0960	3509.0	TENS	146.2	37.3	13.1
TH-533-2		.2500	.2500	1.259	1.505	.0980	3809.0	TENS	155.5	38.5	14.1
TH-533-3		.2500	.2500	1.248	1.510	.0950	3870.0	TENS	162.9	40.8	14.7
TH-541-1		.2500	.2500	1.256	.755	.1260	4135.0	TENS	131.3	32.6	26.0
TH-541-2		.2500	.2500	1.257	.745	.1270	4752.0	TENS	149.7	37.2	30.2
TH-541-3		.2500	.2500	1.250	.755	.1310	4520.0	TENS	138.0	34.5	27.4
TH-543-1		.2500	.2500	1.231	1.005	.1280	5168.0	TENS	161.5	41.2	22.9
TH-543-2		.2500	.2500	1.232	.994	.1290	4942.0	TENS	153.2	39.0	22.0
TH-543-3		.2500	.2500	1.256	.995	.1270	4851.0	TENS	152.8	38.0	22.0
TH-545-1		.2500	.2500	1.226	1.510	.1350	5142.0	TENS	152.4	39.0	13.8
TH-545-2		.2500	.2500	1.258	1.510	.1360	4785.0	TENS	140.7	34.9	12.7
TH-545-3		.2500	.2500	1.258	1.506	.1350	4960.0	TENS	147.0	36.4	13.3

TABLE XXIIIA

TENSION THROUGH-THE-HOLE SPECIMENS

ALL GRAPHITE FIBERS, EPOXY RESIN
FIBER PATTERN - 25 PCT 0, 50 PCT ±π/4, 25 PCT π/2

SI UNITS

SPECIMEN ID	HOLE ID	HOLE DIAM MM	BOLT DIAM MM	PANEL WIDTH MM	EDGE DIST. MM	PANEL THICK. MM	FAILURE LOAD KNEWTON	FAILURE MODE	BEARING STRENGTH MPASCAL	TENSION STRENGTH MPASCAL	SHEAROUT STRENGTH MPASCAL
TH-523-1		4.826	4.826	31.50	12.83	2.489	10.8937	TENS	906.8	164.1	210.1
TH-523-2		4.851	4.826	31.45	12.85	2.451	10.3199	TENS	872.4	158.3	201.9
TH-523-3		4.851	4.826	31.83	12.85	2.311	10.4845	TENS	939.9	168.2	217.5
TH-525-1		4.851	4.826	31.78	19.20	2.261	12.4105	TENS	1137.6	203.9	163.6
TH-525-2		4.851	4.826	31.29	19.20	2.261	11.1206	TENS	1019.3	186.0	146.6
TH-525-3		4.877	4.826	31.95	19.20	2.413	12.6196	TENS	1083.7	193.2	156.0
TH-527-1		4.826	4.826	31.37	32.00	2.332	13.0555	TENS	1160.2	210.9	94.6
TH-527-2		4.826	4.826	31.57	31.88	2.273	13.3224	TENS	1214.3	219.1	99.4
TH-527-3		4.826	4.826	31.93	31.90	2.332	13.3224	TENS	1183.9	210.8	96.9
TH-535-1		4.826	4.826	31.95	12.70	3.429	15.4353	TENS	932.7	165.9	218.8
TH-535-2		4.826	4.826	31.75	12.57	3.378	16.9032	TENS	1036.8	185.8	246.2
TH-535-3		4.826	4.826	31.98	12.57	3.404	16.8187	TENS	1023.9	182.0	243.2
TH-537-1		4.826	4.826	31.90	19.30	3.251	18.2866	TENS	1165.5	207.7	166.5
TH-537-2		4.826	4.826	31.93	19.18	3.353	16.6586	TENS	1029.5	183.3	148.2
TH-537-3		4.826	4.826	31.90	19.18	3.277	17.0145	TENS	1076.0	191.8	154.9
TH-539-1		4.851	4.826	31.93	31.90	3.277	18.7804	TENS	1187.7	211.7	97.2
TH-539-2		4.826	4.826	31.93	31.88	3.200	17.7929	TENS	1152.0	205.1	94.3
TH-539-3		4.826	4.826	31.78	32.00	3.327	20.4396	TENS	1272.9	227.9	103.8

TABLE XXIIIB

TENSION THROUGH-THE-HOLE SPECIMENS

ALL GRAPHITE FIBERS, EPOXY RESIN
FIBER PATTERN - 25 PCT 0 DEG., 50 PCT ±45 DEG., 25 PCT 90 DEG.

US CUSTOMARY UNITS

SPECIMEN ID	HOLE ID	HOLE DIAM IN.	BOLT DIAM IN.	PANEL WIDTH IN.	EDGE DIST. IN.	PANEL THICK. IN.	FAILURE LOAD LB	FAILURE MODE	BEARING STRENGTH KSI	TENSION STRENGTH KSI	SHEAROUT STRENGTH KSI
TH-523-1		.1900	.1900	1.240	.505	.0980	2449.0	TENS	131.5	23.8	30.5
TH-523-2		.1910	.1900	1.238	.506	.0965	2320.0	TENS	126.5	23.0	29.3
TH-523-3		.1910	.1900	1.253	.506	.0910	2357.0	TENS	136.3	24.4	31.5
TH-525-1		.1910	.1900	1.251	.756	.0890	2790.0	TENS	165.0	29.6	23.7
TH-525-2		.1910	.1900	1.232	.756	.0890	2500.0	TENS	147.8	27.0	21.3
TH-525-3		.1920	.1900	1.258	.756	.0950	2837.0	TENS	157.2	28.0	22.6
TH-527-1		.1900	.1900	1.235	1.260	.0918	2935.0	TENS	168.3	30.6	13.7
TH-527-2		.1900	.1900	1.243	1.255	.0895	2995.0	TENS	176.1	31.8	14.4
TH-527-3		.1900	.1900	1.257	1.256	.0918	2995.0	TENS	171.7	30.6	14.1
TH-535-1		.1900	.1900	1.258	.500	.1350	3470.0	TENS	135.3	24.1	31.7
TH-535-2		.1900	.1900	1.250	.495	.1330	3800.0	TENS	150.4	27.0	35.7
TH-535-3		.1900	.1900	1.259	.495	.1340	3781.0	TENS	148.5	26.4	35.3
TH-537-1		.1900	.1900	1.256	.760	.1280	4111.0	TENS	169.0	30.1	24.1
TH-537-2		.1900	.1900	1.257	.755	.1320	3745.0	TENS	149.3	26.6	21.5
TH-537-3		.1900	.1900	1.256	.755	.1290	3825.0	TENS	156.1	27.8	22.5
TH-539-1		.1910	.1900	1.257	1.256	.1290	4222.0	TENS	172.3	30.7	14.1
TH-539-2		.1900	.1900	1.257	1.255	.1260	4000.0	TENS	167.1	29.8	13.7
TH-539-3		.1900	.1900	1.251	1.260	.1310	4595.0	TENS	184.6	33.1	15.1

TABLE XXIVA

TENSION THROUGH-THE-HOLE SPECIMENS

ALL GRAPHITE FIBERS, EPOXY RESIN
FIBER PATTERN - 50 PCT 0, 50 PCT ±π/4

SI UNITS

SPECIMEN ID	HOLE ID	HOLE DIAM MM	BOLT DIAM MM	PANEL WIDTH MM	EDGE DIST. MM	PANEL THICK. MM	FAILURE LOAD KNEWTON	FAILURE MODE	BEARING STRENGTH MPASCAL	TENSION STRENGTH MPASCAL	SHEAROUT STRENGTH MPASCAL
TH-505-1		6.452	6.350	31.67	19.05	2.311	14.2566	SHR	971.3	244.5	194.9
TH-505-2		6.426	6.350	31.62	19.05	2.286	12.9666	SHR	893.3	225.1	179.1
TH-505-3		6.452	6.350	31.50	19.05	2.311	13.7984	SHR	940.1	238.4	188.6
TH-507-1		6.452	6.350	31.52	25.81	2.261	14.7637	SHR	1028.5	260.5	144.6
TH-507-2		6.426	6.350	31.62	25.81	2.311	15.8846	SHR	1082.2	272.7	152.1
TH-507-3		6.452	6.350	31.72	25.40	2.286	15.3019	SHR	1054.1	264.9	150.9
TH-509-1		6.452	6.350	31.98	38.51	2.311	14.8571	BRG	1012.2	251.8	91.1
TH-509-2		6.426	6.350	32.05	38.51	2.362	15.7289	BRG	1048.6	259.8	94.3
TH-509-3		6.426	6.350	31.86	38.51	2.311	15.4131	BRG	1050.1	262.0	94.5
TH-517-1		6.452	6.350	31.83	19.15	3.327	16.9032	TENS	800.0	200.2	159.5
TH-517-2		6.452	6.350	31.83	19.20	3.353	16.7031	TENS	784.5	196.3	155.9
TH-517-3		6.426	6.350	31.95	19.18	3.277	19.4165	TENS	933.2	232.1	185.6
TH-519-1		6.426	6.350	31.83	25.55	3.200	21.0623	TENS	1036.4	259.1	147.3
TH-519-2		6.452	6.350	31.83	25.60	3.200	21.1513	TENS	1040.8	260.5	147.7
TH-519-3		6.452	6.350	31.83	25.45	3.150	18.5713	TENS	928.6	232.4	132.7
TH-521-1		6.452	6.350	31.80	38.20	3.200	19.4832	TENS	958.7	240.2	87.0
TH-521-2		6.452	6.350	31.80	38.28	3.251	19.7946	TENS	958.8	240.2	86.8
TH-521-3		6.452	6.350	31.80	38.23	3.200	21.4404	TENS	1055.0	264.3	95.7

TABLE XXIVB

TENSION THROUGH-THE-HOLE SPECIMENS

ALL GRAPHITE FIBERS, EPOXY RESIN
FIBER PATTERN - 50 PCT 0 DEG., 50 PCT ±45 DEG.

US CUSTOMARY UNITS

SPECIMEN ID	HOLE ID	HOLE DIAM IN.	BOLT DIAM IN.	PANEL WIDTH IN.	EDGE DIST. IN.	PANEL THICK. IN.	FAILURE LOAD LB	FAILURE MODE	BEARING STRENGTH KSI	TENSION STRENGTH KSI	SHEAROUT STRENGTH KSI
TH-505-1		.2540	.2500	1.247	.750	.0910	3205.0	SHR	140.9	35.5	28.3
TH-505-2		.2530	.2500	1.245	.750	.0900	2915.0	SHR	129.6	32.7	26.0
TH-505-3		.2540	.2500	1.240	.750	.0910	3102.0	SHR	136.4	34.6	27.4
TH-507-1		.2540	.2500	1.241	1.016	.0890	3319.0	SHR	149.2	37.8	21.0
TH-507-2		.2530	.2500	1.245	1.016	.0910	3571.0	SHR	157.0	39.6	22.1
TH-507-3		.2540	.2500	1.249	1.000	.0900	3440.0	SHR	152.9	38.4	21.9
TH-509-1		.2540	.2500	1.259	1.516	.0910	3340.0	BRG	146.8	36.5	13.2
TH-509-2		.2530	.2500	1.262	1.516	.0930	3536.0	BRG	152.1	37.7	13.7
TH-509-3		.2530	.2500	1.255	1.516	.0910	3465.0	BRG	152.3	38.0	13.7
TH-517-1		.2540	.2500	1.253	.754	.1310	3800.0	TENS	116.0	29.0	23.1
TH-517-2		.2540	.2500	1.253	.756	.1320	3755.0	TENS	113.8	28.5	22.6
TH-517-3		.2530	.2500	1.258	.755	.1290	4365.0	TENS	135.3	33.7	26.9
TH-519-1		.2530	.2500	1.253	1.006	.1260	4735.0	TENS	150.3	37.6	21.4
TH-519-2		.2540	.2500	1.253	1.008	.1260	4755.0	TENS	151.0	37.8	21.4
TH-519-3		.2540	.2500	1.253	1.002	.1240	4175.0	TENS	134.7	33.7	19.2
TH-521-1		.2540	.2500	1.252	1.504	.1260	4380.0	TENS	139.0	34.8	12.6
TH-521-2		.2540	.2500	1.252	1.507	.1280	4450.0	TENS	139.1	34.8	12.6
TH-521-3		.2540	.2500	1.252	1.505	.1260	4820.0	TENS	153.0	38.3	13.9

TABLE XXVA

TENSION THROUGH-THE-HOLE SPECIMENS

ALL GRAPHITE FIBERS, EPOXY RESIN
FIBER PATTERN - 50 PCT 0, 50 PCT ±π/4

SI UNITS

SPECIMEN ID	HOLE ID	HOLE DIAM MM	BOLT DIAM MM	PANEL WIDTH MM	EDGE DIST. MM	PANEL THICK. MM	FAILURE LOAD KNEWTON	FAILURE MODE	BEARING STRENGTH MPASCAL	TENSION STRENGTH MPASCAL	SHEAROUT STRENGTH MPASCAL
TH- 1-1		4.826	4.826	31.60	13.08	2.367	9.3324	SHR	827.5	149.2	187.2
TH- 1-2		4.902	4.826	31.55	12.70	2.368	9.0299	SHR	783.7	141.9	184.5
TH- 1-3		4.877	4.826	31.75	12.70	2.388	9.1989	SHR	798.3	143.4	187.7
TH-501-1		4.826	4.826	31.62	19.67	2.337	10.8981	SHR	966.4	174.0	143.4
TH-501-2		4.851	4.826	31.57	19.46	2.388	10.8047	SHR	937.7	169.4	132.9
TH-501-3		4.826	4.826	31.70	19.46	2.362	10.2754	SHR	901.4	161.9	127.6
TH-503-1		4.826	4.826	31.88	32.54	2.337	11.8545	BRG	1051.2	187.5	84.2
TH-503-2		4.826	4.826	31.90	32.54	2.311	11.2229	BRG	1006.1	179.3	80.6
TH-503-3		4.826	4.826	32.18	32.16	2.311	11.3074	BRG	1013.7	178.8	82.2
TH-511-1		4.826	4.826	31.80	12.67	3.150	12.8776	TENS	847.2	151.6	199.2
TH-511-2		4.826	4.826	31.80	12.78	3.251	13.5226	TENS	861.8	154.2	200.7
TH-511-3		4.826	4.826	31.80	12.80	3.175	12.3972	TENS	809.1	144.8	187.9
TH-513-1		4.826	4.826	31.80	19.23	3.175	16.7031	TENS	1090.1	195.0	156.4
TH-513-2		4.826	4.826	31.83	19.05	3.200	15.6355	TENS	1012.3	180.9	146.8
TH-513-3		4.826	4.826	31.83	19.18	3.150	14.5101	TENS	954.6	170.6	137.4
TH-515-1		4.826	4.826	31.98	31.98	3.353	17.7751	TENS	1098.5	195.3	89.7
TH-515-2		4.826	4.826	31.85	31.85	3.378	17.8596	TENS	1095.5	195.6	89.8
TH-515-3		4.826	4.826	31.83	32.05	3.327	17.1701	TENS	1069.3	191.1	87.0

TABLE XXVB

TENSION THROUGH-THE-HOLE SPECIMENS

ALL GRAPHITE FIBERS, EPOXY RESIN
FIBER PATTERN - 50 PCT 0 DEG., 50 PCT ±45 DEG.

US CUSTOMARY UNITS

SPECIMEN ID	HOLE ID	HOLE DIAM IN.	BOLT DIAM IN.	PANEL WIDTH IN.	EDGE DIST. IN.	PANEL THICK. IN.	FAILURE LOAD LB	FAILURE MODE	BEARING STRENGTH KSI	TENSION STRENGTH KSI	SHEAROUT STRENGTH KSI
TH- 1-1		.1900	.1900	1.244	.515	.0920	2098.0	SHR	120.0	21.6	27.1
TH- 1-2		.1930	.1900	1.242	.500	.0940	2030.0	SHR	113.7	20.6	26.8
TH- 1-3		.1920	.1900	1.250	.500	.0940	2068.0	SHR	115.8	20.8	27.2
TH-501-1		.1900	.1900	1.245	.735	.0920	2450.0	SHR	140.2	25.2	20.8
TH-501-2		.1910	.1900	1.243	.766	.0940	2429.0	SHR	136.0	24.6	19.3
TH-501-3		.1900	.1900	1.248	.766	.0930	2310.0	SHR	130.7	23.5	18.5
TH-503-1		.1900	.1900	1.255	1.281	.0920	2665.0	BRG	152.5	27.2	12.2
TH-503-2		.1900	.1900	1.256	1.281	.0910	2523.0	BRG	145.9	26.0	11.7
TH-503-3		.1900	.1900	1.267	1.266	.0910	2542.0	BRG	147.0	25.9	11.9
TH-511-1		.1900	.1900	1.252	.499	.1240	2895.0	TENS	122.9	22.0	28.9
TH-511-2		.1900	.1900	1.252	.503	.1280	3040.0	TENS	125.0	22.4	29.1
TH-511-3		.1900	.1900	1.252	.504	.1250	2787.0	TENS	117.3	21.0	27.3
TH-513-1		.1900	.1900	1.252	.757	.1250	3755.0	TENS	158.1	28.3	22.7
TH-513-2		.1900	.1900	1.253	.750	.1260	3515.0	TENS	146.8	26.2	21.3
TH-513-3		.1900	.1900	1.253	.755	.1240	3262.0	TENS	138.5	24.7	19.9
TH-515-1		.1900	.1900	1.259	1.259	.1320	3996.0	TENS	159.3	28.3	13.0
TH-515-2		.1900	.1900	1.254	1.254	.1330	4015.0	TENS	158.9	28.4	13.0
TH-515-3		.1900	.1900	1.253	1.262	.1310	3860.0	TENS	155.1	27.7	12.6

TABLE XXVIA

FILLED-HOLE SPECIMENS
(TENSILE AND COMPRESSIVE LOADING)

ALL GRAPHITE FIBERS, EPOXY RESIN
SI UNITS

SPECIMEN ID	HOLE ID	HOLE DIAM MM	BOLT DIAM MM	PANEL WIDTH MM	EDGE DIST. MM	PANEL THICK. MM	FAILURE LOAD KNEWTON	FAILURE MODE	NET SECT. STRENGTH MPASCAL
			FIBER PATTERN - 25 PCT 0, 75 PCT ±π/4						
TH- 1-1		6.35	6.35	38.25	50.80	1.118	10.3999	TENS	291.7
TH- 1-2		6.35	6.35	38.25	50.80	1.118	9.6571	TENS	270.9
TCL- 1-3		.00	.00	25.35	50.80	1.118	12.1259	TENS	428.0
CCL- 1-4		.00	.00	25.50	50.80	1.143	13.4737	COMPR	462.2
TH- 1-5		25.40	25.40	50.85	50.80	1.143	7.5798	TENS	260.6
CH- 1-6		6.35	6.35	38.35	50.80	1.118	9.3769	COMPR	262.2
CH- 1-7		6.35	6.35	38.33	50.80	1.143	10.6668	COMPR	291.8
			FIBER PATTERN - 50 PCT 0, 50 PCT ±π/4						
TH- 2-1		6.35	6.35	38.15	50.80	1.092	12.9132	TENS	371.8
TH- 2-2		6.35	6.35	38.33	50.80	1.118	12.2415	TENS	342.5
TCL- 2-3		.00	.00	25.40	50.80	1.143	18.0776	TENS	622.7
CCL- 2-4		.00	.00	25.53	50.80	1.118	18.2822	COMPR	640.8
TH- 2-5		25.40	25.40	50.98	50.80	1.118	9.6571	TENS	337.8
CH- 2-6		6.35	6.35	38.28	50.80	1.092	12.9132	COMPR	370.3
CH- 2-7		6.35	6.35	38.20	50.80	1.067	12.4639	COMPR	366.8
			FIBER PATTERN - 75 PCT 0, 25 PCT ±π/4						
TH- 3-1		6.35	6.35	38.25	50.80	1.067	18.0553	TENS	530.5
TH- 3-2		6.35	6.35	38.10	50.80	1.092	19.9903	TENS	576.5
TCL- 3-3		.00	.00	25.48	50.80	1.118	24.7054	TENS	867.7
CCL- 3-4		.00	.00	25.43	50.80	1.118	24.3585	COMPR	857.2
TH- 3-5		25.40	25.40	50.95	50.80	1.092	13.3625	TENS	478.8
CH- 3-6		6.35	6.35	38.18	50.80	1.092	15.1062	COMPR	434.6
CH- 3-7		6.35	6.35	38.28	50.80	1.041	16.0581	COMPR	483.0

TABLE XXVIB

FILLED-HOLE SPECIMENS
(TENSILE AND COMPRESSIVE LOADING)

ALL GRAPHITE FIBERS, EPOXY RESIN
US CUSTOMARY UNITS

SPECIMEN ID	HOLE ID	HOLE DIAM IN.	BOLT DIAM IN.	PANEL WIDTH IN.	EDGE DIST. IN.	PANEL THICK. IN.	FAILURE LOAD LB	FAILURE MODE	NET SECT. STRENGTH KSI
FIBER PATTERN - 25 PCT 0 DEG., 75 PCT ±45 DEG.									
TH- 1-1		.250	.250	1.506	2.000	.0440	2338.0	TENS	42.3
TH- 1-2		.250	.250	1.506	2.000	.0440	2171.0	TENS	39.3
TCL- 1-3		.000	.000	.998	2.000	.0440	2726.0	TENS	62.1
CCL- 1-4		.000	.000	1.004	2.000	.0450	3029.0	COMPR	67.0
TH- 1-5		1.000	1.000	2.002	2.000	.0450	1704.0	TENS	37.8
CH- 1-6		.250	.250	1.510	2.000	.0440	2108.0	COMPR	38.0
CH- 1-7		.250	.250	1.509	2.000	.0450	2398.0	COMPR	42.3
FIBER PATTERN - 50 PCT 0 DEG., 50 PCT ±45 DEG.									
TH- 2-1		.250	.250	1.502	2.000	.0430	2903.0	TENS	53.9
TH- 2-2		.250	.250	1.509	2.000	.0440	2752.0	TENS	49.7
TCL- 2-3		.000	.000	1.000	2.000	.0450	4064.0	TENS	90.3
CCL- 2-4		.000	.000	1.005	2.000	.0440	4110.0	COMPR	92.9
TH- 2-5		1.000	1.000	2.007	2.000	.0440	2171.0	TENS	49.0
CH- 2-6		.250	.250	1.507	2.000	.0430	2903.0	COMPR	53.7
CH- 2-7		.250	.250	1.504	2.000	.0420	2802.0	COMPR	53.2
FIBER PATTERN - 75 PCT 0 DEG., 25 PCT ±45 DEG.									
TH- 3-1		.250	.250	1.506	2.000	.0420	4059.0	TENS	76.9
TH- 3-2		.250	.250	1.500	2.000	.0430	4494.0	TENS	83.6
TCL- 3-3		.000	.000	1.003	2.000	.0440	5554.0	TENS	125.8
CCL- 3-4		.000	.000	1.001	2.000	.0440	5476.0	COMPR	124.3
TH- 3-5		1.000	1.000	2.006	2.000	.0430	3004.0	TENS	69.4
CH- 3-6		.250	.250	1.503	2.000	.0430	3396.0	COMPR	63.0
CH- 3-7		.250	.250	1.507	2.000	.0410	3610.0	COMPR	70.0

TABLE XXVIIA

FILLED-HOLE SPECIMENS
(TENSILE AND COMPRESSIVE LOADING)

ALL GRAPHITE FIBERS, EPOXY RESIN
SI UNITS

SPECIMEN ID	HOLE ID	HOLE DIAM MM	BOLT DIAM MM	PANEL WIDTH MM	EDGE DIST. MM	PANEL THICK. MM	FAILURE LOAD KNEWTON	FAILURE MODE	NET SECT. STRENGTH MPASCAL
FIBER PATTERN - 10 PCT 0, 80 PCT ±π/4, 10 PCT π/2									
TH- 4-1		6.35	6.35	38.28	50.80	1.346	10.7024	TENS	249.0
TH- 4-2		6.35	6.35	38.25	50.80	1.346	11.6188	TENS	270.5
TCL- 4-3		.00	.00	25.48	50.80	1.372	10.0752	TENS	288.3
CCL- 4-4		.00	.00	25.43	50.80	1.397	12.7842	COMPR	359.9
TH- 4-5		25.40	25.40	50.80	50.80	1.397	8.6207	TENS	242.9
CH- 4-6		6.35	6.35	39.70	50.80	1.346	10.9159	COMPR	243.1
CH- 4-7		6.35	6.35	38.13	50.80	1.346	11.5298	COMPR	269.5
FIBER PATTERN - 37.5 PCT 0, 50 PCT ±π/4, 12.5 PCT π/2									
TH- 5-1		6.35	6.35	38.28	50.80	1.118	9.1411	TENS	256.2
TH- 5-2		6.35	6.35	38.10	50.80	1.143	9.8795	TENS	272.2
TCL- 5-3		.00	.00	25.65	50.80	1.194	17.5171	TENS	572.0
CCL- 5-4		.00	.00	25.55	50.80	1.143	20.0303	COMPR	685.8
TH- 5-5		25.40	25.40	53.54	50.80	1.194	11.6232	TENS	346.0
CH- 5-6		6.35	6.35	38.30	50.80	1.092	11.2273	COMPR	321.7
CH- 5-7		6.35	6.35	38.25	50.80	1.143	12.5751	COMPR	344.9
FIBER PATTERN - 50 PCT 0, 40 PCT ±π/4, 10 PCT π/2									
TH- 6-1		6.35	6.35	38.25	50.80	1.372	14.3277	TENS	327.4
TH- 6-2		6.35	6.35	38.38	50.80	1.397	14.5991	TENS	326.3
TCL- 6-3		.00	.00	25.53	50.80	1.397	24.0649	TENS	674.8
CCL- 6-4		.00	.00	25.48	50.80	1.372	27.2009	COMPR	778.4
TH- 6-5		25.40	25.40	51.05	50.80	1.397	12.5929	TENS	351.4
CH- 6-6		6.35	6.35	38.28	50.80	1.397	14.3277	COMPR	321.2
CH- 6-7		6.35	6.35	38.30	50.80	1.346	14.5501	COMPR	338.3
FIBER PATTERN - 87.5 PCT 0, 12.5 PCT π/2									
TH- 7-1		6.35	6.35	38.35	50.80	1.092	22.9083	TENS	655.4
TH- 7-2		6.35	6.35	38.25	50.80	1.143	22.4146	TENS	614.7
TCL- 7-3		.00	.00	25.68	50.80	1.118	29.2070	TENS	017.7
CCL- 7-4		.00	.00	25.50	50.80	1.092	23.2998	COMPR	836.5
TH- 7-5		25.40	25.40	50.95	50.80	1.118	15.6088	TENS	546.6
CH- 7-6		6.35	6.35	38.30	50.80	1.118	11.8456	COMPR	331.7
CH- 7-7		6.35	6.35	38.33	50.80	1.092	13.3536	COMPR	382.3

TABLE XXVIIB

FILLED-HOLE SPECIMENS
(TENSILE AND COMPRESSIVE LOADING)

ALL GRAPHITE FIBERS, EPOXY RESIN
US CUSTOMARY UNITS

SPECIMEN ID	HOLE ID	HOLE DIAM IN.	BOLT DIAM IN.	PANEL WIDTH IN.	EDGE DIST. IN.	PANEL THICK. IN.	FAILURE LOAD LB	FAILURE MODE	NET SECT. STRENGTH KSI
FIBER PATTERN - 10 PCT 0 DEG., 80 PCT ±45 DEG., 10PCT 90 DEG.									
TH- 4-1		.250	.250	1.507	2.000	.0530	2406.0	TENS	36.1
TH- 4-2		.250	.250	1.506	2.000	.0530	2612.0	TENS	39.2
TCL- 4-3		.000	.000	1.003	2.000	.0540	2265.0	TENS	41.8
CCL- 4-4		.000	.000	1.001	2.000	.0550	2874.0	COMPR	52.2
TH- 4-5		1.000	1.000	2.000	2.000	.0550	1938.0	TENS	35.2
CH- 4-6		.250	.250	1.563	2.000	.0530	2454.0	COMPR	35.3
CH- 4-7		.250	.250	1.501	2.000	.0530	2592.0	COMPR	39.1
FIBER PATTERN - 37.5 PCT 0 DEG., 50 PCT ±45 DEG., 12.5 PCT 90 DEG.									
TH- 5-1		.250	.250	1.507	2.000	.0440	2055.0	TENS	37.2
TH- 5-2		.250	.250	1.500	2.000	.0450	2221.0	TENS	39.5
TCL- 5-3		.000	.000	1.010	2.000	.0470	3938.0	TENS	83.0
CCL- 5-4		.000	.000	1.006	2.000	.0450	4503.0	COMPR	99.5
TH- 5-5		1.000	1.000	2.108	2.000	.0470	2613.0	TENS	50.2
CH- 5-6		.250	.250	1.508	2.000	.0430	2524.0	COMPR	46.7
CH- 5-7		.250	.250	1.506	2.000	.0450	2827.0	COMPR	50.0
FIBER PATTERN - 50 PCT 0 DEG., 40 PCT ±45 DEG., 10PCT 90 DEG.									
TH- 6-1		.250	.250	1.506	2.000	.0540	3221.0	TENS	47.5
TH- 6-2		.250	.250	1.511	2.000	.0550	3282.0	TENS	47.3
TCL- 6-3		.000	.000	1.005	2.000	.0550	5410.0	TENS	97.9
CCL- 6-4		.000	.000	1.003	2.000	.0540	6115.0	COMPR	112.9
TH- 6-5		1.000	1.000	2.010	2.000	.0550	2831.0	TENS	51.0
CH- 6-6		.250	.250	1.507	2.000	.0550	3221.0	COMPR	46.6
CH- 6-7		.250	.250	1.508	2.000	.0530	3271.0	COMPR	49.1
FIBER PATTERN - 87.5 PCT 0 DEG., 12.5 PCT 90 DEG.									
TH- 7-1		.250	.250	1.510	2.000	.0430	5150.0	TENS	95.1
TH- 7-2		.250	.250	1.506	2.000	.0450	5039.0	TENS	89.2
TCL- 7-3		.000	.000	1.011	2.000	.0440	6566.0	TENS	147.6
CCL- 7-4		.000	.000	1.004	2.000	.0430	5238.0	COMPR	121.3
TH- 7-5		1.000	1.000	2.006	2.000	.0440	3509.0	TENS	79.3
CH- 7-6		.250	.250	1.508	2.000	.0440	2663.0	COMPR	48.1
CH- 7-7		.250	.250	1.509	2.000	.0430	3002.0	COMPR	55.5

TABLE XXVIIIA

FILLED-HOLE SPECIMENS
(TENSILE AND COMPRESSIVE LOADING)

ALL GRAPHITE FIBERS, EPOXY RESIN
SI UNITS

SPECIMEN ID	HOLE ID	HOLE DIAM MM	BOLT DIAM MM	PANEL WIDTH MM	EDGE DIST. MM	PANEL THICK. MM	FAILURE LOAD KNEWTON	FAILURE MODE	NET SECT. STRENGTH MPASCAL
FIBER PATTERN - 25 PCT 0, 50 PCT ±π/4, 25 PCT π/2									
TH- 8-1		6.35	6.35	38.30	50.80	1.067	8.5361	TENS	250.4
TH- 8-2		6.35	6.35	38.13	50.80	1.143	9.8128	TENS	270.2
TCL- 8-3		.00	.00	25.78	50.80	1.092	11.3430	TENS	402.8
CCL- 8-4		.00	.00	25.32	50.80	1.092	12.3082	COMPR	445.0
TH- 8-5		25.40	25.40	51.08	50.80	1.118	6.9615	TENS	242.6
CH- 8-6		6.35	6.35	38.02	50.80	1.143	10.7825	COMPR	297.8
CH- 8-7		6.35	6.35	38.25	50.80	1.143	12.2771	COMPR	336.7
FIBER PATTERN - 50 PCT 0, 25 PCT ±π/4, 25 PCT π/2									
TH- 9-1		6.35	6.35	38.30	50.80	1.143	10.8715	TENS	297.7
TH- 9-2		6.35	6.35	38.30	50.80	1.118	10.5334	TENS	295.0
TCL- 9-3		.00	.00	25.58	50.80	1.143	19.5410	TENS	668.4
CCL- 9-4		.00	.00	25.55	50.80	1.143	16.6186	COMPR	569.0
TH- 9-5		25.40	25.40	50.95	50.80	1.168	10.1064	TENS	338.5
CH- 9-6		6.35	6.35	38.30	50.80	1.092	10.5556	COMPR	302.5
CH- 9-7		6.35	6.35	38.28	50.80	1.143	13.4737	COMPR	369.2
FIBER PATTERN - 75 PCT 0, 25 PCT π/2									
TH-10-1		6.35	6.35	38.30	50.80	1.092	16.7520	TENS	480.0
TH-10-2		6.35	6.35	38.28	50.80	1.092	17.3614	TENS	497.9
TCL-10-3		.00	.00	25.63	50.80	1.118	24.2562	TENS	846.9
CCL-10-4		.00	.00	25.53	50.80	1.143	22.1210	COMPR	758.2
TH-10-5		25.40	25.40	51.03	50.80	1.118	12.3527	TENS	431.3
CH-10-6		6.35	6.35	38.30	50.80	1.118	12.1259	COMPR	339.6
CH-10-7		6.35	6.35	38.25	50.80	1.143	11.9568	COMPR	327.9
FIBER PATTERN - 100 PCT ±π/4									
TH-11-1		6.35	6.35	38.25	50.80	1.118	6.3120	TENS	177.0
TH-11-2		6.35	6.35	38.35	50.80	1.118	6.9615	TENS	194.6
TCL-11-3		.00	.00	25.53	50.80	1.118	5.1644	TENS	181.0
CCL-11-4		.00	.00	25.60	50.80	1.143	5.3912	COMPR	184.2
TH-11-5		25.40	25.40	50.98	50.80	1.118	6.1208	TENS	214.1
CH-11-6		6.35	6.35	38.30	50.80	1.143	6.5700	COMPR	179.9
CH-11-7		6.35	6.35	38.20	50.80	1.118	6.4232	COMPR	180.4

TABLE XXVIIIB

FILLED-HOLE SPECIMENS
(TENSILE AND COMPRESSIVE LOADING)

ALL GRAPHITE FIBERS, EPOXY RESIN
US CUSTOMARY UNITS

SPECIMEN ID	HOLE ID	HOLE DIAM IN.	BOLT DIAM IN.	PANEL WIDTH IN.	EDGE DIST. IN.	PANEL THICK. IN.	FAILURE LOAD LB	FAILURE MODE	NET SECT. STRENGTH KSI
FIBER PATTERN - 25 PCT 0 DEG., 50 PCT ±45 DEG., 25 PCT 90 DEG.									
TH- 8-1		.250	.250	1.508	2.000	.0420	1919.0	TENS	36.3
TH- 8-2		.250	.250	1.501	2.000	.0450	2206.0	TENS	39.2
TCL- 8-3		.000	.000	1.015	2.000	.0430	2550.0	TENS	58.4
CCL- 8-4		.000	.000	.997	2.000	.0430	2767.0	COMPR	64.5
TH- 8-5		1.000	1.000	2.011	2.000	.0440	1565.0	TENS	35.2
CH- 8-6		.250	.250	1.497	2.000	.0450	2424.0	COMPR	43.2
CH- 8-7		.250	.250	1.506	2.000	.0450	2760.0	COMPR	48.8
FIBER PATTERN - 50 PCT 0 DEG., 25 PCT ±45 DEG., 25 PCT 90 DEG.									
TH- 9-1		.250	.250	1.508	2.000	.0450	2444.0	TENS	43.2
TH- 9-2		.250	.250	1.508	2.000	.0440	2368.0	TENS	42.8
TCL- 9-3		.000	.000	1.007	2.000	.0450	4393.0	TENS	96.9
CCL- 9-4		.000	.000	1.006	2.000	.0450	3736.0	COMPR	82.5
TH- 9-5		1.000	1.000	2.006	2.000	.0460	2272.0	TENS	49.1
CH- 9-6		.250	.250	1.508	2.000	.0430	2373.0	COMPR	43.9
CH- 9-7		.250	.250	1.507	2.000	.0450	3029.0	COMPR	53.5
FIBER PATTERN - 75 PCT 0 DEG., 25 PCT 90 DEG.									
TH-10-1		.250	.250	1.508	2.000	.0430	3766.0	TENS	69.6
TH-10-2		.250	.250	1.507	2.000	.0430	3903.0	TENS	72.2
TCL-10-3		.000	.000	1.009	2.000	.0440	5453.0	TENS	122.8
CCL-10-4		.000	.000	1.005	2.000	.0450	4973.0	COMPR	110.0
TH-10-5		1.000	1.000	2.009	2.000	.0440	2777.0	TENS	62.6
CH-10-6		.250	.250	1.508	2.000	.0440	2726.0	COMPR	49.2
CH-10-7		.250	.250	1.506	2.000	.0450	2688.0	COMPR	47.6
FIBER PATTERN - 100 PCT ±45 DEG.									
TH-11-1		.250	.250	1.506	2.000	.0440	1419.0	TENS	25.7
TH-11-2		.250	.250	1.510	2.000	.0440	1565.0	TENS	28.2
TCL-11-3		.000	.000	1.005	2.000	.0440	1161.0	TENS	26.3
CCL-11-4		.000	.000	1.008	2.000	.0450	1212.0	COMPR	26.7
TH-11-5		1.000	1.000	2.007	2.000	.0440	1376.0	TENS	31.1
CH-11-6		.250	.250	1.508	2.000	.0450	1477.0	COMPR	26.1
CH-11-7		.250	.250	1.504	2.000	.0440	1444.0	COMPR	26.2

TABLE XXIXA

BEARING AND SHEAROUT SPECIMENS
(TENSILE LOADING)

ALL GRAPHITE FIBERS, EPOXY RESIN
SI UNITS

SPECIMEN ID	HOLE ID	HOLE DIAM MM	BOLT DIAM MM	PANEL WIDTH MM	EDGE DIST. MM	PANEL THICK. MM	FAILURE LOAD KNEWTON	FAILURE MODE	BEARING STRENGTH MPASCAL	TENSION STRENGTH MPASCAL	SHEAROUT STRENGTH MPASCAL
FIBER PATTERN - 25 PCT 0, 75 PCT ±π/4											
BS-25-1	A	6.350	6.350	64.01	13.00	4.445	18.1043	TENS	641.4	70.6	78.3
BS-25-1	B	6.350	6.350	64.03	12.90	4.394	15.2129	TENS	545.2	60.0	67.1
BS-25-1	C	6.350	6.350	64.01	37.92	4.445	29.6252	BRG	1049.6	115.6	43.9
BS-25-1	D	6.350	6.350	64.03	37.85	4.394	28.5576	BRG	1023.5	112.7	42.9
BS-25-2	A	6.350	6.350	63.47	13.08	4.318	14.9905	TENS	546.7	60.8	66.3
BS-25-2	B	6.350	6.350	63.35	13.00	4.445	18.4156	TENS	652.4	72.7	79.6
BS-25-2	C	6.350	6.350	63.47	37.95	4.318	28.6910	BRG	1046.4	116.3	43.8
BS-25-2	D	6.350	6.350	63.35	37.92	4.445	25.4438	BRG	901.4	100.4	37.7
FIBER PATTERN - 50 PCT 0, 50 PCT ±π/4											
BS-27-1	A	6.350	6.350	63.45	12.98	4.496	15.1684	TENS	531.3	59.1	65.0
BS-27-1	B	6.350	6.350	63.50	12.80	4.521	16.4807	TENS	574.0	63.8	71.2
BS-27-1	C	6.350	6.350	63.45	47.45	4.496	27.0452	SHR	947.3	105.4	31.7
BS-27-1	D	6.350	6.350	63.50	47.45	4.521	26.6449	BRG	928.1	103.1	31.1
BS-27-2	A	6.350	6.350	62.89	12.78	4.445	14.0564	TENS	498.0	55.9	61.9
BS-27-2	B	6.350	6.350	63.65	12.67	4.470	13.6116	TENS	479.5	53.1	60.1
BS-27-2	C	6.350	6.350	62.89	47.42	4.445	29.0024	SHR	1027.5	115.4	34.4
BS-27-2	D	6.350	6.350	63.65	47.42	4.470	28.1572	SHR	991.9	109.9	33.2
FIBER PATTERN - 75 PCT 0, 25 PCT ±π/4											
BS-29-1	A	6.350	6.350	50.70	12.45	4.369	8.0735	SHR	291.0	41.7	37.1
BS-29-1	B	6.350	6.350	50.77	12.83	4.394	9.6971	SHR	347.5	49.7	43.0
BS-29-1	C	6.350	6.350	50.70	60.10	4.369	24.6432	SHR	888.3	127.2	23.5
BS-29-1	D	6.350	6.350	50.77	60.12	4.394	25.0880	SHR	899.1	128.5	23.7
BS-29-2	A	6.350	6.350	50.85	12.73	4.394	8.5406	SHR	306.1	43.7	38.2
BS-29-2	B	6.350	6.350	50.67	12.95	4.496	10.6090	SHR	371.6	53.2	45.5
BS-29-2	C	6.350	6.350	50.85	60.10	4.394	23.8869	SHR	856.1	122.2	22.6
BS-29-2	D	6.350	6.350	50.67	60.10	4.496	23.2642	SHR	814.9	116.7	21.5

TABLE XXIXB

BEARING AND SHEAROUT SPECIMENS
(TENSILE LOADING)

ALL GRAPHITE FIBERS, EPOXY RESIN
US CUSTOMARY UNITS

SPECIMEN ID	HOLE ID	HOLE DIAM IN.	BOLT DIAM IN.	PANEL WIDTH IN.	EDGE DIST. IN.	PANEL THICK. IN.	FAILURE LOAD LB	FAILURE MODE	BEARING STRENGTH KSI	TENSION STRENGTH KSI	SHEAROUT STRENGTH KSI
FIBER PATTERN - 25 PCT 0 DEG., 75 PCT ±45 DEG.											
BS-25-1	A	.2500	.2500	2.520	.512	.1750	4070.0	TENS	93.0	10.2	11.4
BS-25-1	B	.2500	.2500	2.521	.508	.1730	3420.0	TENS	79.1	8.7	9.7
BS-25-1	C	.2500	.2500	2.520	1.493	.1750	6660.0	BRG	152.2	16.8	6.4
BS-25-1	D	.2500	.2500	2.521	1.490	.1730	6420.0	BRG	148.4	16.3	6.2
BS-25-2	A	.2500	.2500	2.499	.515	.1700	3370.0	TENS	79.3	8.8	9.6
BS-25-2	B	.2500	.2500	2.494	.512	.1750	4140.0	TENS	94.6	10.5	11.6
BS-25-2	C	.2500	.2500	2.499	1.494	.1700	6450.0	BRG	151.8	16.9	6.3
BS-25-2	D	.2500	.2500	2.494	1.493	.1750	5720.0	BRG	130.7	14.6	5.5
FIBER PATTERN - 50 PCT 0 DEG., 50 PCT ±45 DEG.											
BS-27-1	A	.2500	.2500	2.498	.511	.1770	3410.0	TENS	77.1	8.6	9.4
BS-27-1	B	.2500	.2500	2.500	.504	.1780	3705.0	TENS	83.3	9.3	10.3
BS-27-1	C	.2500	.2500	2.498	1.868	.1770	6080.0	SHR	137.4	15.3	4.6
BS-27-1	D	.2500	.2500	2.500	1.868	.1780	5990.0	BRG	134.6	15.0	4.5
BS-27-2	A	.2500	.2500	2.476	.503	.1750	3160.0	TENS	72.2	8.1	9.0
BS-27-2	B	.2500	.2500	2.506	.499	.1760	3060.0	TENS	69.5	7.7	8.7
BS-27-2	C	.2500	.2500	2.476	1.867	.1750	6520.0	SHR	149.0	16.7	5.0
BS-27-2	D	.2500	.2500	2.506	1.867	.1760	6330.0	SHR	143.9	15.9	4.8
FIBER PATTERN - 75 PCT 0 DEG., 25 PCT ±45 DEG.											
BS-29-1	A	.2500	.2500	1.996	.490	.1720	1815.0	SHR	42.2	6.0	5.4
BS-29-1	B	.2500	.2500	1.999	.505	.1730	2180.0	SHR	50.4	7.2	6.2
BS-29-1	C	.2500	.2500	1.996	2.366	.1720	5540.0	SHR	128.8	18.4	3.4
BS-29-1	D	.2500	.2500	1.999	2.367	.1730	5640.0	SHR	130.4	18.6	3.4
BS-29-2	A	.2500	.2500	2.002	.501	.1730	1920.0	SHR	44.4	6.3	5.5
BS-29-2	B	.2500	.2500	1.995	.510	.1770	2385.0	SHR	53.9	7.7	6.6
BS-29-2	C	.2500	.2500	2.002	2.366	.1730	5370.0	SHR	124.2	17.7	3.3
BS-29-2	D	.2500	.2500	1.995	2.366	.1770	5230.0	SHR	118.2	16.9	3.1

TABLE XXXA

BEARING AND SHEAROUT SPECIMENS
(TENSILE LOADING)

ALL GRAPHITE FIBERS, EPOXY RESIN
SI UNITS

SPECIMEN ID	HOLE ID	HOLE DIAM MM	BOLT DIAM MM	PANEL WIDTH MM	EDGE DIST. MM	PANEL THICK. MM	FAILURE LOAD KNEWTON	FAILURE MODE	BEARING STRENGTH MPASCAL	TENSION STRENGTH MPASCAL	SHEAROUT STRENGTH MPASCAL
FIBER PATTERN - 25 PCT 0, 62.5 PCT ±π/4, 12.5 PCT π/2											
BS-31-1	A	6.350	6.350	63.40	13.18	4.420	18.5046	TENS	659.4	73.4	79.4
BS-31-1	B	6.350	6.350	63.42	12.83	4.420	19.8836	TENS	708.5	78.8	87.7
BS-31-1	C	6.350	6.350	63.40	47.42	4.420	28.7355	BRG	1023.9	114.0	34.3
BS-31-1	D	6.350	6.350	63.42	47.45	4.420	27.7124	BRG	987.5	109.9	33.0
BS-31-2	A	6.350	6.350	63.37	12.70	4.496	17.7484	TENS	621.7	69.2	77.7
BS-31-2	B	6.350	6.350	63.27	13.23	4.470	20.2617	TENS	713.8	79.6	85.6
BS-31-2	C	6.350	6.350	63.37	47.40	4.496	29.0024	BRG	1015.9	113.1	34.0
BS-31-2	D	6.350	6.350	63.27	47.32	4.470	24.7766	BRG	872.8	97.4	29.3
FIBER PATTERN - 50 PCT 0, 37.5 PCT ±π/4, 12.5 PCT π/2											
BS-33-1	A	6.350	6.350	63.12	13.06	4.470	13.4336	SHR	473.2	52.9	57.5
BS-33-1	B	6.350	6.350	63.09	13.64	4.470	14.3233	SHR	504.6	56.5	58.7
BS-33-1	C	6.350	6.350	63.12	47.40	4.470	30.0255	BRG	1057.7	118.3	35.4
BS-33-1	D	6.350	6.350	63.09	47.42	4.470	27.4767	BRG	967.9	108.3	32.4
BS-33-2	A	6.350	6.350	63.55	12.80	4.470	14.5012	SHR	510.8	56.7	63.3
BS-33-2	B	6.350	6.350	63.70	12.47	4.470	14.3678	SHR	506.1	56.0	64.4
BS-33-2	C	6.350	6.350	63.55	47.40	4.470	27.7569	BRG	977.8	108.5	32.8
BS-33-2	D	6.350	6.350	63.70	47.42	4.470	27.5790	BRG	971.5	107.6	32.5
FIBER PATTERN - 75 PCT 0, 12.5 PCT ±π/4, 12.5 PCT π/2											
BS-35-1	A	6.350	6.350	50.85	12.50	4.521	8.9632	SHR	312.2	44.5	39.7
BS-35-1	B	6.350	6.350	50.65	12.32	4.521	8.7408	SHR	304.5	43.6	39.2
BS-35-1	C	6.350	6.350	50.85	60.07	4.521	25.4438	BRG	886.2	126.5	23.4
BS-35-1	D	6.350	6.350	50.65	60.10	4.521	26.5559	BRG	925.0	132.6	24.4
BS-35-2	A	6.350	6.350	50.83	12.45	4.496	7.3396	SHR	257.1	36.7	32.8
BS-35-2	B	6.350	6.350	50.72	12.04	4.521	8.1847	CLVG	285.1	40.8	37.6
BS-35-2	C	6.350	6.350	50.83	60.12	4.496	24.2428	BRG	849.2	121.2	22.4
BS-35-2	D	6.350	6.350	50.72	60.10	4.521	27.4455	BRG	956.0	136.8	25.3

TABLE XXXB

BEARING AND SHEAROUT SPECIMENS
(TENSILE LOADING)

ALL GRAPHITE FIBERS, EPOXY RESIN
US CUSTOMARY UNITS

SPECIMEN ID	HOLE ID	HOLE DIAM IN.	BOLT DIAM IN.	PANEL WIDTH IN.	EDGE DIST. IN.	PANEL THICK. IN.	FAILURE LOAD LB	FAILURE MODE	BEARING STRENGTH KSI	TENSION STRENGTH KSI	SHEAROUT STRENGTH KSI
FIBER PATTERN - 25 PCT 0 DEG., 62.5 PCT ±45 DEG., 12.5 PCT 90 DEG.											
BS-31-1	A	.2500	.2500	2.496	.519	.1740	4160.0	TENS	95.6	10.6	11.5
BS-31-1	B	.2500	.2500	2.497	.505	.1740	4470.0	TENS	102.8	11.4	12.7
BS-31-1	C	.2500	.2500	2.496	1.867	.1740	6460.0	BRG	148.5	16.5	5.0
BS-31-1	D	.2500	.2500	2.497	1.868	.1740	6230.0	BRG	143.2	15.9	4.8
BS-31-2	A	.2500	.2500	2.495	.500	.1770	3990.0	TENS	90.2	10.0	11.3
BS-31-2	B	.2500	.2500	2.491	.521	.1760	4555.0	TENS	103.5	11.5	12.4
BS-31-2	C	.2500	.2500	2.495	1.866	.1770	6520.0	BRG	147.3	16.4	4.9
BS-31-2	D	.2500	.2500	2.491	1.863	.1760	5570.0	BRG	126.6	14.1	4.2
FIBER PATTERN - 50 PCT 0 DEG., 37.5 PCT ±45 DEG., 12.5 PCT 90 DEG.											
BS-33-1	A	.2500	.2500	2.485	.514	.1760	3020.0	SHR	68.6	7.7	8.3
BS-33-1	B	.2500	.2500	2.484	.537	.1760	3220.0	SHR	73.2	8.2	8.5
BS-33-1	C	.2500	.2500	2.485	1.866	.1760	6750.0	BRG	153.4	17.2	5.1
BS-33-1	D	.2500	.2500	2.484	1.867	.1760	6177.0	BRG	140.4	15.7	4.7
BS-33-2	A	.2500	.2500	2.502	.504	.1760	3260.0	SHR	74.1	8.2	9.2
BS-33-2	B	.2500	.2500	2.508	.491	.1760	3230.0	SHR	73.4	8.1	9.3
BS-33-2	C	.2500	.2500	2.502	1.866	.1760	6240.0	BRG	141.8	15.7	4.8
BS-33-2	D	.2500	.2500	2.508	1.867	.1760	6200.0	BRG	140.9	15.6	4.7
FIBER PATTERN - 75 PCT 0 DEG., 12.5 PCT ±45 DEG., 12.5 PCT 90 DEG.											
BS-35-1	A	.2500	.2500	2.002	.492	.1780	2015.0	SHR	45.3	6.5	5.8
BS-35-1	B	.2500	.2500	1.994	.485	.1780	1965.0	SHR	44.2	6.3	5.7
BS-35-1	C	.2500	.2500	2.002	2.365	.1780	5720.0	BRG	128.5	18.3	3.4
BS-35-1	D	.2500	.2500	1.994	2.366	.1780	5970.0	BRG	134.2	19.2	3.5
BS-35-2	A	.2500	.2500	2.001	.490	.1770	1650.0	SHR	37.3	5.3	4.8
BS-35-2	B	.2500	.2500	1.997	.474	.1780	1840.0	CLVG	41.3	5.9	5.5
BS-35-2	C	.2500	.2500	2.001	2.367	.1770	5450.0	BRG	123.2	17.6	3.3
BS-35-2	D	.2500	.2500	1.997	2.366	.1780	6170.0	BRG	138.7	19.8	3.7

TABLE XXXIA

BEARING AND SHEAROUT SPECIMENS
(TENSILE LOADING)

ALL GRAPHITE FIBERS, EPOXY RESIN
SI UNITS

SPECIMEN ID	HOLE ID	HOLE DIAM MM	BOLT DIAM MM	PANEL WIDTH MM	EDGE DIST. MM	PANEL THICK. MM	FAILURE LOAD KNEWTON	FAILURE MODE	BEARING STRENGTH MPASCAL	TENSION STRENGTH MPASCAL	SHEAROUT STRENGTH MPASCAL
FIBER PATTERN - 25 PCT 0, 50 PCT ±π/4, 25 PCT π/2											
BS-37-1	A	6.350	6.350	63.55	12.78	4.369	14.2788	TENS	514.7	57.1	64.0
BS-37-1	B	6.350	6.350	63.50	12.83	4.343	16.0136	TENS	580.6	64.5	71.9
BS-37-1	C	6.350	6.350	63.55	47.42	4.369	26.8228	BRG	966.9	107.3	32.4
BS-37-1	D	6.350	6.350	63.50	47.40	4.343	29.2248	BRG	1059.6	117.7	35.5
BS-37-2	A	6.350	6.350	63.42	08.00	4.343	15.2129	TENS	551.6	61.4	.0
BS-37-2	B	6.350	6.350	63.32	12.67	4.369	16.3695	TENS	590.1	65.8	73.9
BS-37-2	C	6.350	6.350	63.42	47.40	4.343	28.3797	BRG	1029.0	114.5	34.5
BS-37-2	D	6.350	6.350	63.32	47.47	4.369	26.6449	BRG	960.5	107.1	32.1
FIBER PATTERN - 50 PCT 0, 25 PCT ±π/4, 25 PCT π/2											
BS-39-1	A	6.350	6.350	63.45	13.00	4.521	13.2557	TENS	461.7	51.3	56.4
BS-39-1	B	6.350	6.350	63.47	12.78	4.445	13.7228	TENS	486.2	54.0	60.4
BS-39-1	C	6.350	6.350	63.45	47.37	4.521	29.2915	BRG	1020.3	113.5	34.2
BS-39-1	D	6.350	6.350	63.47	47.40	4.445	27.1786	BRG	962.9	107.0	32.3
BS-39-2	A	6.350	6.350	63.42	13.13	4.369	13.4559	TENS	485.0	54.0	58.6
BS-39-2	B	6.350	6.350	63.42	12.90	4.343	13.2557	TENS	480.6	53.5	59.1
BS-39-2	C	6.350	6.350	63.42	47.40	4.369	28.4686	BRG	1026.2	114.2	34.4
BS-39-2	D	6.350	6.350	63.42	47.35	4.343	28.7800	BRG	1043.5	116.1	35.0
FIBER PATTERN - 75 PCT 0, 25 PCT π/2											
BS-41-1	A	6.350	6.350	50.95	12.45	4.521	10.1864	SHR	354.8	50.5	45.3
BS-41-1	B	6.350	6.350	50.93	12.95	4.521	9.0744	SHR	316.1	45.0	38.7
BS-41-1	C	6.350	6.350	50.95	60.12	4.521	27.7124	BRG	965.3	137.4	25.5
BS-41-1	D	6.350	6.350	50.93	60.05	4.521	26.2890	BRG	915.7	130.4	24.2
BS-41-2	A	6.350	6.350	50.95	12.57	4.547	9.4747	SHR	328.2	46.8	41.4
BS-41-2	B	6.350	6.350	50.83	11.68	4.496	9.7861	SHR	342.8	48.9	46.6
BS-41-2	C	6.350	6.350	50.85	60.17	4.547	28.2017	BRG	976.8	139.4	25.8
BS-41-2	D	6.350	6.350	50.83	60.05	4.496	27.0897	BPG	948.9	135.5	25.1

TABLE XXXIB

BEARING AND SHEAROUT SPECIMENS
(TENSILE LOADING)

ALL GRAPHITE FIBERS, EPOXY RESIN
US CUSTOMARY UNITS

SPECIMEN ID	HOLE ID	HOLE DIAM IN.	BOLT DIAM IN.	PANEL WIDTH IN.	EDGE DIST. IN.	PANEL THICK. IN.	FAILURE LOAD LB	FAILURE MODE	BEARING STRENGTH KSI	TENSION STRENGTH KSI	SHEAROUT STRENGTH KSI
FIBER PATTERN - 25 PCT 0 DEG., 50 PCT ±45 DEG., 25 PCT 90 DEG.											
BS-37-1	A	.2500	.2500	2.502	.503	.1720	3210.0	TENS	74.7	8.3	9.3
BS-37-1	B	.2500	.2500	2.500	.505	.1710	3600.0	TENS	84.2	9.4	10.4
BS-37-1	C	.2500	.2500	2.502	1.867	.1720	6030.0	BRG	140.2	15.6	4.7
BS-37-1	D	.2500	.2500	2.500	1.866	.1710	6570.0	BRG	153.7	17.1	5.1
BS-37-2	A	.2500	.2500	2.497	0.000	.1710	3420.0	TENS	80.0	8.9	.0
BS-37-2	B	.2500	.2500	2.493	.499	.1720	3680.0	TENS	85.6	9.5	10.7
BS-37-2	C	.2500	.2500	2.497	1.866	.1710	6380.0	BRG	149.2	16.6	5.0
BS-37-2	D	.2500	.2500	2.493	1.869	.1720	5990.0	BRG	139.3	15.5	4.7
FIBER PATTERN - 50 PCT 0 DEG., 25 PCT ±45 DEG., 25 PCT 90 DEG.											
BS-39-1	A	.2500	.2500	2.498	.512	.1780	2980.0	TENS	67.0	7.4	8.2
BS-39-1	B	.2500	.2500	2.499	.503	.1750	3085.0	TENS	70.5	7.8	8.8
BS-39-1	C	.2500	.2500	2.498	1.865	.1780	6585.0	BRG	148.0	16.5	5.0
BS-39-1	D	.2500	.2500	2.499	1.866	.1750	6110.0	BRG	139.7	15.5	4.7
BS-39-2	A	.2500	.2500	2.497	.517	.1720	3025.0	TENS	70.3	7.8	8.5
BS-39-2	B	.2500	.2500	2.497	.508	.1710	2980.0	TENS	69.7	7.8	8.6
BS-39-2	C	.2500	.2500	2.497	1.866	.1720	6400.0	BRG	148.8	16.6	5.0
BS-39-2	D	.2500	.2500	2.497	1.864	.1710	6470.0	BRG	151.3	16.8	5.1
FIBER PATTERN - 75 PCT 0 DEG., 25 PCT 90 DEG.											
BS-41-1	A	.2500	.2500	2.006	.490	.1780	2290.0	SHR	51.5	7.3	6.6
BS-41-1	B	.2500	.2500	2.005	.510	.1780	2040.0	SHR	45.3	6.5	5.6
BS-41-1	C	.2500	.2500	2.006	2.367	.1780	6230.0	BRG	140.0	19.9	3.7
BS-41-1	D	.2500	.2500	2.005	2.364	.1780	5910.0	BRG	132.8	18.9	3.5
BS-41-2	A	.2500	.2500	2.002	.495	.1790	2130.0	SHR	47.6	6.8	6.0
BS-41-2	B	.2500	.2500	2.001	.460	.1770	2200.0	SHR	49.7	7.1	6.8
BS-41-2	C	.2500	.2500	2.002	2.369	.1790	6340.0	BRG	141.7	20.2	3.7
BS-41-2	D	.2500	.2500	2.001	2.364	.1770	6090.0	BRG	137.6	19.6	3.6

TABLE XXXIIA

BEARING AND SHEAROUT SPECIMENS
(TENSILE LOADING)

ALL GRAPHITE FIBERS, EPOXY RESIN
SI UNITS

SPECIMEN ID	HOLE ID	HOLE DIAM MM	BOLT DIAM MM	PANEL WIDTH MM	EDGE DIST. MM	PANEL THICK. MM	FAILURE LOAD KNEWTON	FAILURE MODE	BEARING STRENGTH MPASCAL	TENSION STRENGTH MPASCAL	SHEAROUT STRENGTH MPASCAL
FIBER PATTERN - 100 PCT ±π/4											
BS-45-1	A	6.350	6.350	63.73	12.62	4.572	14.7903	TENS	509.4	56.4	64.1
BS-45-1	B	6.350	6.350	63.70	12.42	4.572	14.0119	TENS	482.6	53.4	61.7
BS-45-1	C	6.350	6.350	63.73	42.34	4.572	15.3241	BRG	527.8	58.4	19.8
BS-45-1	D	6.350	6.350	63.70	29.97	4.572	14.4122	BRG	496.4	55.0	26.3
BS-45-2	A	6.350	6.350	63.40	12.65	4.572	13.9229	TENS	479.6	53.4	60.2
BS-45-2	B	6.350	6.350	63.40	12.85	4.521	14.4567	TENS	503.5	56.0	62.2
BS-45-2	C	6.350	6.350	63.40	31.24	4.572	13.9229	BRG	479.6	53.4	24.4
BS-45-2	D	6.350	6.350	63.40	30.61	4.521	14.6347	BRG	509.7	56.7	26.4

TABLE XXXIIB

BEARING AND SHEAROUT SPECIMENS
(TENSILE LOADING)

ALL GRAPHITE FIBERS, EPOXY RESIN
US CUSTOMARY UNITS

SPECIMEN ID	HOLE ID	HOLE DIAM IN.	BOLT DIAM IN.	PANEL WIDTH IN.	EDGE DIST. IN.	PANEL THICK. IN.	FAILURE LOAD LB	FAILURE MODE	BEARING STRENGTH KSI	TENSION STRENGTH KSI	SHEAROUT STRENGTH KSI
FIBER PATTERN - 100 PCT ±45 DEG.											
BS-45-1	A	.2500	.2500	2.509	.497	.1800	3325.0	TENS	73.9	8.2	9.3
BS-45-1	B	.2500	.2500	2.508	.489	.1800	3150.0	TENS	70.0	7.8	8.9
BS-45-1	C	.2500	.2500	2.509	1.667	.1800	3445.0	BRG	76.6	8.5	2.9
BS-45-1	D	.2500	.2500	2.508	1.180	.1800	3240.0	BRG	72.0	8.0	3.8
BS-45-2	A	.2500	.2500	2.496	.498	.1800	3130.0	TENS	69.6	7.7	8.7
BS-45-2	B	.2500	.2500	2.496	.506	.1780	3250.0	TENS	73.0	8.1	9.0
BS-45-2	C	.2500	.2500	2.496	1.230	.1800	3130.0	BRG	69.6	7.7	3.5
BS-45-2	D	.2500	.2500	2.496	1.205	.1780	3290.0	BRG	73.9	8.2	3.8

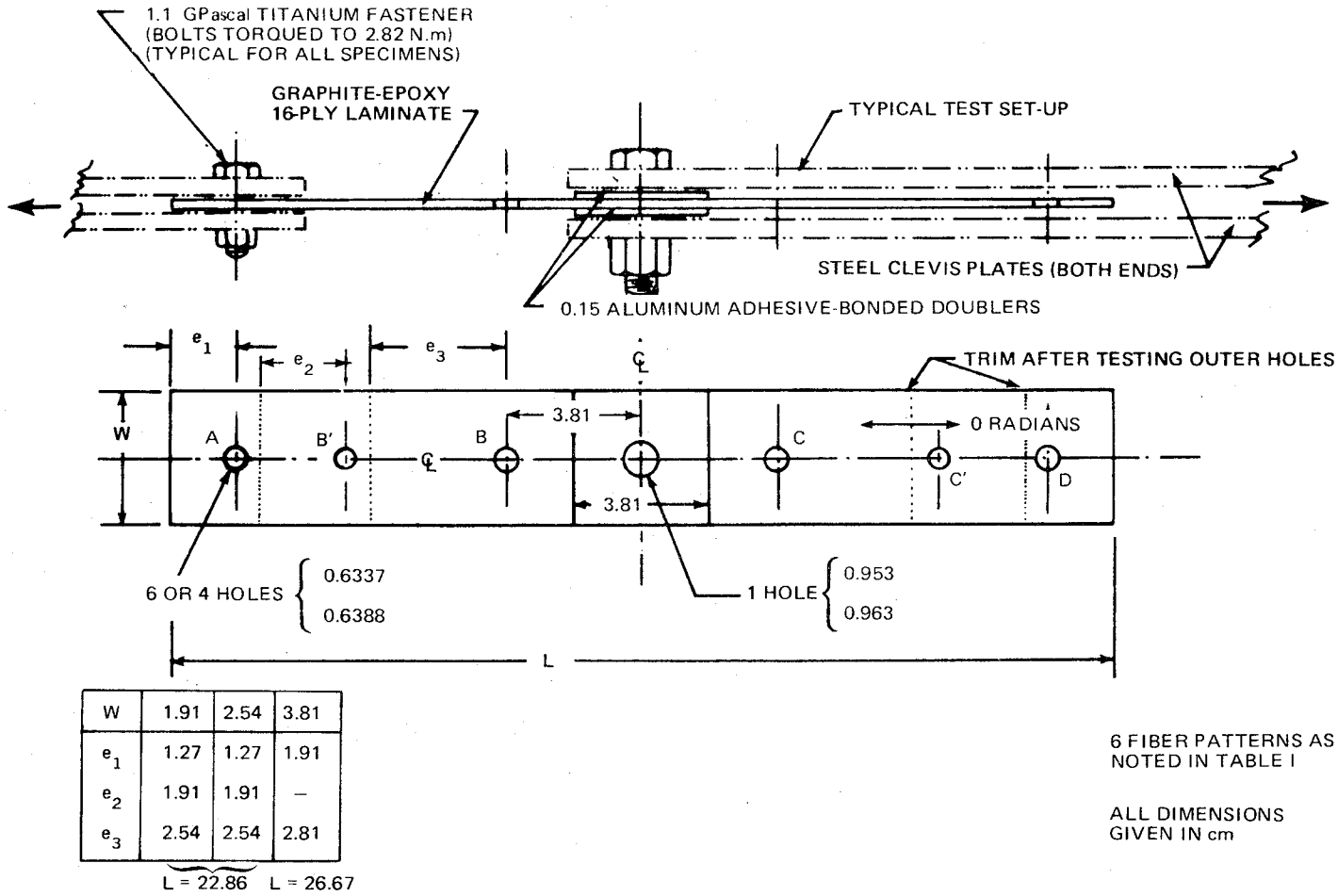

W	1.91	2.54	3.81
e_1	1.27	1.27	1.91
e_2	1.91	1.91	—
e_3	2.54	2.54	2.81
	L = 22.86		L = 26.67

FIGURE 1. TEST SPECIMEN AND SET-UP FOR TENSION-THROUGH-THE-HOLE FAILURE MODE

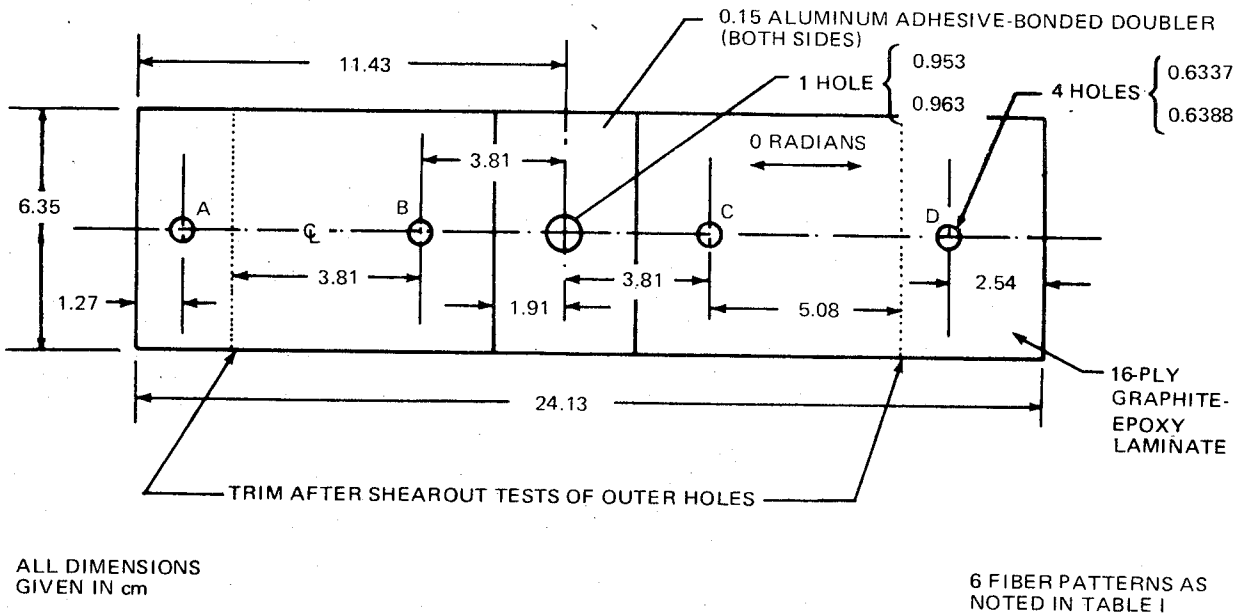

FIGURE 2. SHEAROUT AND BEARING (TENSILE) TEST SPECIMENS

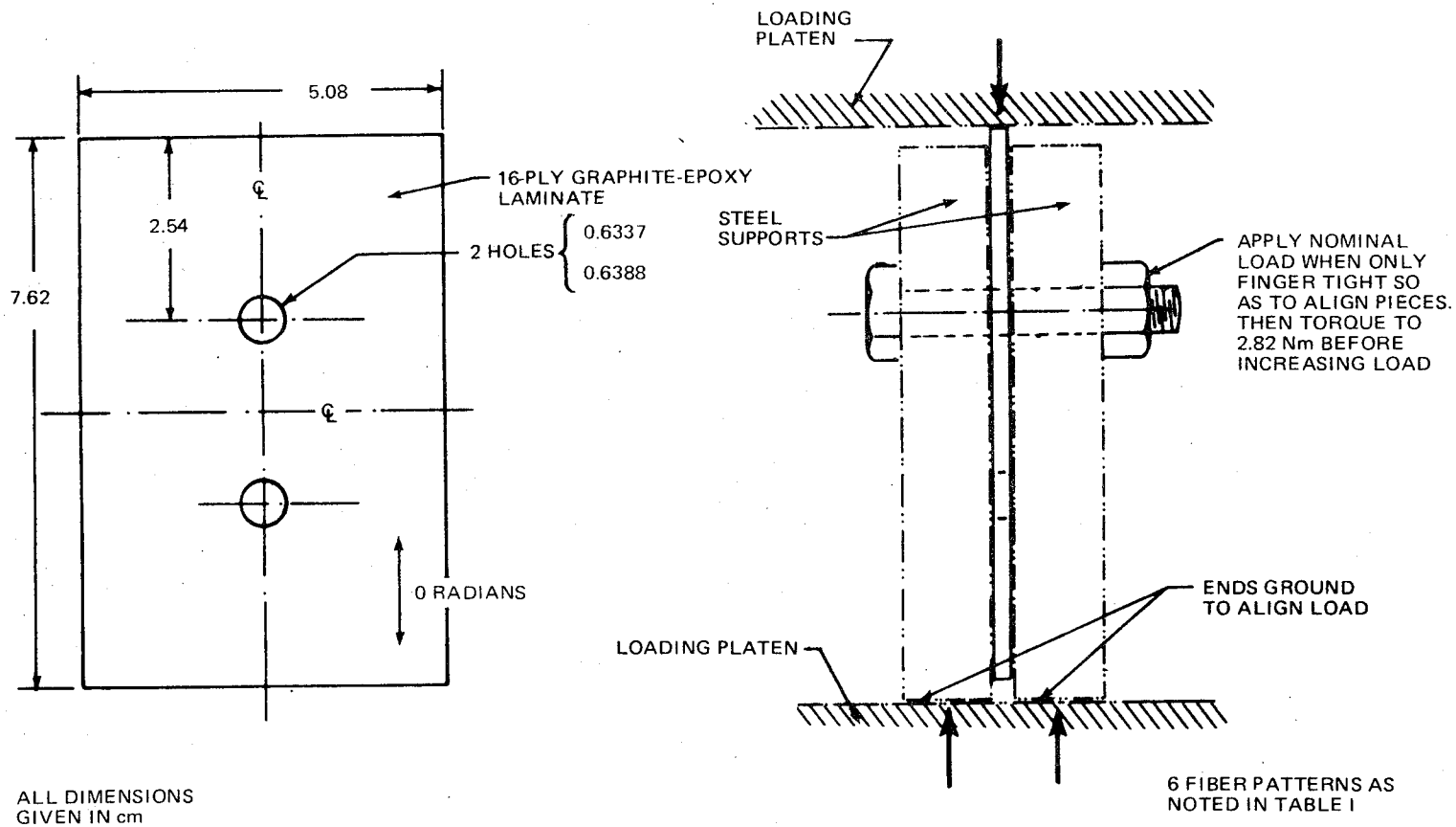

FIGURE 3. COMPRESSION BEARING TEST SPECIMEN AND FIXTURE

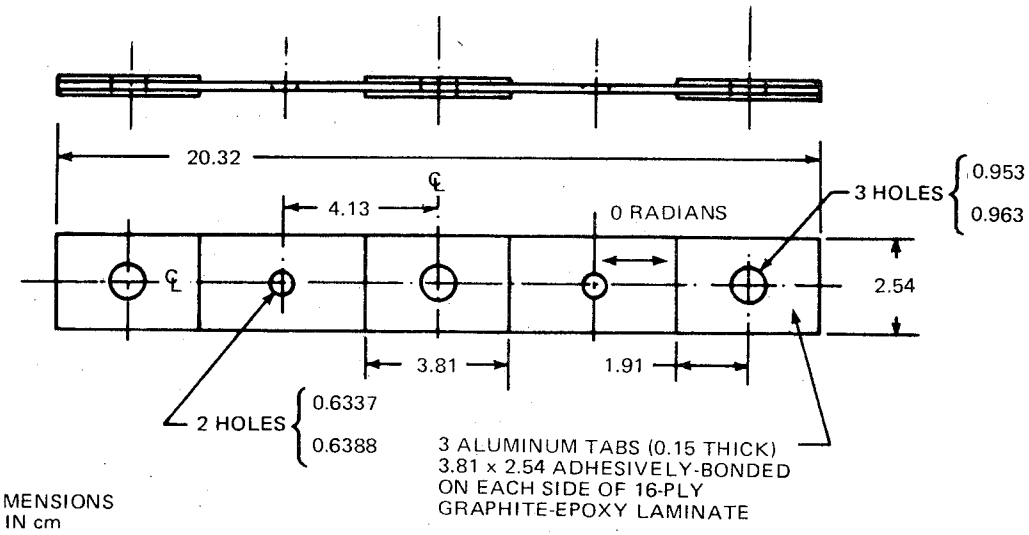

FIGURE 4. OPEN-HOLE STRESS-CONCENTRATION TEST COUPON (TENSILE LOADING)

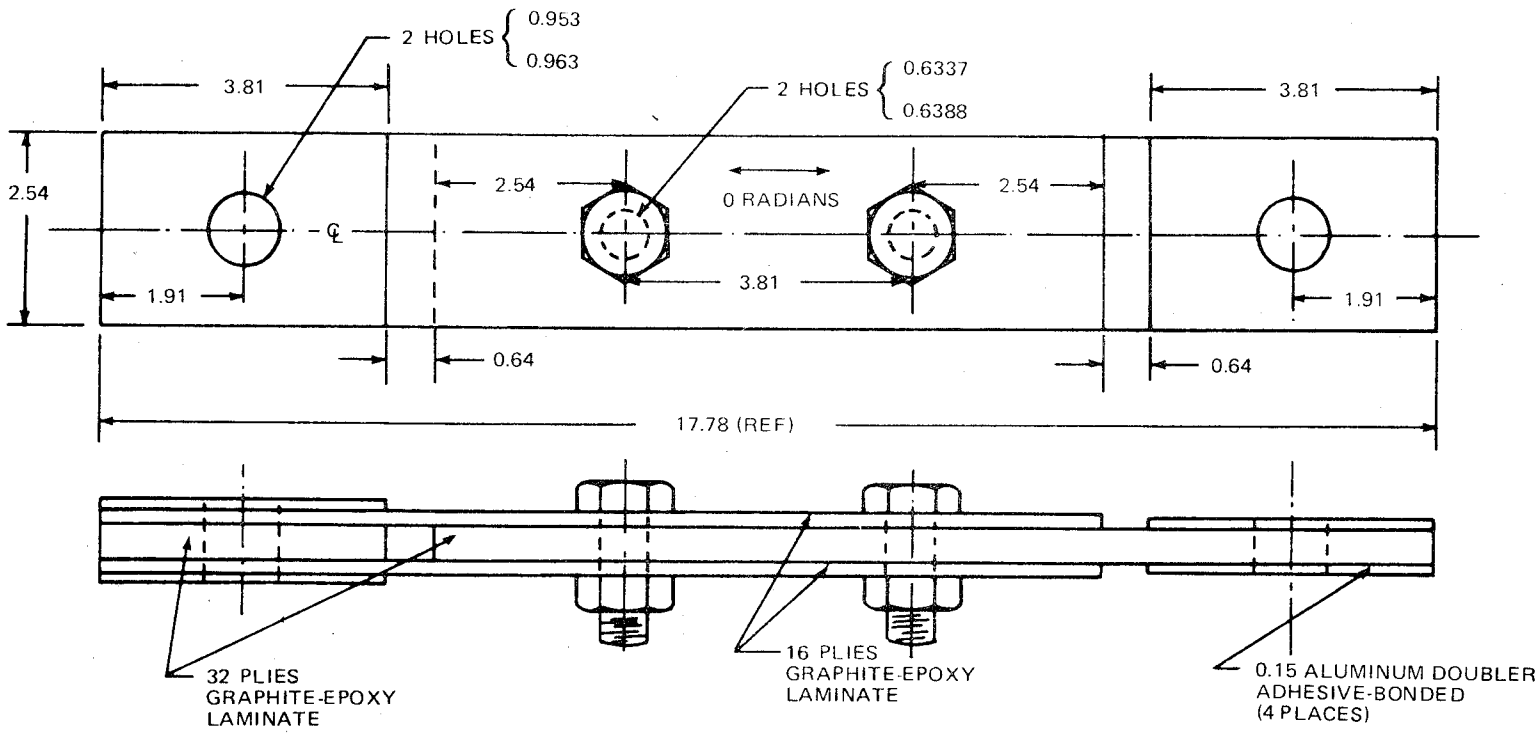

ALL DIMENSIONS
GIVEN IN cm

6 FIBER PATTERNS AS NOTED
IN TABLE I

FIGURE 5. STRESS-CONCENTRATION INTERACTION TEST SPECIMEN (TENSILE AND COMPRESSIVE LOADINGS)

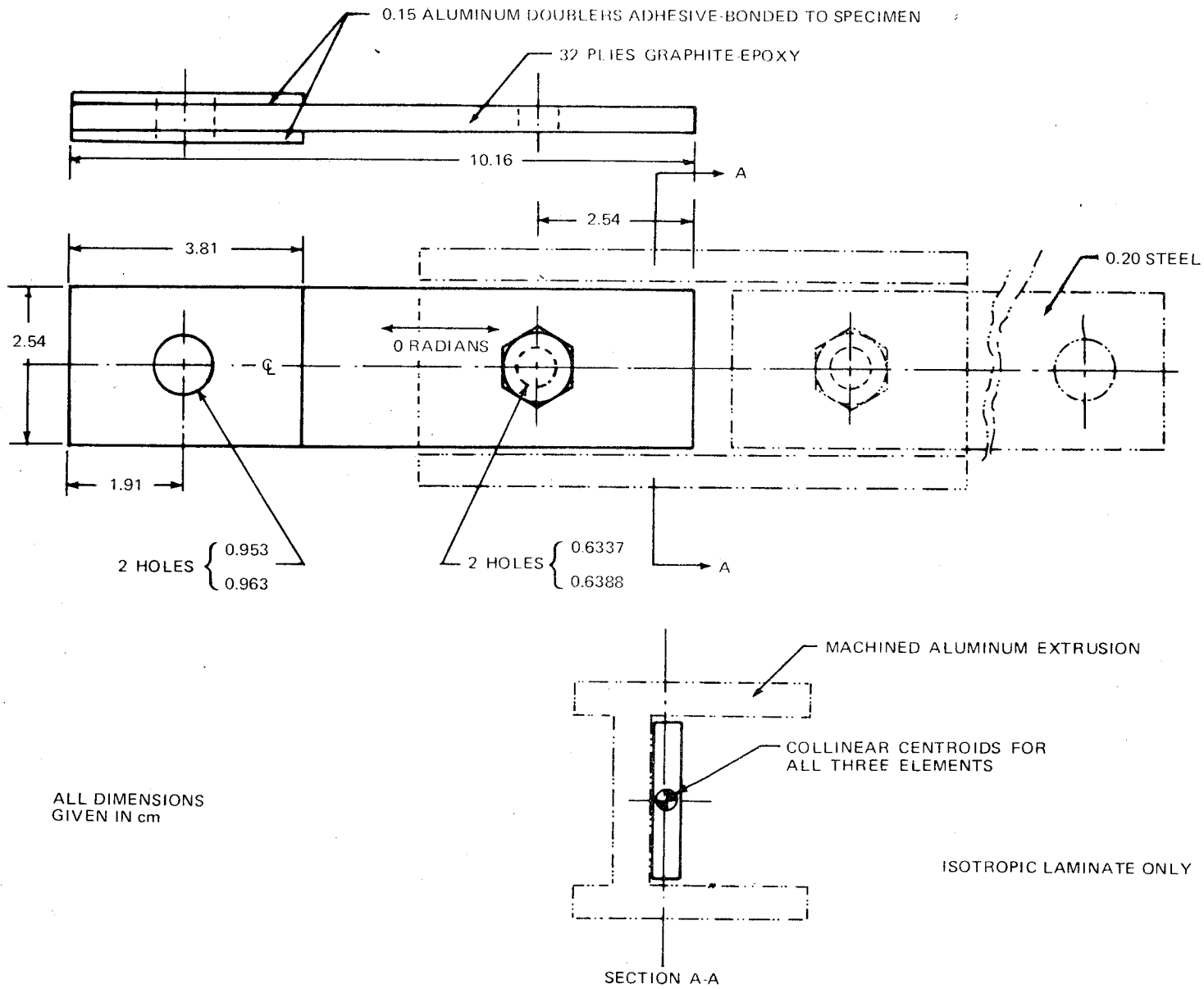

FIGURE 6. SINGLE-LAP TEST SPECIMEN AND MINIMIZED ECCENTRICITY TEST SET-UP (TENSILE LOADING)

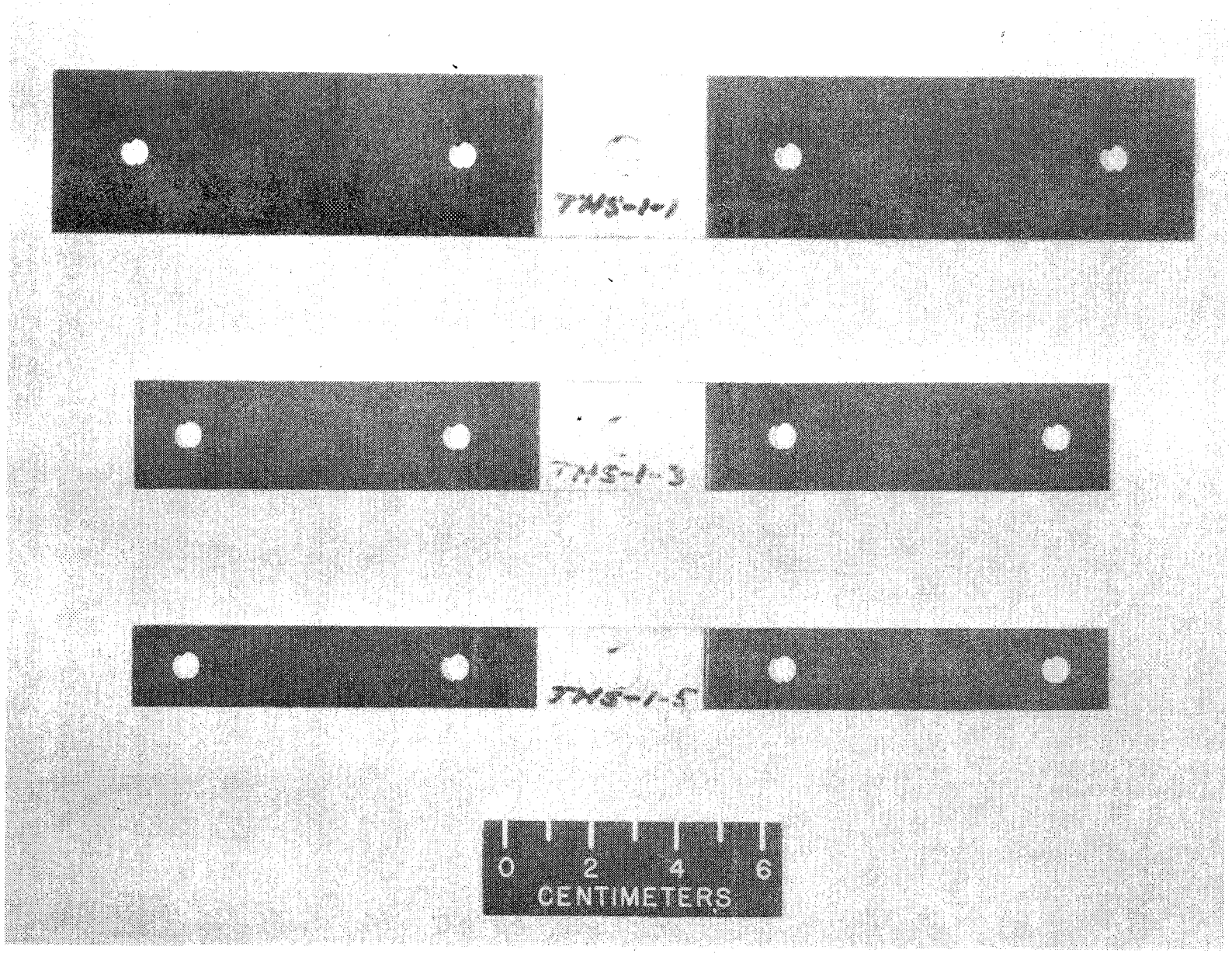

FIGURE 7. TENSION-THROUGH-THE-HOLE TEST SPECIMENS (GRAPHITE/EPOXY)

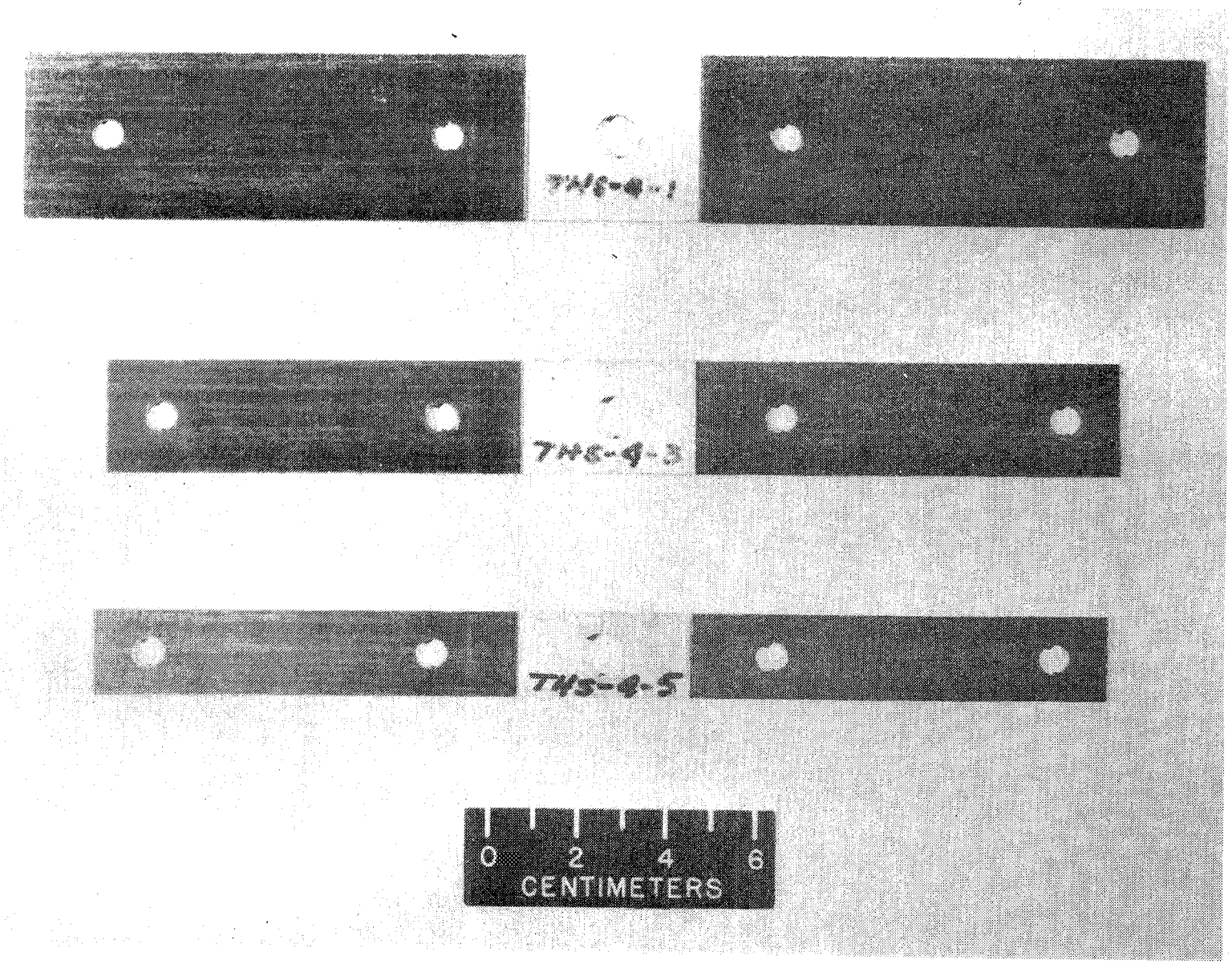

FIGURE 8. TENSION-THROUGH-THE-HOLE TEST SPECIMENS (GRAPHITE/GLASS/EPOXY)

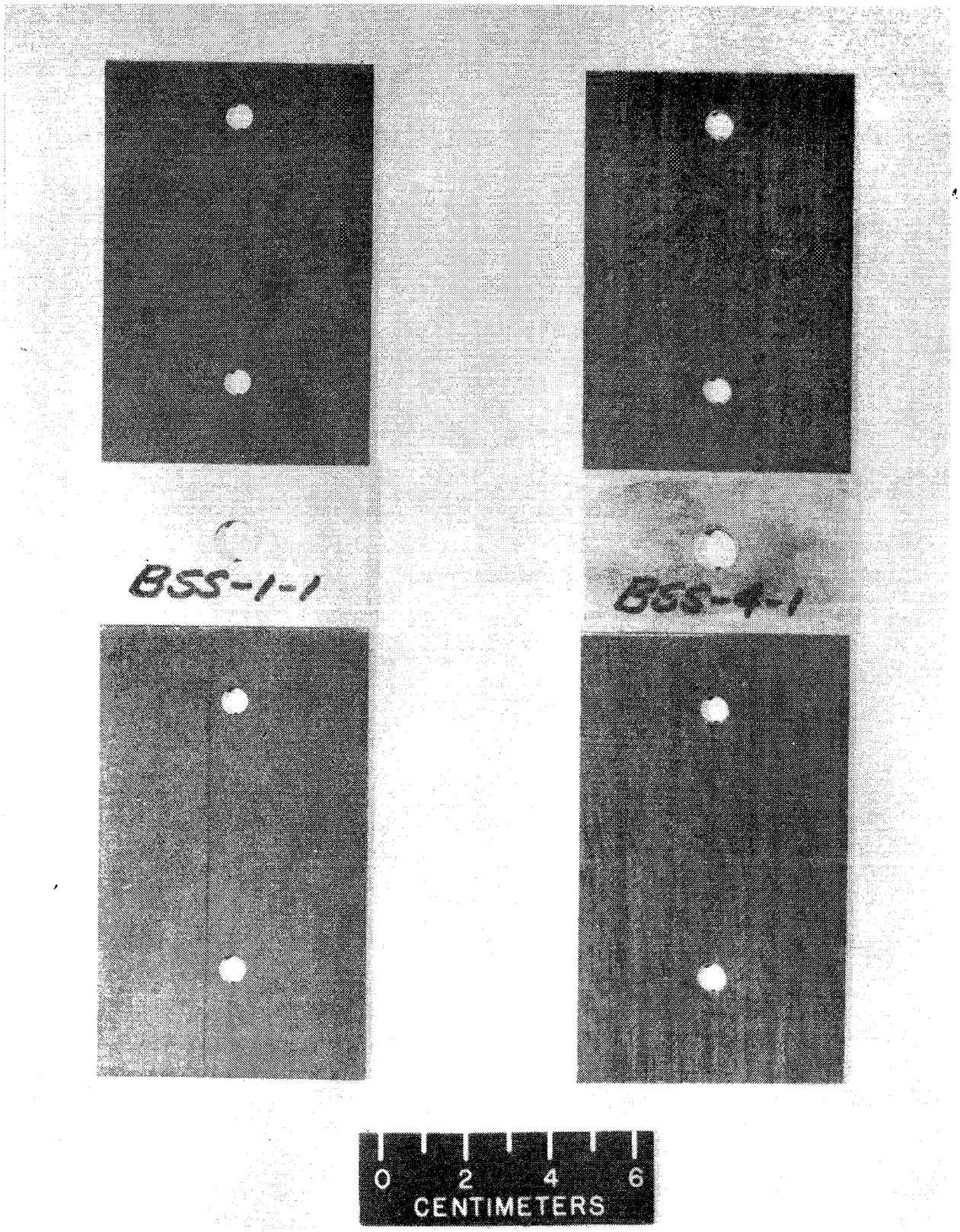

FIGURE 9. BEARING AND SHEAROUT TEST SPECIMENS

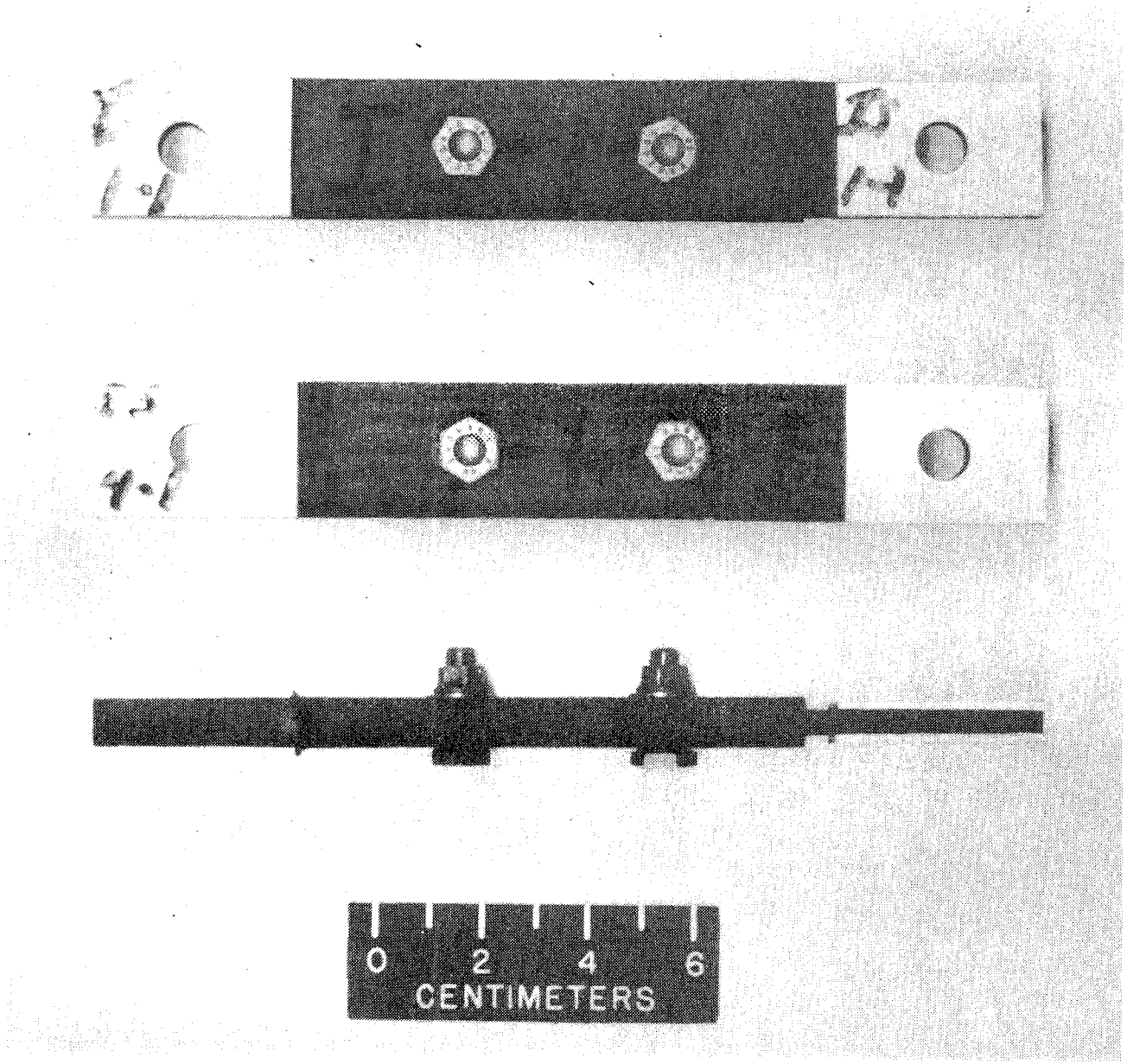

FIGURE 10. STRESS-CONCENTRATION INTERACTION TEST SPECIMENS

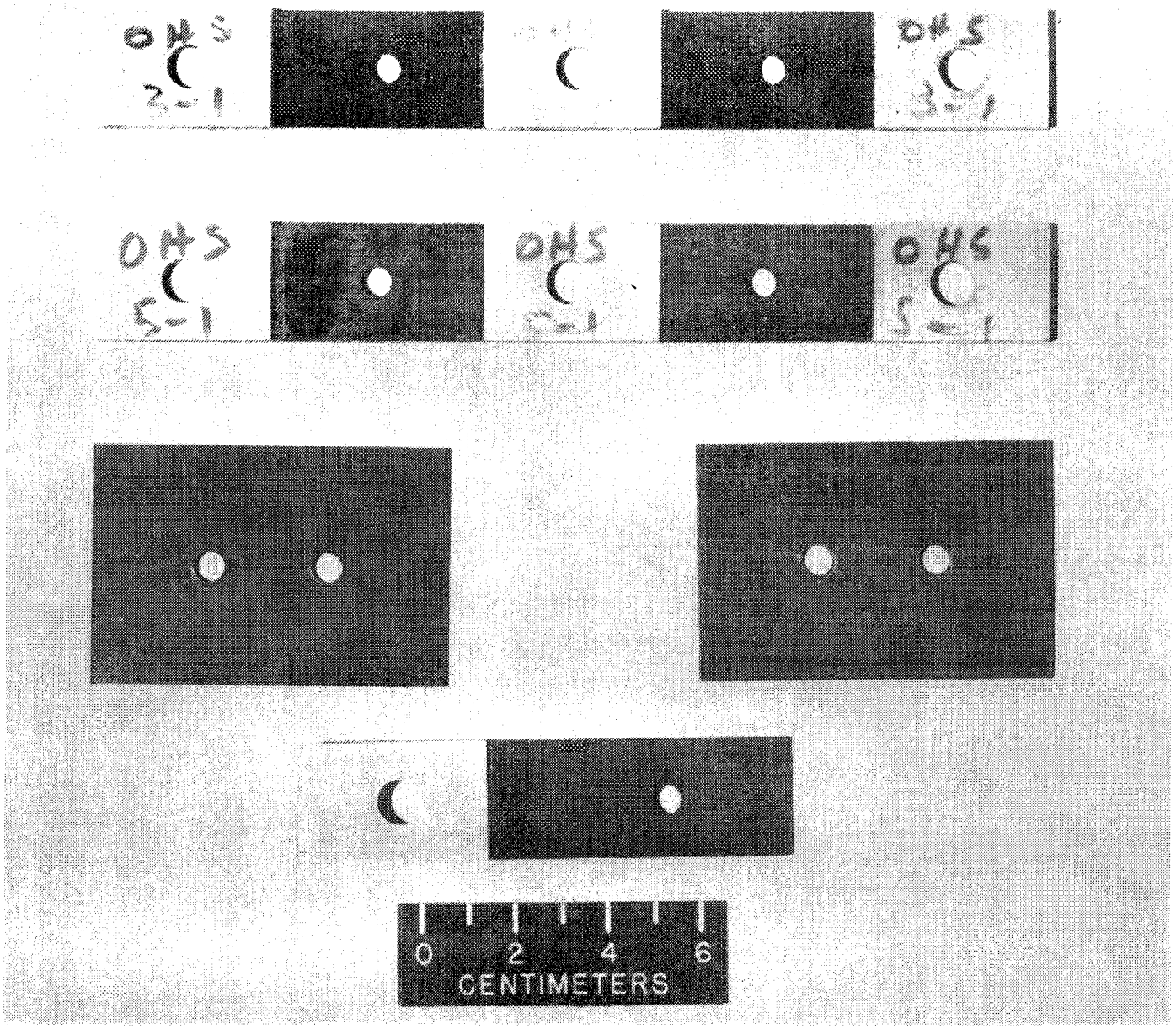

FIGURE 11. OPEN-HOLE, COMPRESSION BEARING, AND SINGLE-LAP TEST SPECIMENS

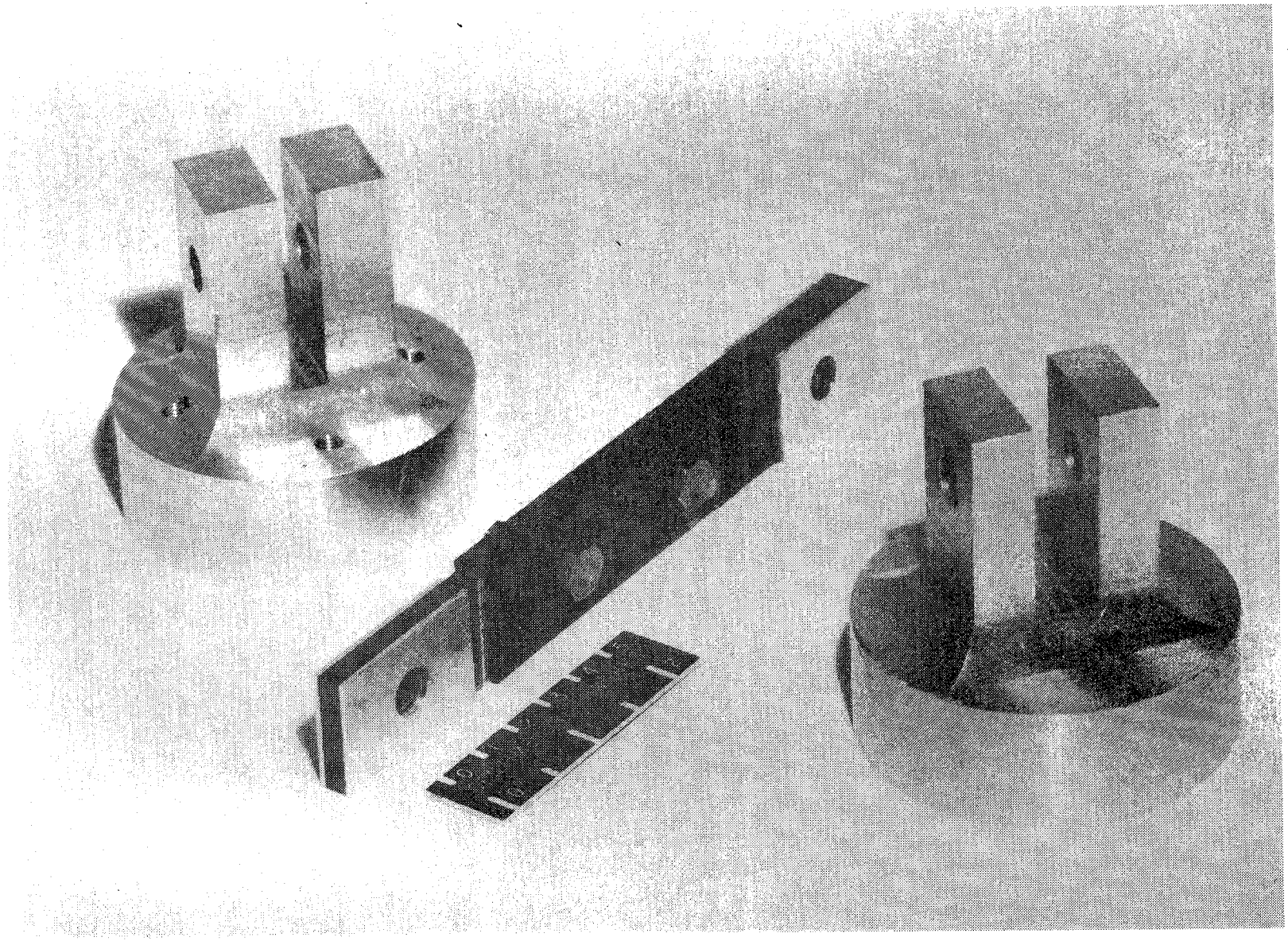

FIGURE 12. LOAD-INTRODUCTION FIXTURE FOR COMPRESSION OF INTERACTION SPECIMENS

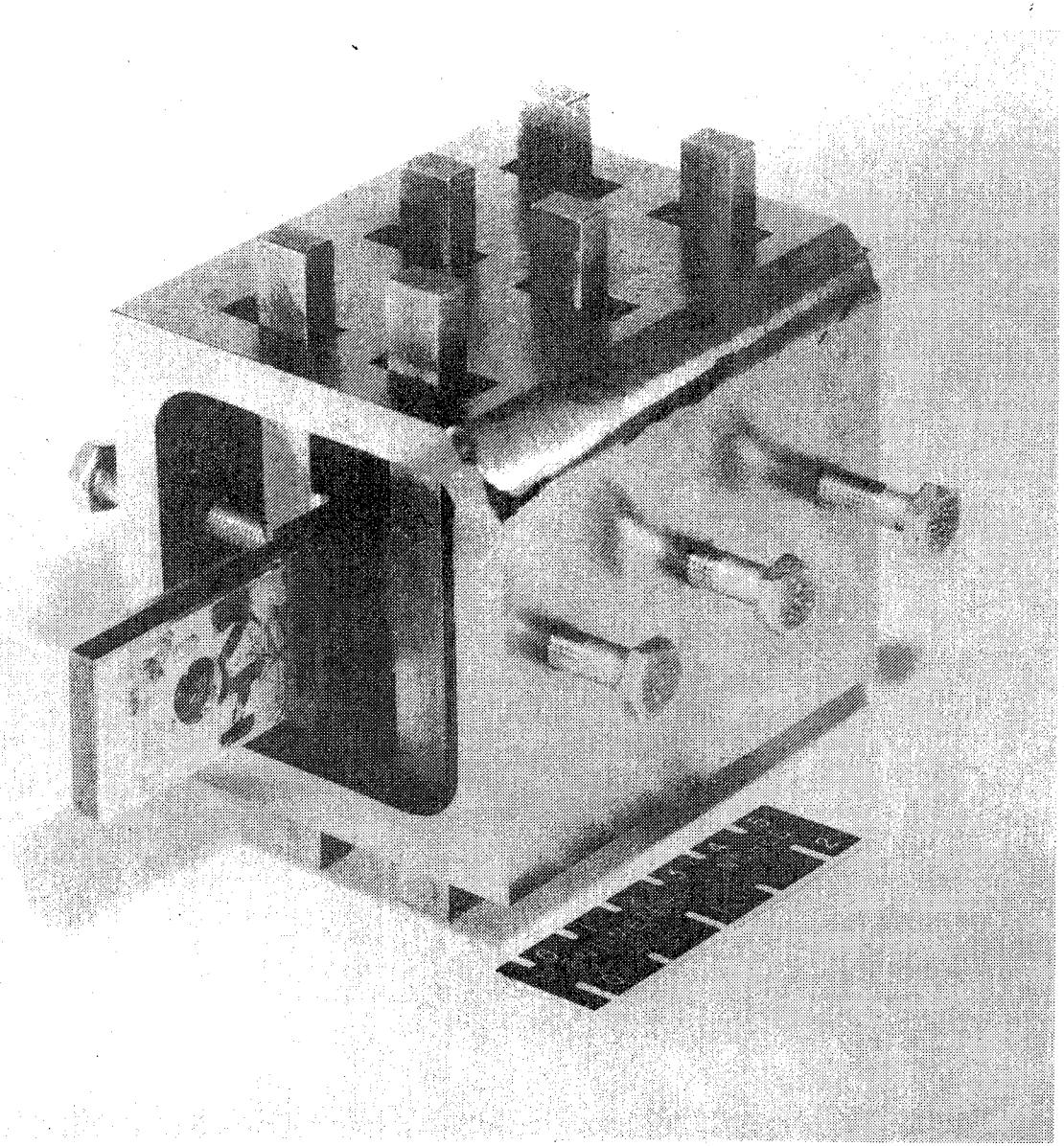

FIGURE 13. LATERAL SUPPORT FIXTURE FOR COMPRESSION TESTS OF INTERACTION SPECIMENS

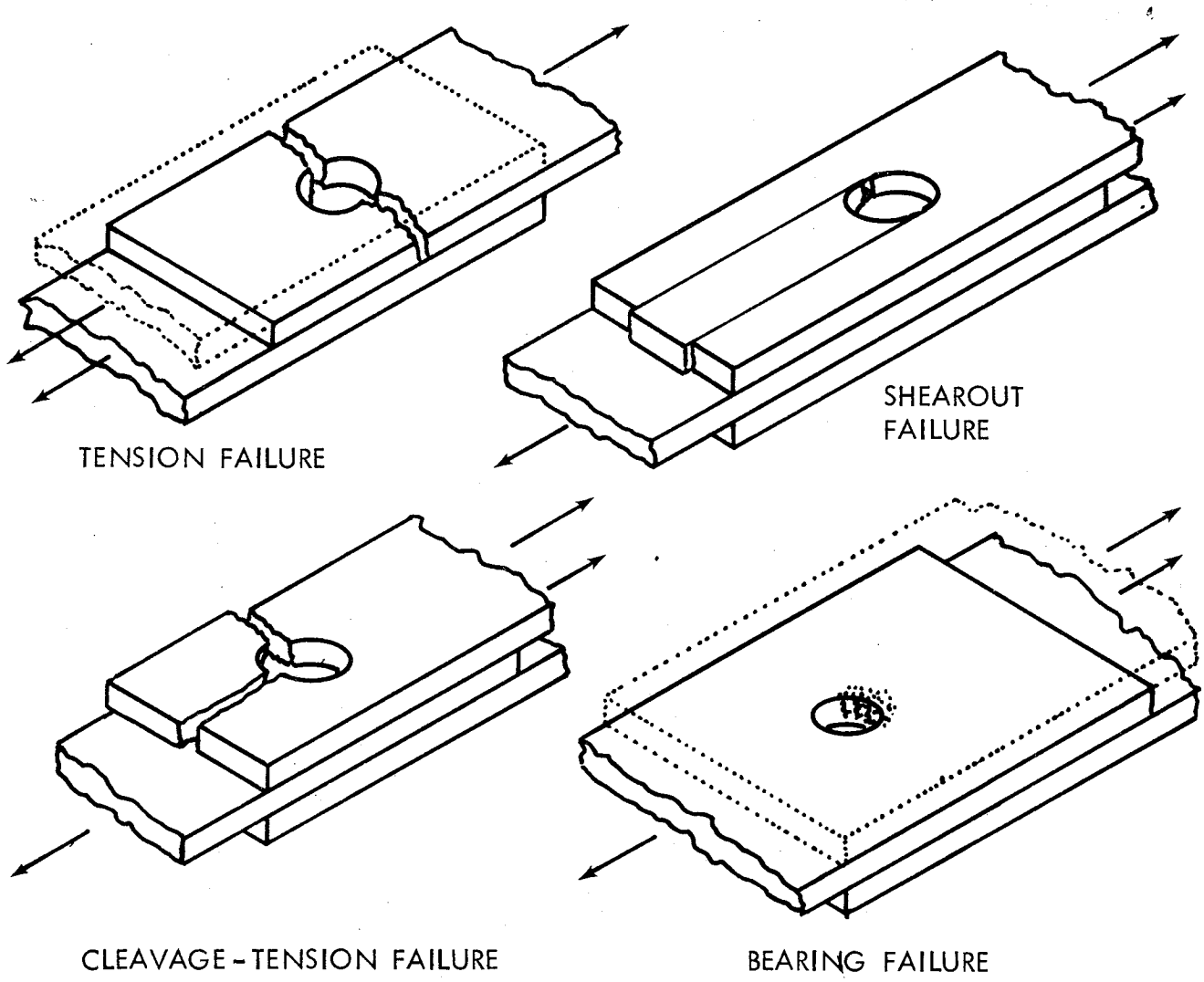

FIGURE 14. MODES OF FAILURE FOR BOLTED JOINTS IN ADVANCED COMPOSITES

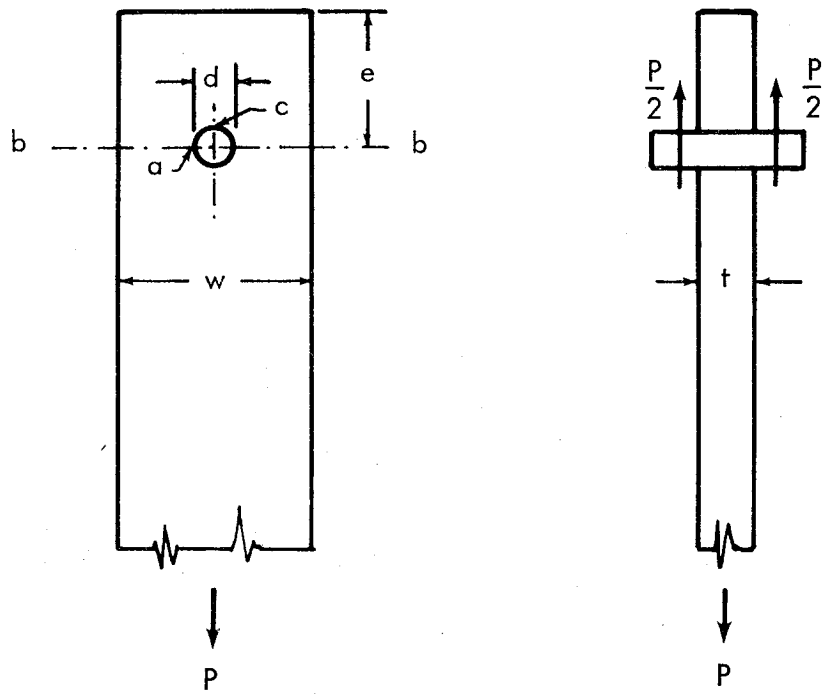

FIGURE 15. GEOMETRY OF DOUBLE-LAP BOLTED JOINT

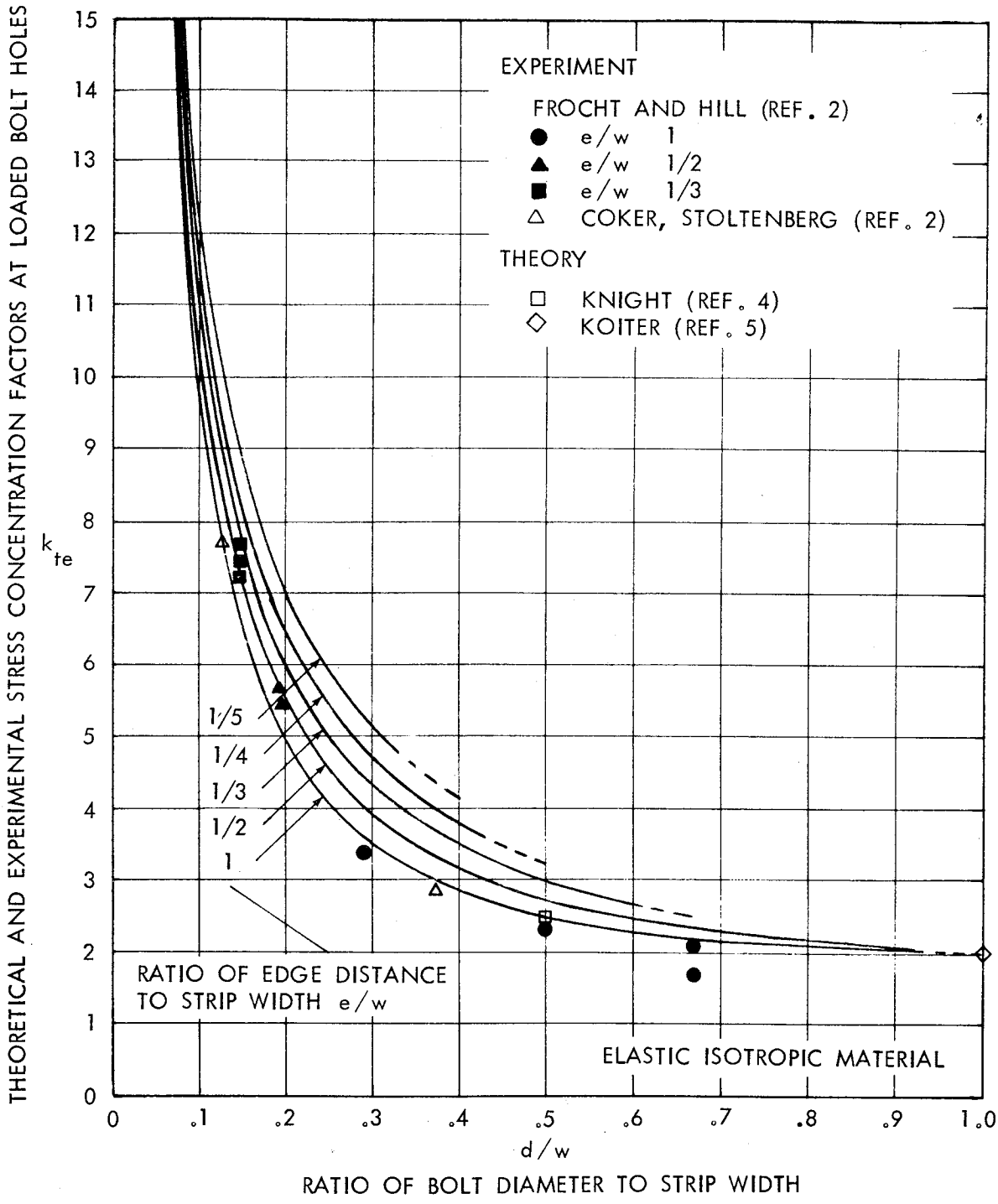

FIGURE 16. ELASTIC ISOTROPIC STRESS CONCENTRATION FACTORS FOR LOADED BOLT HOLES, WITH REFERENCE TO NET SECTION

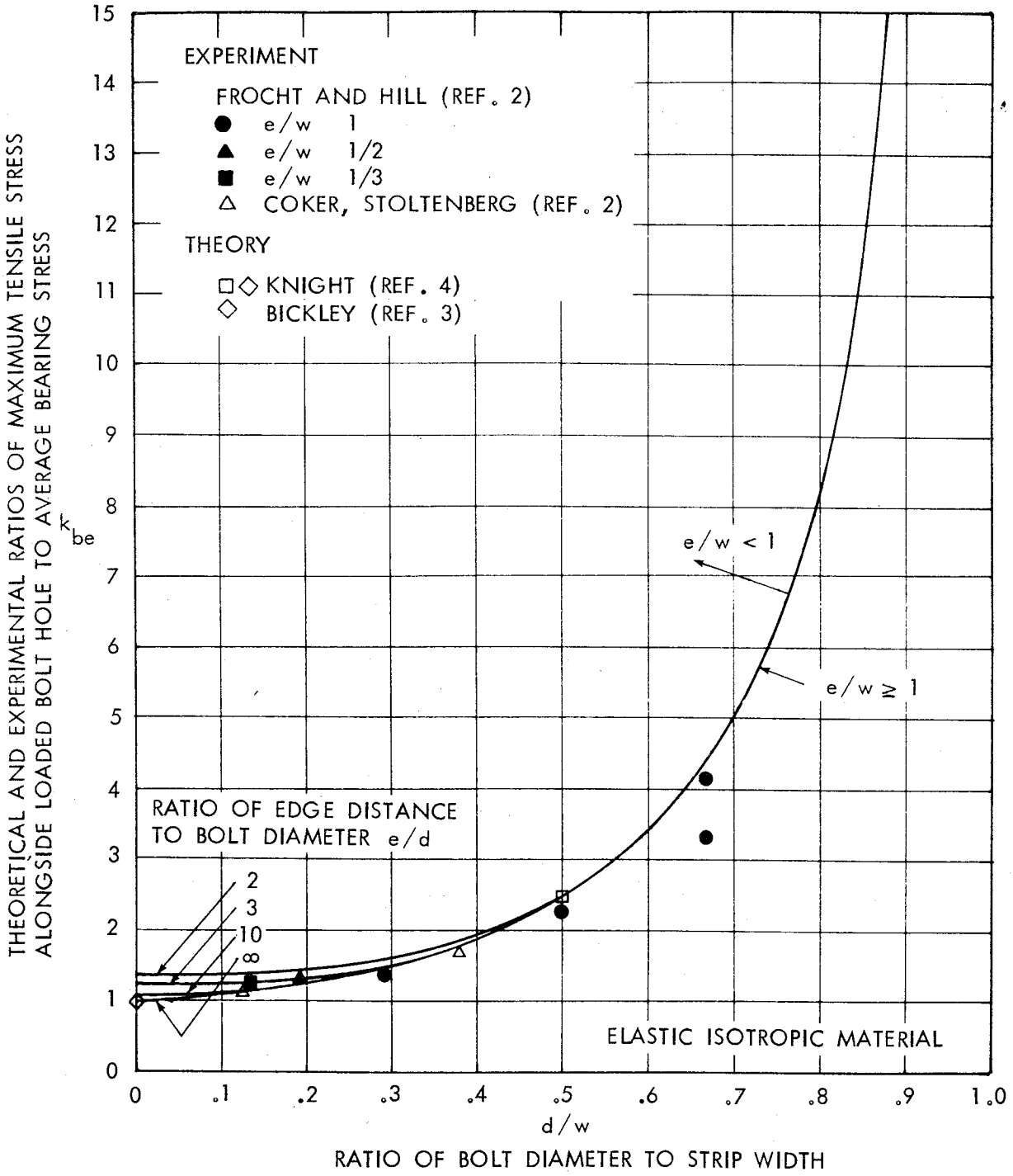

FIGURE 17. ELASTIC ISOTROPIC STRESS CONCENTRATION FACTORS FOR LOADED BOLT HOLES, WITH REFERENCE TO BOLT BEARING AREA

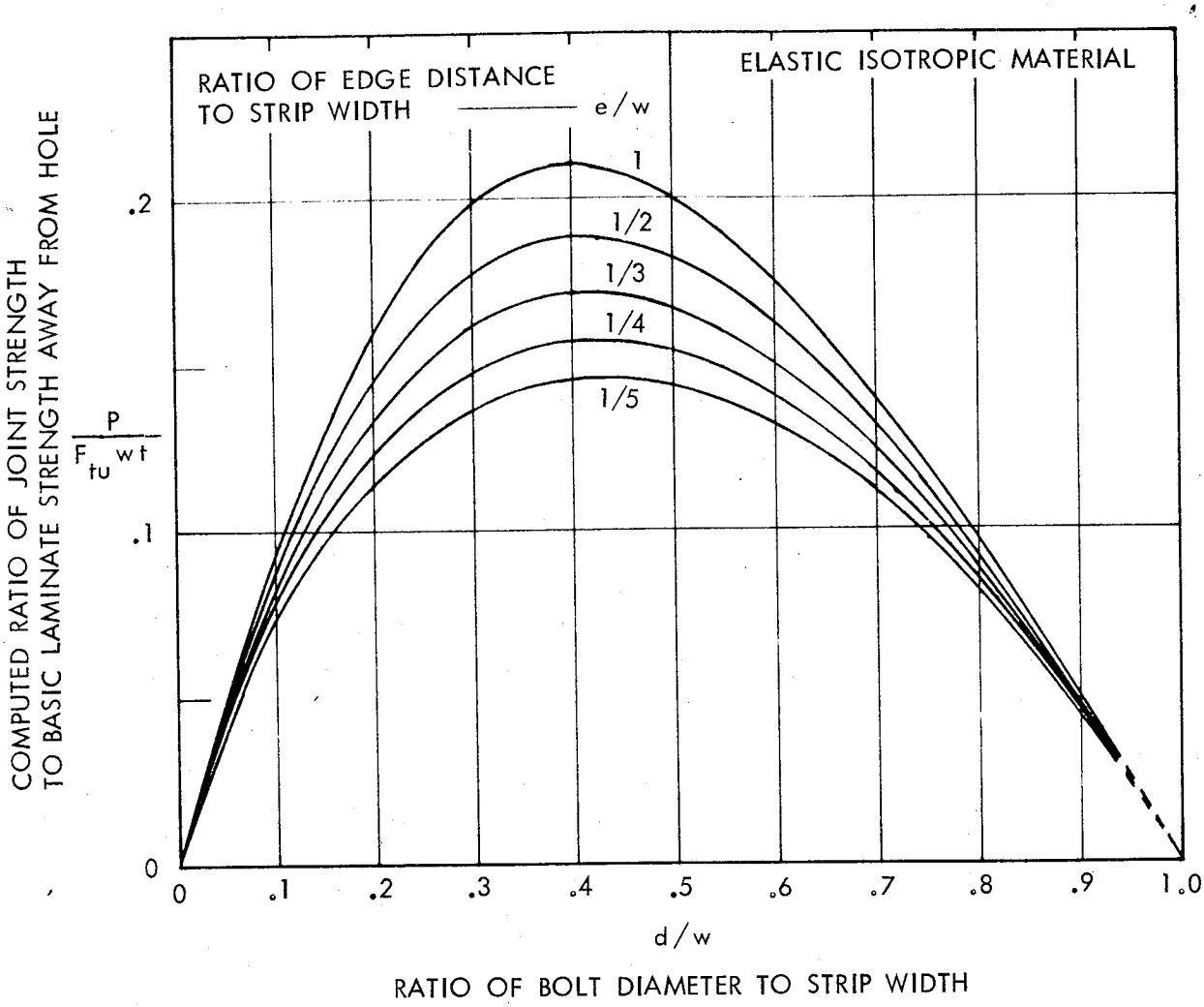

FIGURE 18. INFLUENCE OF JOINT GEOMETRY ON ELASTIC STRENGTH OF BOLTED JOINTS IN ISOTROPIC MATERIAL

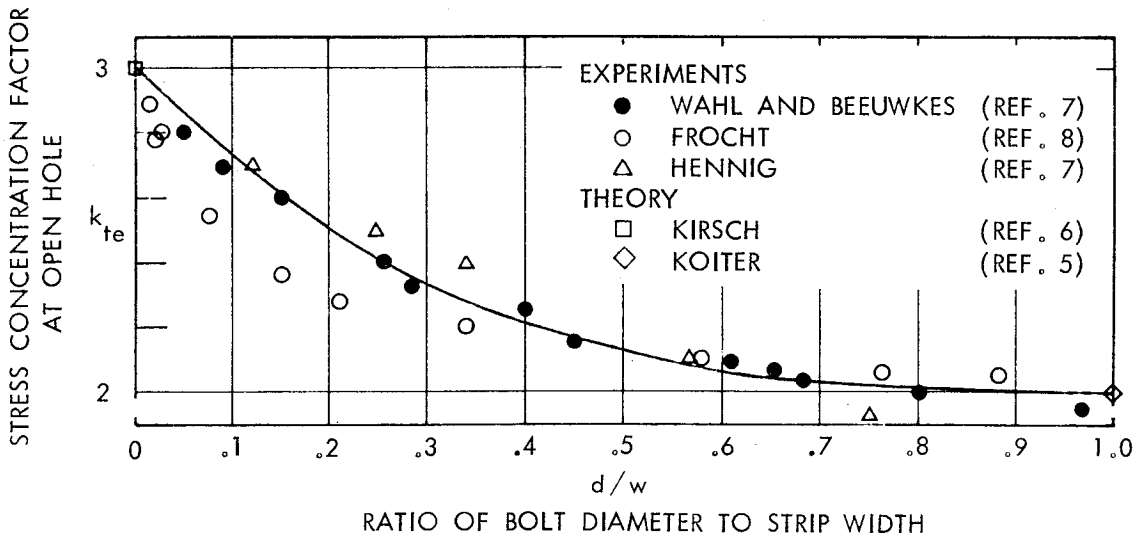

FIGURE 19. ELASTIC ISOTROPIC STRESS CONCENTRATION FACTORS FOR OPEN HOLES IN STRIPS OF FINITE WIDTH

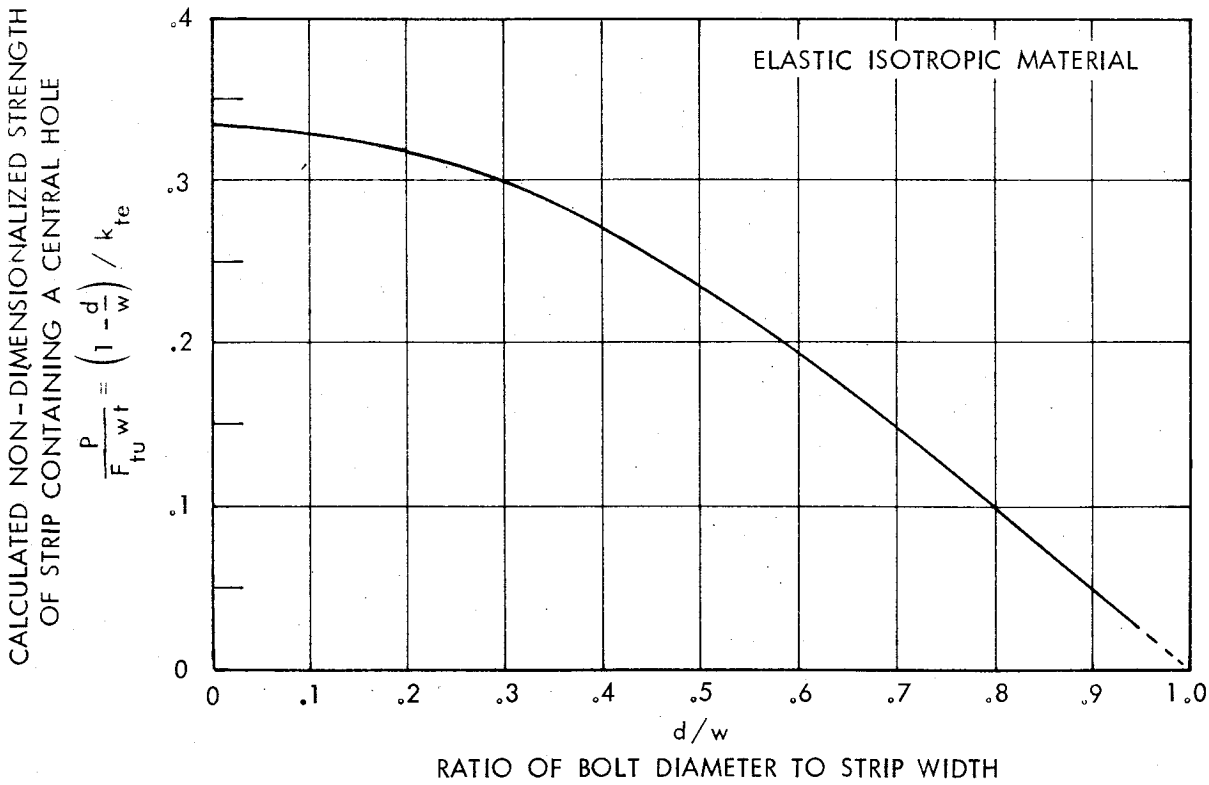

FIGURE 20. INFLUENCE OF JOINT GEOMETRY ON ELASTIC STRENGTH OF FINITE-WIDTH STRIPS CONTAINING OPEN HOLES

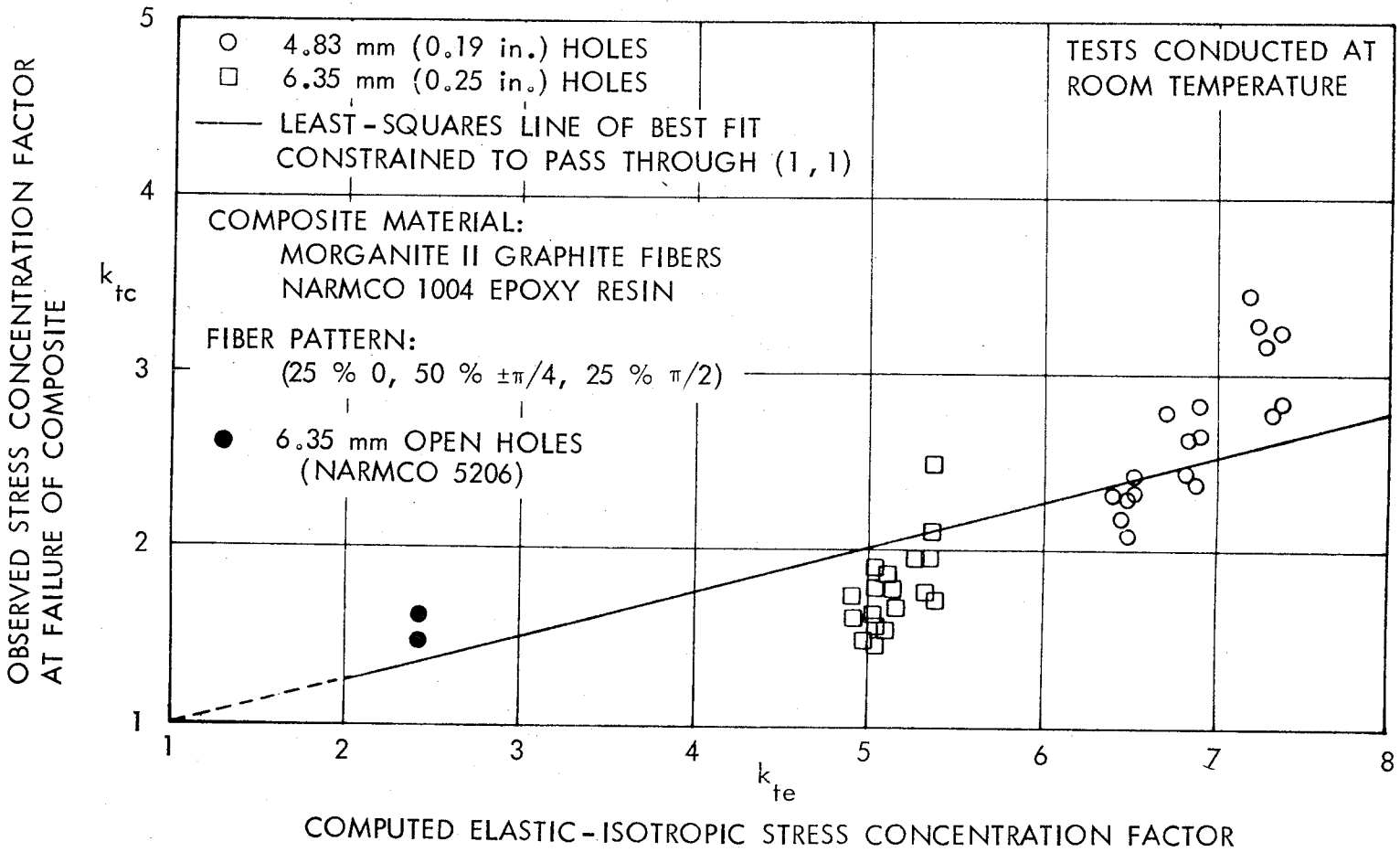

FIGURE 21. STRESS CONCENTRATION FACTORS AT FAILURE FOR BOLTED JOINTS IN MORGANITE II / NARMCO 1004 GRAPHITE-EPOXY (QUASI-ISOTROPIC PATTERN)

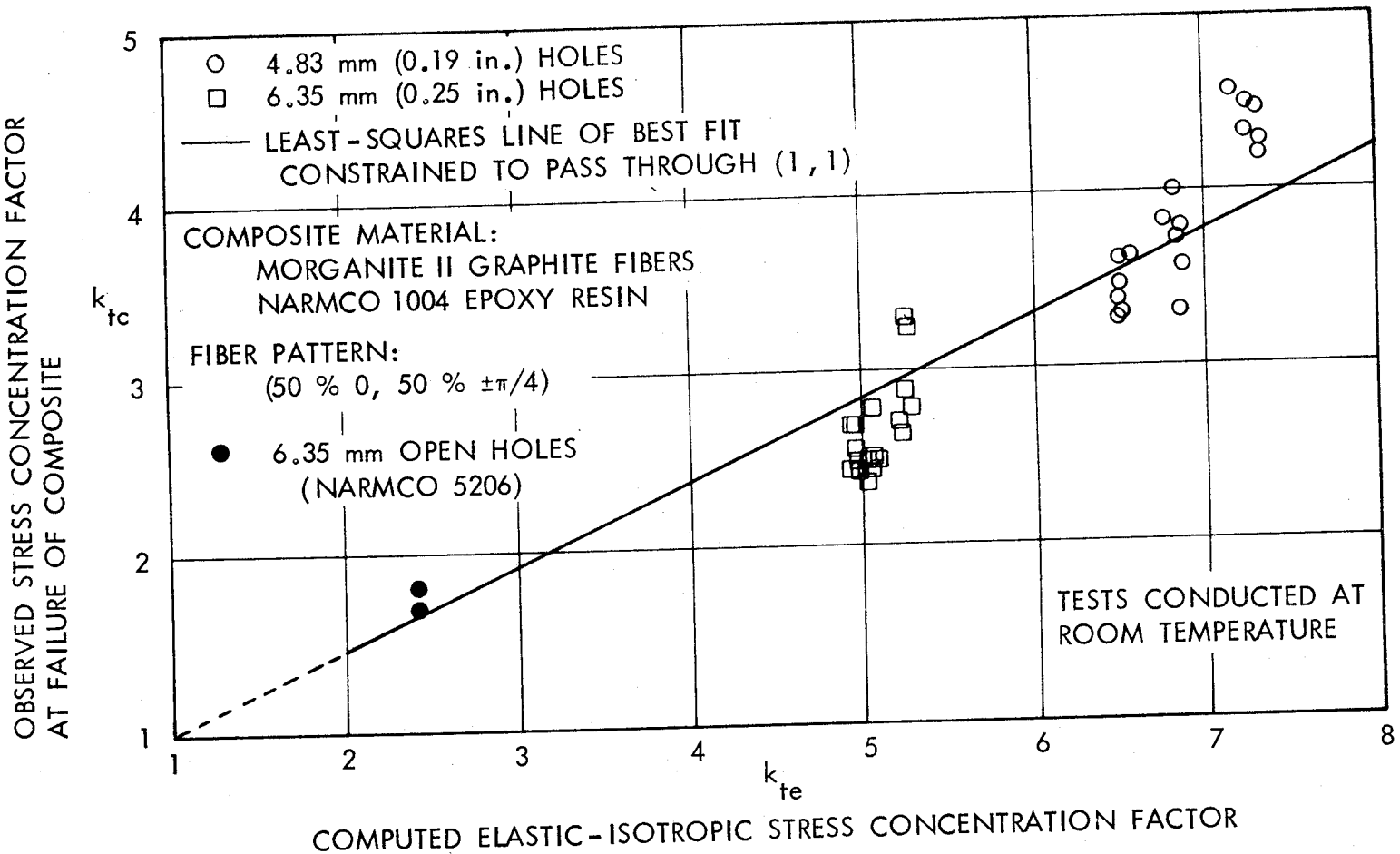

FIGURE 22. STRESS CONCENTRATION FACTORS AT FAILURE FOR BOLTED JOINTS IN MORGANITE II / NARMCO 1004 GRAPHITE-EPOXY (ORTHPTROPIC PATTERN)

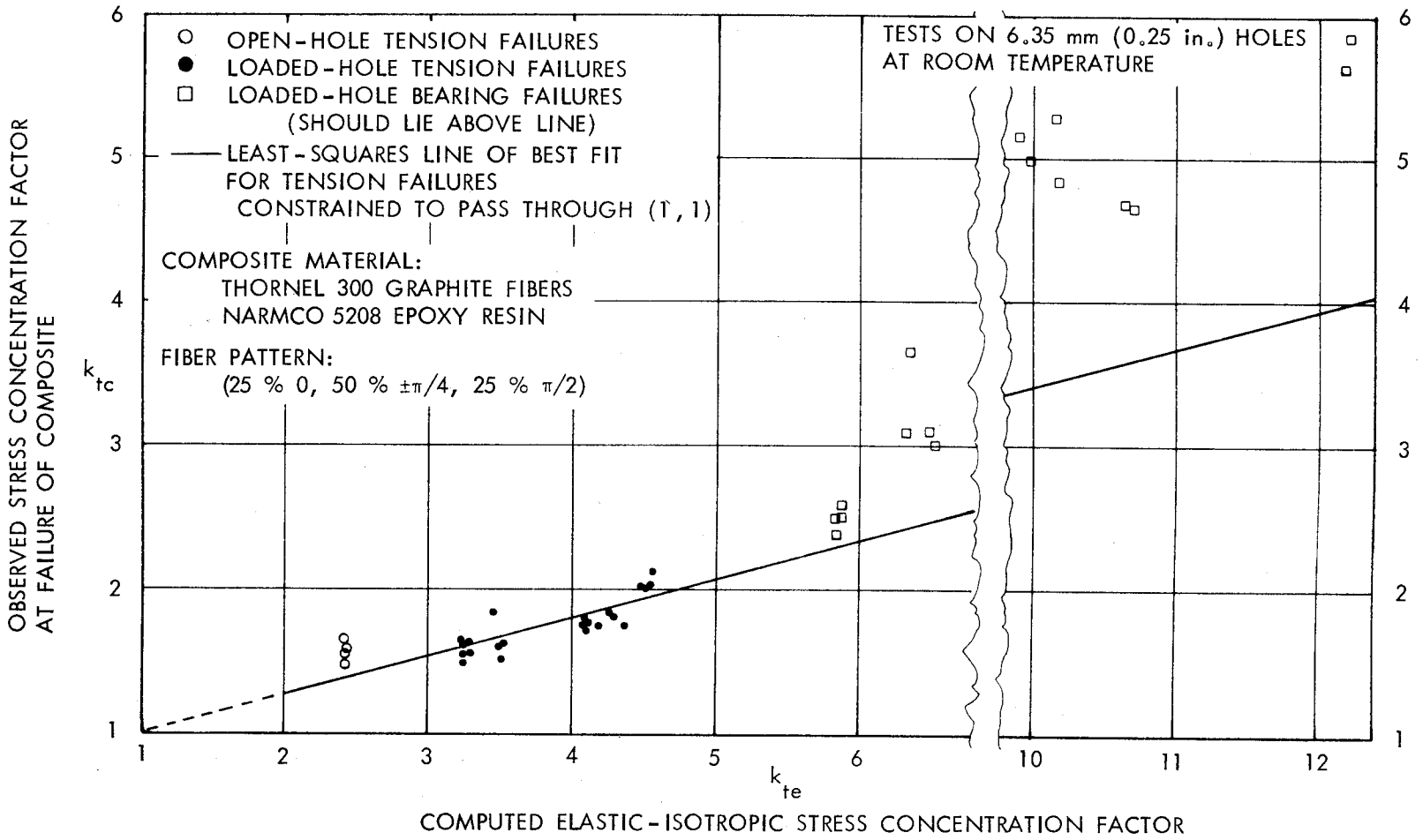

FIGURE 23. STRESS CONCENTRATION FACTORS AT FAILURE FOR BOLTED JOINTS IN THORNEL 300 / NARMCO 5208 GRAPHITE-EPOXY (QUASI-ISOTROPIC PATTERN)

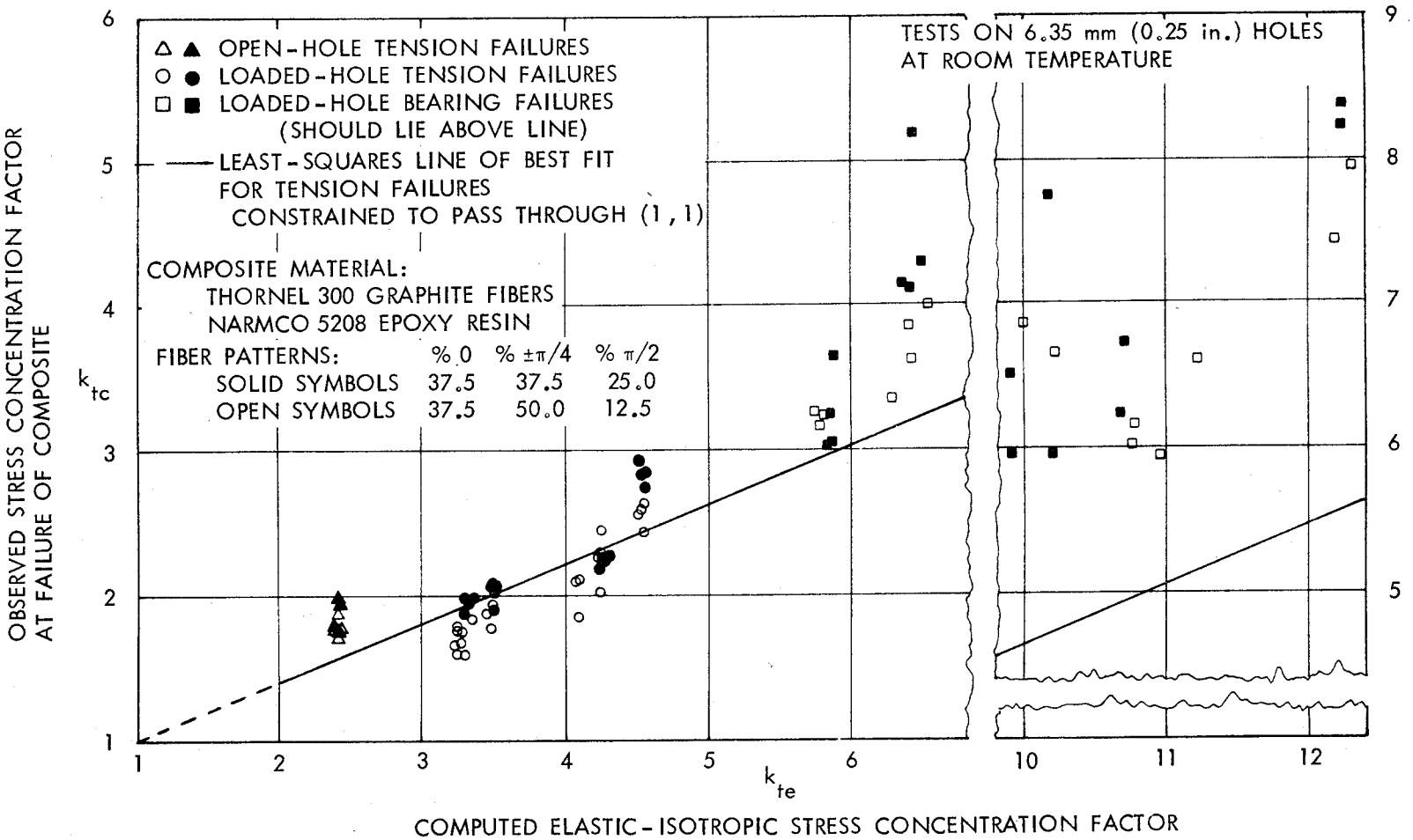

FIGURE 24. STRESS CONCENTRATION FACTORS AT FAILURE FOR BOLTED JOINTS IN THORNEL 300 / NARMCO 5208 GRAPHITE-EPOXY (ORTHOTROPIC PATTERNS)

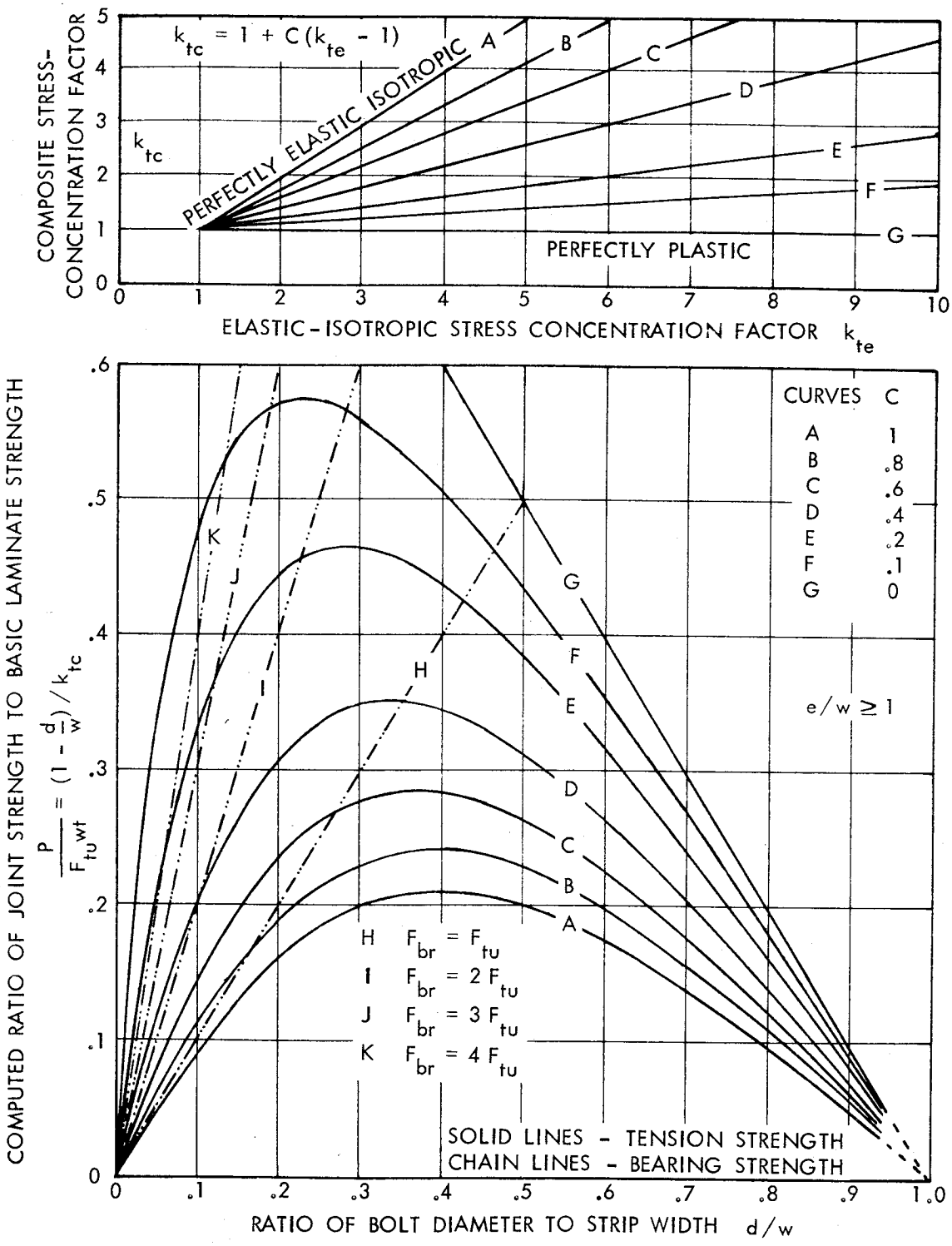

FIGURE 25. INFLUENCE OF JOINT GEOMETRY ON PREDICTED TENSILE STRENGTHS OF BOLTED JOINTS IN COMPOSITES

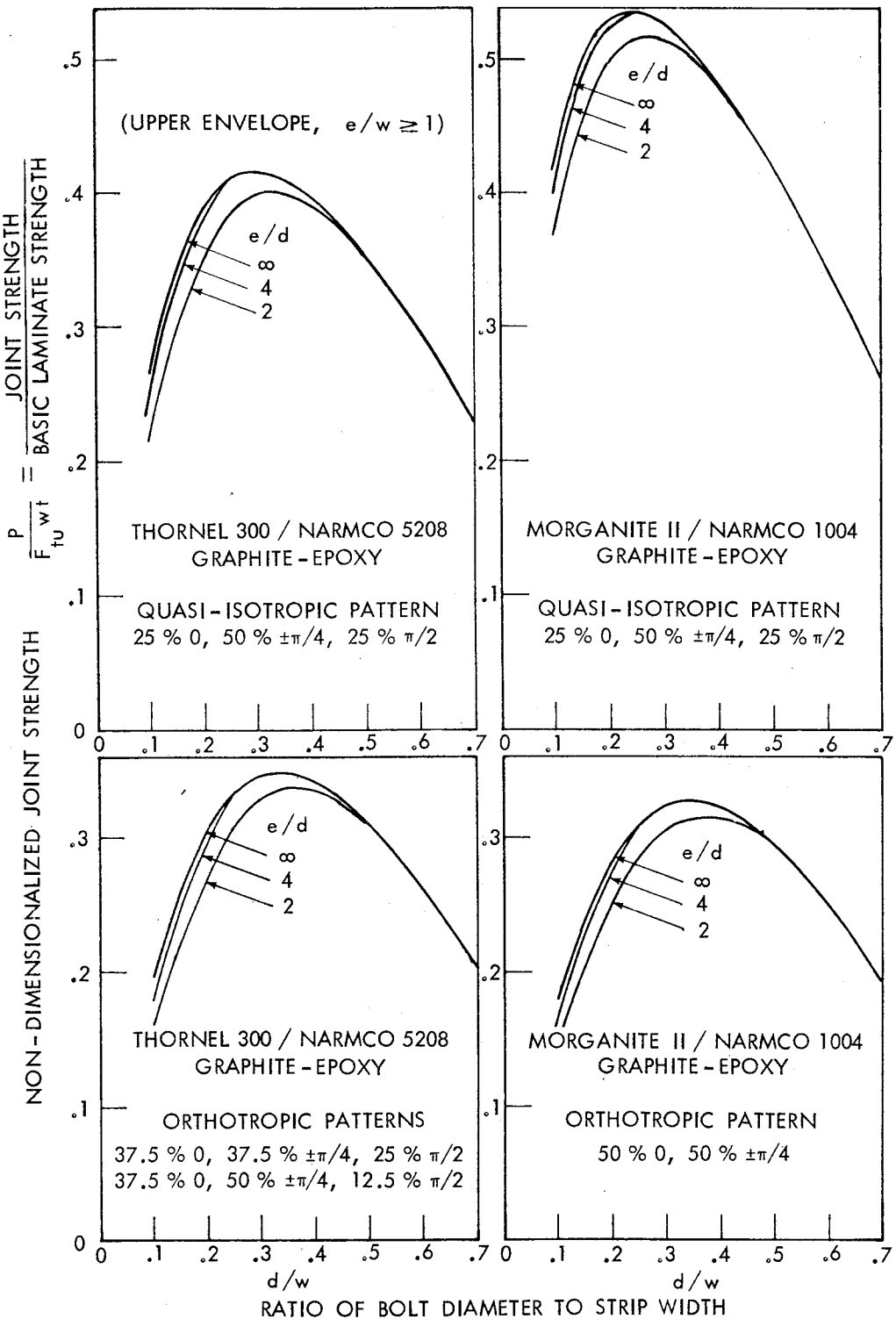

FIGURE 26. INFLUENCE OF JOINT GEOMETRY ON NET-SECTION TENSION STRENGTHS (PREDICTED EMPIRICALLY) FOR GRAPHITE EPOXIES

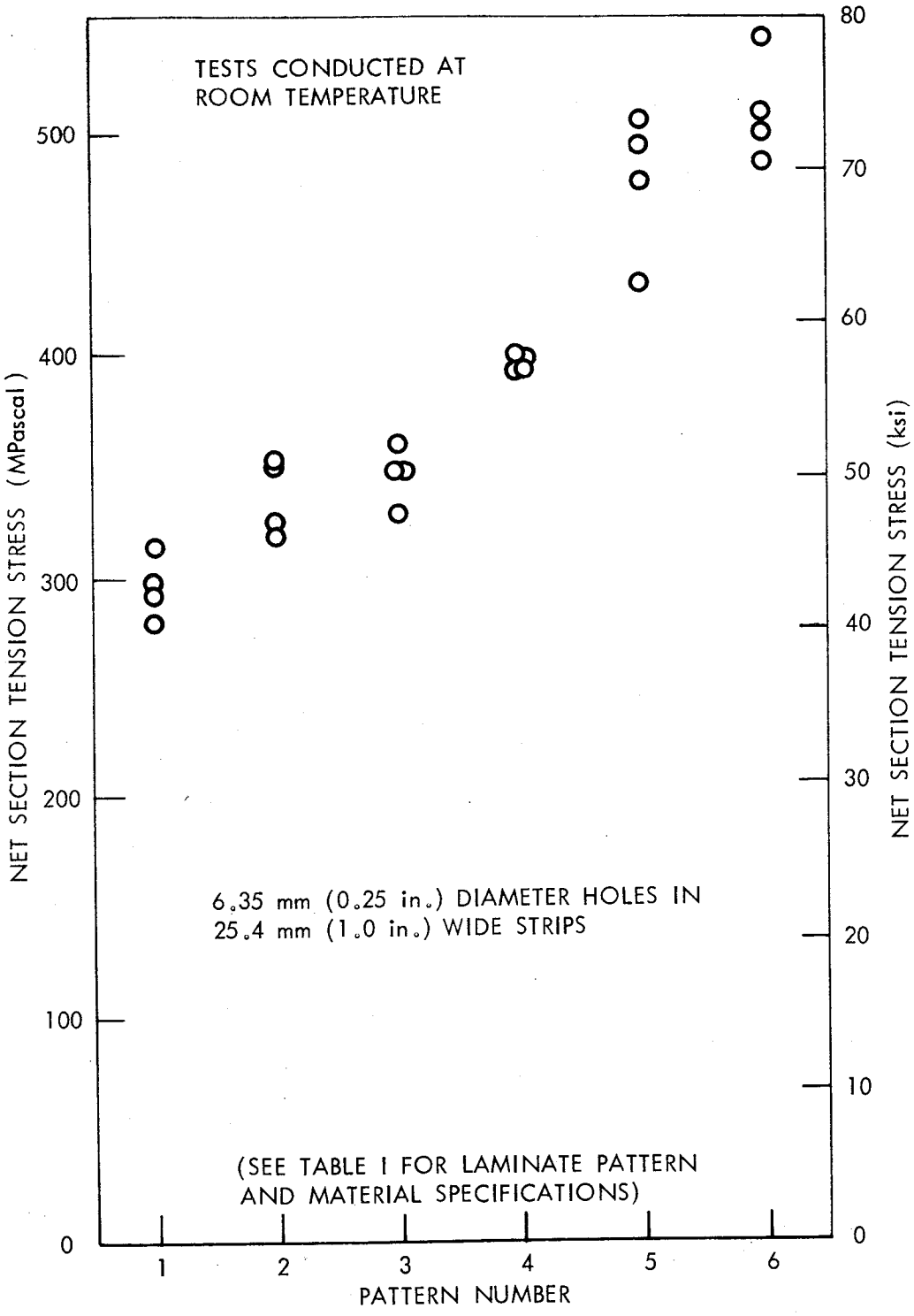

FIGURE 27. NET-SECTION FAILURE STRESSES FOR THORNEL 300 / NARMCO 5208 GRAPHITE-EPOXY AND S-1014 / THORNEL 300 / NARMCO 5208 GLASS-GRAPHITE-EPOXY COMPOSITE STRIPS CONTAINING OPEN HOLES

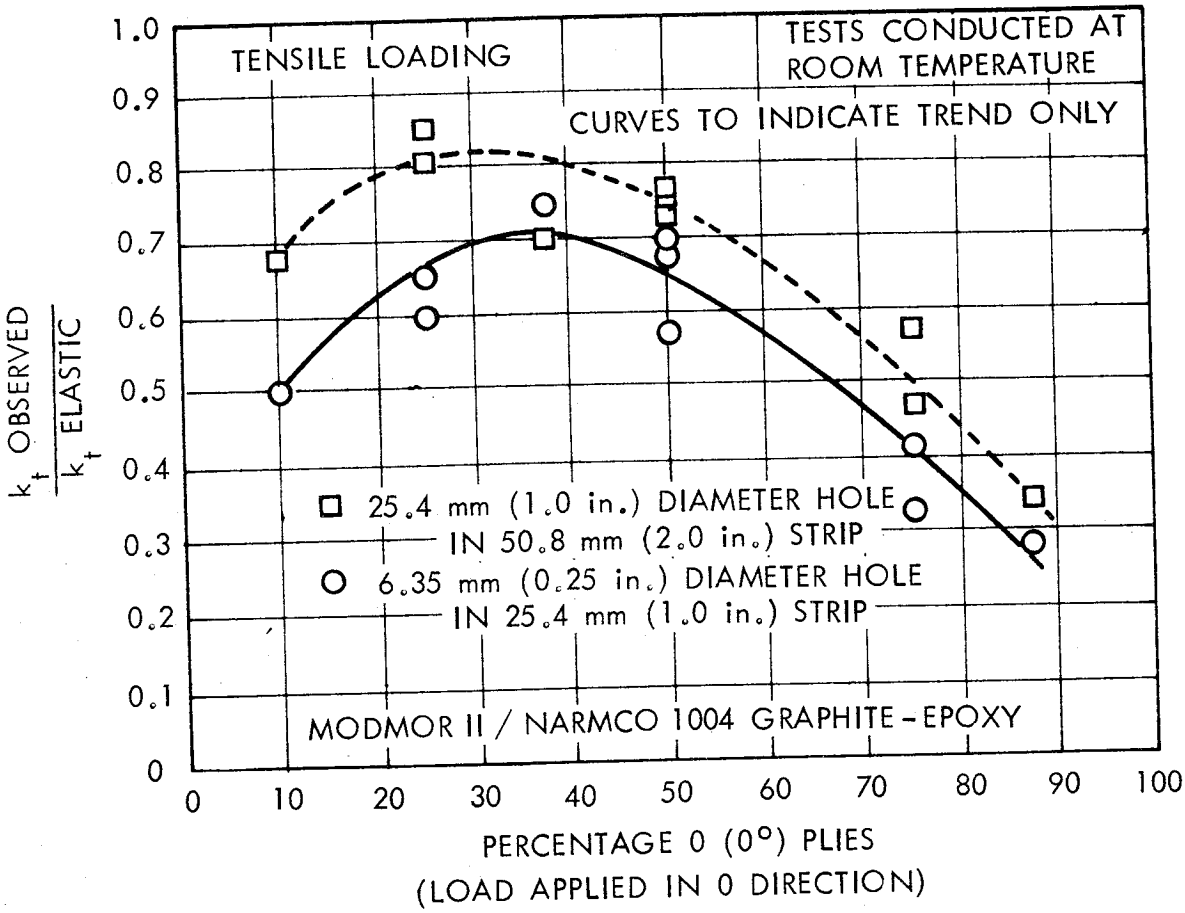

FIGURE 28. ASSESSMENT OF SCALE EFFECT AND INFLUENCE OF FIBER PATTERN ON STRESS CONCENTRATIONS AT FILLED (UNLOADED) HOLES IN MODMOR II / NARMCO 1004 GRAPHITE-EPOXY COMPOSITE UNDER TENSILE LOADING

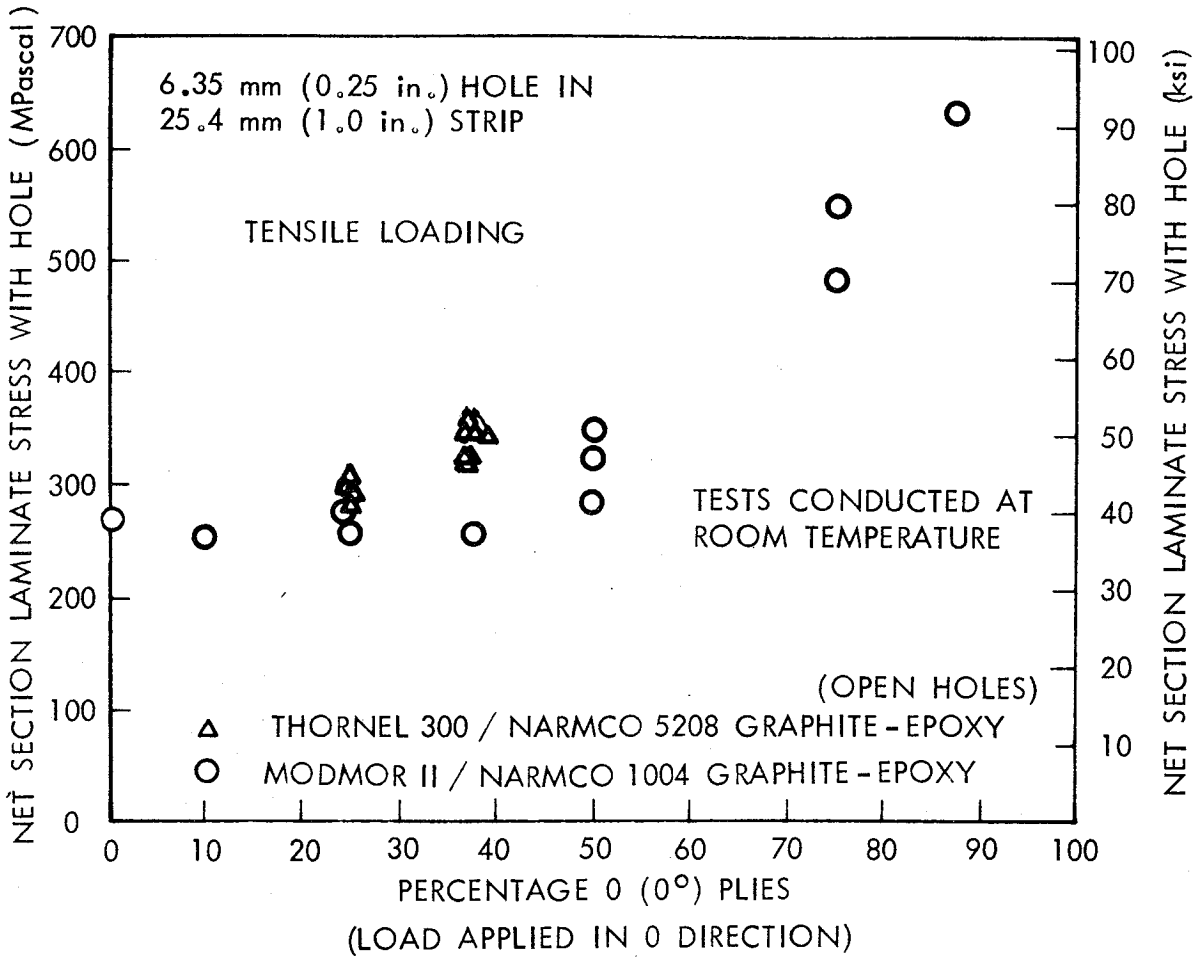

FIGURE 29. INFLUENCE OF FIBER PATTERN ON TENSILE STRENGTH OF MODMOR II / NARMCO 1004 GRAPHITE-EPOXY COMPOSITE STRIPS CONTAINING FILLED (UNLOADED) HOLES

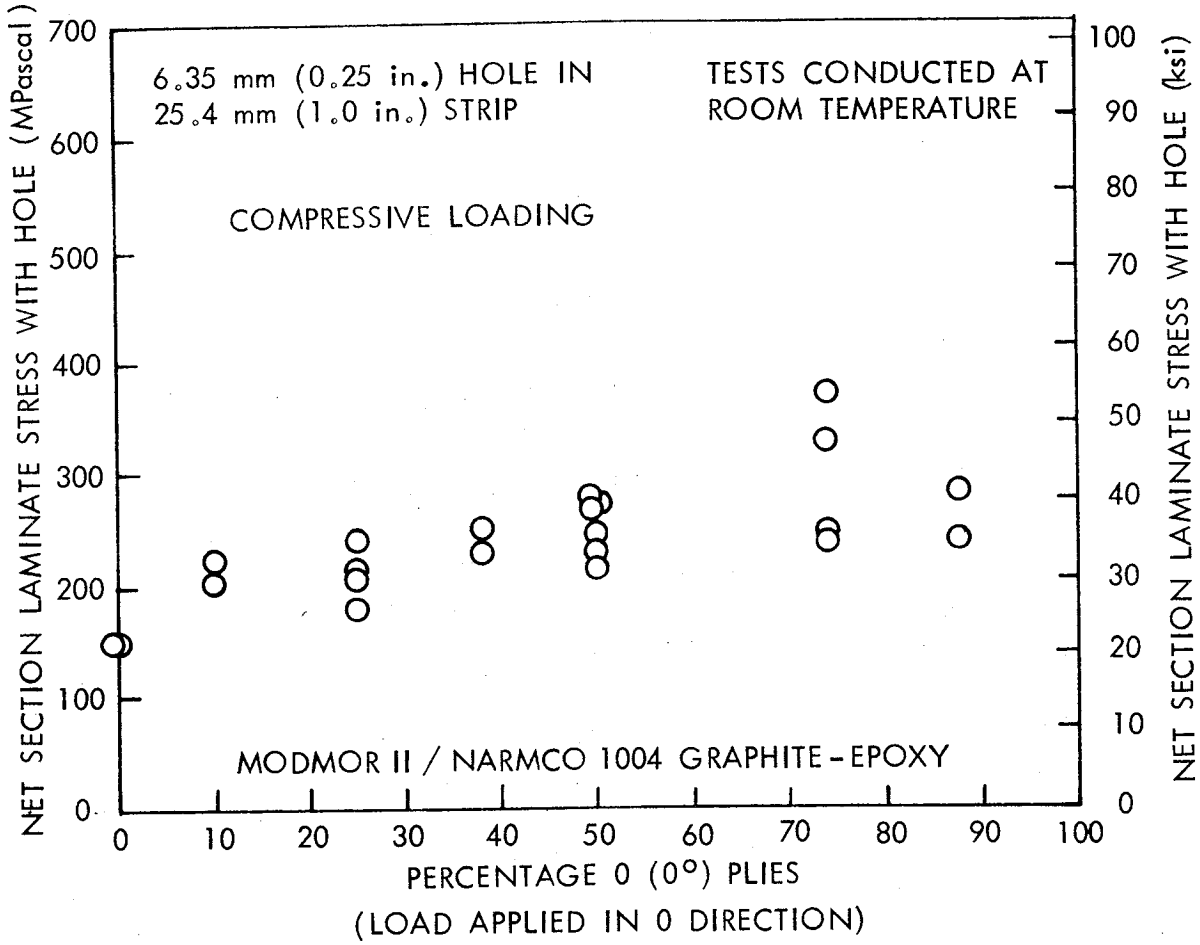

FIGURE 30. INFLUENCE OF FIBER PATTERN ON COMPRESSIVE STRENGTH OF MODMOR II / NARMCO 1004 GRAPHITE-EPOXY COMPOSITE STRIPS CONTAINING FILLED (UNLOADED) HOLES

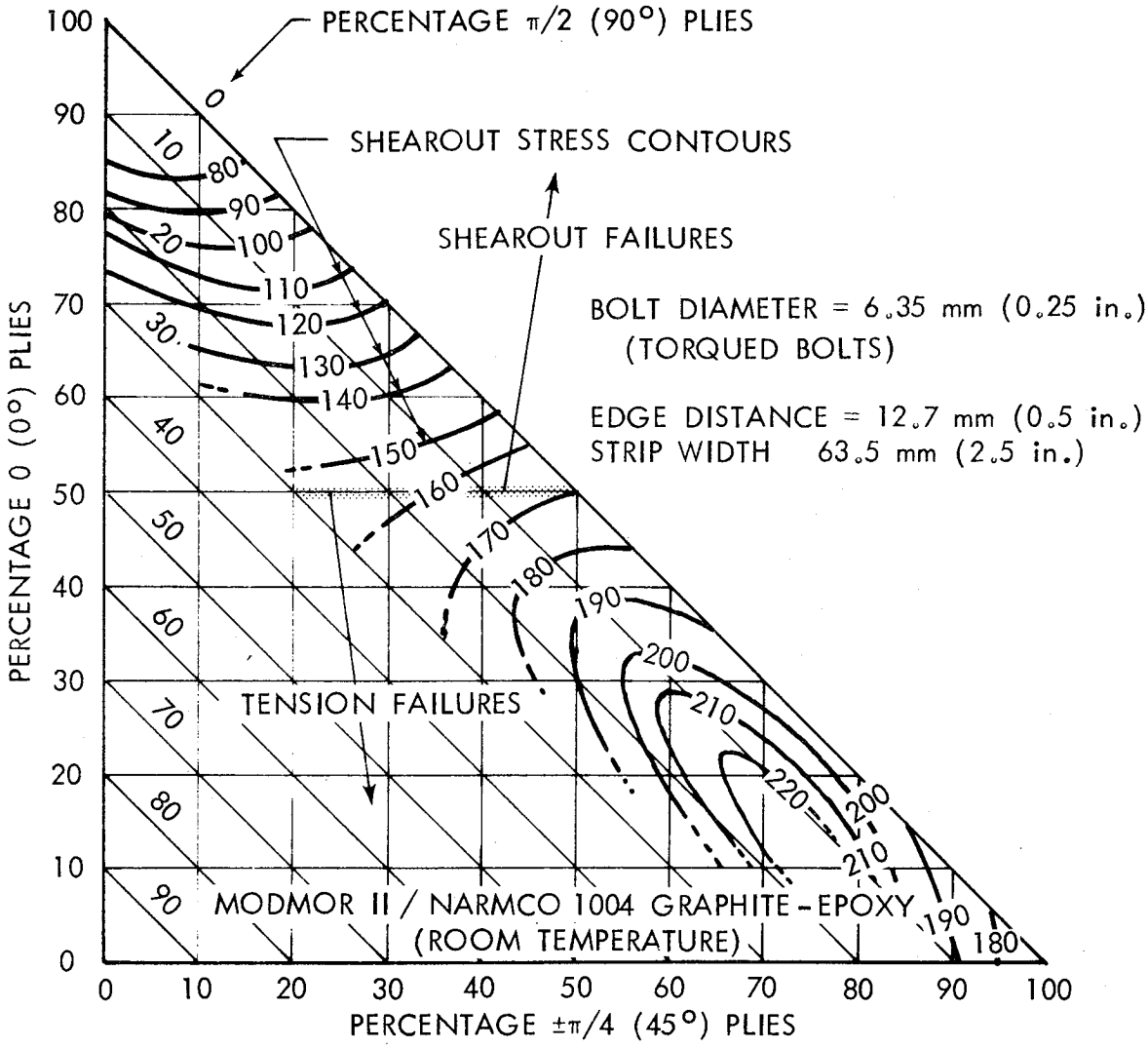

FIGURE 31. SHEAROUT STRESS CONTOURS FOR VARIOUS LAMINATE PATTERNS OF MODMOR II / NARMCO 1004 GRAPHITE-EPOXY COMPOSITES

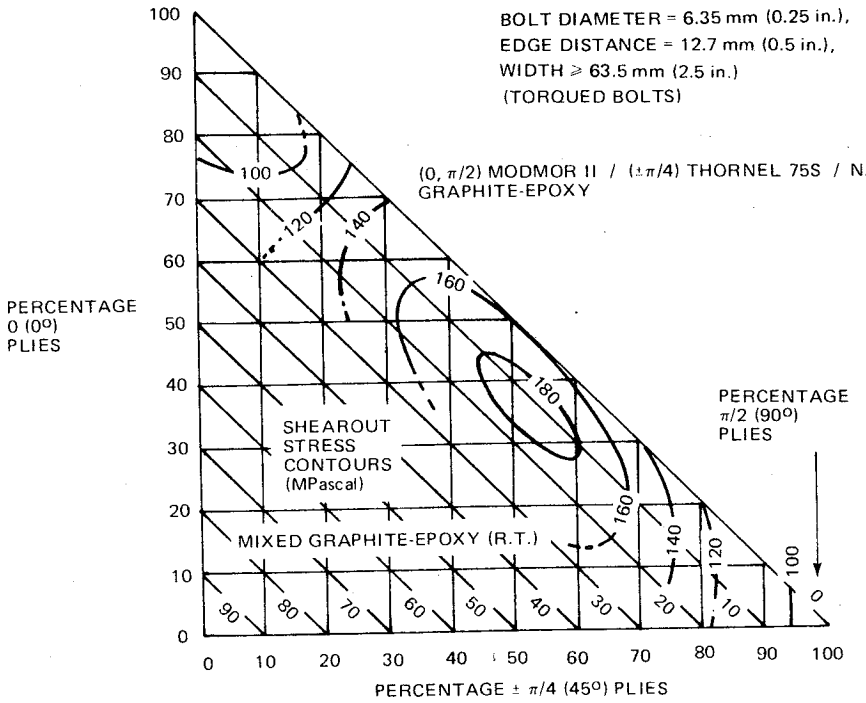

FIGURE 32. SHEAROUT STRESS CONTOURS FOR VARIOUS LAMINATE PATTERNS OF MODMOR II / THORNEL 75S / NARMCO 1004 GRAPHITE-EPOXY

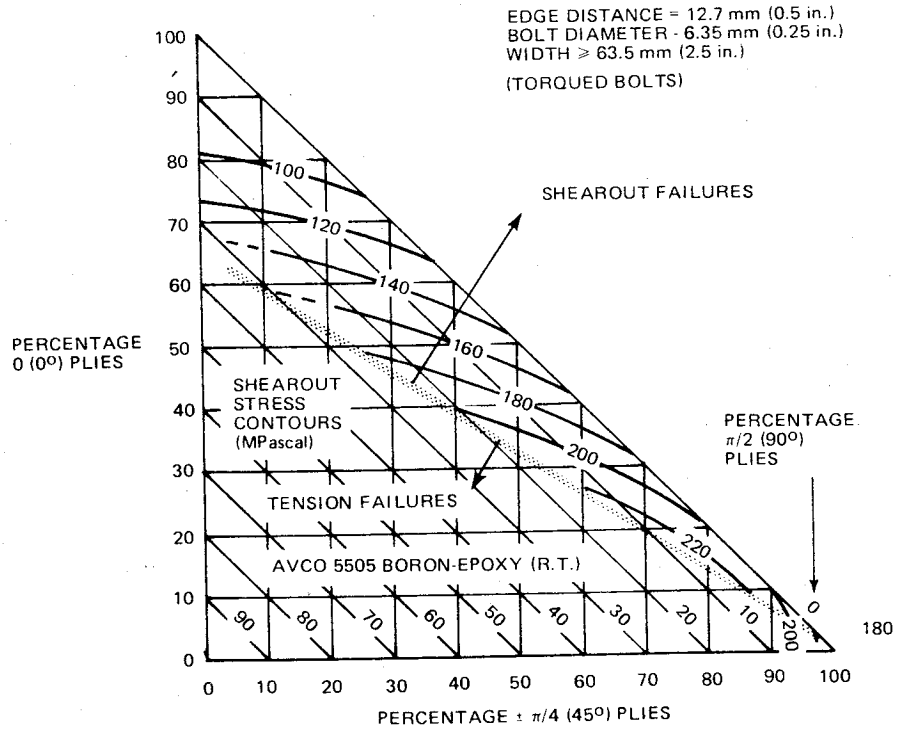

FIGURE 33. SHEAROUT STRESS CONTOURS FOR VARIOUS LAMINATE PATTERNS OF AVCO 5505 BORON-EPOXY COMPOSITE

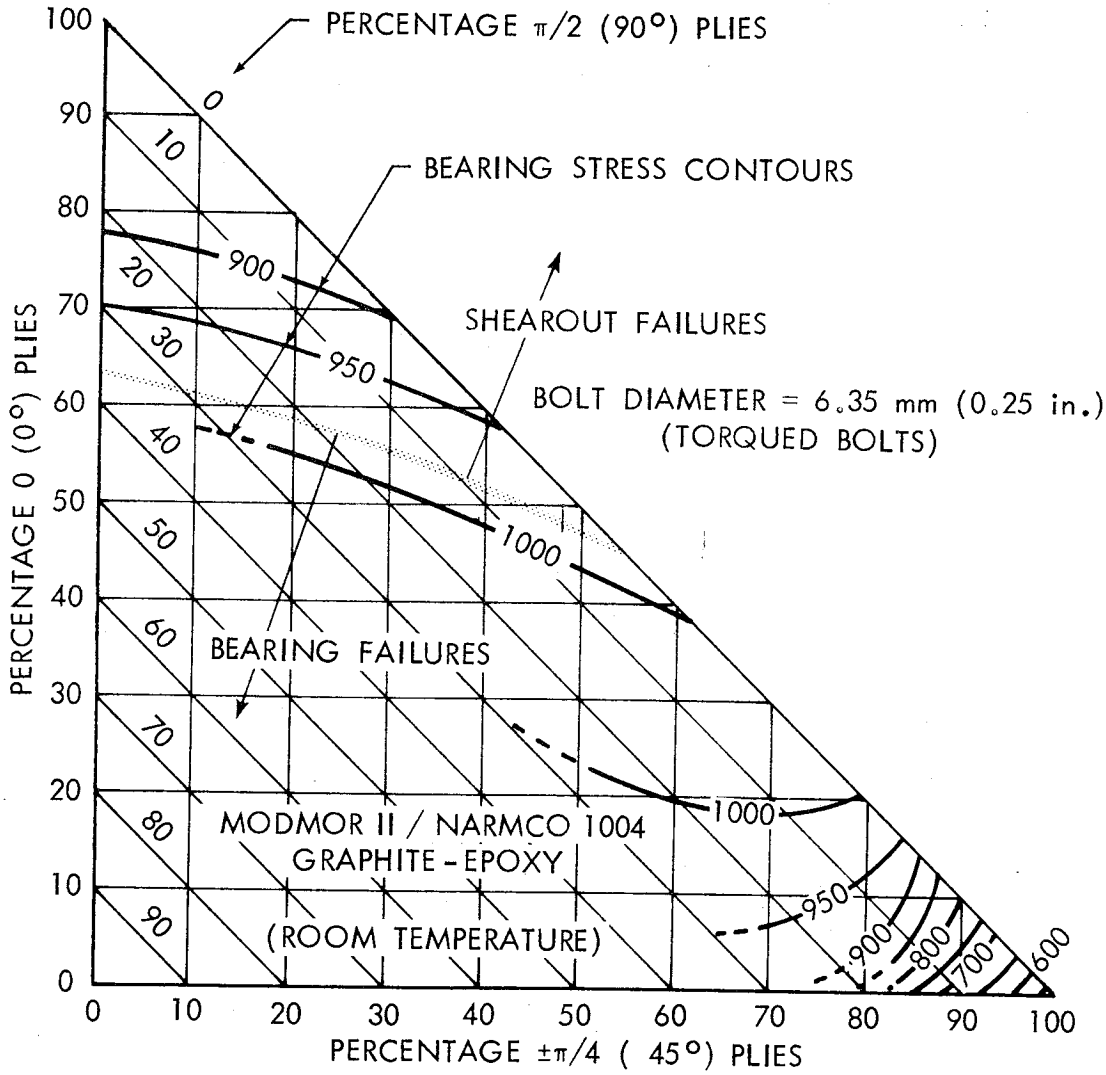

FIGURE 34. BEARING STRESS CONTOURS FOR VARIOUS LAMINATE PATTERNS OF MODMOR II / NARMCO 1004 GRAPHITE-EPOXY COMPOSITE

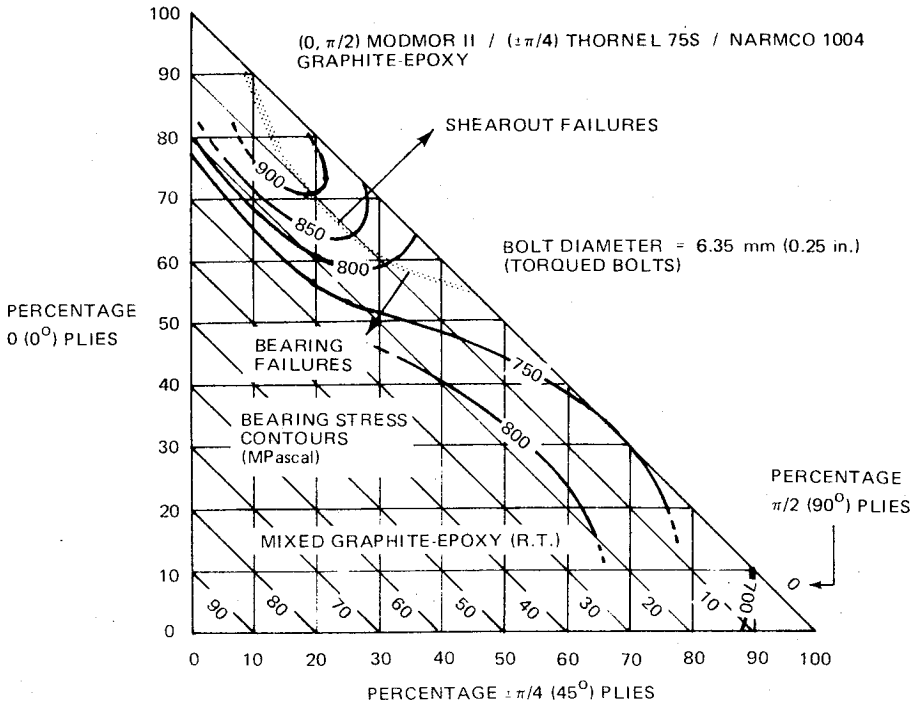

FIGURE 35. BEARING STRESS CONTOURS FOR VARIOUS LAMINATE PATTERNS OF MODMOR II / THORNEL 75S / NARMCO 1004 GRAPHITE-EPOXY

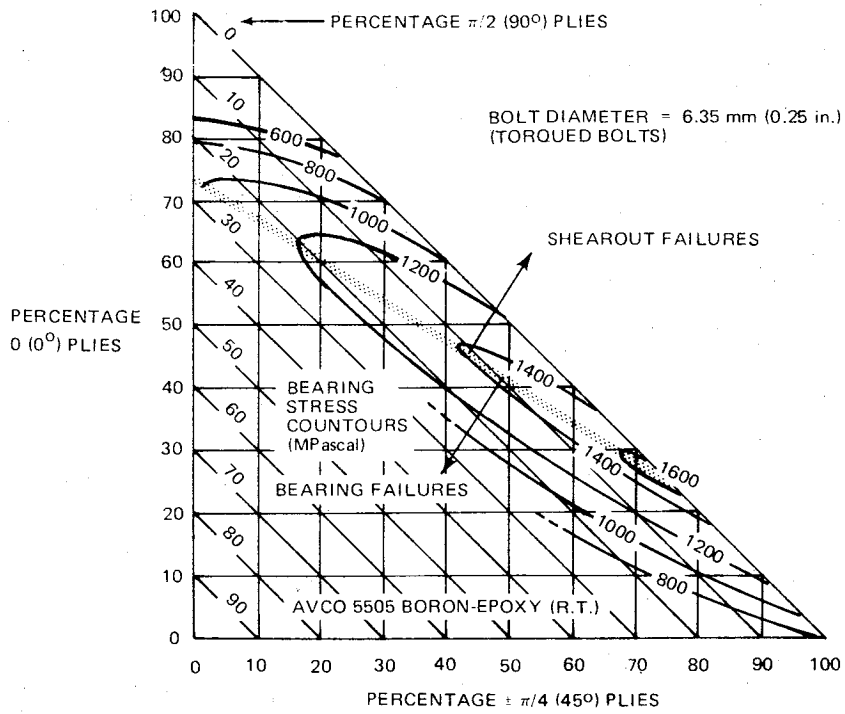

FIGURE 36. BEARING STRESS CONTOURS FOR VARIOUS LAMINATE PATTERNS OF AVCO 5505 BORON-EPOXY COMPOSITE

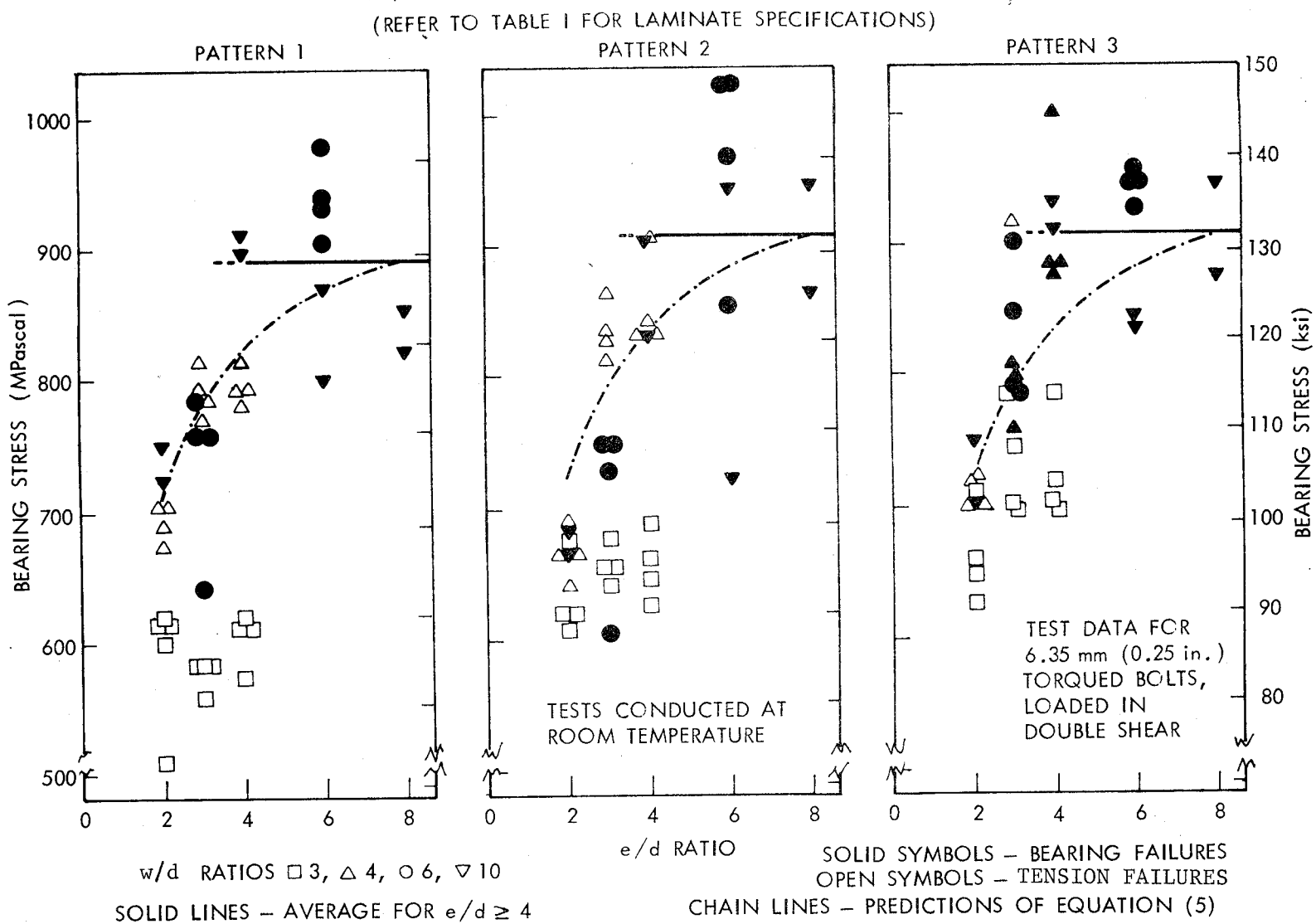

FIGURE 37. BEARING STRESS AS FUNCTION OF EDGE DISTANCE TO BOLT DIAMETER RATIO FOR THORNEL 300 / NARMCO 5208 GRAPHITE-EPOXY

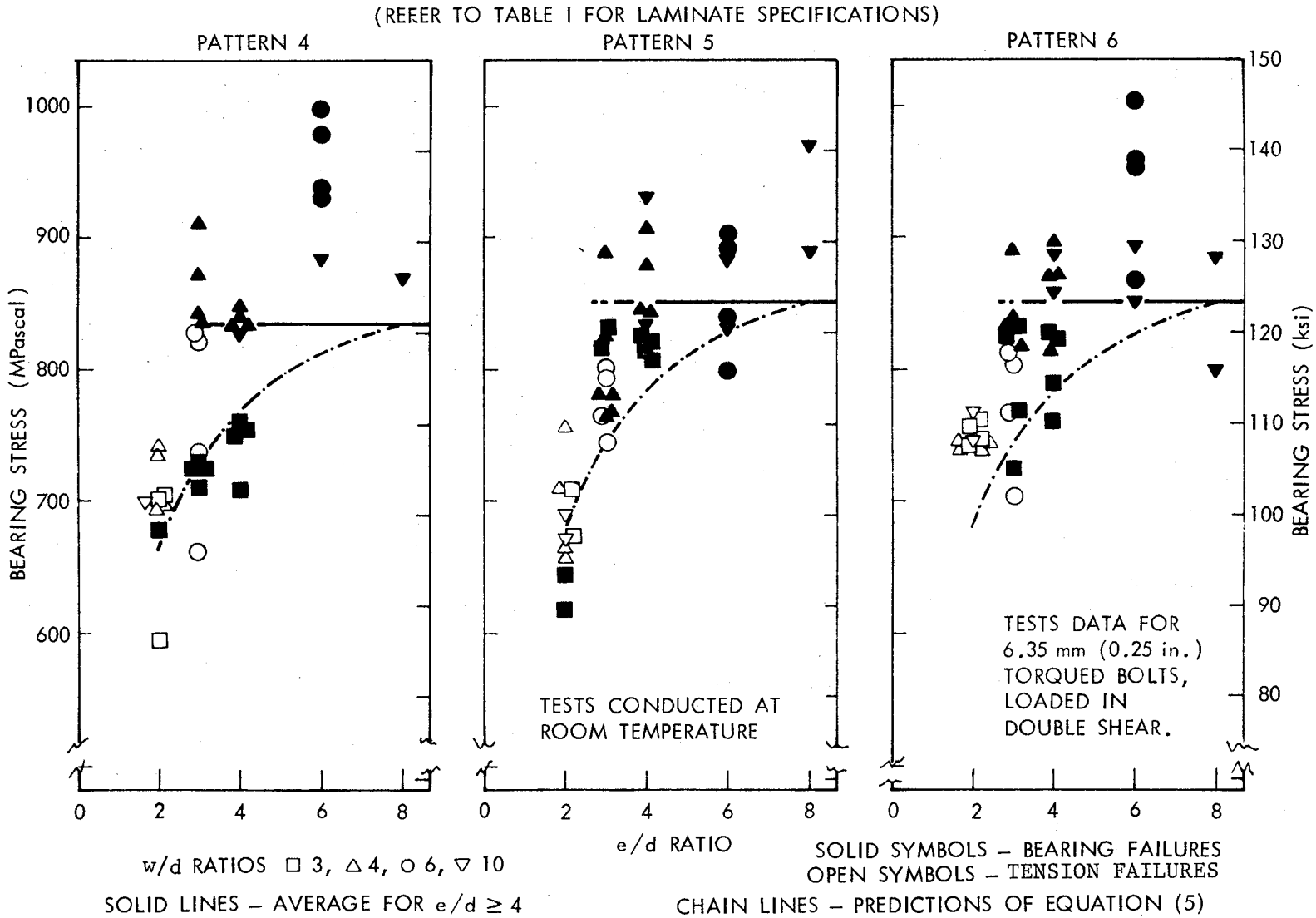

FIGURE 38. BEARING STRESS AS FUNCTION OF EDGE DISTANCE TO BOLT DIAMETER RATIO FOR S-1014 / THORNEL 300 / NARMCO 5208 GLASS-GRAPHITE-EPOXY

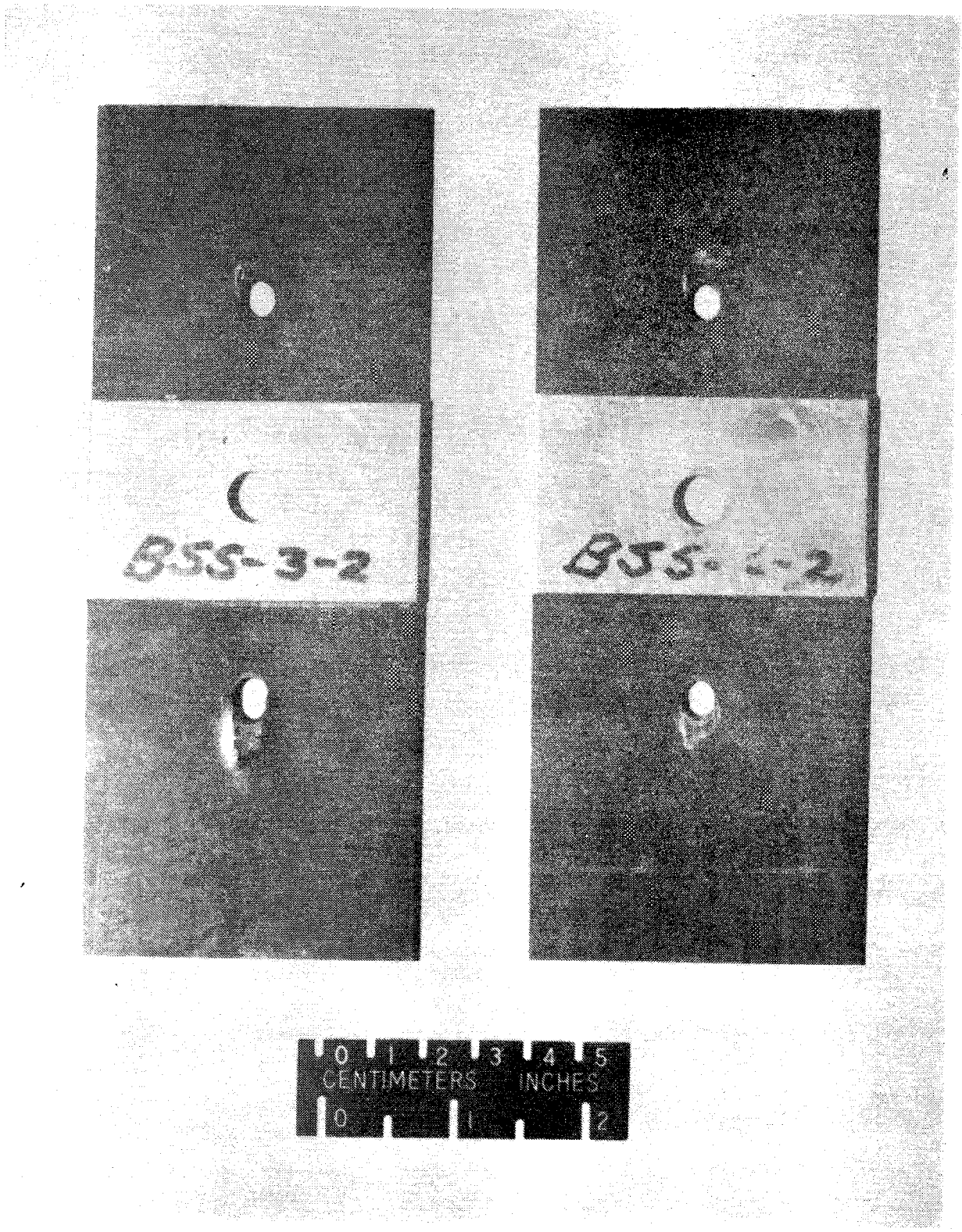

FIGURE 39. TYPICAL TENSILE-BEARING FAILURES OF BOLTED JOINTS IN GRAPHITE-EPOXY AND GLASS-GRAPHITE-EPOXY COMPOSITES

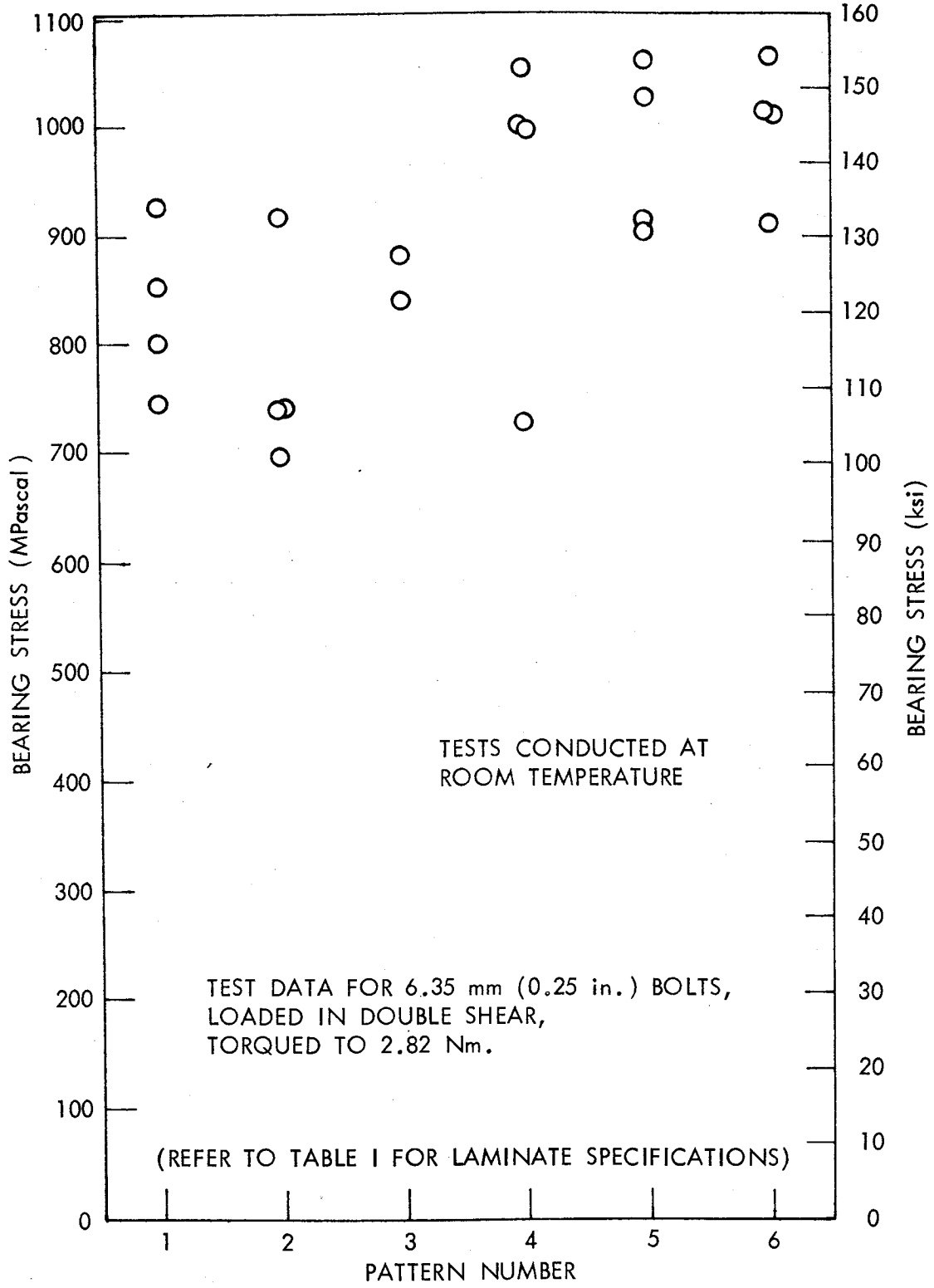

FIGURE 40. COMPRESSIVE - BEARING STRESSES FOR THORNEL 300 / NARMCO 5208 GRAPHITE - EPOXY AND S-1014 / THORNEL 300 / NARMCO 5208 GLASS - GRAPHITE - EPOXY

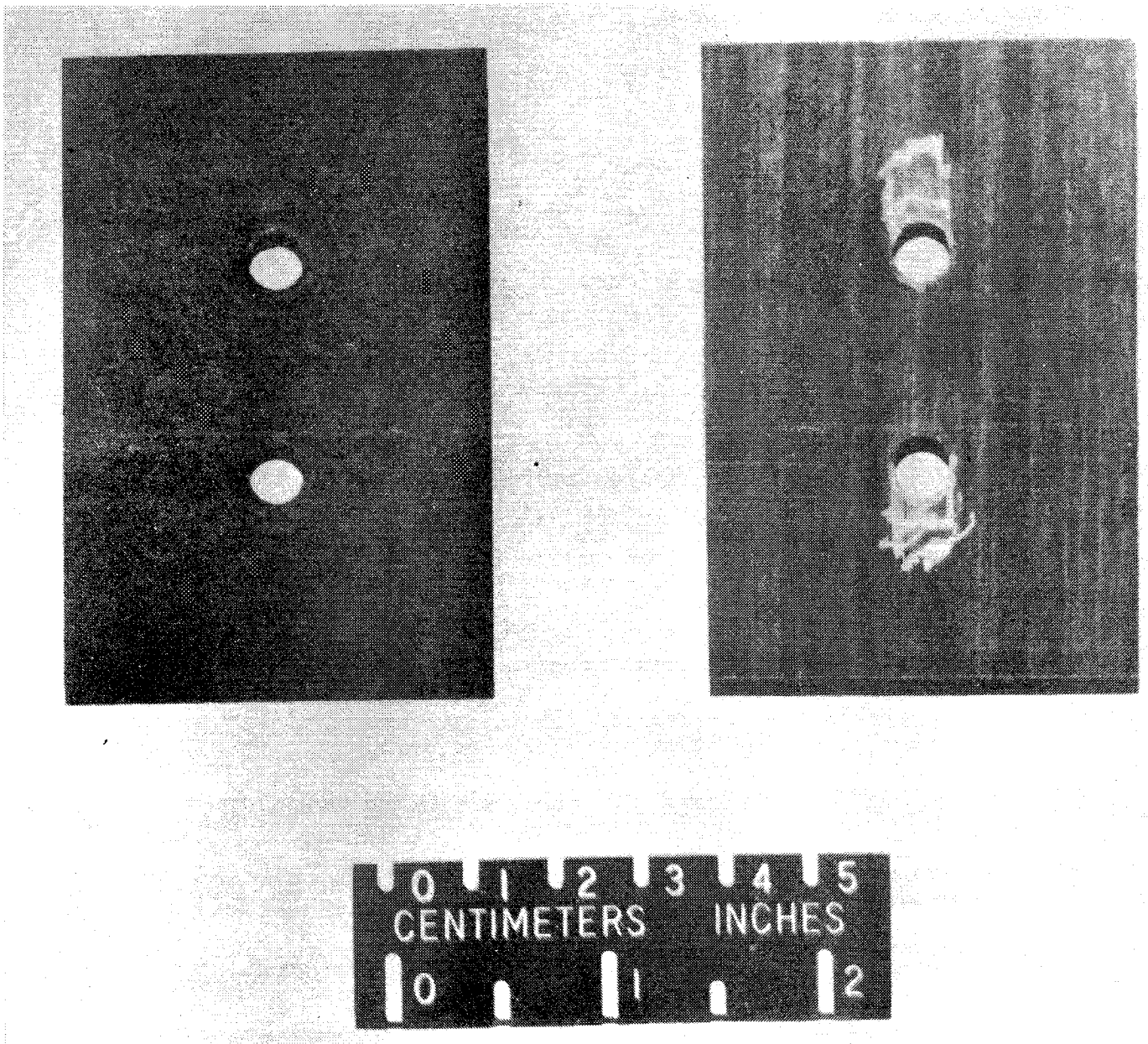

FIGURE 41. TYPICAL FAILURES OF BOLTED JOINTS UNDER COMPRESSIVE BEARING IN GRAPHITE-EPOXY AND GLASS-GRAPHITE-EPOXY COMPOSITES

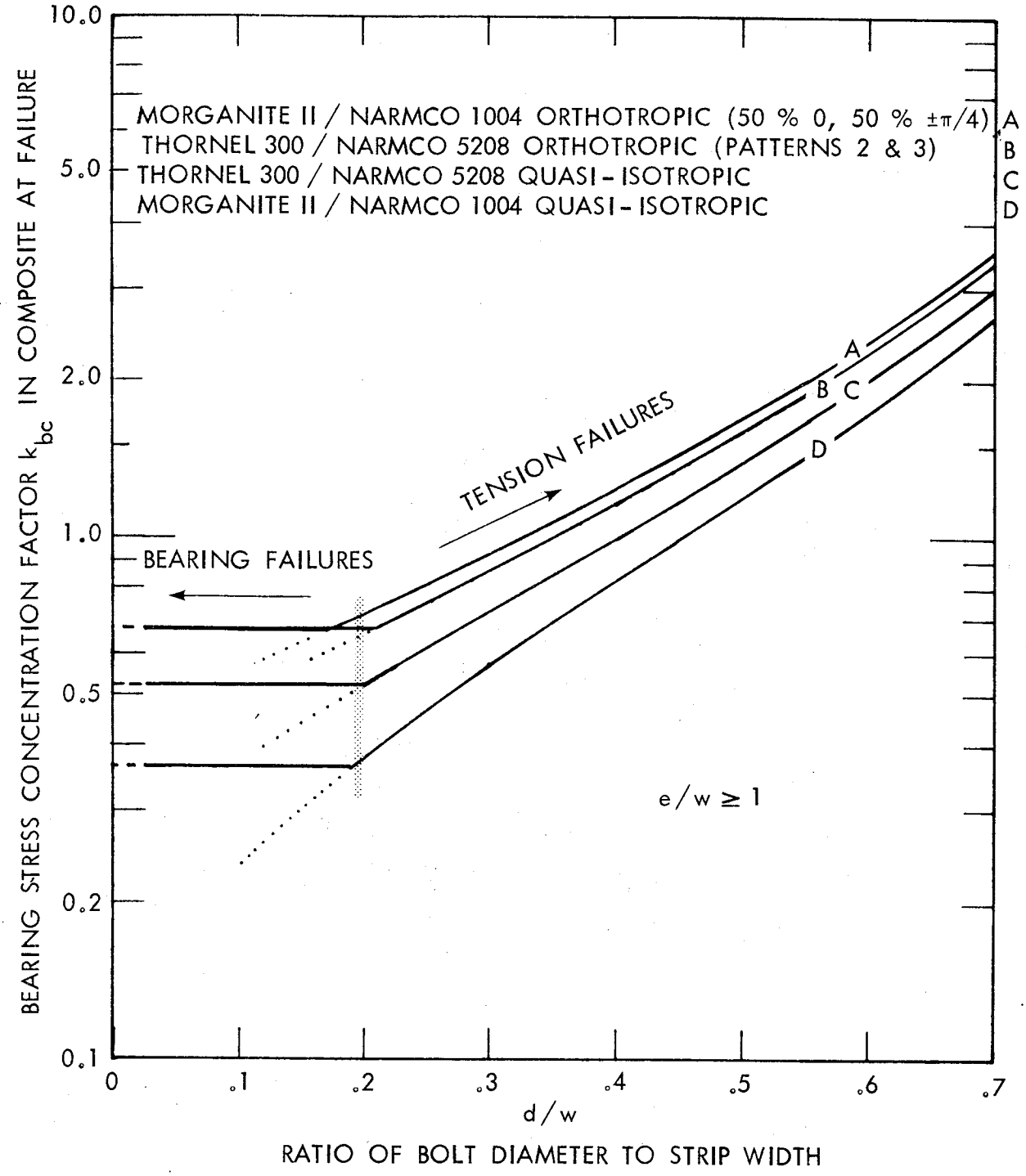

FIGURE 42. STRESS CONCENTRATION FACTORS IN BEARING AND TENSION AS FUNCTIONS OF JOINT GEOMETRY FOR GRAPHITE-EPOXIES

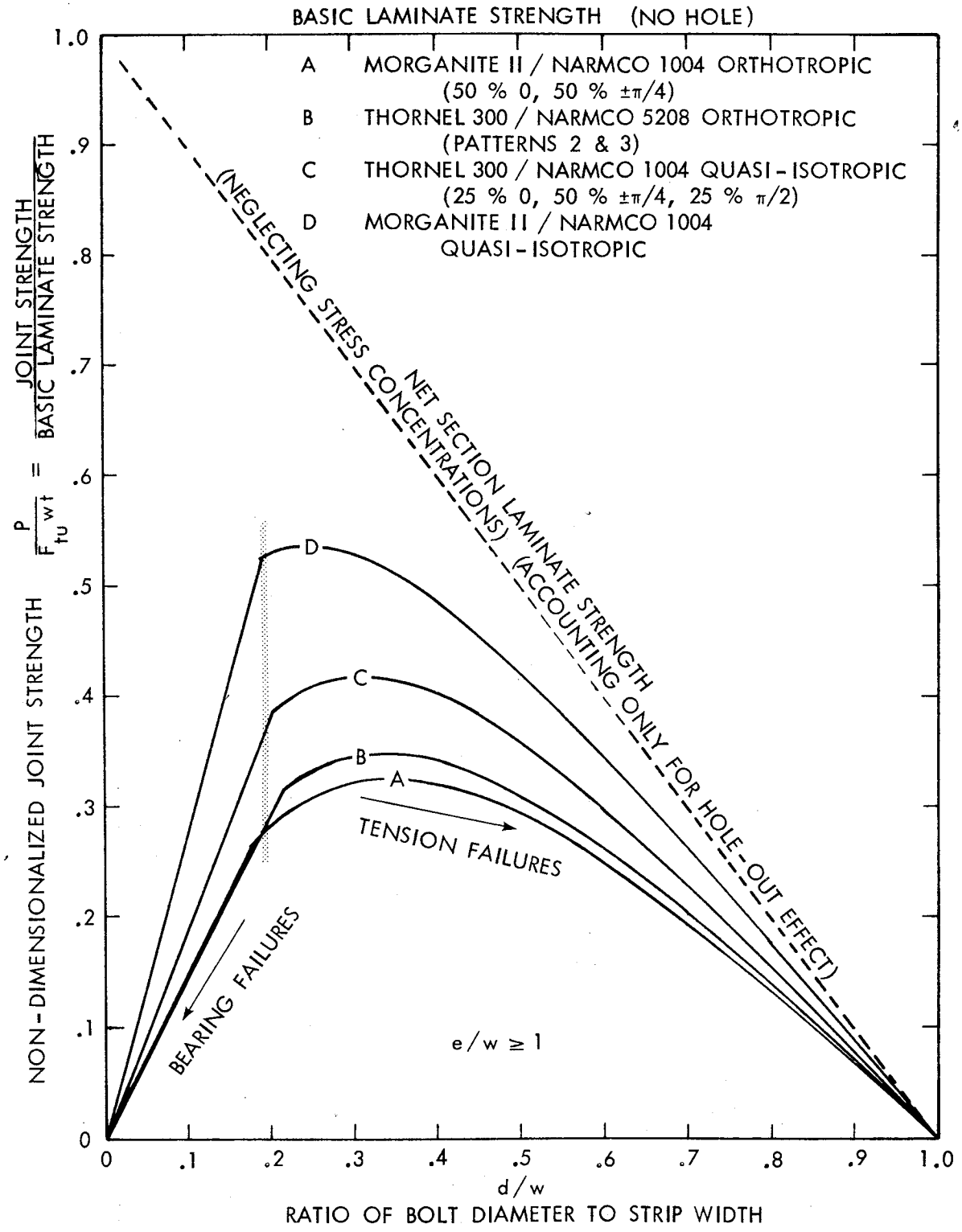

FIGURE 43. NON-DIMENSIONALIZED JOINT STRENGTHS AND FAILURE MODES AS FUNCTIONS OF JOINT GEOMETRY FOR GRAPHITE-EPOXIES

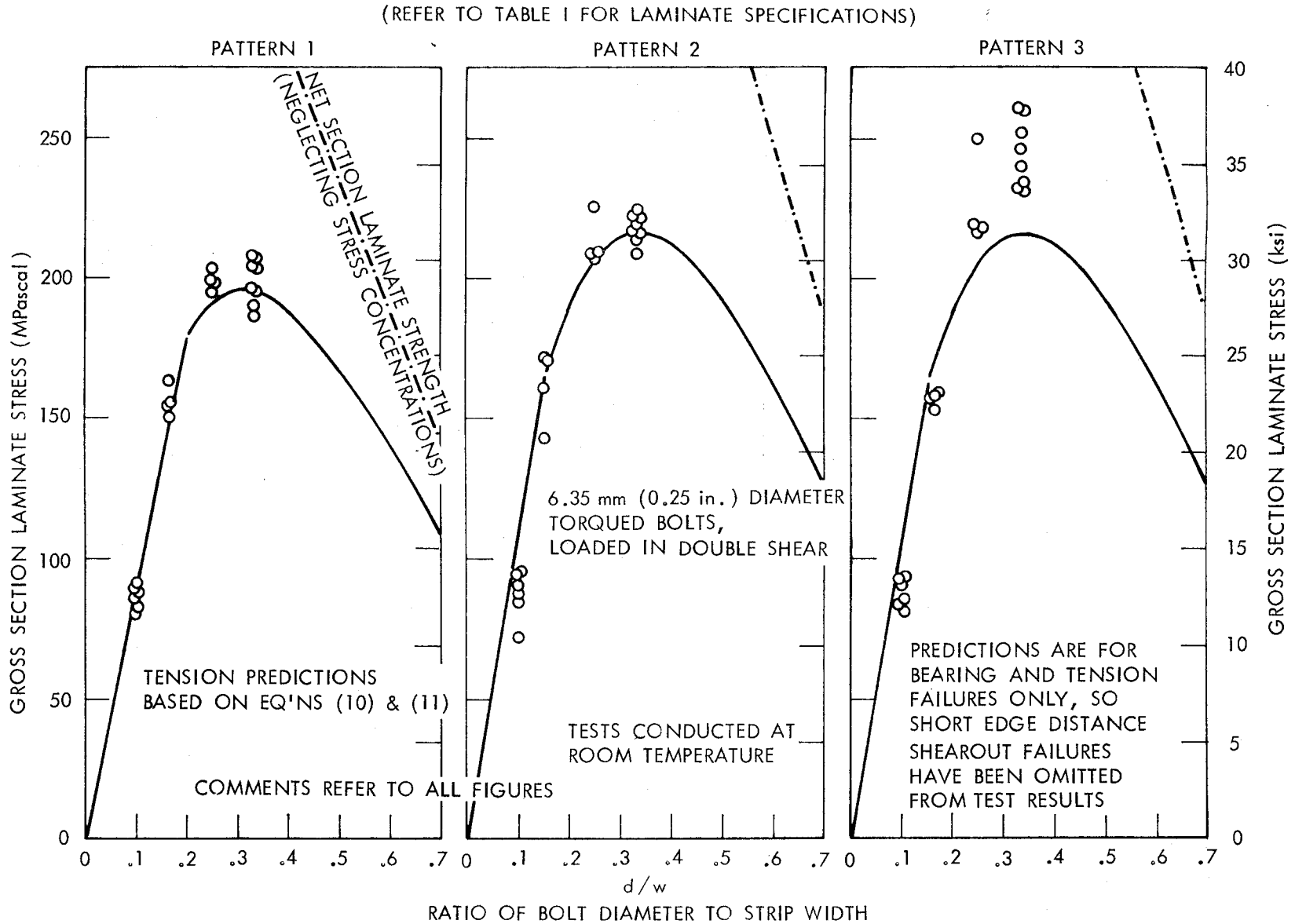

FIGURE 44. COMPARISON BETWEEN PREDICTED AND OBSERVED JOINT STRENGTHS FOR THORNEL 300 / NARMCO 5208 GRAPHITE-EPOXY

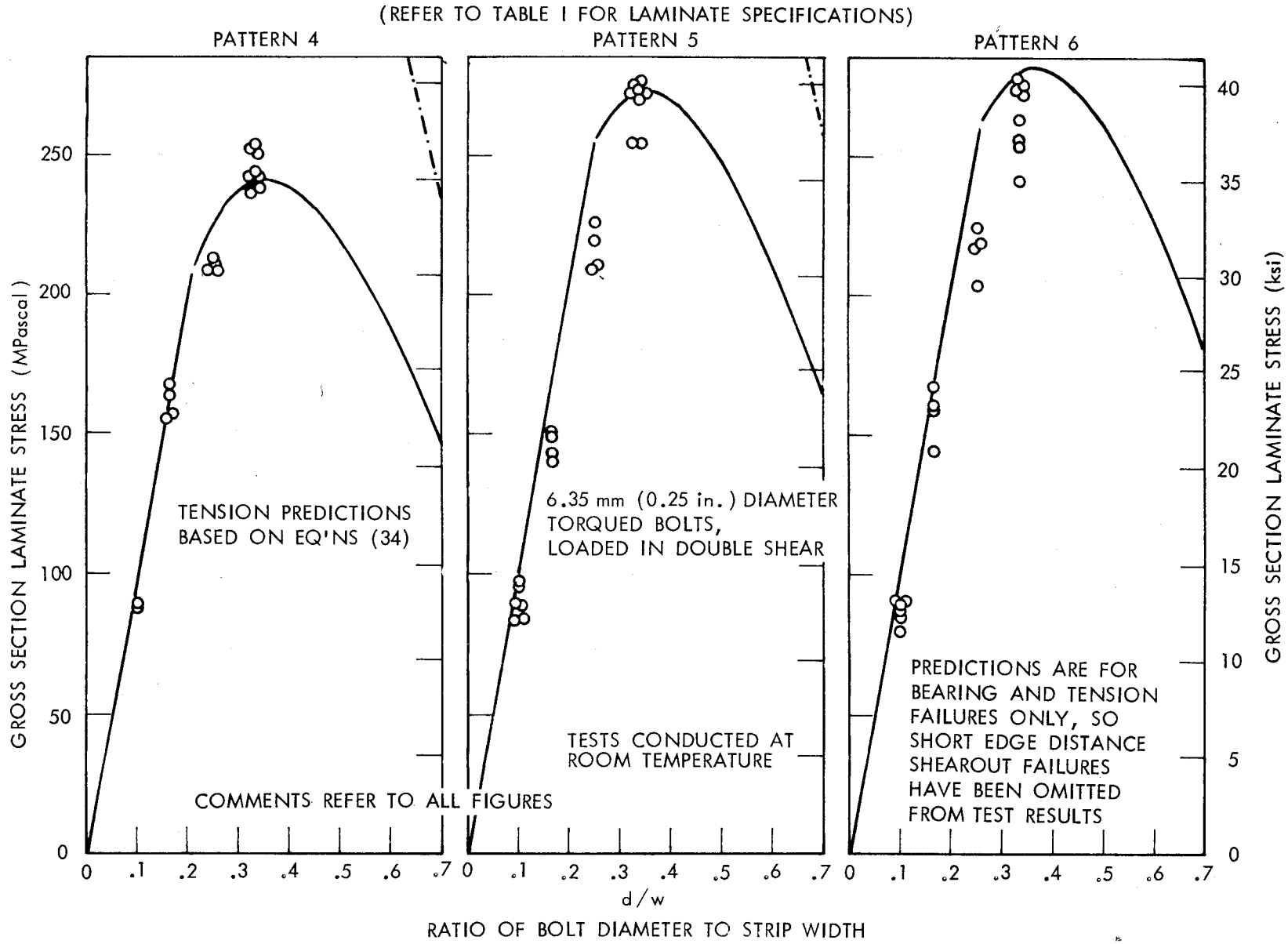

FIGURE 45. COMPARISON BETWEEN PREDICTED AND OBSERVED JOINT STRENGTHS FOR S-1014 / THORNEL 300 / NARMCO 5208 GLASS-GRAPHITE-EPOXY

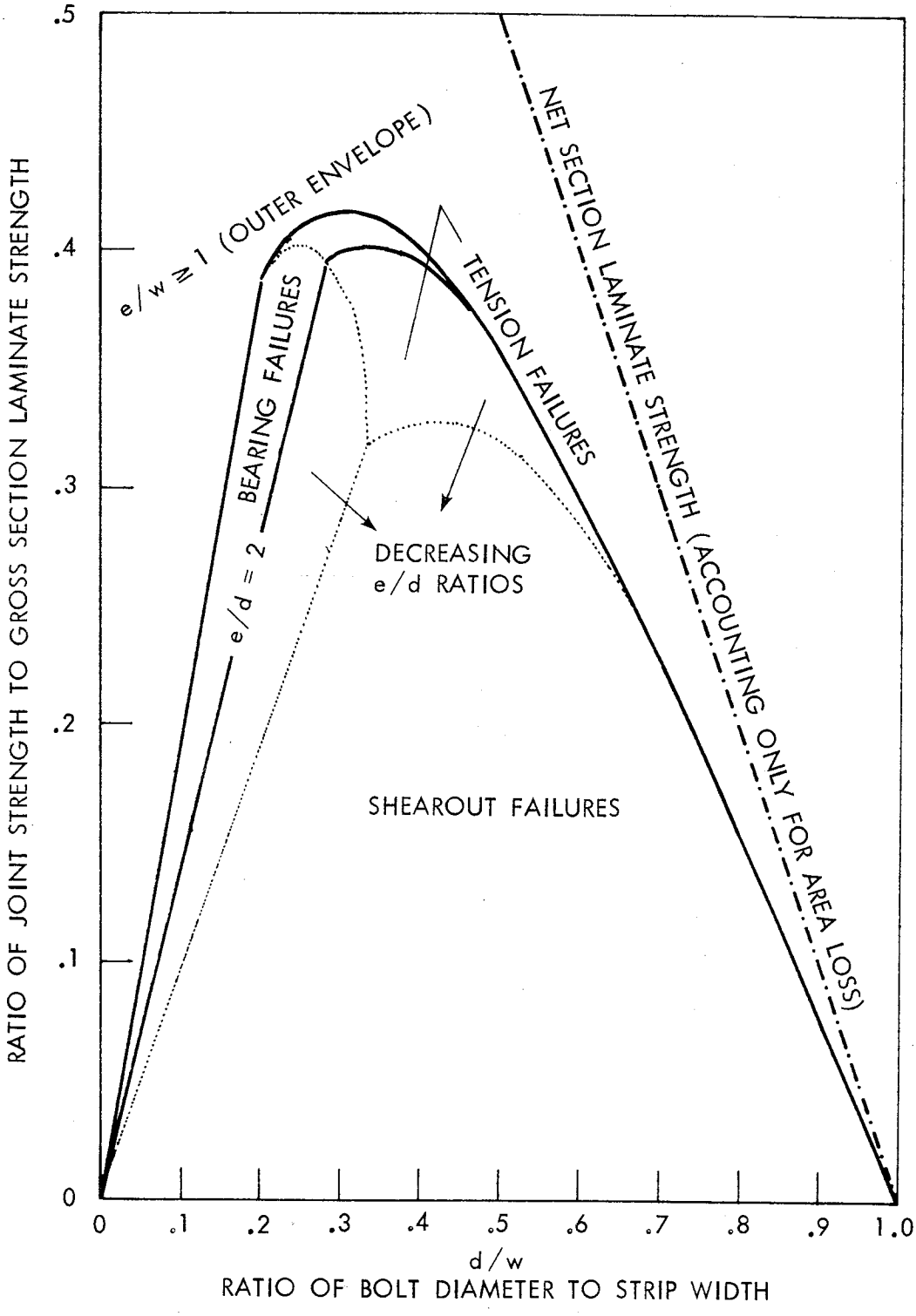

FIGURE 46. INTER-RELATIONSHIP BETWEEN FAILURE MODES AS A FUNCTION OF BOLTED JOINT GEOMETRY FOR GRAPHITE-EPOXY COMPOSITES

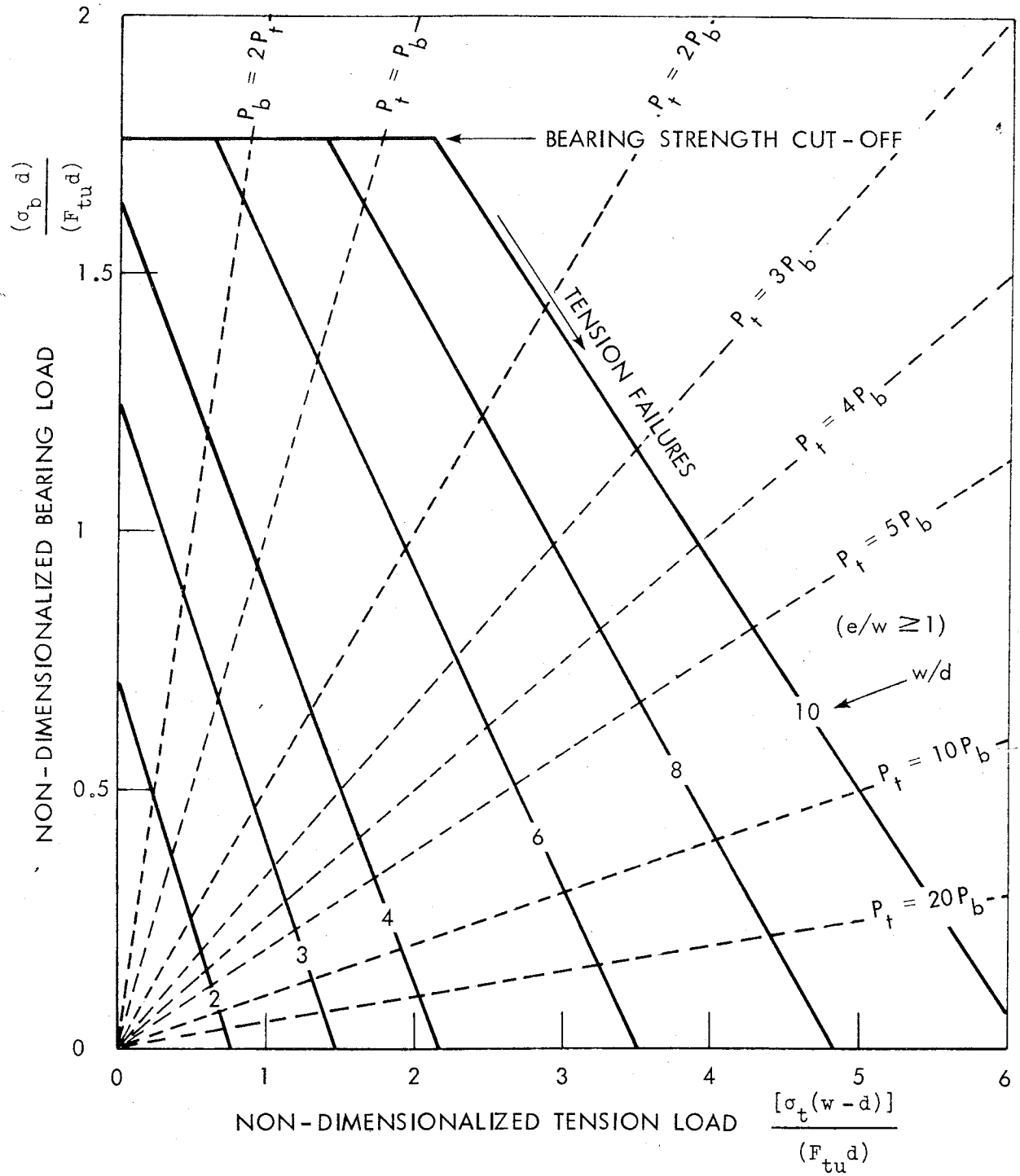

FIGURE 47. CALCULATED INTERACTIONS BETWEEN BEARING AND TENSION LOADS ON TWO-ROW BOLTED JOINTS IN GRAPHITE-EPOXY COMPOSITES

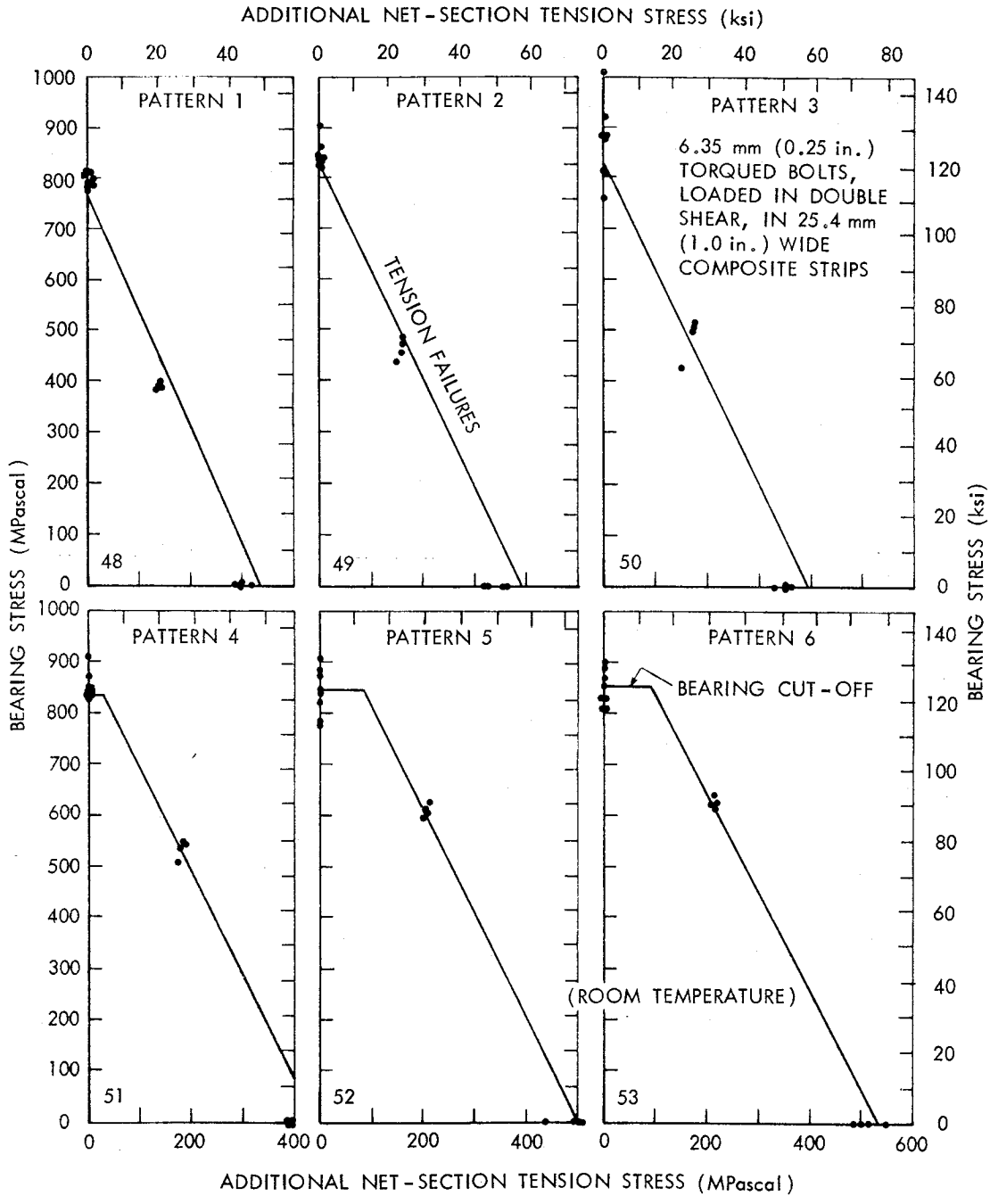

FIGURES 48 - 53. EXPERIMENTAL INTERACTIONS BETWEEN BEARING AND TENSION LOADS ON TWO-ROW BOLTED COMPOSITE JOINTS

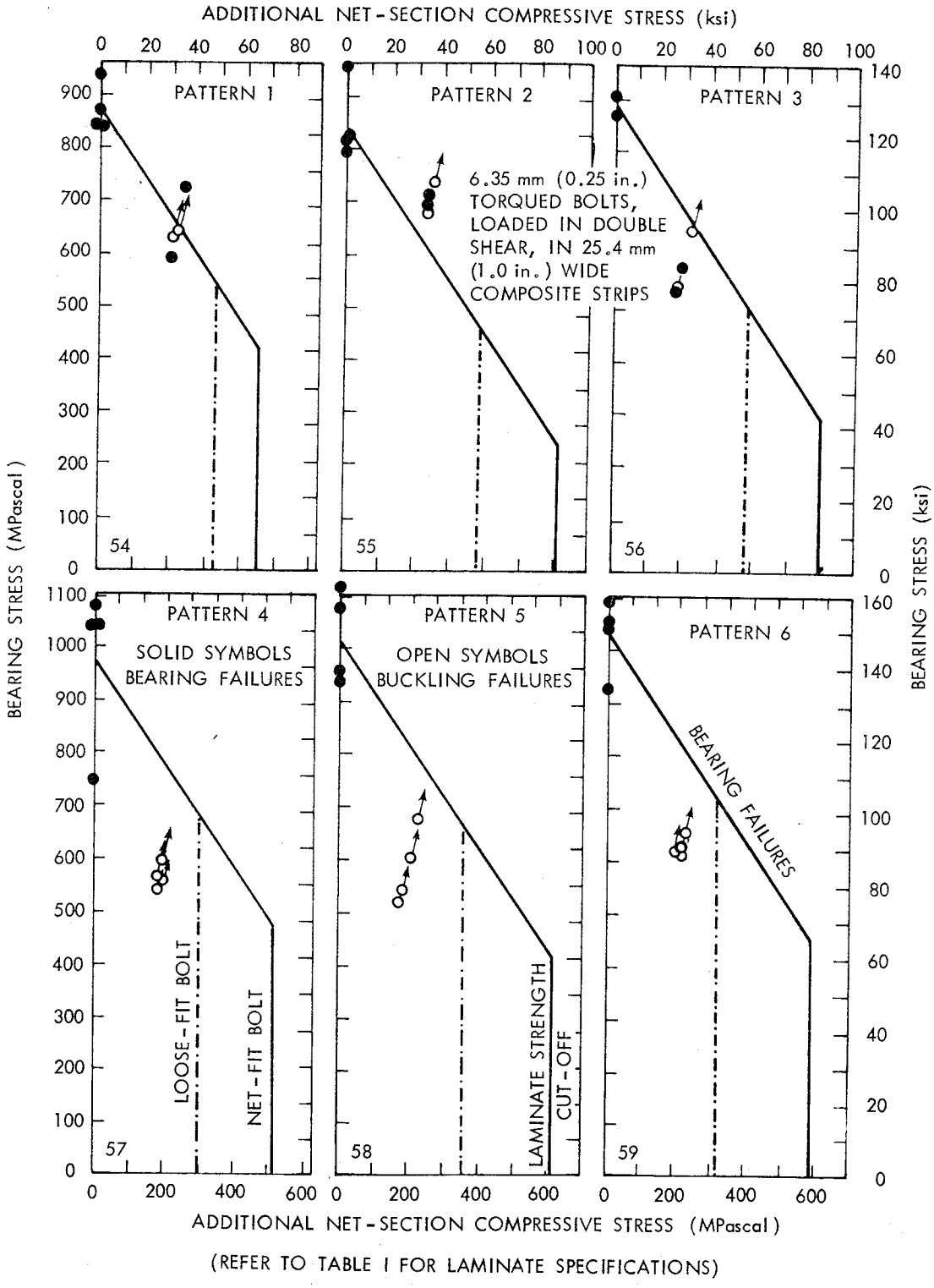

FIGURES 54 - 59. EXPERIMENTAL INTERACTIONS BETWEEN BEARING AND COMPRESSION LOADS ON TWO-ROW BOLTED COMPOSITE JOINTS

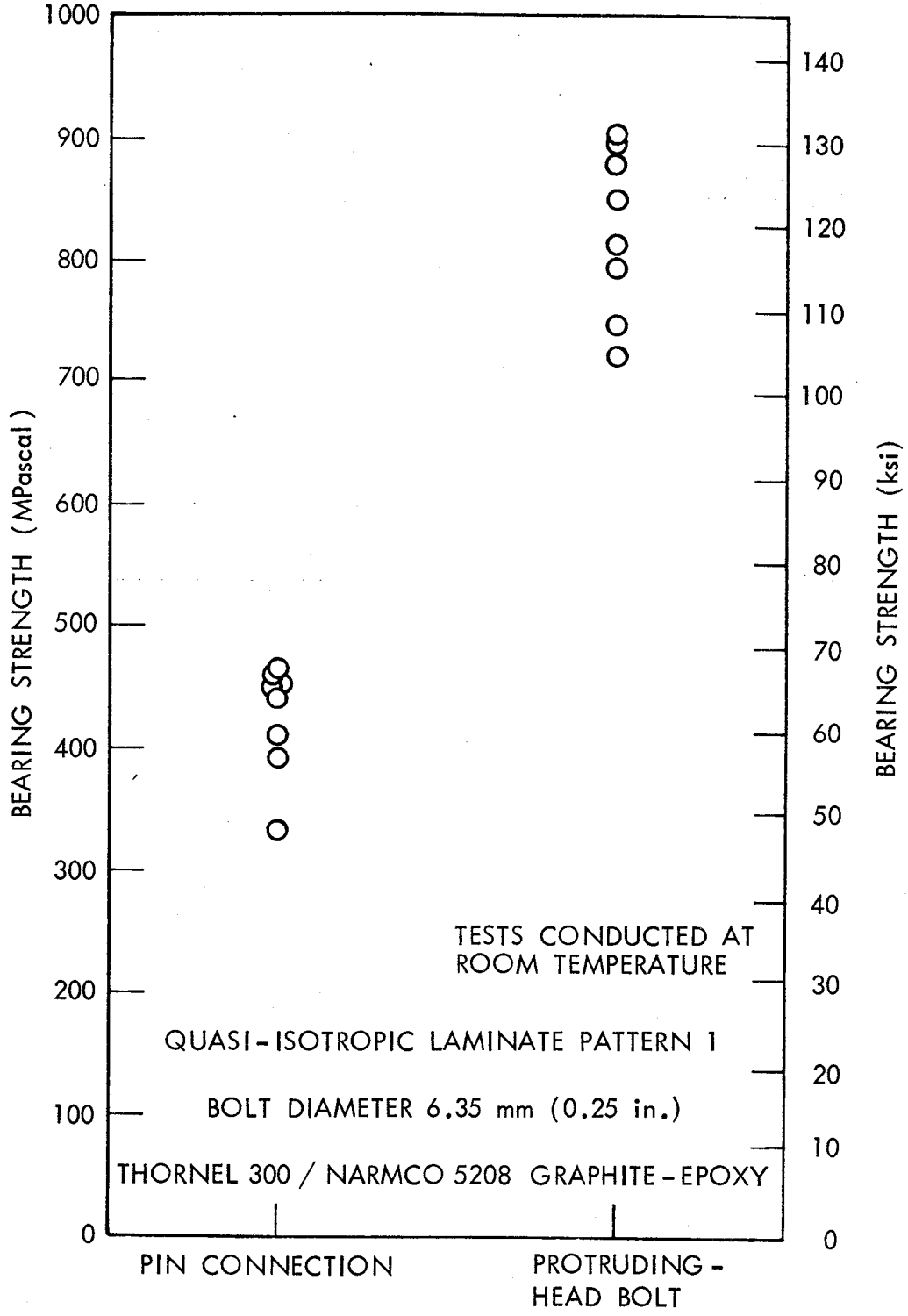

FIGURE 60. COMPARISON BETWEEN BEARING STRENGTHS FOR PIN-LOADING AND REGULAR (TORQUED) BOLTS

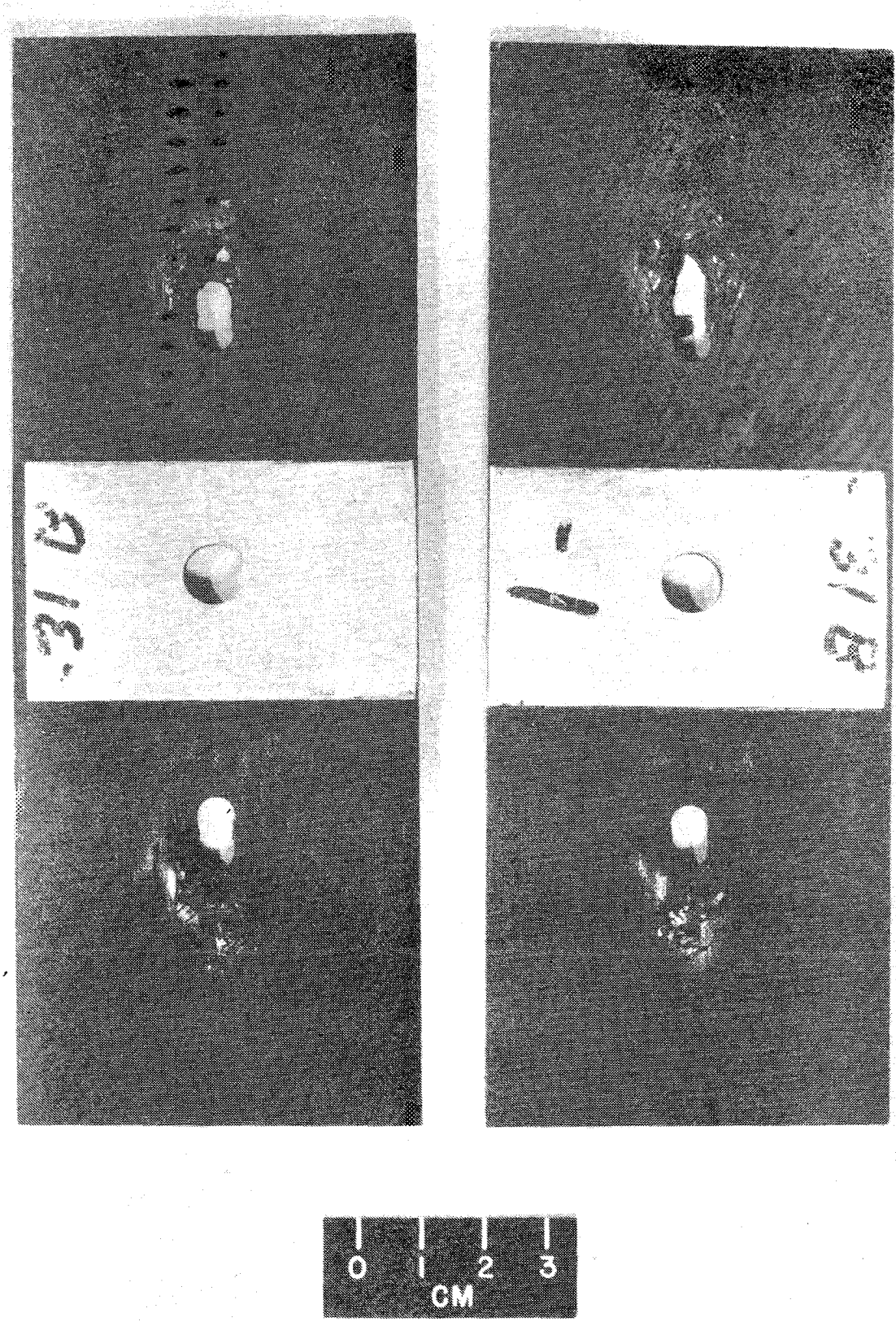

FIGURE 61. BEARING DAMAGE AT BOLT HOLES IN GRAPHITE-EPOXY COMPOSITES

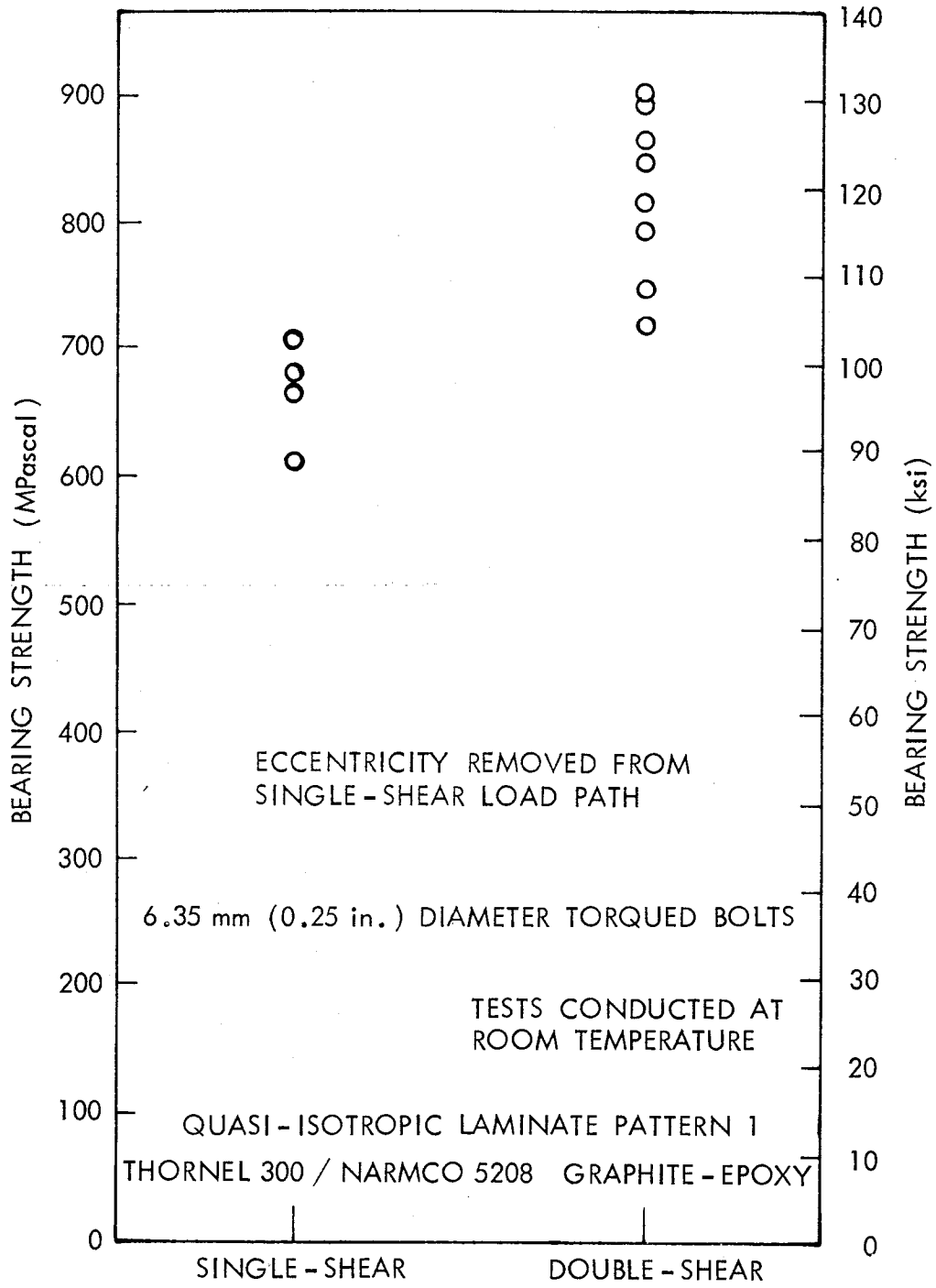

FIGURE 62. COMPARISON BETWEEN BOLT BEARING STRENGTHS IN SINGLE- AND DOUBLE-SHEAR FOR GRAPHITE-EPOXY LAMINATES